The interaction of heparan sulfate proteoglycans with the amyloid β protein

ISBN 978-94-91027-03-1

The interaction of heparan sulfate proteoglycans with the amyloid β protein
Thesis Radboud University Nijmegen with summary in Dutch

Cover design: Henk Kampen
Lay-out: Jan-Rienk Timmer

The work described in this thesis was supported by grants from the Internationale Stichting Alzheimer Onderzoek (no. 03517 and 07510), the Hersenstichting Nederland (no. 14F06.18) and Zon-MW Innovational Research (Vidi program, no. 917.46.331).

The publication of this thesis was financially supported by the Internationale Stichting Alzheimer Onderzoek, Alzheimer Nederland, the Donders Institute for Brain, Cognition and Behaviour and the Radboud University Nijmegen Medical Centre.

Printed by Ipskamp Drukkers, Nijmegen

The interaction of heparan sulfate proteoglycans with the amyloid β protein

Een wetenschappelijke proeve op het gebied van de Medische Wetenschappen

Proefschrift

Ter verkrijging van de graad van doctor
aan de Radboud Universiteit Nijmegen
op gezag van de rector magnificus **prof. Mr. S.C.J.J. Kortmann**,
volgens besluit van het college van decanen
in het openbaar te verdedigen op donderdag **13 januari 2011**
om **13.00 uur** precies

door

Nienke Minke Timmer
geboren op **30 oktober 1979**
te **Groningen**

Promotor:	Prof. Dr. H.P.H. Kremer
Copromotor:	Dr. Ir. M.M. Verbeek Dr. R.M.W. de Waal
Manuscriptcommissie:	Prof. Dr. P. Wesseling (voorzitter) Prof. Dr. G.J.M. Martens Prof. Dr. P.G.M. Luiten

The best-laid schemes o' mice an' men, Gang aft agley
Robert Burns 'To a mouse'

Contents

List of frequently used abbreviations

α1-ACT	α1-antichymotrypsin
α2M	α2-macroglobulin
AA	inflammation-associated amyloid A
Aβ	amyloid beta
AD	Alzheimer's disease
ADAM	a disintegrin and metalloprotease
APP	amyloid precursor protein
APPswe	amyloid precursor protein with the Swedish mutation
Aph-1	anterior pharynx defective 1
apoE	apolipoprotein E
BACE1	beta-site APP cleavage enzyme
BBB	blood brain barrier
CAA	cerebral amyloid angiopathy
CD	circular dichroism
CdS-Hep	N-acetyl-de-O-sulfated (completely desulfated) heparin
CLAC	collagenous Alzheimer amyloid plaque component
CR1	complement receptor 1
CS	chondroitin sulfate
DAβ1-40	amyloid β containing the Dutch mutation
DeN-Hep	de-N-sulfated heparin
DxS	dextran sulfate
EM	electron microscope
Enox	enoxaparin
GAG	glycosaminoglycan
HBP	human brain pericyte
HCHWA(-D)	hereditary cerebral haemorrhage with amyloidosis (of the Dutch type)
HS	heparan sulfate
HSPG	heparan sulfate proteoglycan
ICAM-1	intercellular adhesion molecule 1
IDE	insulin-degrading enzyme
IEM	immuno-electron microscopy
LRP	lipoprotein receptor-related protein
Nct	nicastrin
NEP	neprilysin
NFT	neurofibrillary tangle
NT	non-transgenic
PBS	phosphate buffered saline
PS1	presenilin-1
PS1dE9	presenilin-1 with a deletion in exon 9
PS2	presenilin-2
Pen-2	presenilin enhancer 2
PG	proteoglycan
RAGE	receptor for advanced glycation end products
SAP	serum amyloid P
sHsp	small heat shock protein

SP	senile plaque
Tg	transgenic
TGF-β1	transforming growth factor-β1
TgSwDI	transgenic mouse model expressing the amyloid precursor protein with the Swedish, Dutch and Iowa mutation
WT	wildtype

Chapter 1

General Introduction

Alzheimer's disease

With increasing medical knowledge, life expectancy has greatly increased in the past decades. Therefore, age-related diseases such as Alzheimer's disease (AD) have also become more prevalent. It is estimated that in 2050 more than 100 million people will suffer from AD world-wide, a disease that is clinically characterized by a global loss of cognitive functions such as memory and language and symptoms such as apathy and depression [209]. The very first recognized AD patient, a woman suffering from severe memory failure and disorientation, was described by Alois Alzheimer in 1907 [209, 302]. Upon examination of her brain, Alzheimer noticed atrophy of brain cells combined with "clumps of filaments between cells". These clumps are now known to consist of amyloid β (Aβ). Besides Aβ, hyperphosphorylated tau protein also accumulates as neurofibrillary tangles (NFT), but unlike Aβ, which accumulates in the brain parenchyma as senile plaques (SP) or in the vasculature as cerebral amyloid angiopathy (CAA), tau accumulates intracellularly.

The most important risk factor for AD is age, with sporadic AD cases representing >99% of total AD cases. However, there are other risk factors, such as possession of the ε4 allele of apolipoprotein E (apoE). ApoE is a lipoprotein that can exist in several different isoforms (i.e. apoE2, apoE3, apoE4). In the general population apoE3 is most common [126], but about 65% of sporadic AD patients carry at least one apoE4 allele [50]. Indeed, it has been found that about 50% of individuals carrying one ε4 allele and over 90% of individuals carrying two alleles were affected by AD, with a mean age of disease onset about 10 to 15 years earlier than that of non-carriers [51]. It is thought that the increased risk associated with apoE4 is mediated by less efficient binding to Aβ [245] or a diminished production of this specific isoform [30]. This, in turn, may reduce clearance of Aβ, as apoE is involved in Aβ transport across the blood brain barrier (BBB). In contrast, possession of the ε2 allele seems to be protective, as it is capable of lowering the risk for AD four-fold [50]. However, the ε2 allele does seem to be related to an increased risk for CAA-related hemorrhages [176]. Besides apoE, several other proteins have recently also been linked to an increased risk for AD, i.e. clusterin (CLU), phosphatidylinositol-binding clathrin assembly protein (PICALM) and complement receptor 1 (CR1) [93, 141].

A commonly accepted mechanism that may explain the etiology of AD is the amyloid cascade hypothesis [149]. It suggests that abnormal production and/or clearance of Aβ and subsequent fibrillization of Aβ is responsible for AD development. This hypothesis has received much attention in the past decades, based on the fact that Aβ deposition is such a characteristic part of AD pathology.

Amyloid cascade hypothesis

Production of Aβ

The Aβ peptide is a 4 kDa cleavage product of the amyloid precursor protein (APP), a transmembrane protein that can be cleaved into several different products [81, 165, 208] (Fig. 1A). In neurons, APP is present in synapses [205], where it may be involved in synapse formation and synaptic transmission [186]. Several other functions of APP have been suggested, including a role in cell-cell interaction, although the exact function of APP and its cleavage products remains elusive [165, 209, 211].

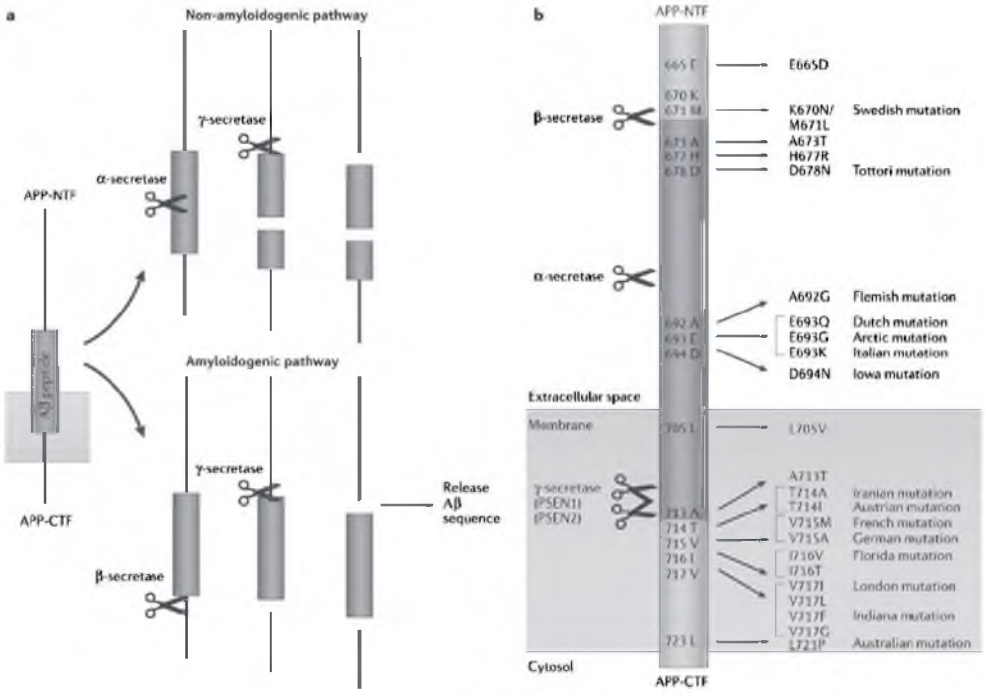

Figure 1: *Amyloid precursor protein (APP) processing involves proteolytic cleavage by several secretases (A). The non-amyloidogenic pathway is initiated by α-secretase cleavage, which occurs in the middle of the amyloid β (Aβ) sequence (red), and results in the release of several soluble APP fragments. The amyloidogenic pathway releases Aβ peptides through cleavage by α- and β-secretases. (B) Part of the APP amino-acid sequence; mutations associated with early-onset Alzheimer's disease have been highlighted. Most mutations are clustered in the close vicinity of secretase-cleavage sites, thereby influencing APP processing, and are named after the nationality or location of the first family in which that specific mutation was demonstrated. The Aβ sequence is indicated in red. Reprinted with permission from Macmillan Publishers Ltd: [Nature Reviews Drug Discovery] [247], copyright (2006)*

Cleavage of APP is performed by three proteolytic enzymes: α-, β- and γ-secretase (reviewed in [44]). Most α-secretases are members of the ADAM (a disintegrin and metalloprotease) family of proteases and of this family, ADAM 9, 10, 17 and 19 are known to have α-secretase activity [8, 236]. BACE1 (beta-site APP cleavage enzyme) is considered the main β-secretase, while γ-secretase operates as a complex of four different proteins: a presenilin (PS), nicastrin (Nct), anterior pharynx defective 1 (Aph-1) and presenilin enhancer 2 (Pen-2). Presenilin, either presenilin-1 or -2, forms the protease part of this secretase, with the other three proteins acting as co-factors, stabilizing presenilin and modifying its enzymatic activity [234].

Cleavage by α- and β-secretase releases two soluble extracellular APP fragments, sAPPα and sAPPβ, respectively. The remaining membrane-embedded fragments, C83 and C99 respectively, can subsequently be cleaved by γ-secretase to release p3 from C83 and

Aβ from C99. Aβ can generally vary in length between 38 and 43 amino acids long, but the main Aβ species generated are Aβ40 and Aβ42. Normally, Aβ40 makes up 90% of all produced Aβ and Aβ42 only 10%. However, in both sporadic and familial AD, brain levels of Aβ42 are elevated, altering the ratio between Aβ40 and Aβ42. It is thought that this increase in Aβ42 leads to deposition of Aβ, as Aβ42 is particularly prone to aggregation [114]. In patients suffering from familial AD, the cause of increased production of Aβ42 is the presence of one or more mutations in an AD-related gene, while in sporadic AD cases it is believed that impaired removal of Aβ from the brain causes Aβ levels to increase.

Familial mutations

Gene mutations in familial cases of AD explain only a minority of AD cases (<1%). Most of these are linked to missense mutations in the presenilins that are part of the γ-secretase complex, with mutations in PS1 being more frequent than in PS2 [208]. Mutations in γ-secretase are known to result in a (partial) loss of its proteolytic function [19]. As the cleavage site for Aβ42 seems less affected than the cleavage site for Aβ40, this leads to a prevalent production of Aβ42 and therefore a (relative) increase in Aβ42 levels in familial AD cases.

There are also a number of known APP mutations (Fig. 1B), all named after the area in which they were first identified [247]. Mutations near β-secretase cleavage sites result in increased production of both Aβ40 and Aβ42, while the preferential generation of Aβ42 seems to occur as a result of mutations near γ-secretase cleavage sites. Furthermore, mutations within the Aβ sequence (i.e. Flemish A692G, Dutch E693Q or Iowa D694N) can accelerate the aggregation of Aβ into oligomers and ultimately fibrils [81]. Mutations may also direct the accumulation of Aβ into specific types of Aβ deposit (i.e. SP or CAA). For example, patients carrying APP with the Dutch mutation (Glu22Gln amino acid substitution) specifically develop CAA accompanied by hemorrhages and suffer from a condition called hereditary cerebral hemorrhage with amyloidosis of the Dutch type (HCHWA-D) [251].

Clearance of Aβ

In healthy individuals, Aβ is generally cleared in two different ways, either by proteolytic degradation or by transport across the BBB [210, 270, 303]. There are several proteases involved in the normal degradation of Aβ, including endothelin converting enzyme (ECE), insulin-degrading enzyme (IDE) and neprilysin (NEP), with the latter two having received most attention [270]. IDE is a thiol metalloendopeptidase of about 110 kDa that can degrade a number of proteins such as insulin, glucagon and monomeric, but not oligomeric, extracellular Aβ [188, 210, 261]. The Aβ-degrading capacity of NEP, another metalloendopeptidase, was revealed when inhibition of this protease suppressed the degradation of intracerebrally injected Aβ in rats [109]. Unlike IDE, NEP can degrade both monomeric and oligomeric Aβ species [120]. With age and in AD, the levels of IDE and NEP decrease, specifically in brain areas that are most vulnerable to Aβ pathology (i.e. cortex and hippocampus) [36, 297].

Transport of Aβ across the BBB is mediated by two receptors, the lipoprotein receptor-related protein (LRP) and the receptor for advanced glycation end products (RAGE). Aβ, either alone or complexed with apoE or α2-macroglobulin can be transported out of the brain by LRP [60, 216], while RAGE is considered an influx receptor [59]. In AD, the expression of LRP, but not RAGE, diminishes, perhaps explaining in part the observed

increase in brain Aβ levels [60, 216, 296]. In contrast, we have previously demonstrated an Aβ-induced increase of LRP-1 in cerebrovascular cells [283], which may be a (temporary) compensatory mechanism to enhance Aβ clearance.

Aggregation and toxicity

When Aβ levels increase in the brain, Aβ starts to aggregate. To this end, its conformation switches from an α-helix to a β-sheet [23]. Monomeric Aβ can assemble into oligomers (dimer, trimers, and larger aggregates), protofibrils (4-11 nm in diameter and <200 nm in length) and mature fibrils (6-10 nm in diameter, indeterminate length) [81, 128], ultimately forming the Aβ deposits visible in AD brain (Fig. 2). Furthermore, accumulation can also occur intracellularly [138].

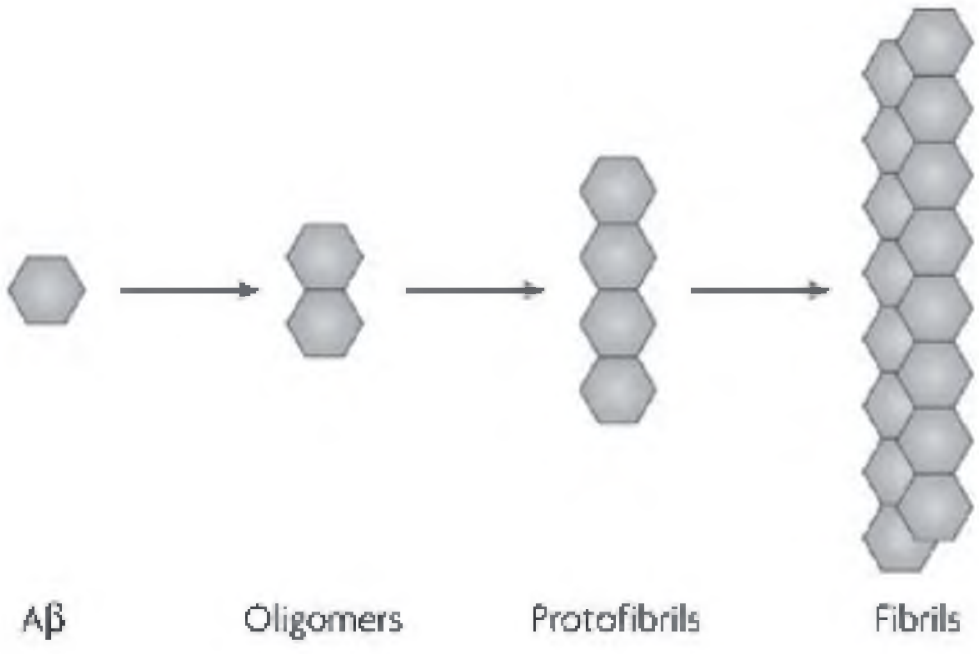

Figure 2: *Amyloid β (Aβ) can exist in multiple assembly states — monomers, oligomers, protofibrils and fibrils. In its monomeric state, Aβ does not appear to be neurotoxic. By contrast, oligomeric and protofibrillar species are considered potent blockers of long-term potentiation, a form of synaptic plasticity. Reprinted with permission from Macmillan Publishers Ltd: [Nature Reviews Neuroscience] [138], copyright (2007).*

It has long been thought that Aβ fibrils are the toxic species in AD, but it is now known there is little correlation between dementia and fibrillar amyloid deposits. Indeed, there is much more evidence that oligomeric and protofibril species of Aβ are toxic [128, 168]. This toxicity is in part thought to be mediated by Aβ-induced inflammation and/or oxidative stress [18, 209]. Furthermore, (oligomeric) Aβ species are considered synaptotoxic, as they can, for example, reduce long-term potentiation (LTP) (reviewed in [238]). Ultimately, Aβ-induced toxicity results in the substantial loss of neurons seen in AD.

Inflammation and Aβ-associated proteins

Aβ deposition in AD is accompanied by neuroinflammation, as it activates and attracts microglial cells, the innate immune cells of the brain. Furthermore, astrocytes also become activated and are surrounding Aβ deposits (reviewed in [4]). Both these glial cells have pro- and anti-inflammatory activities and can therefore enhance brain damage but also protect the brain from (Aβ-induced) toxicity [207]. In their pro-inflammatory state, glial cells release numerous inflammatory factors, including cytokines and complement factors [4], that contribute to neurodegeneration. However, glial cells have also been demonstrated to phagocytose Aβ and in this way may have a protective function against Aβ-induced toxicity [274].

The inflammatory factors excreted by glial cells, such as complement factors, can be found co-deposited with Aβ [72, 73, 264] and other inflammatory proteins, such as acute phase proteins [72, 264] and intercellular adhesion molecule 1 (ICAM-1) [267], are also found near or within Aβ deposits. In fact, many proteins co-deposit with Aβ and some of them, including heparan sulfate proteoglycans [254, 255] and small heat shock proteins [280, 284], have been proven to bind Aβ with high affinity and influence Aβ aggregation in vitro.

Heparan sulfate proteoglycans (HSPG)

HSPG are part of a family of proteoglycans that also include chondroitin sulfate, keratan sulfate and dermatan sulfate proteoglycans [91, 256]. In general, proteoglycans consist of a glycosaminoglycan (GAG) chain attached to a protein core via a specific serine residue. The GAG chains are long sulfated polysaccharide chains synthesized in the Golgi apparatus. The repeating disaccharide units that make up the GAG chains are unique for each proteoglycan family member. For HSPG, the disaccharide unit consists of N-acetylglucosamine with a uronic acid. The type of uronic acid depends on the enzymatic modifications of the chain that occur during the synthesis process. Various Golgi enzymes modify GAG chains to contain highly sulfated regions with iduronic acid and relatively unmodified regions with glucuronic acid [22, 256].

There are several different HSPG, each characterized by a different core protein. In general, HSPG can divided into two groups: extracellular matrix-associated HSPG, including perlecan, agrin [108] and collagen XVIII [88] and various cell surface HSPG, like the glypicans and syndecans [22]. The different HSPG have numerous functions, although most are involved in developmental processes. For example, functions of perlecan include involvement in cartilage formation and blood vessel development in embryogenesis [89], while agrin is involved in organizing synapses in the neuromuscular junction [199] and maintaining BBB impermeability [14]. Cell surface HSPG can bind extracellular proteins for internalization or act as co-receptors (reviewed in [22]). HSPG have also been linked to several pathological conditions, including all types of amyloidosis [225].

In AD, HSPG can be found co-localized with Aβ deposits. Agrin and the cell surface HSPG glypican-1 have the most prominent co-deposition, as they can be found associated with nearly all types of Aβ deposits (i.e. fibrillar and non-fibrillar SP, CAA) [254, 255]. Syndecans can only be detected in a minority of SP with some deposition of syndecan-2, but not the other syndecans, in CAA [255]. Collagen XVIII can be found in all Aβ deposits, except fibrillar SP [257]. The association of perlecan with Aβ deposits is still unclear, as some describe this HSPG to have the strongest association [222, 224], whereas we and others have been unable to detect perlecan in CAA or SP [254, 255, 263]. There is evidence that other proteoglycans can also be found in the vicinity of Aβ deposits, but never to the same extent as HSPG [65, 221, 223].

Small heat shock proteins (sHsp)

Small Hsp are chaperone proteins, involved in the proper folding of proteins [32]. There are ten members of the sHsp family [121], each possessing an α-crystallin domain and all ranging between 16-25 kDa in size. Some sHsp are expressed in the eye lens, where they help refract incoming light and maintain transparency of lens fluid [105]. Many members are also expressed in skeletal and cardiac muscle tissues. In AD, Hsp20, Hsp27, HspB2/B3 and HspB8 co-localize with SP, while HspB2/B3 is only associated with Aβ in CAA [280, 284]. The only sHsp not co-deposited with Aβ is αB-crystallin, although this sHsp can be detected in glial cells near Aβ deposits [284].

As would be expected from their close association with Aβ in vivo, both HSPG and sHsp can bind Aβ with high affinity [41, 52, 279] and protect cells against Aβ-induced cellular toxicity [279, 290]. By binding to Aβ, HSPG can stimulate Aβ fibrillization [41, 52] and protect Aβ from proteolytic degradation [52, 87]. In contrast, sHsp, especially αB-crystallin, seem to inhibit Aβ fibrillization [279].

Mouse models for AD

To investigate disease mechanisms and test new therapeutic interventions, transgenic mouse models have been created. There are several different methods for creating transgenics, including homologous recombination and pronuclear injection [74, 97]. Homologous recombination relies on targeted disruption of endogenous mouse genes, thereby altering gene function or even generating full knockouts. However, as mice do not necessarily possess the genes responsible for human disease, this technique is not always suitable to mimic their pathology. With pronuclear injection, human genes can be inserted into the mouse genome. To accomplish this, the gene of interest is inserted into a vector, containing a (tissue-specific) promoter, that is then injected into a pronuclear mouse zygote. This results in the development of a transgenic mouse that will (over)express the human gene.

Most transgenic mouse models for AD express the human APP gene [67, 74, 80] (for a summary of models mentioned in this thesis: see Table 1). Initial attempts to generate an APP-expressing model revealed that wildtype APP, although expressed, did not generate the (robust) Aβ pathology seen in humans [35, 98, 293]. However, inserting APP with one (or more) of the pathogenic mutations found in familial AD cases did generate mice with AD-like pathology. The first model expressing mutated APP, the PDAPP mouse expressing APP with the Indiana mutation, developed Aβ plaques at about 6 months of age [79] (Table 1) accompanied by impaired cognition [68].

To facilitate APP cleavage, many models also express (mutated) PS1 [67, 74, 80].

Table 1: *Characteristics of the AD mouse models mentioned in this thesis (Adapted from [74])*

Mouse model	Mutations	Promotor	Amyloid pathology (age of onset)	Reference
APPwe/PS1dE9	APP-Swedish PS1 exon 9 deleted	PrP	Parenchymal plaques (4-6 months of age)	[82]
TgSwDI	APP-Swedish + Dutch + Iowa	Thy1.2	Severe vascular deposition + parenchymal plaques (3-6 months of age)	[55]
PDAPP	APP-Indiana	PDFG-β	Parenchymal plaques (6-9months of age)	[293]
Tg2576	APP-Swedish	PrP	Parenchymal plaques (9-12 months of age)	[106]
TgCRND8	APP-Swedish + Indiana	PrP	Aggressive parenchymal plaques (3 months of age)	[42]
PSAPP	PS1M146V APP-Swedish (Tg2576)	-	Earlier and more extensive plaque pathology compared to Tg2576 mice	[101]
Triple transgenic	APP-Swedish PS1M146V Tau P301L	Thy1.2	Parenchymal plaques (6 months of age) + tau pathology (12 months of age)	[181]

The fastest approach to create double-transgenics is to co-inject both genes, although it has long been done by mating the single transgenic mice with each other [112]. Generally, expression of PS1 accelerates and exacerbates Aβ pathology in models [101]. However, even with robust Aβ deposition, AD models still do not mimic all (Aβ-related) characteristics of AD, such as neurodegeneration [80], Aβ modifications (e.g. N-terminal cleavage) [136] and tau pathology. To further model the disease, a triple transgenic mouse (3xTg), expressing APP, PS1 and a mutated tau protein, has now been created [181]. These 3xTg mice accumulate Aβ, develop tau tangles and demonstrate synaptic dysfunction.

Therapeutic interventions

Currently, only five drugs are approved for the treatment of AD [175]. Four of these drugs are acetylcholinesterase inhibitors, including donepezil and rivastigmine. These inhibitors aim to prevent the degradation of acetylcholine, as levels of this neurotransmitter are severely diminished in AD brains due to the loss of cholinergic neurons [276]. The other drug, memantine, is an antagonist of the N-methyl-d-aspartate (NMDA) glutamate receptor and currently used to treat moderate to severe AD cases [192]. In blocking the NMDA receptor, memantine is thought to reduce excitotoxicity triggered by the neurotransmitter glutamate. Although all these drugs can at least stabilize the symptoms [90, 192], they cannot prevent or cure AD. Curing this disease requires addressing the underlying (neurotoxic) causes of the disease (reviewed in [209]). For example, lowering oxidative stress by administering substances with anti-oxidant properties, such as titerpenoids [70], can improve memory of AD mice. It has to be mentioned that effective treatment of AD is hindered by the late diagnosis of this disease, although advances are being made to identify patients at an earlier stage of AD [47].

Most new therapeutic strategies target Aβ directly. For example, Aβ production can potentially be modulated by inhibition of β- or γ-secretase cleavage of APP [179]. A whole number of β-secretase inhibitors are now being developed and tested, with GRL-8234 lowering plasma and brain Aβ40 levels in Tg2576 mice [84]. The potent γ-secretase inhibitor LY411575, a benzodiazepine analogue, was demonstrated to lower brain Aβ levels in Tg2576 mice [143] and a similar, but slightly less potent, γ-secretase inhibitor, LY450139 has now entered clinical trials [217].

Another therapeutic strategy is to inhibit Aβ aggregation. Indeed, scyllo-inositol, a known inhibitor of Aβ aggregation, can significantly improve cognition of TgCRND8 mice [77]. Most promising of all potential new therapeutic strategies, however, is immune therapy, aimed at the removal, or clearance, of Aβ. This form of therapy not only affects brain Aβ pathology and cognition, it also provides insights into the mechanisms responsible for Aβ removal from the brain.

Immune therapy

There are two different types of immune therapy, active and passive immunization. With active immunization, Aβ or fragments of Aβ are administered, together with an adjuvant, to trigger an immune response. With passive immunization, antibodies against Aβ are injected directly, circumventing the necessity for patients to generate an immune response and allowing for a better regulation of the immune response. In vitro studies have demonstrated that antibodies may inhibit Aβ aggregation and Aβ-induced cellular toxicity [228, 229] and therefore the feasibility of in vivo immune therapy was soon investigated in AD mouse models.

The first immunization studies were performed in PDAPP mice [16, 203]. When actively immunizing these mice, by injecting Aβ42 for a number of months, mice developed a significant antibody titer against Aβ, which was accompanied by a reduction in brain Aβ burden [203]. This was not only true when injections started prior to Aβ pathology development (11 weeks old), but also when injections were started when severe Aβ pathology was already prominent (11 months old).

Similar to active immunization, passive immunization of PDAPP mice with anti-Aβ antibodies also reduced brain Aβ burden when administered before or during development of Aβ pathology [16]. These antibodies were found associated with Aβ in the brain, apparently having been able to cross the blood brain barrier (BBB), even though integrity of the BBB remained intact. In general, it appeared that antibodies directed against the N-terminus of Aβ were more effective in reducing brain Aβ deposition than those directed against the C-terminus [15], which is in line with the idea that the N-terminus is the most accessible part of the aggregated Aβ protein [124]. After these first immunization treatments, many more animal studies revealed the promising effects of both active and passive immune therapy on brain Aβ levels (reviewed in [83]). Furthermore, immunization was also demonstrated to improve cognitive impairment [66, 113, 172] and to reduce pathological features such as gliosis, neuritic dystrophy [203] and loss of synapses [34]. Administration of anti-Aβ antibodies could even facilitate development of diagnostic tests, as it was demonstrated that plasma Aβ levels of PDAPP mice are highly correlated to brain Aβ levels only after administration of the m266 antibody [62].

Since immunization protocols had such positive results in different AD mouse models [83], human trials started not long after the first mouse results were published. In the very first clinical trials, patients were actively immunized using Aβ42 with the adjuvant QS21 (AN1792). AN1792 not only induced production of anti-Aβ antibodies [99], but could also reduce brain Aβ levels [160, 177] and slow the rate of cognitive decline [100]. Long-term effects of AN1792 however were minimal [102]. Six years after receiving AN1792, brain Aβ levels were lower in immunized patients than in unimmunized controls, but there was no sign of an attenuation of cognitive decline. Furthermore, in a Phase II trial, immunization with AN1792 resulted in the development of meningoencephalitis in 6% of the enrolled patients, causing the trial to be interrupted [183].

Immunization protocols are now being modified to improve efficacy and ensure safety in clinical trials. For example, to minimize negative side-effects, Aβ peptides are being shortened to create small epitopes specifically recognized by antibodies, but not T-cells [158]. Choosing alternative administration routes, such as intranasal administration, may also further increase safety of immunization [145]. In general, passive immunization protocols appear to be safer (i.e. associated with a low risk of encephalitis) than active immunization and can also be further modified to improve safety. For example, deglyco-

sylation of antibodies diminishes their interaction with microglial Fc-receptors and complement factors that can trigger a harmful neuroinflammatory response (i.e. microglial and complement activation) [235]. This modification neither affects binding affinity to Aβ nor does it reduce the ability to lower brain Aβ levels and improve cognition [278].

There are several proposed biological mechanisms Aβ antibodies may use to reduce brain Aβ levels (reviewed in [227, 268]) (Fig. 3). First, antibodies may trigger the uptake of Aβ by microglia (Fig. 3A) [16]. This process is likely mediated by Fc receptors on microglial membranes as specific antibodies against these receptors could inhibit Aβ uptake. However, experiments with deglycosylated antibodies [235], antibody fragments lacking the Fc-binding region [9] and Fc-receptor knockout mice [53] proved that there are also non-Fc-mediated mechanisms responsible for antibody-mediated clearance of Aβ. One of these alternative mechanisms is inhibition or disruption of Aβ aggregation by antibodies that directly associate with Aβ in the brain (Fig. 3B), a process that has been demonstrated in in vitro studies [228, 229]. For this latter mechanism, antibodies need to enter the brain.

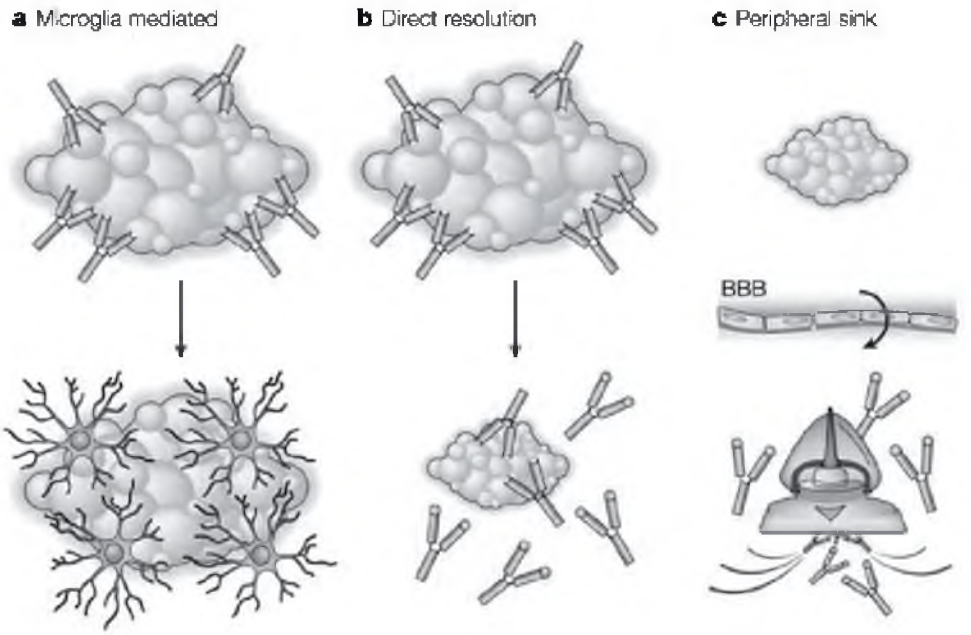

Figure 3: *Three biological mechanisms that are not mutually exclusive have been proposed. Small amounts of anti-amyloid antibodies reach amyloid deposits in the brain and trigger a phagocytic response by microglia (A). Anti-amyloid antibodies reach amyloid deposits in the brain and resolve them directly through interaction of the antibody with the amyloid deposit (B). Anti-amyloid antibodies act as a peripheral sink for soluble amyloid β species, leading ultimately to the resolution of brain deposits by mass action (B). BBB, blood–brain barrier. Reprinted with permission from Macmillan Publishers Ltd: [Nature Reviews Neuroscience] [46], copyright (2004).*

Indeed, peripherally administered antibodies have been found associated with brain Aβ in PDAPP mice, and therefore were apparently able to cross the BBB [16]. However, there are also antibodies that can reduce brain Aβ levels without entering the brain [61]. These antibodies may act as so-called peripheral sink agents (Fig. 3C).

Peripheral sink hypothesis

The peripheral sink hypothesis was first postulated by DeMattos et al. in 2001 [61], who found that passively immunizing PDAPP mice with the monoclonal antibody m266 significantly increased plasma Aβ levels, while decreasing brain Aβ load. They suggested that, by binding to plasma Aβ, antibodies caused a net efflux of Aβ from the brain. Indeed, m266 has been found in complex with Aβ in CSF and plasma of PDAPP mice [66]. Aβ/antibody complexes can be degraded in peripheral organs such as liver or kidneys [200], which disturbs the equilibrium that is known to exist between brain and peripheral Aβ pools [63]. To reestablish this equilibrium, soluble Aβ is transported from the brain to the plasma, explaining the decrease in brain Aβ levels. It should be mentioned that fibrillar Aβ remains in the brain, as it cannot cross the BBB.

After the first description of the peripheral sink hypothesis [61], a number of studies, both immune and non-immune, have been performed that support this hypothesis. For example, actively immunized PSAPP mice demonstrated an increase in serum Aβ levels, accompanied by a reduction in brain Aβ levels [146]. Furthermore, the previously mentioned deglycosylated antibodies also significantly increased plasma Aβ levels in triple transgenic (APP, PS1, tau) AD mice, without entering the brain [235]. Immunization of TgSwDI mice provided additional proof of the existence of a peripheral sink mechanism. TgSwDI mice produce Aβ that, due to the Dutch and Iowa mutations, has less affinity for the receptor that is involved in Aβ clearance from the brain (i.e. LRP-1) and Aβ is retained within the cerebral vascular wall [56, 60]. Indeed, it was demonstrated that immunizing TgSwDI mice with an antibody against Aβ neither reduced the deposition of Aβ in the brain nor dissolved established Aβ deposits [259]. Only when directly delivered to the brain, this antibody cleared already established deposits.

As previously mentioned, immune therapy can be accompanied by neuroinflammatory responses that are detrimental to AD patients [183]. Therefore, the use of non-immune substances as peripheral sink agents has also received attention. To act as peripheral sink agents, binding Aβ is key. Gelsolin and GM1, a secretory protein and ganglioside respectively, can both bind Aβ and it was found that both could reduce brain Aβ levels of PSAPP mice without entering the brain [163]. Furthermore, GM1, but not gelsolin, influenced plasma Aβ levels. As it has a high binding affinity to Aβ, part of the Nogo-66 receptor (NgR(310)ecto-Fc) has also been tested as a peripheral sink agent [184]. NgR(310)ecto-Fc administered to APPswe/PS1dE9 did not enter the brain, but lowered brain Aβ levels. Furthermore, it reduced the number of dystrophic neurites and gliosis and improved cognition of these mice. However, like gelsolin, it did not alter plasma Aβ levels, demonstrating that altered plasma Aβ levels may not always be a good measure of the presence of a peripheral sink mechanism. Another potential peripheral sink agent is part of the LRP-1 receptor (binding domain LRP-IV) that can reduce brain Aβ levels of APPswe mice while increasing plasma Aβ levels [200]. Furthermore, a peripheral sink action has also been suggested for several Congo red derivates [164] and for an analogue of heparan sulfate proteoglycans, the low-molecular weight heparin enoxaparin [20].

Aim of this study

As HSPG are such prominent components of human Aβ deposits, we aimed to further investigate the interaction between Aβ and HSPG. Using cerebrovascular cells and the APPswe/PS1dE9 mouse model for AD, we explored the capacity for Aβ to trigger HSPG expression and GAG chain modification in vitro **(Chapters 2 and 3)** and in vivo **(Chapter 4)**. Furthermore, we reviewed the literature on co-deposition of HSPG and several other co-depositing factors (e.g. complement factors and acute phase proteins) in different AD mouse models **(Chapter 5)**. Finally, we investigated if a HSPG analogue, enoxaparin **(Chapter 6)**, and the sHsp αB-crystallin **(Chapter 7)** could be potential therapeutic agents and possibly even act as peripheral sink agents.

Outline of this thesis

Chapter 2
Of all HSPG, agrin and glypican-1 are most commonly found in association with Aβ. However, it is still largely unknown what causes the association of heparan sulfate proteoglycans with Aβ deposits in human brains. Therefore, we examined the role of Aβ in the expression and production of these two HSPG in vitro. Furthermore, using human brain pericytes, we studied the cellular location of agrin and glypican-1 in the absence or presence of Aβ.

Chapter 3
Sulfated glycosaminoglycan chains of HSPG are not only found in association with parenchymal Aβ deposits, they can also be detected in CAA, suggesting a role for GAGs in vascular Aβ deposition. Their sulfate moieties in particular are said to be key in the interaction of GAGs with Aβ in plaques. We investigated if sulfate moieties have a similar role in GAG association with vascular Aβ. Furthermore, we studied the effect of several different GAGs (heparin, chondroitin sulfate, heparan sulfate) on aggregation of Aβ and Aβ-induced toxicity of cerebrovascular cells.

Chapter 4
The close association of HSPG with Aβ deposits in human AD patients is well-established and proven to influence Aβ deposition. We aimed to characterize the association of HSPG with Aβ deposits in the APPswe/PS1dE9 mouse model for AD in order to get a better understanding of the differences of mouse and human Aβ deposits and to investigate if there is a temporal relation between HSPG and Aβ deposition.

Chapter 5
In this chapter we reviewed the co-deposition of several factors with mouse Aβ deposits that are known to be associated with human Aβ deposits. These factors include: HSPG, apolipoproteins, complement factors, acute phase proteins, ICAM-1, cystatin C and CLAC.

Chapter 6
Enoxaparin is a low molecular weight heparin that is known to reduce brain Aβ levels when prophylactically administered to a mouse model for AD. We investigated what effect prophylactic and therapeutic injections of enoxaparin had on cognition and brain Aβ levels of APPswe/PS1dE9 mice.

Chapter 7
According to the peripheral sink hypothesis, Aβ can be removed from the body by degradation in peripheral organs after forming macromolecular complexes, e.g. by binding to anti-Aβ antibodies in the blood. To restore the balance of the Aβ pool in the blood and brain, Aβ is then transported out of the brain. Since αB-crystallin can bind Aβ with high affinity, we investigated if this sHsp can act as a peripheral sink agent in two mouse models for AD.

Chapter 8
In this chapter we summarize and discuss the results of this thesis and propose future research plans.

Chapter 2

Amyloid β induces cellular relocalization and production of agrin and glypican-1

Nienke M. Timmer[a,*], Jack van Horssen[b,*], Irene Otte-Holler[c], Micha M.M. Wilhelmus[d], Guido David[d], Joyce van Beers[c], Rob M.W de Waal[c], Marcel M. Verbeek[a]

[a]Department of Neurology, Laboratory of Pediatrics and Neurology, Donders Centre for Brain, Cognition and Behavior, Alzheimer Centre Nijmegen, Radboud University Nijmegen Medical Centre, Nijmegen, The Netherlands, [b]Department of Molecular Cell Biology and Immunology, VU University Medical Center, Amsterdam, The Netherlands, [c]Department of Pathology, Radboud University Nijmegen Medical Centre, Nijmegen, The Netherlands, [d]Department of Anatomy and Neurosciences, VU University Medical Centre, Amsterdam, The Netherlands, [e]The Center for Human Genetics, University of Leuven and Flanders Interuniversity Institute for Biotechnology, Leuven, Belgium

Brain Research **1260**, 38-46 (2009)

* Authors contributed equally

Abstract

The major component of senile plaques and vascular amyloid in Alzheimer's disease (AD) brains is the amyloid β protein (Aβ). Besides Aβ, several other proteins have been identified in these lesions, in particular heparan sulfate proteoglycans (HSPG). However, it is still unclear, what causes the excessive accumulation of HSPG in AD brains. Therefore, we investigated if Aβ may influence production and expression of two major Aβ-associated HSPG species, agrin and glypican-1. When human brain pericytes (HBP) were cultured in the presence of Aβ, protein and mRNA expression of both agrin and glypican-1 were increased and more radioactive sulfate was incorporated in the glycosaminoglycan fraction of Aβ-treated HBP. Furthermore, after Aβ treatment these HSPG were found in association with the amyloid fibrils attached to the cell membrane, in contrast to the intracellular agrin and glypican-1 staining observed in untreated cells. We conclude that Aβ can modulate the cellular expression of agrin and glypican-1, which may contribute to the accumulation of these HSPGs in AD lesions.

Introduction

The major pathological lesions in Alzheimer's disease (AD) brains comprise neurofibrillary tangles (NFT), senile plaques (SP) and cerebral amyloid angiopathy (CAA). NFTs are composed of fibrillar hyperphosphorylated tau protein [159]. The major component of SPs and CAA-affected vessels is the amyloid β protein (Aβ), a proteolytic cleavage product of the amyloid precursor protein (APP) [208]. Next to the presence of these abnormal protein aggregates, several other proteins accumulate in AD lesions, including inflammatory proteins [72, 73, 267], apolipoprotein E [173, 287], small heat shock proteins [280, 284] and heparan sulfate proteoglycans (HSPG) [225, 254-257].

HSPG are complex macromolecules involved in a variety of biological processes, such as proliferation, differentiation and cell adhesion [189]. They are composed of long sulfated polysaccharide side-chains covalently attached to a specific serine residue of the core protein. These glycosaminoglycan (GAG) side-chains may undergo a series of enzymatic modifications leading to variable sequences with highly sulfated regions alternated by relatively unmodified regions [22, 91, 256]. In the sulfated regions of HSPG, the disaccharide units consist of N-acetylglucosamine in combination with iduronic acid, while in the unmodified regions N-acetylglucosamine is combined with glucuronic acid. HSPG can be divided into two major groups: the extracellular matrix-associated HSPG, including perlecan, agrin and collagen XVIII [88, 108], and cell surface HSPG of the syndecan and glypican families [22].

We previously demonstrated a differential expression pattern of several HSPG subtypes in AD lesions [254, 255, 257]. Unlike the syndecans, perlecans and collagen XVIII, the HSPG agrin and glypican-1 are the only two HSPG that are expressed in all types of AD lesions. Agrin and glypican-1 expression was detected in the majority of SP present in AD patients [254]. In CAA of AD patients a variable, sometimes weak agrin expression was detected [255]. A much stronger association of agrin with Aβ in CAA was found in patients suffering from hereditary cerebral haemorrhage with amyloidosis of the Dutch type (HCHWA-D), a rare autosomal dominant disease characterized by vascular depositions of Aβ [251]. Of all HSPG, glypican-1 was most predominant, accumulating in CAA-affected vessels of both AD and HCHWA-D patients [255]. Interestingly, glypican-1 could not be detected in normal vessels, suggesting a particular role for this HSPG in CAA pathogenesis.

In AD lesions, HSPG expression not only occurs at the same location, but also virtually at the same time as Aβ deposition [222], which suggests a close association between HSPG and Aβ. It has indeed been reported that HSPG can bind to Aβ with high affinity [41, 52] through a connection between the GAG side-chains and the Aβ protein, although the core protein is also involved [219]. The effect of HSPG on Aβ accumulation may in fact be caused by their tight association. Indeed, HSPG can induce aggregation of Aβ, stabilize Aβ plaques [41, 52] and inhibit Aβ degradation [52, 87]. There is also evidence that the heparan sulfate (HS) GAG side-chains can prevent β-secretase cleavage of Aβ from its precursor protein [17, 204]. Since it is well known that Aβ, agrin and glypican-1 are tightly associated in AD brains, we investigated in vitro if Aβ directly affects cellular expression of these HSPG and the degree of sulfation of GAG side-chains in general. We used human brain pericytes (HBP) as an in vitro model system, since these cerebrovascular cells are tightly associated with one of the Aβ-containing lesions in AD brains, namely CAA [262].

Materials and methods

Antibodies

We used primary monoclonal antibodies directed against the core protein of agrin (JM72) [249] and glypican-1 (S1) [57]. For immunocytochemistry we used FITC-labeled sheep anti-mouse as secondary antibody (Vector, Burlingame, CA) and for Western blot analysis we used peroxidase-labeled rabbit anti-mouse (Vector, Burlingame, CA).

Aβ peptides

We used Aβ containing the Dutch mutation (Glu22-->Gln22) as found in HCHWA-D ($DA\beta_{1-40}$), since this protein is biology active towards cerebrovascular cells [54]. $DA\beta_{1-40}$ was purchased either from Biosource (89% pure, Etten-Leur, The Netherlands) or from Quality Controlled Biochemicals (QCB; Hopkinton, Massachusetts, USA, 96% pure). $A\beta_{40-1}$ was purchased from QCB (Hopkinton, Massachusetts, USA). In previous experiments it was demonstrated that $A\beta_{40-1}$, unlike the $DA\beta_{1-40}$ peptide, has no biological activity towards HBPs in viability assays [283].

We used two different ways of preparing stock solutions of the DAβ1-40 peptides: in sterile water (250 μM) [280] or by dissolving the peptide in hexafluoroisopropanol (HFIP), removing the solvent by evaporation and subsequently dissolving it in DMSO (5 mM). The former procedure yields an $DA\beta_{1-40}$ preparation that is in a monomeric state for more than 90%; the latter procedure is commonly used by researchers to yield a robust solution of monomeric Aβ. $A\beta_{40-1}$ was dissolved in HFIP and DMSO (5 mM). Aliquots were stored at –80°C prior to use. Neither the source of the peptide nor the procedure used to dissolve the peptide affected the results in the experiments.

Cell cultures

HBP were isolated and characterized as described previously [265]. For the different experiments HBP were maintained in fibronectin-coated flasks containing Eagle's modified essential medium (EMEM; Bio-Whittaker, Verviers, Belgium) with L-glutamine containing 10% human serum, 20% newborn calf serum, 1 ng/ml basic fibroblast growth factor and 2% penicillin/streptomycin. Prior to experiments, HBP were incubated in EMEM containing 0.1% bovine serum albumin (EMEM-BSA) and antibiotics for at least 4 hours. Next, cells were incubated in fresh EMEM-BSA, either supplemented or not with 8-25 μM synthetic $DA\beta_{1-40}$ peptide for 1-3 days depending on the specific assay.

Immunofluorescence staining of DAβ1-40-treated HBP

To study the effects of $DA\beta_{1-40}$ on the expression of agrin and glypican-1 at the immunocytochemical level, HBP were cultured in sterile gelatin-coated 8-well chamber slides, and incubated either with or without 25 μM $DA\beta_{1-40}$ for three days. After fixation with periodate-lysine-paraformaldehyde (PLP) for 10 minutes, cells were incubated overnight at 4°C with primary antibodies. Finally, cells were incubated with the secondary antibody for 1 hour and mounted in Vectashield (Vector, Burlingame, CA, USA). Between incubation steps, cells were thoroughly washed with PBS. All antibodies were diluted in PBS containing 0.1% BSA, which also served as a negative control. Nuclei were stained with Topro3 (Molecular probes, Eugene, Ore., USA, dilution 1:1000). Immunofluorescence staining was examined using a confocal laser-scanning microscope (Leica, Wetzlar, Germany).

Immuno-electron microscopical (IEM) analysis
HBP were cultured on fibronectin-coated foil bottom dishes (WillCo Wells BV, Amsterdam, The Netherlands) and subsequently incubated for three days with fresh EMEM-BSA with or without 12.5 µM DA$\beta_{1\text{-}40}$. After washing twice with PBS, HBP were fixed in PLP for 2 hours, followed by washing with PBS and blocking with 20% goat serum in PBS with 0.1% BSA for 1 hour. Cell preparations were pre-treated with 0.05% Triton-X in PBS for 30 minutes to increase permeability of the cells. Incubation with primary antibodies was performed overnight at 4°C. After washing four times with PBS, samples were incubated with ultra-small gold conjugated goat anti-mouse antibodies (Aurion, Wageningen, The Netherlands) overnight at 4°C. Again, samples were washed with PBS and fixed for 10 minutes in 2% glutaraldehyde, washed with PBS, followed by 10 minutes post-fixation with 2% osmium tetroxide. After intense washing with PBS and ultrapure water the preparations were silver-enhanced with the Aurion R-Gent SE-EM kit and the reaction was stopped after 20 minutes in ultra pure water. Then, cells were washed in 30% ethanol, en-bloc stained with 2% uranyl acetate in 30% ethanol for 30 minutes at 4°C and washed again in 30% ethanol. Subsequently, samples were dehydrated with increasing concentrations of ethanol followed by mixtures of epon (Agar Scientific, Stansted, England) with 100% ethanol and finally pure epon resin. The foil was cut with a razor blade and embedded in pure epon resin. Ultrathin sections were cut on a Leica Ultracut (Leica, Wetzlar, Germany) and stained with uranyl acetate and lead citrate. Photographs were taken on a Jeol 1200 EX/II electron microscope at 60 kV (Jeol, Tokyo, Japan).

Western blot analysis
HBP were cultured with or without 8-25 µM DA$\beta_{1\text{-}40}$ in EMEM-BSA for 3 to 6 days. Cell culture medium was removed for Western blot analysis and cells were thoroughly rinsed three times with 0.9 % NaCl. Subsequently, cells were treated with 8 M urea (Sigma-Aldrich Chemie, Zwijndrecht, the Netherlands) to lyse the cells. Cell culture medium and cell lysates were diluted 1:1 with reducing sample buffer (2.3 % sodiumdodecylsulfate (SDS), 12.5 % Tris-HCL (0.5 M, pH 6.8), 77 % glycerol, 3% dithiothreitol (DTT) and bromophenol blue in milliQ). This mixture was heated for 5 minutes at 100 °C and equal amounts of protein were subsequently separated by SDS-polyacrylamide gel electrophoresis (SDS-PAGE). Proteins were electrophoretically transferred onto nitrocellulose membranes (Hybond; Amersham Corp, Arlington Heights, IL, USA) in blotting buffer (25 mM Tris pH 8.6, 192 mM glycine and 20% methanol). Blots were incubated for 15 minutes in blocking solution (PBS/0.05% Tween-20 (PBS-T) containing 5% low fat milk powder), rinsed three times in PBS-T and subsequently incubated overnight at 4°C with specific primary antibodies in PBS-T with 0.5% low fat milk powder. The blots were then rinsed three times in PBS-T and incubated with the appropriate secondary antibody in PBS-T with 0.5% low fat milk powder for 1 hour at room temperature. Blots were washed three times in PBS-T and finally rinsed in PBS. Detection was performed by chemiluminescence according to the manufacturer's protocol (Roche, Basel, Switzerland) and exposed to Kodak X-OMAT-R films. Each experiment was repeated three times.

Total RNA isolation
HBP were cultured in 6 well plates and subsequently incubated for 1-3 days with or without 8-10 µM DA$\beta_{1\text{-}40}$ or A$\beta_{40\text{-}1}$ in EMEM-BSA medium. Total RNA was isolated following with Trizol reagent (1 ml per well; Invitrogen, Carlsbad, CA, USA) following the manufactu-

rer's instructions. The total RNA pellet was washed with 75% ethanol and finally dissolved in RNA-free water. A Nanodrop® ND-1000 UV-Vis spectrophotometer (Nanodrop Technologies, Wilmington, DE, USA) was used to determine amount and purity of total RNA isolated and a small sample was separated on a 1% agarose gel to check for the presence of the characteristic 18S and 28S bands.

cDNA synthesis

To quantify mRNA expression of agrin and glypican-1, cDNA was synthesized from isolated total RNA. Total RNA (0.5-1.0 µg) was incubated with random primers in a mixture of 5mM dNTPs, RNAsin, 5x first strand buffer, 0.1 M DTT and M-MLV transcriptase (Invitrogen). The samples were incubated for 10 min at room temperature and for one hour at 37°C, followed by a 3 minute M-MLV inactivation at 70°C. A solution containing all components of the mix except M-MLV served as a negative control. A PCR of the housekeeping gene β-2 microglobulin (B2M) was performed to exclude contamination of the samples with genomic DNA. Amount and purity of cDNA was determined on the Nanodrop® ND-1000 UV-Vis spectrophotometer (Nanodrop Technologies).

Quantitative PCR

For real-time RT-PCR, 2x Taqman Universal PCR Master Mix (Applied Biosystems, Foster City, CA, USA) was used. A 20x Taqman gene expression assay mix of agrin, glypican-1 or lipoprotein-related protein 1 (LRP-1), an Aβ receptor, was added to a mixture of Taqman universal mastermix, RNAse-free water and 50 ng of cDNA. We used LRP-1 expression as a positive control as we have previously demonstrated that LRP-1 protein expression is upregulated by Aβ treatment [283]. Forward (5'-GGCAATGCGGCTGCAA-3') and reverse (5'-GGGTACCCACGCGAATCAC-3') primers for the housekeeping gene porphobilinogen deaminase (PBGD) and a probe (5'-CTCATCTTTGGGCTGTTTTCTTCCGCC-3') labeled with AllGloTM were from Biolegio (Nijmegen, The Netherlands). The PCR was performed using the ABI PRISM 7700 sequence detection system. A standard curve of mRNA expression was created with mRNA isolated from a 75-cm2 flask of untreated HBP.

Three separate RT-PCR experiments were performed. In each experiment, cDNA samples were analyzed in duplicate and the standard curve method was used to calculate the mRNA expression of agrin, glypican-1 and LRP-1 of $DA\beta_{1-40}$ or $A\beta_{40-1}$ -treated cells. Expression was normalized to PBGD and an unpaired two-sided t-test was used to compare expression levels of treated and untreated HBP. Data of one representative experiment are presented as mean expression ± standard error relative to untreated cells.

Assessment of ^{35}S-sulfate incorporation

HBP were cultured for 24 h in EMEM-BSA, in the presence or absence of 12.5 µM DAβ1-40. Transforming growth factor-β1 (TGF-β1) increased the production of various extracellular matrix proteins, including HSPG [131], and was therefore used as positive control (2 ng/ml). Subsequently, ^{35}S-labeled sulfate (25 µCi/ml) (PerkinElmer, Boston, MA, USA) was added to the medium for 24 hours. Then, cells were washed in EMEM three times and digested for 2 h at 65°C in a papain solution containing a chondroitin sulfate as carrier. Cells were centrifuged for 10 minutes at 1,000x g to remove cell debris and 0.2% cetylpyridinium chloride solution was added to the supernatant in equal amounts and incubated for 2 h at 37°C to precipitate the GAGs. After incubation, the mixture was centrifuged for 10 minutes at 10,000x g to collect the precipitate. Finally, the precipitated residue was rinsed

twice and dissolved in Lumasolve (Omnilabo, Breda, The Netherlands). Subsequently, the dissolved precipitated residue was diluted in Optifluor (Packard BioScience, Groningen, The Netherlands) and ^{35}S-sulfate incorporation was measured by liquid scintillation counting (PerkinElmer 1450 Microbeta, Boston, MA, USA) and expressed as counts per minute (cpm). One-sided unpaired t-tests were performed to compare the effects of TGF-β1 or $DA\beta_{1-40}$ on ^{35}S-sulfate incorporation. Each experiment was repeated three times. All values are expressed as mean ± standard deviation.

Results

Aβ-induced agrin and glypican-1 immunoreactivity

To determine the effects of Aβ on expression of agrin and glypican-1, $DA\beta_{1-40}$-treated HBP were immunocytochemically stained. The JM72 antibody, directed against the core protein of agrin, demonstrated increased immunoreactivity after incubation with $DA\beta_{1-40}$ (Fig. 1B) when compared to untreated cells (Fig. 1A). The glypican-1 antibody S1, directed against the glypican core protein, showed a similar increase of immunoreactivity after $DA\beta_{1-40}$ treatment (Fig. 1C and D).

Furthermore, immunocytochemical analyses showed that agrin was confined to a perinuclear localization in cultured HBP (Fig. 1A), whereas glypican-1 was distributed throughout the cytoplasm (Fig. 1C). $DA\beta_{1-40}$ treatment caused a cellular redistribution of agrin towards the cell membrane (Fig. 1B).

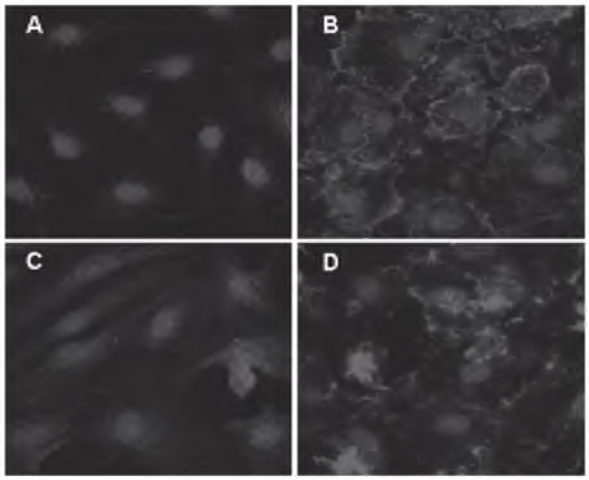

Figure 1: *Immunofluorescence staining of untreated (A, C) and $DA\beta_{1-40}$–treated (B, D) HBP for agrin (A, B) and glypican-1 (C, D). Protein expression of both agrin and glypican-1 was increased after treatment. Original magnification 630x.*

Subcellular localization of agrin and glypican-1

To further investigate the cellular localization of agrin and glypican-1, ultrastructural analysis of agrin and glypican-1 localization by IEM analysis was performed (Fig. 2). Untreated cells demonstrated agrin immunoreactivity in phagosome-like structures (Fig. 2A). Upon $DA\beta_{1-40}$ treatment, agrin was predominantly found in close association with $DA\beta_{1-40}$ fibrils attached to the cell surface (Fig. 2B and E) but also in DAβ1-40-containing phagosomes (Fig. 2B and F). Glypican-1 immunoreactivity in untreated cells was mainly observed at the cell surface and sporadically in the cytoplasm (Fig. 2C). After $DA\beta_{1-40}$ treatment glypican-1, like agrin, co-localized with amyloid fibrils attached to the cell surface (Fig. 2D). Additionally, glypican-1 immunoreactivity was also detected throughout the cytoplasm of $DA\beta_{1-40}$-treated HBP.

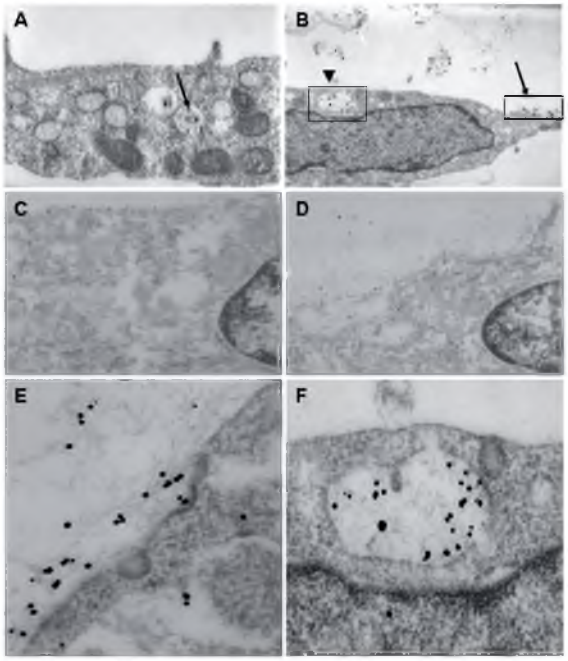

Figure 2: *Immuno-electron microscopical analysis of untreated (A, C) and DAβ$_{1-40}$-treated (B, D, E, F) HBP for localization of agrin (A, B, E, F) and glypican-1 (C, D). In control HBP, agrin is mainly found in phagosomal bodies (A; arrow). After DAβ$_{1-40}$ treatment, agrin co-localized with DAβ$_{1-40}$ fibrils on the cell surface (B; arrow; shown at higher magnification in E) and in phagosomal bodies (B; arrowhead; shown at higher magnification in F). In untreated cells, glypican-1 is closely associated with the cell surface (C) and, after DAβ$_{1-40}$ treatment, associated with Aβ fibrils on the cell surface as well as distributed throughout the cytoplasm (D). Original magnification A, B, C, D 12.000x and E, F 25.000x.*

Aβ-induced protein expression of agrin and glypican-1

To determine protein expression and secretion of agrin and glypican-1 in DAβ$_{1-40}$-treated HBP, cell-lysates and cell culture medium were analysed for the presence of these HSPG by Western blot analysis. Both untreated and DAβ$_{1-40}$-treated HBP cell lysates demonstrated the typical bands of the agrin (Fig. 3A; 212 kDa) and glypican-1 (Fig. 3B; 64 kDa) unglycosylated core protein. The expression of these core proteins increased after DAβ$_{1-40}$-treatment (Fig. 3A and B, lane 2). In addition to the core protein, we observed a high molecular weight smear (>>200 kDa) immunoreactive with anti-agrin antibodies (Fig. 3A, lane 2) after treatment with DAβ$_{1-40}$. A similar smear was observed for glypican-1 (Fig. 3B, lane 2) in the absence of DAβ$_{1-40}$, which became more intense after DAβ$_{1-40}$-treatment.

Agrin and glypican-1 could not be detected in cell culture medium of treated and untreated cells by Western blot analysis (data not shown).

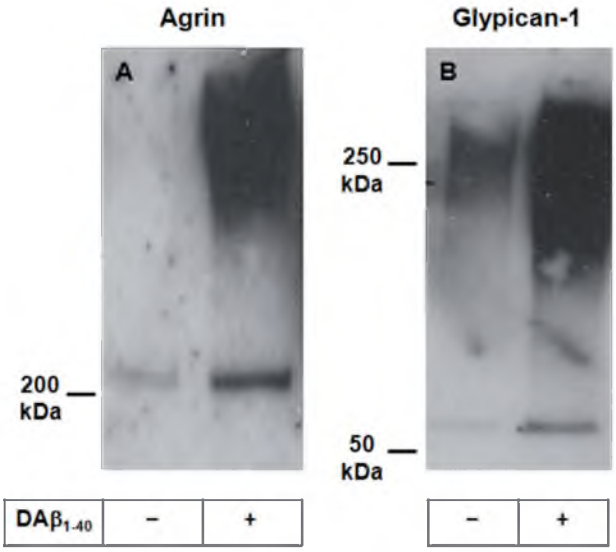

Figure 3: *Western blot analysis of agrin (A) and glypican-1 (B) extracted from control HBP (lane 1) and DA$\beta_{1\text{-}40}$-treated HBP (lane 2) showed increased expression of core protein and an increased high molecular weight smear after DA$\beta_{1\text{-}40}$ treatment.*

Aβ-induced mRNA expression of agrin and glypican-1

To test whether the increases in agrin and glypican-1 immunoreactivity represent changes in production of these HSPG, we analyzed normalized mRNA expression of agrin, glypican-1 and the positive control LRP-1 after 1-3 days of DA$\beta_{1\text{-}40}$ treatment relative to expression in untreated HBP by quantitative PCR (Fig. 4).

After one day of treatment with DA$\beta_{1\text{-}40}$, relative LRP-1 expression was significantly ($p<0.05$) increased (1.58 ± 0.03) compared to untreated cells (Fig. 4A). A lower, near significant ($p<0.10$), increase in expression was detected on day 2 (1.42 ± 0.13) with an unsignificant increase on day 3 (1.21 ± 0.10). Agrin expression on day 1 demonstrated a near significant ($p<0.10$) increase (1.66 ± 0.24; Fig. 4B) with an unsignificant increase on day 2 (1.53 ± 0.17) and day 3 (1.15 ± 0.20). DAβ1-40-induced expression of glypican-1 was increased on day 1 (1.45 ± 0.20; Fig. 4C) and even significantly ($p<0.05$) increased on day 2 (1.47 ± 0.04). On day 3, expression of glypican-1 was unsignificantly increased (1.18 ± 0.19).

The differences in agrin or glypican-1 expression between Aβ-treated and untreated HBP were consistent in three separate experiments, but did not always reach statistical significance. A$\beta_{40\text{-}1}$, an Aβ peptide with an inverse sequence, was used as a negative control and did not influence mRNA expression of LRP-1, agrin and glypican-1 (data not shown), indicating that the increases in mRNA expression of both LRP-1 and the HSPGs are specific for DA$\beta_{1\text{-}40}$.

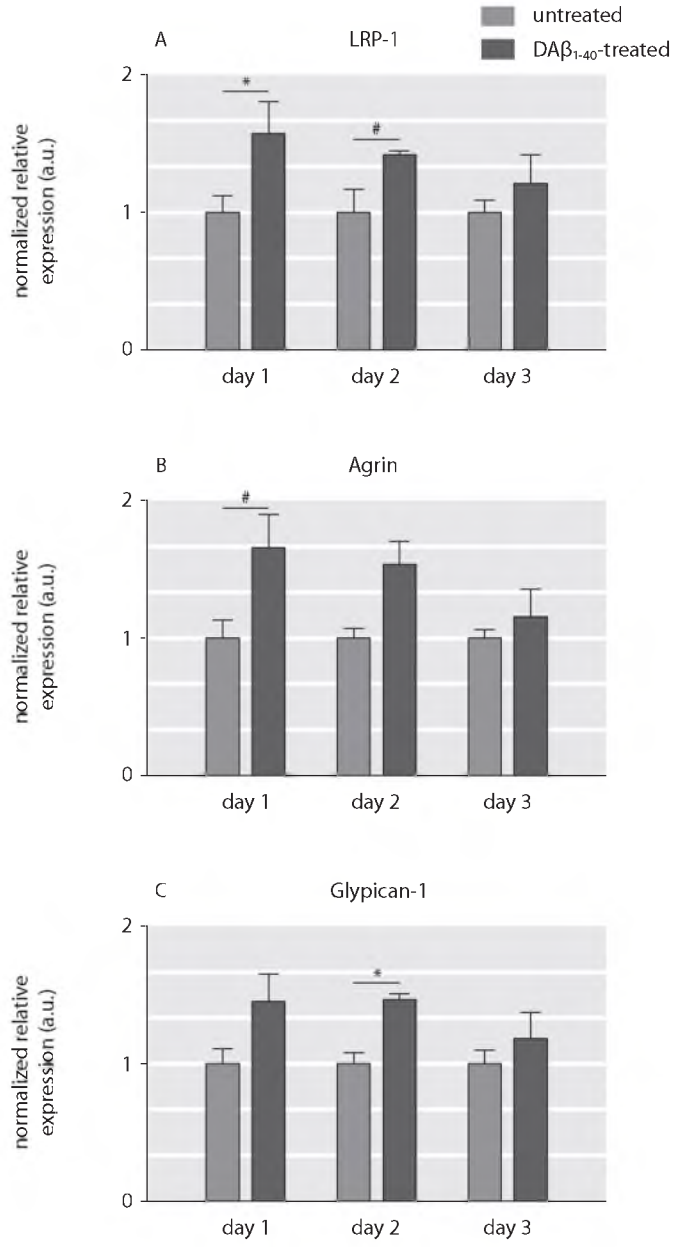

Figure 4: *Normalized relative mRNA expression of LRP-1 (A), agrin (B) and glypican-1 (C) in untreated (white bars) and 1-3 days DAβ$_{1-40}$ treated HBP (grey bars). Expression of all three genes was increased after treatment with DAβ$_{1-40}$ compared to expression in untreated cells. Expression was highest on the first day of treatment. # p<0.10, * p<0.05*

Aβ-induced ^{35}S-sulfate incorporation

The size and composition of GAG chains influence the biological function of HSPG [91]. Sulfation of the disaccharide units for example appears to be very selective and depends on the specific function of the HSPG. To investigate the influence of Aβ on sulfation of the GAG chains, incorporation of radioactively labeled sulfate by HBP was assessed.

The incorporation of ^{35}S-sulfate was significantly enhanced in TGF-β1-treated HBP, compared to untreated control HBP ($p < 0.01$; Fig. 5). Addition of $DA\beta_{1-40}$ resulted in a significant 3-fold increase in ^{35}S-sulfate incorporation compared to untreated HBP ($p < 0.01$).

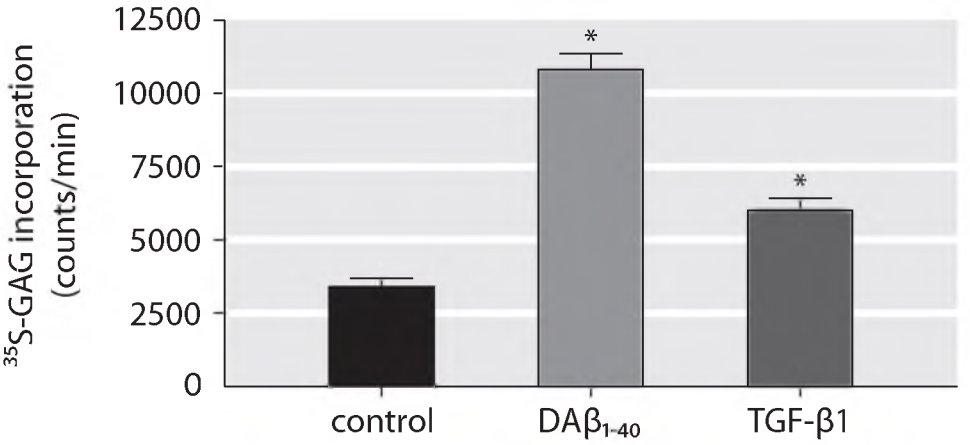

Figure 5: *Effect of $DA\beta_{1-40}$ on ^{35}S-sulfate incorporation in human brain pericytes. TGF-β1 treatment markedly enhanced ^{35}S-sulfate incorporation (*: $p < 0.01$) compared to untreated control HBP. Incubation with $DA\beta_{1-40}$ resulted in a significant 3-fold increase in ^{35}S-sulfate incorporation (*: $p < 0.01$) compared to untreated HBP.*

Discussion

HSPG expression is observed in various pathological lesions in AD brain tissue and the timing of HSPG deposition parallels that of Aβ. This suggests a direct relation between Aβ and HSPG, implying that HSPG may play a role in Aβ aggregation and accumulation. Binding of HSPG to Aβ does indeed stimulate aggregation of Aβ and may affect cleavage of Aβ from its precursor protein [17, 204]. In this study, we demonstrated that Aβ increases the production of agrin and glypican-1.

Treatment of cultured HBP with $DA\beta_{1-40}$ resulted in increased immunoreactivity of both agrin and glypican-1 (Fig. 1). Furthermore, the immunocytochemical analyses revealed that after treatment of HBP with $DA\beta_{1-40}$, agrin could be found in association with amyloid fibrils attached to the cell surface, whereas in untreated cells agrin was found in the cytosol (phagosomes). This result was confirmed by our IEM analyses (Fig. 2). Binding of agrin to amyloid fibrils is in line with earlier findings of agrin associated with Aβ in vitro and with the presence of agrin in the different Aβ-containing lesions of Alzheimer's disease [52, 69, 254, 255]. After $DA\beta_{1-40}$ treatment, some agrin was still present in phagosomal bodies. In these bodies, agrin could be found together with Aβ, suggesting that both Aβ and agrin were targeted for degradation, either as individual proteins or in a complex. We did not observe glypican-1 in phagosomal bodies.

Glypican-1 is a cell surface HSPG and could, accordingly, be observed at the cell membrane of untreated HBP. After incubation with $DA\beta_{1-40}$ glypican-1, like agrin, was detected in association with Aβ fibrils attached to the cell surface as well as in the cytoplasm. Our immunocytochemical and IEM studies suggest that the cell surface-associated Aβ fibrils function as a HSPG retention reservoir. This may also be the molecular basis for accumulation of HSPGs in the Aβ-containing lesions of AD brains.

An increased immunoreactivity may reflect enhanced agrin and glypican-1 production after Aβ treatment. We therefore investigated Aβ-induced expression of these HSPG and found that both protein and mRNA expression of agrin and glypican-1 were increased after Aβ treatment. Our Western blot analysis demonstrated an Aβ-induced increase in core protein levels of glypican-1 and agrin (Fig. 3). Furthermore, a (more pronounced) high molecular weight smear characteristic of glycosylated proteoglycans appeared after Aβ treatment in both HSPG. The presence of this smear suggests that the degree of glycosylation of glypican-1 and agrin was altered when HBP were treated with $DA\beta_{1-40}$, perhaps because Aβ triggers the newly synthesized pool of agrin or glypican-1 to become more heavily glycosylated. Since it is known that nitrocellulose membranes have a relatively low affinity for highly glycosylated proteoglycans, it is possible that we underestimated the amount of heavily glycosylated HSPG present in treated and untreated HBP. Finally, the absence of both agrin and glypican-1 in cell culture medium may suggest that these HSPGs do not reach the cell culture medium or that the concentration of these HSPG in the medium was too low to be detected in our Western blot.

Together with the increased protein levels we found that mRNA levels of agrin and glypican-1 were increased after treatment with $DA\beta_{1-40}$, but not with the inactivated $A\beta_{40-1}$. Although it was already known that Aβ can upregulate gene expression in HBP [195], to the best of our knowledge this is the first report of Aβ-induced gene expression of a protein involved in Aβ aggregation.

Close examination of the mRNA expression during three days of culturing in the presence of $DA\beta_{1-40}$ revealed that the highest expression levels were found during the first two days. On the third day, expression levels had returned to control levels, which may

reflect a negative feedback mechanism. It is unlikely that the decreased expression on the third day is a result of increased cell death, that is observed after several days of culturing with $DA\beta_{1-40}$ [282], since expression levels of agrin and glypican-1 were normalized against a housekeeping gene that should be similarly affected by this degeneration.

Another way to examine Aβ-induced biosynthesis of (HS)PG is by measuring sulfate incorporation into GAG side-chains. We demonstrated that $DA\beta_{1-40}$ increased ^{35}S-sulfate incorporation into GAG chains of HBP (Fig. 4), suggesting that Aβ is able to influence GAG composition, e.g. by activating or inducing expression of enzymes involved in the synthesis of (HS) GAG chains, such as sulfotransferases and epimerases [256]. This may then contribute to the production of the highly glycosylated and sulfated forms of PG found in AD brains, but this remains to be investigated. However, it cannot be excluded that GAG chains other than HS chains, such as chondroitin sulfate (CS) chains, incorporated radioactive sulfate as well. Indeed, others [190] have demonstrated that radioactive sulfate incorporation into CS chains in the presence of TGF-β, our positive control, was increased more than 6-fold. Future sulfate incorporation experiments under CS degrading conditions may resolve the specific sulfate incorporation into HS chains. Furthermore, since Aβ fibrils may act as a HSPG reservoir, Aβ-treated cells may retain larger amounts of GAGs that have incorporated ^{35}S-sulfate, relative to untreated HBP. Finally, it is known that Aβ can interfere with HSPG metabolism by inhibiting the degradation of HSPG by heparanases [13], which may contribute to both the relatively high sulfate incorporation and the relatively high HSPG expression in Aβ-treated cells.

In any case, our data suggest that $DA\beta_{1-40}$ not only increases HSPG expression but also influences GAG composition. Since it is known that the sulfate moieties of proteoglycan GAG chains stimulate Aβ fibril formation [40], Aβ may indirectly stimulate its own aggregation, by induction of sulfate incorporation into HSPG.

In summary, we have demonstrated that Aβ treatment of HBP induces an increased cellular production of both agrin and glypican-1, which are likely also modified by increased sulfate incorporation. Furthermore, after Aβ treatment, agrin and glypican-1 bind the Aβ fibrils that attach to the cell surface. Interestingly, agrin and glypican-1 are not only the most predominant HSPG species accumulating in senile plaques [263], CAA and NFTs in AD brains, they are also the only two HSPG that have been demonstrated to interact directly with Aβ [52, 271]. Since HSPG, and particularly the sulfate moieties of the GAG side-chains, stimulate Aβ aggregation, our findings suggest that Aβ-regulated HSPG production may contribute to AD pathogenesis in general and HSPG accumulation in particular.

Acknowledgements

This work was supported by grants from the Internationale Stichting Alzheimer Onderzoek (no. 03517 and 07510), the Hersenstichting Nederland (no. 14F06.18) and Zon-MW Innovational Research (Vidi program, no. 917.46.331). We thank dr. L. Joosten (Dept. of Rheumatology, Radboud University Nijmegen Medical Centre) and dr. L v.d. Locht (Dept. of Haematology, Radboud University Nijmegen Medical Centre) for their technical assistence.

Chapter 3

Aggregation and cytotoxic properties towards cultured cerebrovascular cells of Dutch-mutated Aβ40 ($DA\beta_{1-40}$) are modulated by sulfate moieties of heparin

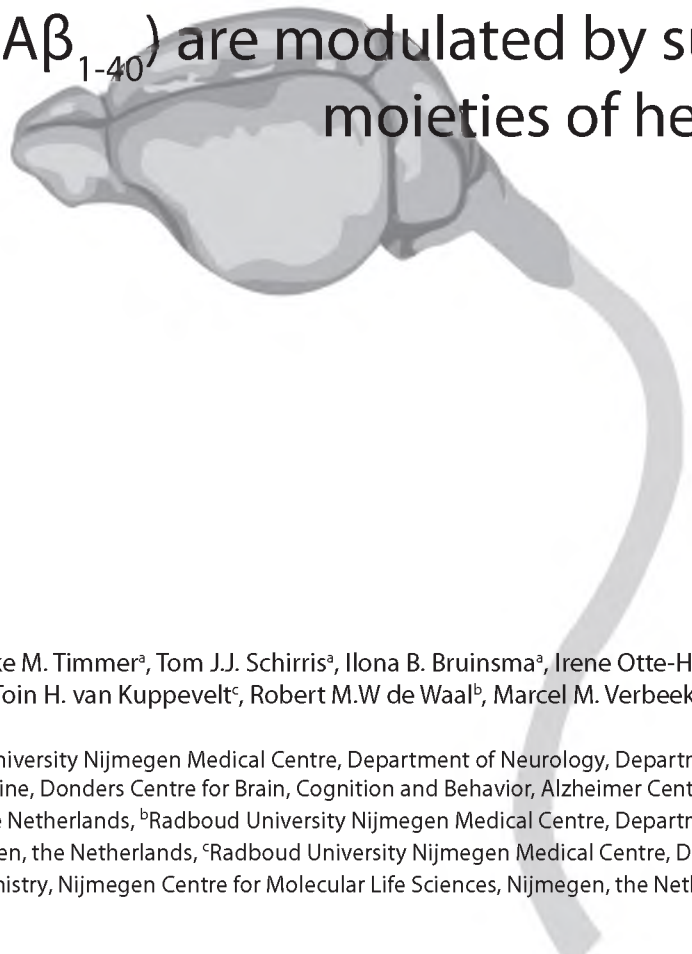

Nienke M. Timmer[a], Tom J.J. Schirris[a], Ilona B. Bruinsma[a], Irene Otte-Höller[b], Toin H. van Kuppevelt[c], Robert M.W de Waal[b], Marcel M. Verbeek[a]

[a]Radboud University Nijmegen Medical Centre, Department of Neurology, Department of Laboratory Medicine, Donders Centre for Brain, Cognition and Behavior, Alzheimer Centre Nijmegen, Nijmegen, the Netherlands, [b]Radboud University Nijmegen Medical Centre, Department of Pathology, Nijmegen, the Netherlands, [c]Radboud University Nijmegen Medical Centre, Department of Biochemistry, Nijmegen Centre for Molecular Life Sciences, Nijmegen, the Netherlands

Neuroscience Research **66**(4), 380-389 (2010)

Abstract

Glycosaminoglycans (GAGs), in particular as part of heparan sulfate proteoglycans, are associated with cerebral amyloid angiopathy (CAA). Similarly, GAGs are also associated with the severe CAA found in patients suffering from hereditary cerebral hemorrhage with amyloidosis of the Dutch type (HCHWA-D), where the amyloid β (Aβ) peptide contains the Dutch mutation ($DA\beta_{1-40}$). This suggests a role for GAGs in vascular Aβ aggregation. It was the aim of this study to investigate the effect of different GAGs (heparin, chondroitin sulfate, heparan sulfate), the macromolecule dextran sulfate and, using desulfated heparins, the role of GAG sulfate moieties on the in vitro aggregation of CAA-associated $DA\beta_{1-40}$ and on $DA\beta_{1-40}$-induced toxicity of cultured cerebrovascular cells. We also aimed to study the in vivo distribution of various sulfated heparan sulfate GAG epitopes in CAA. Of all GAGs tested, heparin was the strongest inducer of aggregation of $DA\beta_{1-40}$ in the different aggregation assays, with both heparin and heparan sulfate reducing Aβ-induced cellular toxicity. Furthermore, (partial) removal of the sulfate moieties of heparin partially abolished the effects of heparin on aggregation and cellular toxicity, suggesting an essential role for the sulfate moieties in heparin. Finally, we demonstrated the in vivo association of sulfated heparan sulfate (HS) GAGs with CAA. We conclude that sulfate moieties within GAGs, like heparin and HS, have an important role in Aβ aggregation in CAA and in Aβ-mediated toxicity of cerebrovascular cells.

Introduction

Accumulation of the amyloid β (Aβ) protein into senile plaques and cerebral amyloid angiopathy (CAA) is one of the major pathological characteristics of Alzheimer's disease (AD). Aβ is a 4 kDa protein that is cleaved from the amyloid precursor protein (APP) by γ- and β-secretases [81, 208]. After its cleavage, Aβ can adopt a β-sheet conformation and accumulate as insoluble deposits.

CAA is mostly found in cortical areas [241], with the occipital lobe being most severely affected. The hippocampus on the other hand, a brain area that is early and extensively affected by senile plaque formation, is not substantially affected by CAA [193]. When Aβ is deposited within the vessel walls, degradation of cerebrovascular cells such as smooth muscle cells and human brain pericytes (HBP) is observed with subsequent loss of vessel integrity [262]. Severe and widespread CAA is found in patients suffering from hereditary cerebral hemorrhage with amyloidosis of the Dutch type (HCHWA-D) [251]. HCHWA-D is caused by a Glu-->Gln at amino acid 22 of the Aβ protein leading to extensive CAA accompanied by severe secondary pathology (i.e. hemorrhagic stroke).

We have previously demonstrated that several proteins, such as the small heat shock protein HspB2 [284], and the heparan sulfate proteoglycans (HSPG) glypican-1 and agrin [255] co-deposit with vascular amyloid deposits in AD and HCHWA-D. HSPG are part of a family of proteoglycans that consist of sulfated glycosaminoglycan (GAG) chains attached to a core protein [91]. It is known that HSPG via their GAG chains, and to a lesser extent via their core protein, bind to Aβ with high affinity [219]. In this way they may influence the formation and stabilization of Aβ plaques [41, 52]. Other members of the GAG family are dermatan sulfate, keratan sulfate and chondroitin sulfate (CS) [256]. Although less abundant than HSPG, these proteoglycans can also be found in the vicinity of some Aβ deposits [65, 221, 223].

The GAG chains of proteoglycans are composed of different disaccharide units, each comprising either N-acetylgalactosamine or N-acetylglucosamine in combination with glucuronic or iduronic acid [91]. In case of HSPG, this disaccharide unit contains glucuronic or iduronic acid and N-acetylglucosamine. Disaccharide units, in turn, are variably N- and O-sulfated, with different GAGs having a different number of sulfate moieties per disaccharide unit (Table 1). Notably, N-sulfates are essential for GAG chains to become subsequently sulfated at the 2-O and 6-O positions [201]. It appears that the biological function of proteoglycans is dependent on their level of sulfation and saccharide sequence [91].

Given the relation between Aβ and cellular degeneration in CAA and the close association of HSPG and GAGs with CAA, we aimed to investigate the role of different GAGs, and in particular their sulfate moieties, in $DA\beta_{1-40}$ aggregation and $DA\beta_{1-40}$-induced cellular toxicity of cultured cerebrovascular cells. In addition, we studied the association of differently sulfated HS in CAA-affected vessels using different HS domain-specific antibodies.

Materials and Methods

GAGs and (desulfated) heparins

Heparin, heparan sulfate (HS) and chondroitin sulfate (CS) as well as N-acetyl-de-O-sulfated (completely desulfated) heparin (CdS-Hep) and de-N-sulfated heparin (DeN-Hep) were purchased from Sigma-Aldrich (St. Louis, MO, USA) and dissolved in Milli Q water (1 mg/ml stock solutions). The different GAGs were chosen based on their level of sulfation (Table 1). Dextran sulfate (DxS), a GAG-related macromolecule (Sigma-Aldrich), was chosen for its high level of sulfation.

HCHWA-D $A\beta_{1-40}$-protein

We used Aβ containing the Dutch mutation (Glu22-->Gln22) as found in HCHWA-D ($DA\beta_{1-40}$) as a model peptide, since this peptide has robust and reproducible aggregation properties and cytotoxic properties in vitro [54] and is associated with conditions of severe CAA formation in vivo, i.e. HCHWA-D. $DA\beta_{1-40}$ was purchased from Quality Controlled Biochemicals (QCB; Hopkinton, Massachusetts, USA, 96% pure). We made a stock solution by dissolving the peptide in hexafluoroisopropanol, removing the solvent by evaporation and subsequently dissolving it in DMSO (5 mM). For circular dichroism analysis, stock solutions of the peptides were made in sterile water (250 µM). Aliquots were stored at -80°C prior to use.

Thioflavin T analysis

$DA\beta_{1-40}$ (50 µM) was incubated up to 48 hours at 37°C with or without GAGs or the desulphated heparins (250 µg/ml) in Tris/NaCl buffer (50 mM Tris, 150 mM NaCl, 0.01% sodium azide pH 7.4). After several time intervals (1, 7, 24 and 48 hours), 20 µl samples were taken from the incubation mixture. These samples were added to 980 µl Thioflavin-T solution (50 mM glycine pH 9.2, 3 µM Thioflavin-T). Samples were excited at 450 nm (slit width 5 nm) and emission fluorescence was measured twice for each sample at 482 nm (slid width 10 nm). Each experiment was repeated at least three times. Mean emission fluorescence of one representative analysis ± standard error was plotted as a function of time. At each time point, an unpaired two-sided t-test was performed to compare aggregation of $DA\beta_{1-40}$ with and without the different GAGs and desulfated heparins.

Electron microscopy

After 48 hours of incubation, 3 µl samples were taken from the Thioflavin-T assay incubation mixtures to analyse by electron microscope (EM). The samples were diluted 10 times in ultra pure water, 5 µl aliquots were placed on a formvar-coated Ni-grids and grids were then left to dry overnight at 37°C. The following day, grids were washed with ultra pure water and negatively stained for 30 minutes with 4% filtered uranyl acetate solution. Finally, grids were air dried and examined using a Jeol 1200 EX/II electron microscope (Jeol Ltd., Tokyo, Japan) at 60 kV.

Circular dichroism (CD) analysis

$DA\beta_{1-40}$ (50 µM) dissolved in sterile water was incubated in Tris/NaCl buffer (50 mM Tris, 150 mM NaCl, 0.01% sodium azide) with or without (desulfated) heparins (250 µg/ml) or GAGs (250 µg/ml) for 48 hours at 37°C. All samples were kept on ice before measuring far UV spectra at 4°C with 1 nm intervals (240-195 nm). Measurements were performed on a Jasco J-810 spectropolarimeter (Jasco Inc., Easton, MD, USA) using a quartz cuvette (path

length 1 mm). Spectra are an average of 15 scans recorded at a speed of 20 nm/min with 5 scans of the Tris/NaCl buffer used as baseline.

Viability assay

HBP were isolated and characterized as previously described [265]. Cells were maintained in uncoated culture flasks at 37°C with complete medium containing Eagle's modified culture medium (EMEM), 20% fetal calf serum, 10% human serum (Lonza BioWhittaker Benelux BV, Breda, the Netherlands), 0.1% basic fibroblast growth factor and antibiotics. For the viability assay, HBP were transferred to 8-well chamber slides (Nunc, Roskilde, Denmark) coated with gelatin (1%) and cross-linked with glutaraldehyde (0.1%). After one day of culturing in complete medium, HBP were incubated with EMEM with 0.1% bovine serum albumin (EMEM-BSA) overnight. The next day, cells were incubated with EMEM-BSA containing 10 μM $DA\beta_{1-40}$ with or without either 50 μg/ml GAGs or desulfated heparins. Controls were cells incubated without $DA\beta_{1-40}$ and without GAGs or desulfated heparins. After six days in culture, cell viability was quantified using a fluorescent Life/Dead® viability kit (Invitrogen Molecular Probes, Eugene, Oregon, USA). Four fields per well were counted using a Leica DMI inverted fluorescence microscope (magnification 10x) and the percentage dead cells was calculated. Assays were repeated at least twice and data of one representative is presented as mean ± standard error. An unpaired two-sided t-test was performed to compare the effects of the different GAGs and desulfated heparins on $DA\beta_{1-40}$-induced cell death.

Table 1: *The number of sulfate moieties present in each disaccharide of different GAGs and a GAG related macromolecule*

Glycosaminoglycan	**Sulfate moieties per disaccharide unit** [1]
Dextran sulfate [2]	4 - 6
Heparin	1.6 - 3
Heparan sulfate	0.4 - 2
Chondroitin sulfate	0.1 - 1.3

[1] adapted from [94]
[2] GAG-related macromolecule

Immunofluorescent staining of Aβ on the cell surface of HBP

HBP were cultured for three days in 8-well chamber slides incubated with 10 μM $DA\beta_{1-40}$ and either 50 μg/ml GAGs or 50 μg/ml desulfated heparins. HBP were then fixed for 10 minutes with periodate-lysine-paraformaldehyde and incubated overnight with rabbit anti-Aβ antibody 40-4 (1:200; generously provided by Dr. William van Nostrand). Subsequently, cells were incubated for one hour with the secondary antibody Alexa 594-labeled anti-rabbit (1:200; Invitrogen, Breda, The Netherlands). Topro-3 (1:1000; Vector laboratories, Burlingame, California, USA) was used to stain nuclei. All antibodies were diluted in PBS/1% BSA. Staining was analyzed using a confocal laser-scanning microscope (Leica, Wetzlar, Germany).

Human autopsy material

Occipital lobe tissue samples of a female AD patient (age 75 years, NFT Stage (Braak) VI, Plaque score (CERAD) C, CAA grade ++) were obtained after a rapid autopsy procedure, snap-frozen in liquid nitrogen and stored at -80°C until sectioning. Informed consent was obtained according to European guidelines.

Antibodies

The phage display antibodies directed against specific HS GAG motifs and the dilutions used are listed in Table 2. Phage antibodies were detected by monoclonal mouse anti-VSV (P5D4; Sigma-Aldrich Chemie BV, Zwijndrecht, NL). Anti-VSV was subsequently detected with goat anti-mouse 594 Alexa (Invitrogen, Carlsbad, CA, USA).

Immunohistochemistry

Cryosections (4µm) of the occipital neocortex were stained with the different phage display antibodies (Table 2). In short, sections were air-dried and fixed in 4% paraformaldehyde for 10 minutes. Phage display antibodies were diluted in PBS/1% BSA, and incubated overnight at 4 °C. Sections were then incubated with anti-VSV antibody (1:200) and subsequently with goat-anti mouse 594 Alexa (1:200) for one hour each. For the detection of fibrillar Aβ, sections were double stained with Thioflavin S (1% w/v in distilled water) for 5 minutes at room temperature, in the dark. Then, sections were dehydrated with 70% ethanol. Finally, sections were mounted in Vectashield (Vector Laboratories) and staining patterns were analyzed using a fluorescence microscope (Leica, Wetzlar, Germany).

Table 2: *Phage display antibodies that recognize different sulfated HS GAG motifs*

Antibody	Moieties involved in binding	Dilution [5]
AO4B08 [1]	N-sulfation 2-O-sulfation 6-O-sulfation (high) C5-epimerization	1:1
EV3C3 [2]	N-sulfation 2-O-sulfation C5-epimerization	1:5
HS4C3 [3]	N-sulfation 2-O-sulfation 6-O-sulfation 3-O-sulfation	1:2
HS4E4 [1]	N-sulfation N-acetylation C5-epimerization	1:1
RB4EA12 [4]	N-sulfation N-acetylation 6-O-sulfation	1:1

[1] [137]
[2] unpublished data
[3] [239]
[4] [277]
[5] dilution used in immunohistochemical staining

Results

GAGs affect Aβ aggregation and Aβ-mediated cell death

The effect of different GAGs, i.e. chondroitin sulfate (CS), heparan sulfate (HS), and heparin and the GAG-related macromolecule dextran sulfate (DxS) on aggregation of Aβ was studied using several different aggregation assays, i.e. Thioflavin T assay, electron microscopy and circular dichroism. Furthermore, we studied the pathological effects of these GAGs on Aβ-mediated toxicity of cultured HBP.

In the Thioflavin T assay (Fig. 1), heparin and the highly sulfated DxS increased $DA\beta_{1-40}$ aggregation, although this increase was only measurable after 24 hours of incubation. At this time point, heparin and DxS increased $DA\beta_{1-40}$ fluorescence emission significantly ($p<0.01$ and $p<0.05$, respectively) three- to four-fold. After 48 hours of incubation only heparin significantly ($p<0.001$) increased $DA\beta_{1-40}$ aggregation (3.5-fold). HS and CS had no significant effect on $DA\beta_{1-40}$ aggregation at any time point.

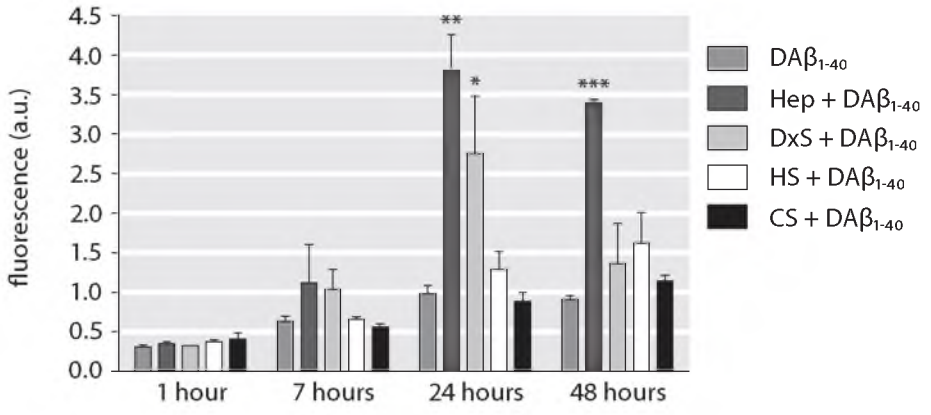

Figure 1: *Thioflavin-T analysis of $DA\beta_{1-40}$ aggregated up to 48 hours (37°C) with different GAGs. heparin treatment significantly increased thioflavin-T fluorescence after 24 and 48 hours of incubation. DxS significantly increased fluorescence, but only after 24 hours of incubation. The other GAGs had no effect on aggregation. DxS: dextran sulfate; Hep: heparin; HS: heparan sulfate; CS: chondroitin sulfate. * $p<0.05$; ** $p<0.01$, *** $p<0.001$*

Using electron microscopy to visualize aggregation, it was revealed that aggregation of $DA\beta_{1-40}$ alone for 48 hours resulted in compact aggregates of Aβ, whereas individual fibrils could hardly be detected (Fig. 2A). It was not possible to dissolve these compact aggregates by further dilution of samples either before or after incubation (data not shown). When $DA\beta_{1-40}$ was co-incubated with heparin, extensive networks of long Aβ fibrils were observed (Fig. 2B) in between compact aggregates that were much smaller in number than observed without heparin incubation. Similar to heparin, incubation with DxS induced the formation of an extensive network of Aβ fibrils with only a small number of compact aggregates (Fig. 2C). Co-incubation with HS (Fig. 2D) or CS (Fig. 2E) resulted in an intermediate situation characterized by compact aggregates of $DA\beta_{1-40}$ interconnected with long, mostly laterally aggregated, Aβ fibrils.

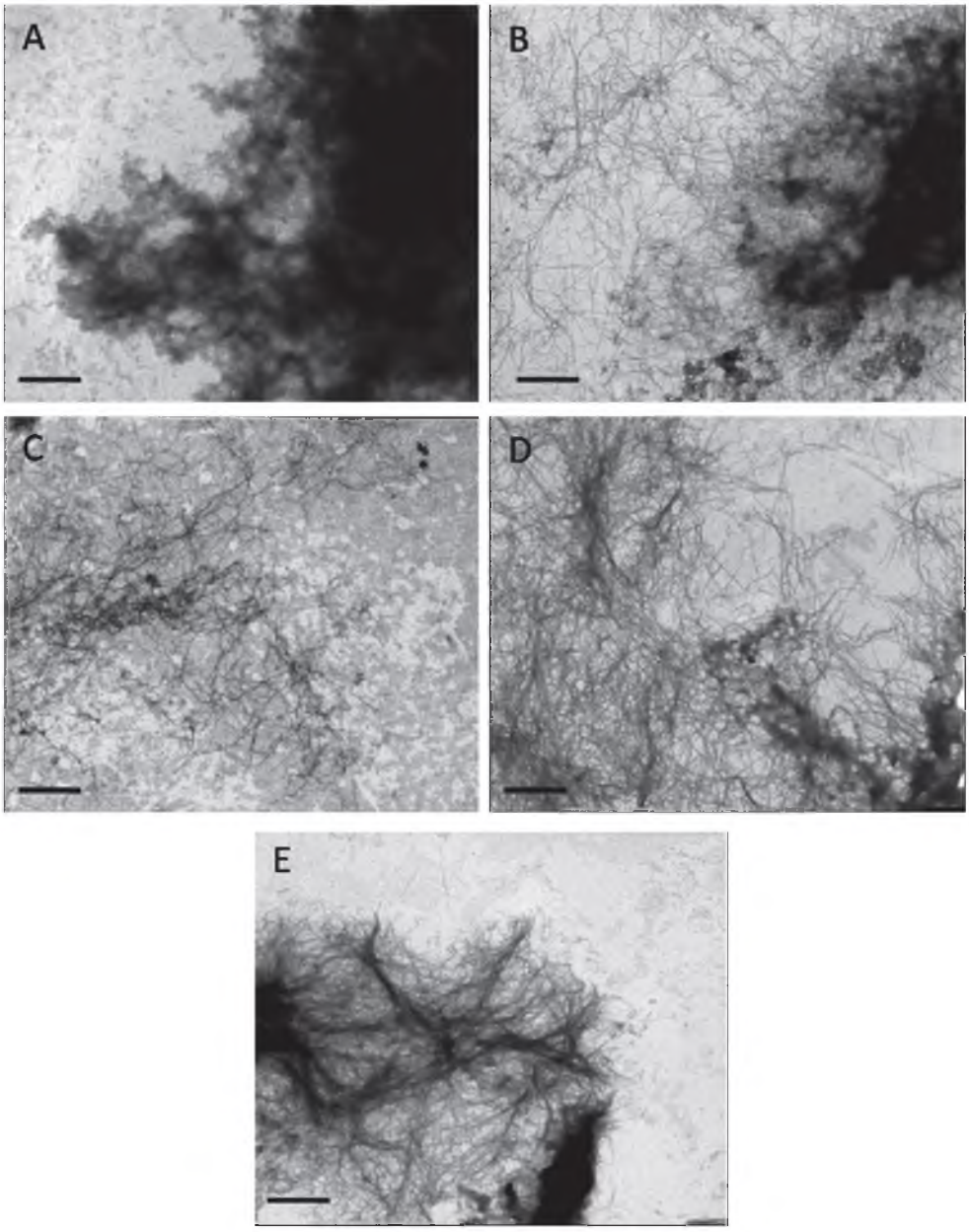

Figure 2: *Electron microscopic analysis of DA$\beta_{1\text{-}40}$ aggregated up to 48 hours (37°C) with different GAGs. Co-incubation with heparin (B) resulted in a network of fibrils in between the compact aggregates seen in untreated DA$\beta_{1\text{-}40}$ (A). A similar aggregation pattern can be seen after co-incubation with DxS treatment (C; compact aggregates present, but not shown). After co-incubation with HS (D) and CS (E), compact DA$\beta_{1\text{-}40}$ aggregates interconnected with laterally aggregated fibrils are visible.*
Magnification 10.000x; scale bar: 100 µm

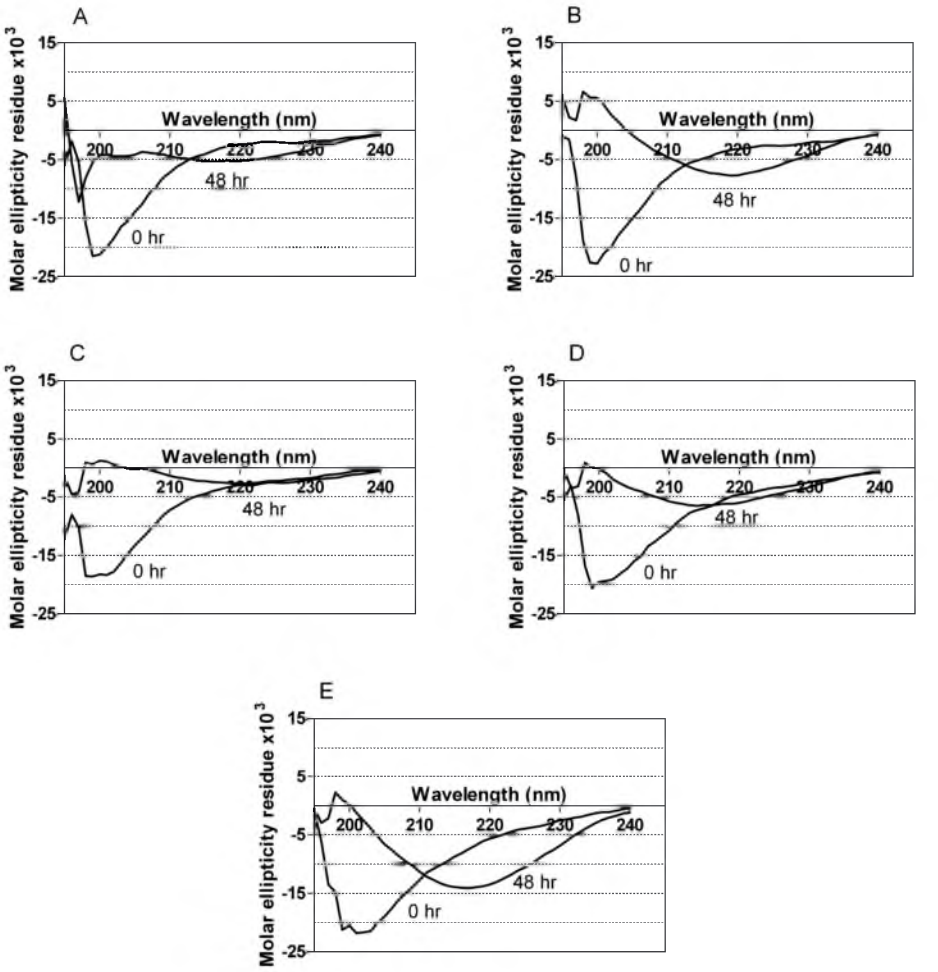

Figure 3: *CD analysis of DAβ$_{1-40}$ aggregated for 0 or 48 hours (37°C) in the presence of different GAGs. After 48 hours of incubation DAβ$_{1-40}$ alone (A) has a conformation in between random coil (minimum 197 nm) and β-sheet (minimum 220 nm, maximum 200 nm). In the presence of heparin (B) and CS (E), DAβ$_{1-40}$ adopts a β-sheet conformation after 48 hours, whereas in the presence of DxS (C) and HS (D) a conformation in between random coil and β-sheet was detected. At 0 hours of incubation DAβ$_{1-40}$ alone or in combination with the GAGs is in a random coil conformation (A-E).*

To determine the conformation (i.e. random coil, β-sheet) of DAβ$_{1-40}$ when incubated for 48 hours with or without GAGs, we performed CD analysis (Fig. 3). Before incubation (0 hours), a typical random coil conformation was observed (minimum at 197 nm) for DAβ$_{1-40}$ alone or in combination with the different GAGs. After 48 hours of incubation, however, the spectrum of DAβ$_{1-40}$ alone demonstrated a conformation that had characteristics of both a β-sheet and random coil conformation (minimum signal between 200 to 220 nm) (Fig. 3A). DAβ$_{1-40}$ incubated with heparin (Fig. 3B) resulted in a CD spectrum with a minimum signal at 220 nm and a maximum at 200 nm, basically resembling a β-sheet conformation. DAβ$_{1-40}$ with either DxS (Fig. 3C) or HS (Fig. 3D) had an intermediate conformation (minimum signal at 220 nm and 213 nm, respectively), although a β-sheet structure was more prominent than with DAβ$_{1-40}$ alone. The CD spectrum of DAβ$_{1-40}$ incubated with CS (Fig. 3E) demonstrated a minimum around 216 nm, indicative of a β-sheet conformation.

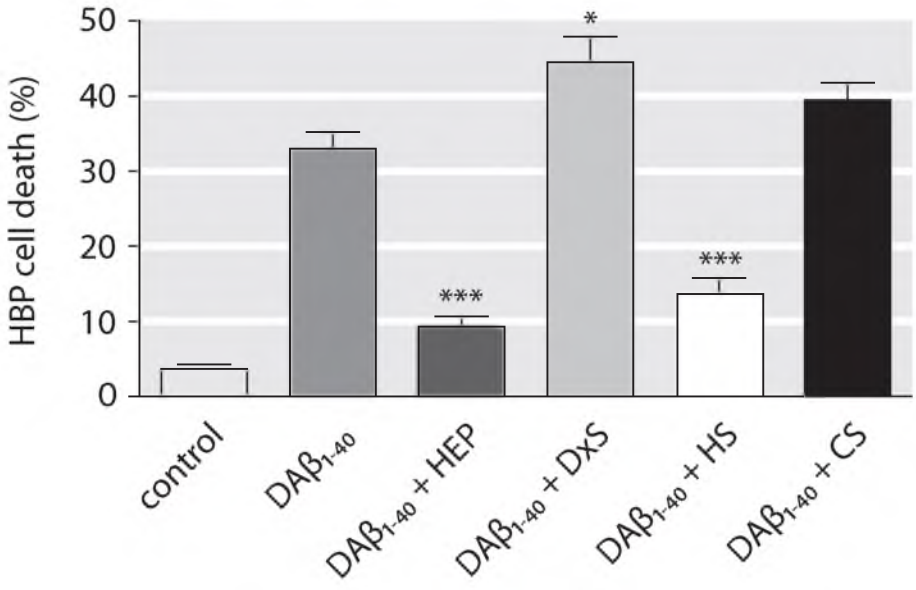

Figure 4: *Viability assay of HBP incubated for 6 days with DAβ$_{1-40}$ with different GAGs. Incubation of DAβ$_{1-40}$ with heparin and HS significantly reduced DAβ$_{1-40}$ – induced cell death, whereas DxS significantly increased HBP cell death. CS had no effect.*
*DxS: dextran sulfate; Hep: heparin; HS: heparan sulfate; CS: chondroitin sulfate. * p<0.05; ***p<0.001*

Finally, we examined toxicity of HBP when they were cultured with Aβ in combination with the GAGs (Fig. 4). Incubation of HBP with $DA\beta_{1-40}$ increased cell death of HBP from an average of 4 ± 1% in controls to 33 ± 2%. The GAGs alone had no effect on cell death compared to controls (data not shown). Both heparin and HS significantly ($p<0.0001$) reduced Aβ-mediated cell death in cultured HBP (9 ± 1% and 13 ± 2%), whereas DxS significantly ($p<0.05$) increased HBP death (44.5 ± 3%) and CS had no effect (39.5 ± 2%). To determine whether aggregation of Aβ on the cell surface was related to the observed cellular toxicity, immunofluorescent imaging of HBP incubated with $DA\beta_{1-40}$ and the GAGs was performed. There were no obvious differences in $DA\beta_{1-40}$ aggregation on the cell surface when comparing $DA\beta_{1-40}$ alone or in combination with heparin (Fig. 5) or any of the other GAGs (data not shown). As mentioned earlier, the different GAGs used have different levels of sulfation (Table 1). To study the influence of sulfation on Aβ aggregation and toxicity, we next used desulfated forms of heparin.

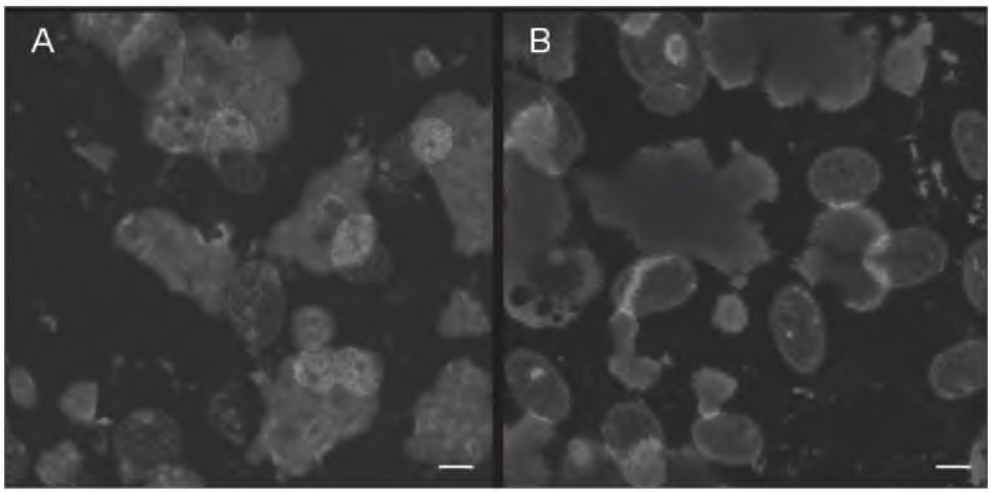

Figure 5: *Immunofluorescent staining of confluent cultures of HBP incubated with $DA\beta_{1-40}$ alone (A) or in combination with heparin (B). No obvious change in the association of Aβ (40-4; red) with the cultured cells (Topro-3; blue nuclei) was visible when $DA\beta_{1-40}$ was incubated with heparin. Magnification 630x. Scale bar: 1 mm*

Pathological effects of heparin are dependent on sulfate moieties

We studied the effects heparins with various degrees of sulfation, i.e. fully sulfated heparin, deN-sulfated heparin (DeN-Hep) and completely desulfated heparin (CdS-Hep), on Aβ aggregation by using the same assays as previously mentioned. In the Thioflavin T assay, the influence of sulfated heparin on $DA\beta_{1-40}$ aggregation again became measurable only after 24 hours of incubation (Fig. 6); from that time point on it significantly increased fluorescence emission ($p<0.001$) four-fold compared to the emission level seen with $DA\beta_{1-40}$ alone. As seen before (Fig. 1) this significant increase remained until at least 48 hours of incubation. In contrast, neither DeN-Hep nor CdS-Hep affected $DA\beta_{1-40}$ fluorescence at any time point between 1 and 48 hours (Fig. 6).

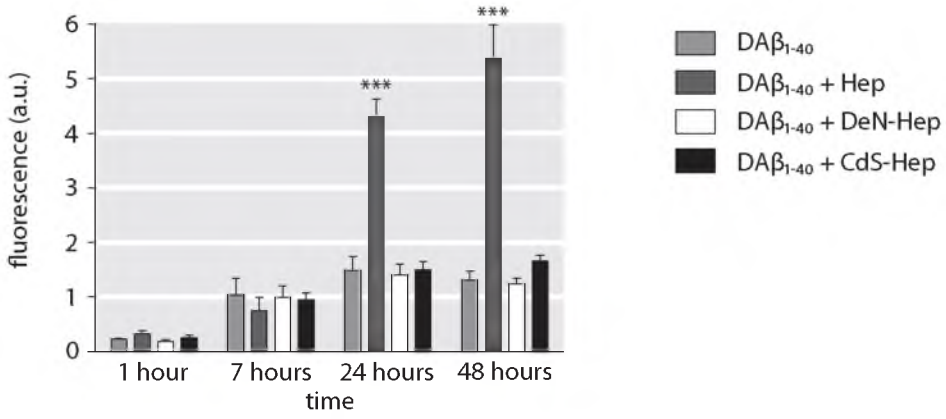

Figure 6: *Thioflavin-T analysis of DAβ$_{1-40}$ aggregated up to 48 hours (37°C) with different (desulfated) heparins. Heparin treatment significantly increased thioflavin-T fluorescence at 24 and 48 hours of incubation. DeN-Hep and CdS-Hep had no effect on aggregation. DeN-Hep: de-N sulfated heparin; CdS-Hep: completely desulfated heparin. ***p<0.001*

Electron microscopy revealed that after co-incubation with DeN-Hep (Fig. 7C), unlike the vast network of fibrils seen when incubated with heparin (Fig. 7B), only a limited number of individual fibrils extending from the compact DAβ1-40 aggregates were observed. Co-incubation with CdS-Hep demonstrated compact aggregates similar to DAβ$_{1-40}$ alone (Fig. 7D).

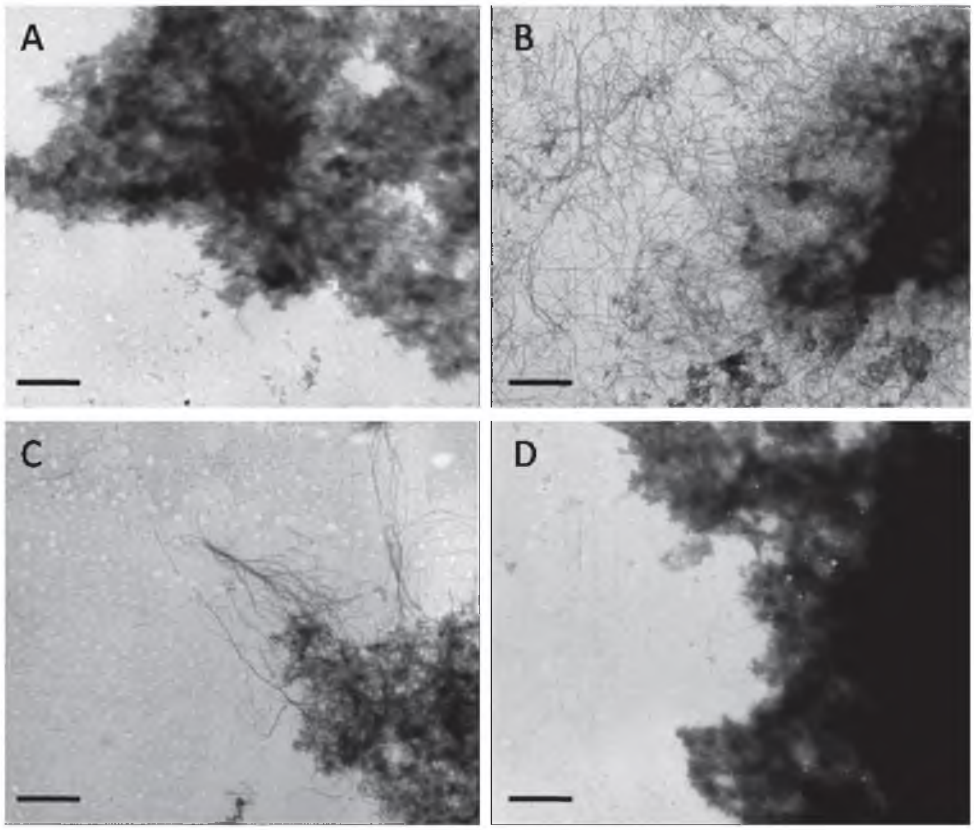

Figure 7: *Electron microscopic analysis of DAβ_{1-40} aggregated up to 48 hours (37°C) in the presence of different (desulfated) heparins. Co-incubation with heparin (B) resulted in a network of fibrils between the compact aggregates that were also seen in untreated DAβ_{1-40} (A). Some individual fibrils protruding from compact aggregates are detected after coincubation with DeN-Hep (C). Incubation with CdS-Hep had no effect on DAβ_{1-40} aggregation. Magnification 10.000x; scale bar: 100 µm*

When we examined the conformation of DAβ_{1-40} in the presence of desulfated heparins, it was revealed that DAβ_{1-40} incubated with DeN-Hep (Fig. 8C) resulted in a CD spectrum with a minimum signal at 220 nm and a maximum at 200 nm, basically resembling a β-sheet conformation. This spectrum is therefore similar to the spectrum of DAβ_{1-40} incubated with heparin (Fig. 8B). Incubation with CdS-Hep (Fig. 8D) also resulted in an intermediary conformation (minimum at 210 nm, maximum 195 nm), but with relatively more aspects of a random coil structure than DAβ_{1-40} alone (Fig. 8A). Before incubation (0 hours), the conformation of DAβ_{1-40}, either with or without the (desulfated) heparins, was a typical random coil conformation (minimum at 197 nm) (Fig. 8 A-D).

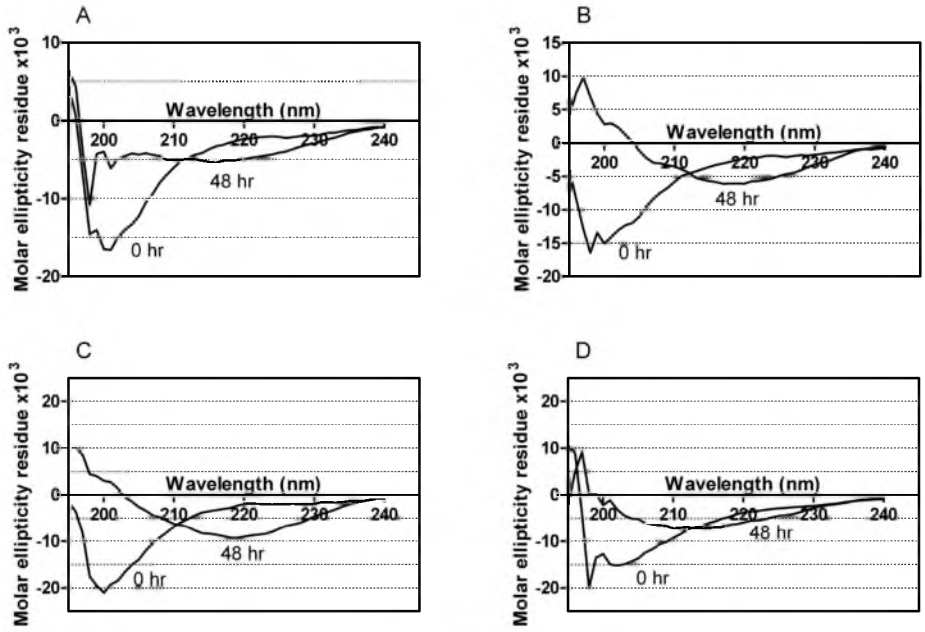

Figure 8: *CD analysis of DAβ_{1-40} aggregated for 0 or 48 hours (37°C) with different (desulfated) heparins. After 48 hours of incubation DAβ_{1-40} alone (A) has a conformation in between random coil (minimum 197 nm) and β-sheet (minimum 220 nm, maximum 200 nm). After co-incubation for 48 hours with heparin (B) and DeN-Hep (C), DAβ_{1-40} has a β-sheet conformation, whereas co-incubation with CdS-Hep(D) results in an intermediate conformation between random coil and β-sheet . At 0 hours of incubation DAβ_{1-40} alone or in combination with the heparins is in a random coil conformation (A-D).*

In the cell culture experiment, the addition of heparin to DAβ_{1-40} significantly ($p<0.05$) decreased cell death from 46 ± 6% to 25 % ± 5% (Fig. 9). Addition of DeN-Hep or CdS-Hep to DAβ_{1-40} resulted in cell death rates of 47 ± 6% and 37 ± 14% respectively, comparable with that of DAβ_{1-40} alone (46 ± 6%). Incubation of HBP with the (desulfated) heparins alone did not influence cell death (data not shown). Confocal imaging of HBP incubated with DAβ_{1-40} and the (desulfated) heparins did not show a difference in DAβ_{1-40} accumulation on the cell surface (data not shown).

Sulfated HS are associated with CAA in vivo

CAA-positive vessels were double-stained for Thioflavin-S and a variety of phage display antibodies directed against specific sulfated HS motifs (Table 2) to determine if there is an in vivo association of sulfated HS with vascular amyloid pathology (Fig. 10). Strong staining of Thioflavin-S positive vessels was observed with AO4B08, EV3C3, HS4E4 and HS4C3 (Fig. 10 K-N). RB4E12 showed little staining of Thioflavin-S positive vessels (Fig. 10 O).

Notably, whereas Thioflavin-S staining was localized to the outer layers of the vessels where Aβ is typically deposited (Fig. 10 A-E), sulfated HS were observed in the

entire vessel wall (Fig. 10 F-J), which also includes basement membranes that surround vascular endothelial cells.

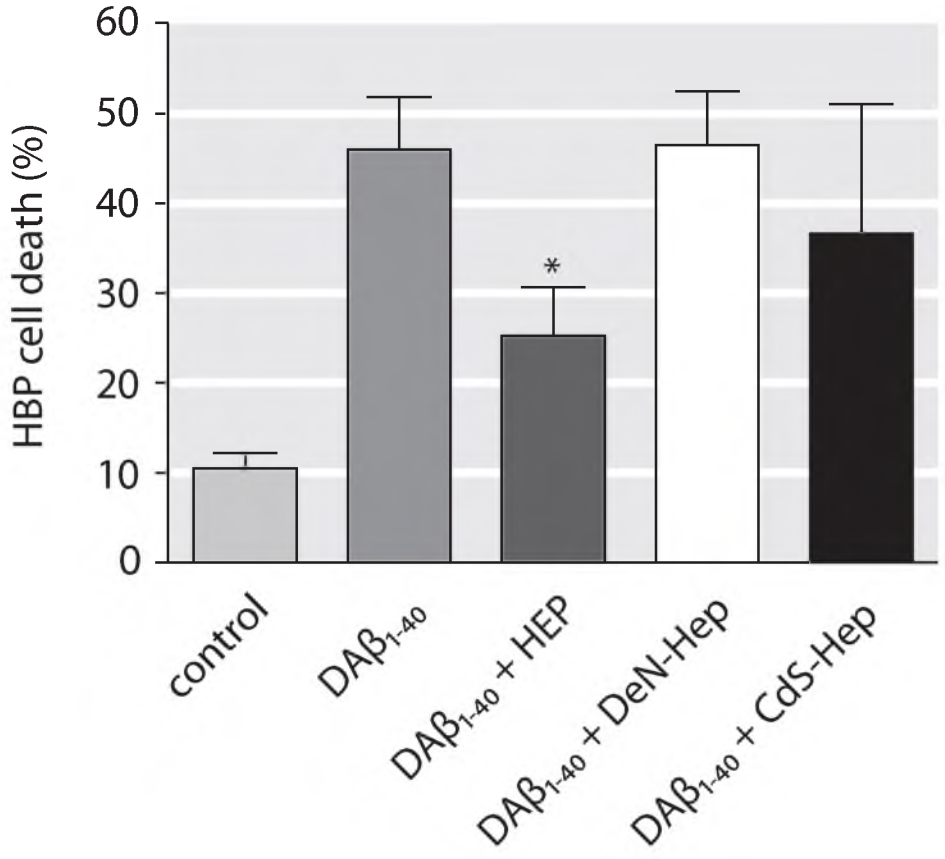

Figure 9: *Viability assay of HBP incubated for 6 days with $DA\beta_{1-40}$ with different (desulfated) heparins. Incubation of $DA\beta_{1-40}$ with heparin significantly reduced $DA\beta_{1-40}$ – induced cell death, whereas DeN-Hep and CdS-Hep had no effect.*
Hep: heparin; DeN-Hep: deN-sulfated heparin; CdS-Hep: completely desulfated heparin.
** $p<0.05$*

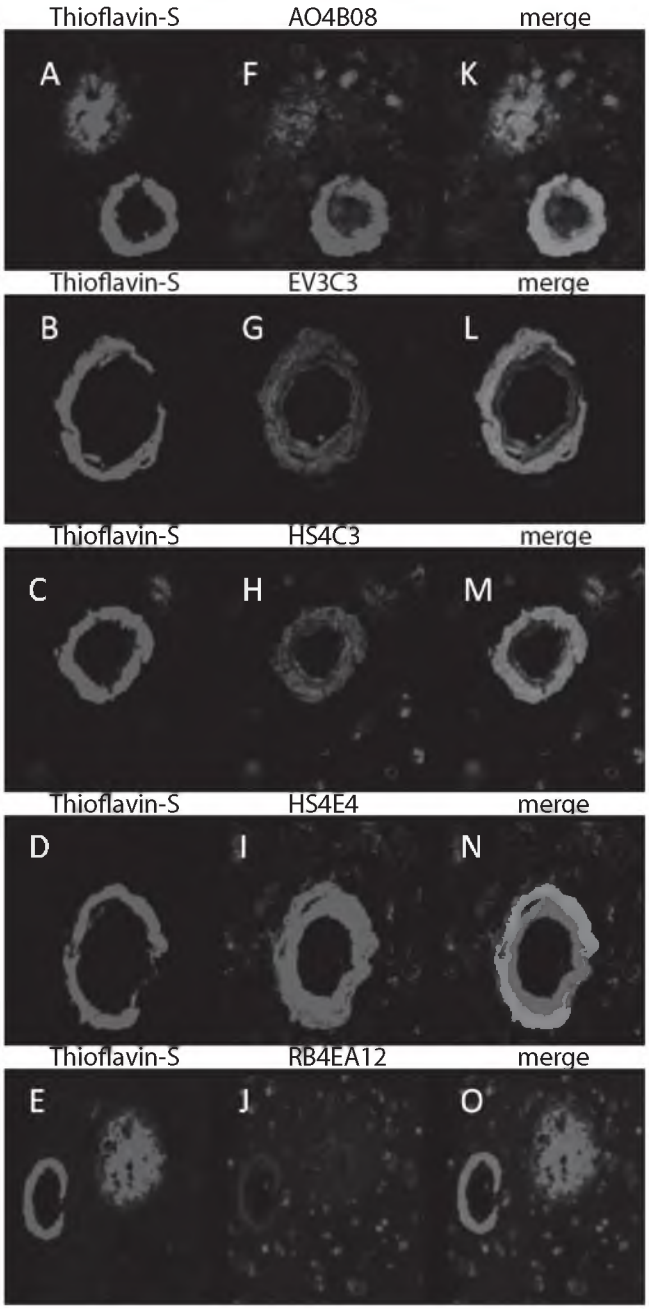

Figure 10: *Immunofluorescent staining of Thioflavin-S positive cortical vessels of an AD patient (A-E) with different phage display antibodies that recognize different HS sulfate motives (F-J). In K-O, Thioflavin-S and HS staining is merged. Vessels with fibrillar Aβ deposits were positive for most antibodies (K-N), but negative for RB4EA12 (O). Original magnification 630x.*

Discussion

Aggregated Aβ in CAA is predominantly present in a fibrillar form. Since GAGs are abundantly present in CAA of AD and HCHWA-D, it is possible that they contribute to the aggregation of Aβ in these vascular deposits. The main findings of our study are the following: 1) heparin increases $DA\beta_{1-40}$ aggregation and inhibits $DA\beta_{1-40}$ -mediated cytotoxicity of cultured cerebrovascular cells, 2) this effect is mainly mediated by the sulfate moieties in heparin, since desulfated forms of heparin are less active or even inactive, 3) heparan sulfate, but not dextran or chondroitin sulfate, also inhibits $DA\beta_{1-40}$ -mediated cytotoxicity of cultured cerebrovascular cells, although it has less pronounced effects on $DA\beta_{1-40}$ aggregation, 4) GAGs with various sulfation motifs are closely associated with CAA in AD brains, supporting a biological role for sulfated GAGs in the pathology of CAA.

Previous studies, using a limited number of aggregation assays and wild type Aβ40 or amylin, suggested that GAGs could affect amyloid formation [39, 40]. In the present study, we found that several GAGs can affect aggregation of $DA\beta_{1-40}$, a peptide that mainly deposits in the cerebral vasculature. In particular, the highly sulfated heparin and DxS stimulated Aβ aggregation and fibrillization as visualized in the Thioflavin T assay (Fig. 1), CD spectroscopy (Fig. 3) and also by EM analysis (Fig. 2). The moderately sulfated CS and HS had a stimulatory effect on aggregation as observed in CD spectroscopy and EM analysis, but not in the Thioflavin T assay. Therefore, we demonstrated that sulfate moieties of GAGs, in particular those of heparin, influence Aβ aggregation, apparently regardless of the level of sulfation. The effects of the various GAGs on Aβ aggregation, however, are likely not completely attributable to sulfate modifications only. For example, the exact composition of the sugar chains themselves varies greatly between GAGs, with each GAG being characterized by a different disaccharide unit. These differences may therefore also influence Aβ aggregation, although, as far as we know, this has not been investigated.

Our data suggested that sulfation of heparin, was critical in the effect of heparin on the aggregation of $DA\beta_{1-40}$, which is in concurrence with previous observations [40]. Removal of N-sulfates from heparin showed the same prevention of aggregation in the Thioflavin-T analysis as completely desulfated heparin (Fig. 6), suggesting that N-sulfates are of predominant importance in Aβ fibril formation. In contrast, in EM analysis (Fig. 7), which shows more details of the architecture of the aggregates and fibrils that are formed, De-N-sulfated heparin had some effect on the fibril formation of DAβ1-40, whereas co-incubation of fully desulfated heparin with $DA\beta_{1-40}$ resulted in compact aggregates indistinguishable from aggregates formed by $DA\beta_{1-40}$ alone. This suggests that O-sulfation has a dominant effect over N-sulfation of heparin, which was supported by a similar observation in CD spectroscopy (Fig. 8). Our data are thus contradictory with respect to the specific and relative roles of N- and O-sulfation and are only partly in line with others [39, 40], where it was suggested that O-sulfation is more important in enhancing fibril formation than N-sulfation. The limited availability of de-O sulfated heparin prevented us from specifically studying the effects of O-sulfation of heparin.

It has to be mentioned that we did find some discrepancies in determining Aβ aggregation state since the Thioflavin T results for CS and HS did not match the results found with CD spectroscopy and EM. This may be explained by the fact that information on aggregation retrieved from the different assays is partly overlapping. For example, EM analysis reveals structural information, but is not sensitive enough to demonstrate β-sheet formation in smaller peptide aggregates; CD spectroscopy results in spectra that

are often reminiscent of mixed α-helix and β-sheet conformations rather than the pure forms of protein folding and with the Thioflavin T assay protein the type of aggregation that is detected is not exactly defined.

When cerebrovascular cells are cultured with Aβ, Aβ accumulates at the cell surface and induces cellular degeneration over time [262]. Previous studies demonstrated that the cytotoxic interaction of Aβ with the cell can be inhibited in several ways, e.g. by proteolytic breakdown of Aβ [196], by binding to the Aβ protein thereby blocking its interaction with binding sites [194, 279] or, finally, by blocking possible intracellular signaling cascades [116]. In our case, the protective effect of heparin towards $DA\beta_{1-40}$-mediated cell death (Fig. 4 and Fig. 9) may be explained by the increased propensity of $DA\beta_{1-40}$ to aggregate in solution when heparin is present. This could then prevent the interaction of toxic monomeric, oligomeric or prefibrillar species of $DA\beta_{1-40}$ with the cell surface. Although this may form a mechanistic explanation for our findings, our immunofluorescence experiments leave room for one of the alternative explanations, since we did not observe differences in the association of $DA\beta_{1-40}$ with the cell surface under the influence of the various (desulfated) GAGs. Furthermore, HS inhibited $DA\beta_{1-40}$-mediated cell death in the absence of an overt effect on $DA\beta_{1-40}$ aggregation and DxS increased DAβ1-40 aggregation and $DA\beta_{1-40}$-mediated cell death. Therefore, it is possible that heparin and HS may also protect cells against $DA\beta_{1-40}$-mediated death in another way, for example by affecting intracellular signaling cascades that lead to cell death. Future studies will have to reveal if and how such pathways are affected by these GAGs. In any case, the pathological effect of heparin was abolished after (partial) desulfation of heparin, suggesting a crucial role for sulfate moieties of GAGs in their interaction with $DA\beta_{1-40}$.

In previous studies we demonstrated the presence of HS GAGs in CAA of AD brains [255]. Furthermore, with antibodies directed against HS core proteins, we demonstrated that the heparan sulfate proteoglycans agrin, glypican-1, syndecan-2 [255] and collagen XVIII [257] co-deposit with CAA. In the present study, we stained CAA vessels with antibodies directed against different motifs of sulfated HS (Table 2) and demonstrated that the HS chains that are associated with Thioflavin-S-positive vessels are in fact sulfated (Fig. 10). Apparently, there is some variation in the sulfation and epimerization pattern of HS in CAA-vessels, since not all HS motifs were found in these vessels, but the relevance of this variation remains to be investigated. Unfortunately, we could not determine the level of sulfation (i.e. high vs. low) of HS near CAA vessels, although a previous study suggested that HS of AD patients are more sulfated than HS of controls [152]. Finally, it must be mentioned that only one patient was examined, therefore, in the future a more elaborate study of sulfation of CAA-associated HS should be performed to further substantiate our results.

Given the close association of cerebrovascular cells with the HS(PG) in CAA, the question arises if HSPG are produced locally by pericytes and smooth muscle cells or, like Aβ itself, are produced by neurons and transported with the interstitial fluid to blood vessel walls [275]. In line with the former possibility, our immunohistochemical stainings revealed the presence of sulfated HS in the entire vessel wall, suggesting production by vascular cells. Indeed, we recently demonstrated that cultured HBP can produce HSPG, in particular – but not restricted to - agrin and glypican-1, and its production is stimulated by $DA\beta_{1-40}$ [244]. Furthermore, we showed that $DA\beta_{1-40}$ also increased sulfate incorporation into GAG chains, suggesting that HSPG modifications are induced by $DA\beta_{1-40}$. Therefore, these in vitro data may explain our immunohistochemical observations of the association

of sulfated HS with CAA vessels.

In summary, our data show the importance of GAG sulfate moieties within heparin, and probably also in other GAGs, in regulating CAA-associated Aβ aggregation and thus influencing Aβ-induced cytotoxicity. Given the close association of sulfated GAGs in CAA, this may provide a mechanistic basis for the observation that Aβ is highly aggregated in CAA.

Acknowledgments

This study was supported by a grant from the Internationale Stichting Alzheimer Onderzoek (ISAO, no. 07510), the Netherlands Organization for Scientific Research (NWO/ZonMW, Vidi program, no. 917.46.331) and the Hersenstichting Nederland (no. 14F06.18).

Chapter 4

Limited expression of heparan sulfate proteoglycans associated with Aβ deposits in the APPswe/PS1dE9 mouse model for Alzheimer's Disease

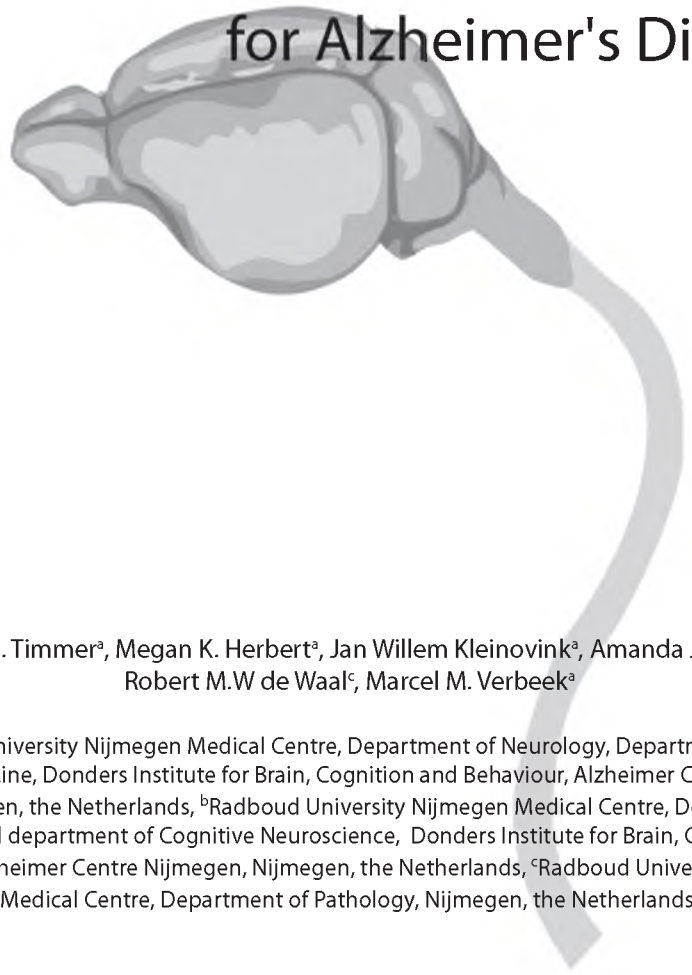

Nienke M. Timmer[a], Megan K. Herbert[a], Jan Willem Kleinovink[a], Amanda J. Kiliaan[b], Robert M.W de Waal[c], Marcel M. Verbeek[a]

[a]Radboud University Nijmegen Medical Centre, Department of Neurology, Department of Laboratory Medicine, Donders Institute for Brain, Cognition and Behaviour, Alzheimer Centre Nijmegen, Nijmegen, the Netherlands, [b]Radboud University Nijmegen Medical Centre, Department of Anatomy and department of Cognitive Neuroscience, Donders Institute for Brain, Cognition and Behaviour, Alzheimer Centre Nijmegen, Nijmegen, the Netherlands, [c]Radboud University Nijmegen Medical Centre, Department of Pathology, Nijmegen, the Netherlands

Neuropathology and Applied Neurobiology **36**, 478-486 (2010)

Abstract

Alzheimer's disease (AD) is characterized by deposition of the amyloid beta (Aβ) peptide in brain parenchyma and vasculature. Several proteins co-deposit with Aβ, including heparan sulfate proteoglycans (HSPG). HSPG have been suggested to contribute to Aβ aggregation and deposition, and may influence plaque formation and persistence by stimulating Aβ fibrillization and by protecting Aβ against degradation. Mouse models for AD, expressing the human amyloid precursor protein (APP), produce Aβ deposits similar to humans. These models may be used to study disease pathology and to develop new therapeutic interventions. We aimed to investigate whether co-deposition of HSPG in AD brains can be replicated in the APPswe/PS1dE9 mouse model for AD and if a temporal association of HSPG with Aβ exists. We studied the co-deposition of several HSPG and of the glycosaminoglycan (GAG) side-chains of HSPG in the APPswe/PS1dE9 model at different ages by immunohistochemistry. We found that, although APPswe/PS1dE9 mice did develop severe Aβ pathology with age, co-deposition of HS GAG chains and the various HSPG (agrin, perlecan and glypican-1) was scarce (<10-30% of the Aβ deposits were stained). Therefore, our data suggest that the molecular composition of Aβ deposits in the APPswe/PS1dE9 mouse, with respect to the several HSPG investigated in this study, does not accurately reflect the human situation. The near absence of HSPG in Aβ deposits in this transgenic mouse model may, in turn, hinder the translation of preclinical intervention studies from mice to men.

Introduction

In order to study Alzheimer's disease (AD) pathology, many different mouse models have been developed to test new therapeutic agents and to develop potentially new diagnostic tools [49]. All these transgenic mice express one or more human proteins involved in AD pathology, usually (a mutant form of) the amyloid precursor protein (APP). In humans, APP cleavage may result in the production of the amyloid β (Aβ) peptide and, in turn, Aβ fibrillizes and accumulates in AD brains. Aβ deposits can be found in the brain parenchyma as fibrillar or non-fibrillar senile plaques (SP) and in the vasculature as cerebral amyloid angiopathy (CAA). Transgenic expression of APP in mice leads to similar Aβ depositions. In addition to human APP, some models express (mutant) human presenilin-1 (PS1), which is an essential component of the γ-secretase enzyme complex that mediates cleavage of APP [208], to accelerate development of Aβ pathology.

In humans, Aβ aggregation is thought to be facilitated by several co-depositing proteins, including apolipoprotein E [173], small heat shock proteins [280, 284] and heparan sulfate proteoglycans (HSPG). HSPG consist of a core protein with glycosaminoglycan (GAG) chains attached [256]. There are several different HSPG, some (perlecan, agrin and collagen XVIII) associated with the extracellular matrix, some (glypican and syndecan) associated with cell membranes. The co-deposition of HSPG with Aβ has long been described [220] as has the association of different subtypes of HSPG with Aβ deposits [52, 254, 255]. Remarkably, HSPG seem to be associated with virtually all types of human amyloidoses, e.g. in amyloid A (AA) and amyloid light chain (AL) amyloidosis [225, 226].

The HSPG agrin and glypican-1 were strongly associated with almost all SP in cerebral cortex, cerebellum and hippocampus of AD patients [254, 263]. Syndecan expression, however, could only be observed in a minority of cortical and hippocampal SP. Glypican-1 was the most common HSPG in CAA, with some deposition of agrin and syndecan-2 within vascular Aβ deposits. Perlecan could neither be detected in SP nor in CAA, although this HSPG was previously thought to be most commonly associated with the pathological lesions of AD [222, 224].

The close association of HSPG with Aβ in vivo suggests an important role for these molecules in Aβ deposition. Indeed, in vitro studies have shown that HSPG can regulate Aβ production [17, 147, 204] and stimulate Aβ aggregation [41, 52]. Furthermore, Aβ plaques may be protected from degradation by HSPG [87] and Aβ, in turn, can protect HSPG from degradation [13]. We also recently demonstrated that mRNA expression of agrin and glypican-1 is induced by Aβ in human brain pericytes [244]. Although Aβ and HSPG mutually influence each other's production and degradation, and furthermore deposit simultaneously [222], it is yet unclear if HSPG are already associated with the earliest cerebral Aβ depositions.

Since HSPG appear to be crucial in human Aβ deposition, we aimed to investigate if transgenic mouse models for AD recapitulate the findings in AD brains. To this end, we used the frequently described transgenic APPswe/PS1dE9 mouse model, a well-characterized model [82] exhibiting a severe amyloid pathology starting from about 4-6 months of age. Since transgenic mouse models allow for study of the temporal association of HSPG with Aβ, we investigated expression of several HSPG and of their GAG side-chains at different ages, in order to get a good understanding of the possible role of HSPG in the different stages of AD pathogenesis.

Materials and Methods

APPswe/PS1dE9 mice

A colony of APPswe/PS1dE9 mice was established at the Central Animal Laboratory of the Radboud University Nijmegen Medical Centre, Nijmegen, The Netherlands, after obtaining founder animals from Johns Hopkins University, Baltimore (MA), USA. In short, this model was created by co-injecting the two transgenes with a prion protein promoter in the pronucleus of single cell C57Bl/6 embryos [112].

Female APPswe/PS1dE9 mice were group-housed in standard cages with nestlets and an igloo as cage enrichment. There was a 12 hour light-dark cycle (lights on at 7 am), with a constant temperature of 21±1°C, humidity control and background music during the light phase. Standard food pellets and acidified water (pH 2.5-3) were given ad libitum. This study was approved by the Animal Care Committee of the Radboud University Nijmegen Medical Centre (RU-DEC) and was performed according to the guidelines of the Dutch Council for Animal Care and the European Communities Council Directive of 24 November 1986 (86/609/EEC). Our study was also in concurrence with the European regulations on ethics and responsible conduct regarding scientific communication.

Transcardial perfusion

At 5 (n=5), 8 (n=5), 12 (n=4), 15 (n=3) and 18 months (n=4) of age, mice were anesthetized with 2-4% isoflurane and transcardially perfused with sterile phosphate buffered saline (PBS; Roche, Mannheim, Germany). After perfusion, mice were decapitated and brains were collected. One hemisphere was snap-frozen in liquid nitrogen and stored at -80°C until further analysis.

Immunohistochemical staining

Serial 5 µm sagittal cryosections were stained for Aβ and different HSPG (Table 1). In short, brain tissue was fixed with acetone and incubated with 20% normal serum from the host species of the secondary antibody used. Sections were incubated with primary antibody overnight at 4°C and after which they were incubated with biotin-labeled secondary antibodies for one hour at room temperature. As secondary antibody, horse-anti-mouse was used for 6C6, goat-anti-mouse IgM for JM403, goat-anti-rabbit for M95 and C40 and C42, horse-anti-goat for Bl31 and rabbit-anti-rat for MAB1948. Subsequently, sections were incubated with an avidin-biotin complex (ABC) solution (Vector, CA, USA) for 45 minutes. Staining was developed using 5% diaminobenzidine (DAB) and 0.5% hydrogen peroxide. Copper sulfate (0.5% in saline) and haematoxylin were used to counterstain the surrounding tissue. For each different HSPG staining, four sections of each mouse were used, separated by 50 µm (for Aβ eight slices per mouse were stained). The number of Aβ plaques and the number of HSPG-positive Aβ plaques were counted manually. Two of the authors, who were blinded to the age of the mice, counted five microscopical fields (magnification 200x) per randomized section. The number of HSPG-positive plaques is given as the percentage of Aβ plaques that stained for a specific HSPG. Finally, percentages of co-deposition determined in the sections were averaged for each age group.

Statistical analysis

For the different age groups, the average number of Aβ plaques and the percentage of plaques positive for HSPG were compared using One-way ANOVA with Bonferroni post hoc tests (SPSS).

Table 1: *Primary antibodies used to stain Aβ and the different HSPG*

Antibody	Antigen	Dilution	Source
6C6	Aβ	1:1000	Elan pharmaceuticals, San Francisco, CA, USA
C40	Aβ40	1:500	dr. T. Saido, Tokyo, Japan
C42	Aβ42	1:500	dr. T. Saido, Tokyo, Japan
JM403	HS GAG	1:500	[248]
M-95	Glypican-1	1:50	Santa Cruz Biotechnology, Santa Cruz, CA, USA
BI31	Agrin	1:750	[250]
MAB1948	Perlecan	1:500	Millipore, Billerica, MA, USA

Results

Aβ plaque number increases with age

The average number of plaques (Aβ staining) increased with age (Fig. 1A), with a slight decrease at 18 months. At 12 months, plaque number was significantly ($p<0.05$) higher than at 5 months. At 15 and 18 months this number was significantly ($p<0.05$) higher than at 5 and 8 months. Aβ-positive vessels were low in number or absent in mice between 5 and 15 months old (Fig. 1B). At 18 months there was a significant ($p<0.05$) increase in the number of Aβ-positive vessels compared to all other age groups. Because the number of Aβ-positive vessels was very low, we did not quantify co-deposition of these vessels with the different HSPG.

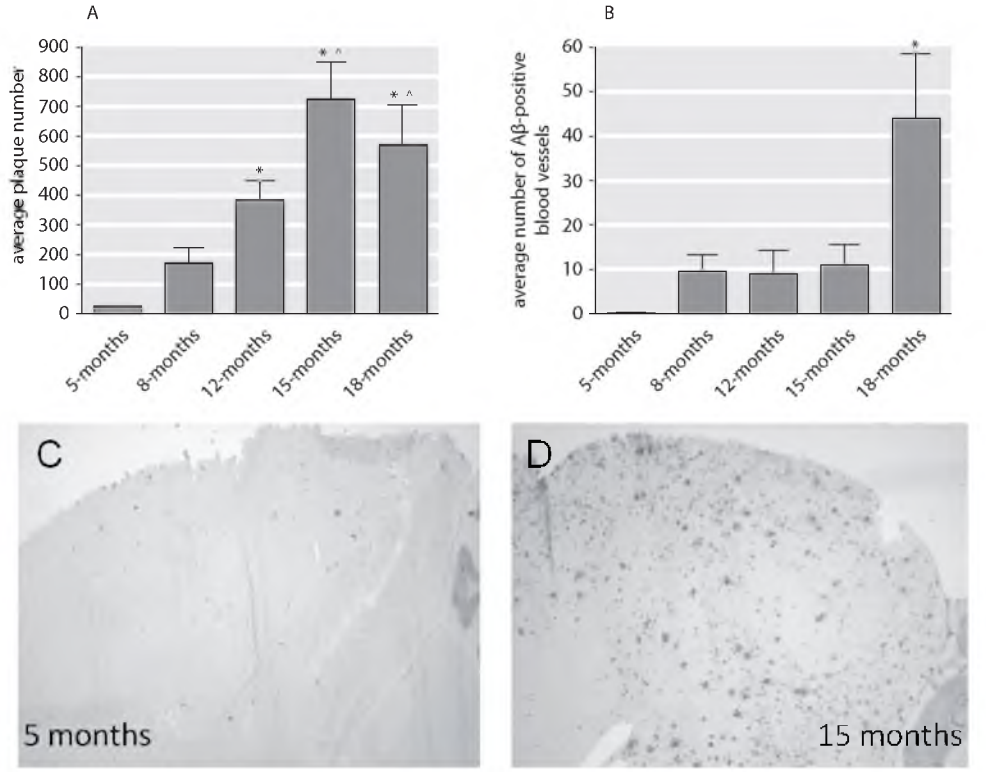

Figure 1: *The average Aβ plaque number (±S.E.M.) increased with age in the APPswe/PS1dE9 mouse model (A), whereas the average number of Aβ-positive blood vessels (±S.E.M.) was low (B), except in the 18-month-old mice. Sagittal sections (5 µm) of mice aged 5 months (C) or 15 months (D) were stained for Aβ using the 6C6 antibody and plaques and Aβ-positive vessels were counted in 8 sections per mouse. (A) * $p<0.05$ compared to 5 months old. ^ $p<0.05$ compared to 8 months old. (B) * $p<0.05$ compared to all other groups. Magnification 200x.*

Expression of HS GAGs and the membrane-associated HSPG glypican-1

To assess HS GAG deposition in APPswe/PS1dE9 mice, the JM403 antibody was used. At 5 months of age, approximately 29% of Aβ plaques were positive for GAG (Fig. 2A). This number decreased to 18% at 8 months and showed a steady incline to 34% at higher

ages, but these changes were not significant (p>0.05). Both Aβ-positive and Aβ-negative cerebral vessels (Fig. 2D) were stained for GAG in all sections. Approximately 9% of Aβ plaques were positive for the glypican-1 antibody (M95) at all ages (Fig. 2B). Although some vessels were stained with M95 (Fig. 2E), vascular staining for glypican-1 was minimal. The immunohistochemical stainings did reveal staining of glial cells with the glypican-1 antibody (inset Fig. 2E).

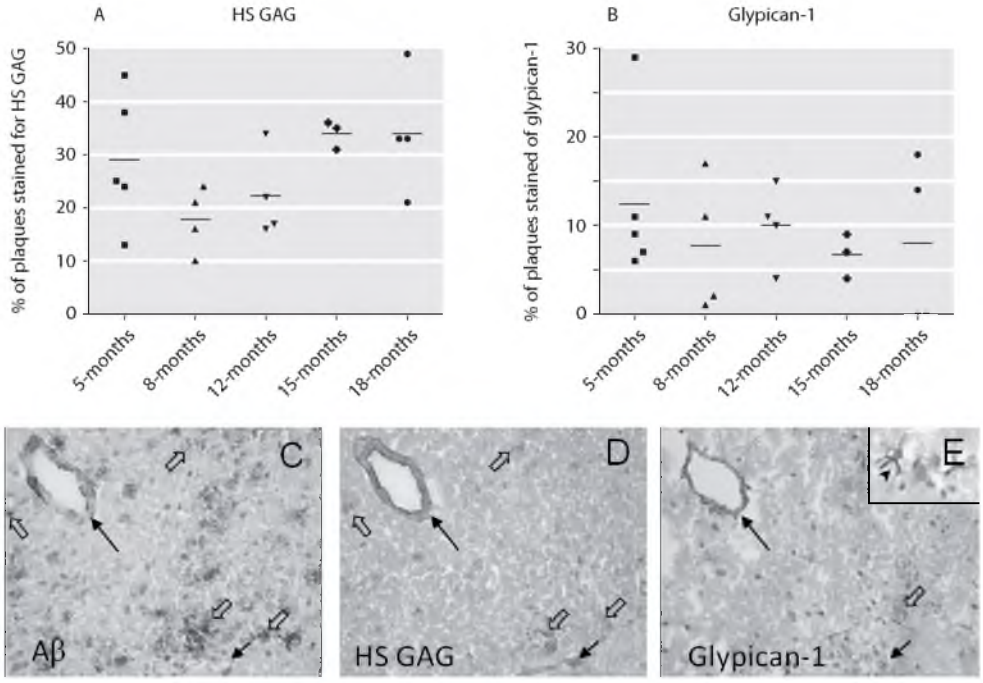

Figure 2: *Percentage of plaques positive for HS GAG (A) and glypican-1 (B). At and above the age of 8 months, the number of HS GAG-positive plaques increased with age (A). However, in 5-month-old mice there was more HS GAG (29%) co-deposition with Aβ than in 8-month-old mice (18%) but this was not significant (p>0.05). The number of glypican-1 positive plaques was low and remained constant with increasing age (B). Immunohistochemical analysis (C-E) of a 15-month-old mouse demonstrated HS GAG and glypican-1 positive plaques (open arrows). An Aβ-negative vessel was positive for HS-GAG (short closed arrow; D) and an Aβ-positive vessel (long closed arrow) was positive for both HS GAG (D) and glypican-1 (E). The inset (E) shows a glial cell positive for glypican-1 (arrowhead). Magnification 200x; magnification inset 400x.*

To assess HS GAG co-deposition with different Aβ species, a serial staining for HS GAG, Aβ40 and Aβ42 was performed (Fig. 3). In 15-month-old APPswe/PS1dE9 mice, Aβ42 plaques were more numerous than Aβ40 plaques, with all Aβ40-positive deposits also being positive for Aβ42 (Fig. 3A vs. 3B). Both Aβ42- and Aβ40- positive plaques were stained for HS GAG (Fig. 3B vs. 3C).

Expression of the extracellular matrix-associated HSPG agrin and perlecan

Staining of plaques with the agrin antibody (BI31) was most frequent at 5 months of age with 11% of plaques being positive for this HSPG (Fig. 4A). Co-localization of agrin with Aβ was not significantly lower (3-7%; $p>0.05$) at 8-18 months and, in general, staining was weak (Fig. 4D). Agrin staining was also detected in many cerebral blood vessels (Fig. 4G), including several Aβ-positive vessels. Antibody MAB1948 for perlecan only weakly stained Aβ plaques for all age groups tested (1-4%; Fig. 4B). However, strong staining for perlecan was detected in many cerebral blood vessels (Fig. 4E and H).

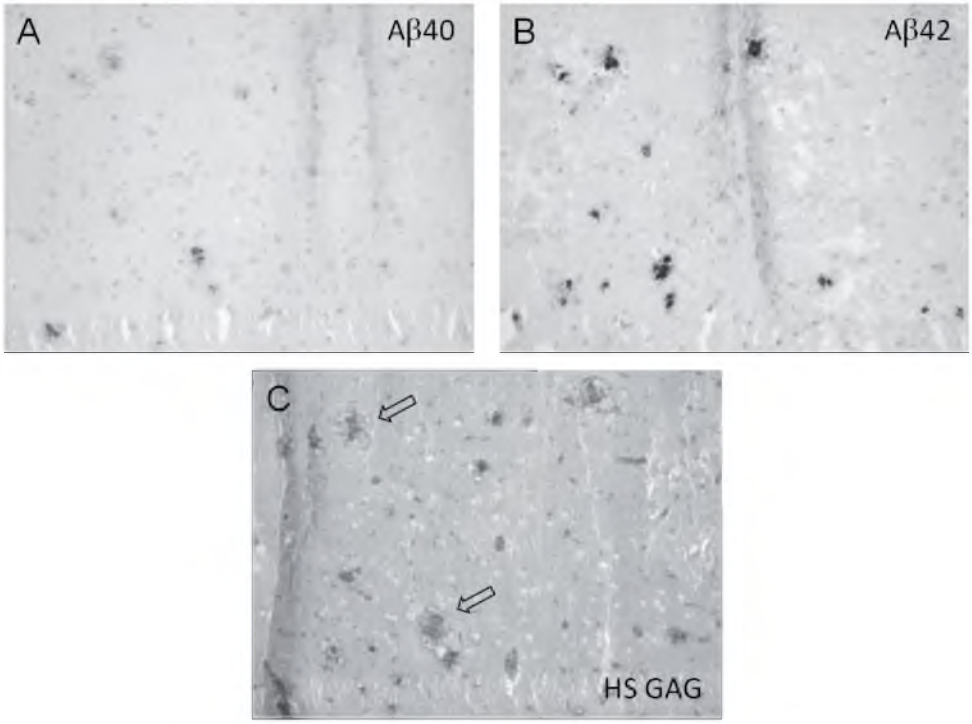

Figure 3: *Aβ40- (A) and Aβ42-positive (B) plaques and co-deposition with HS GAG (C) in a 15-month-old APPswe/PS1dE9 mouse. Aβ42-positive plaques were more numerous than Aβ40-positive plaques. All Aβ40-positive plaques were positive for Aβ42. HS GAG staining could be observed in both Aβ42- and Aβ40-containing plaques (open arrows).*

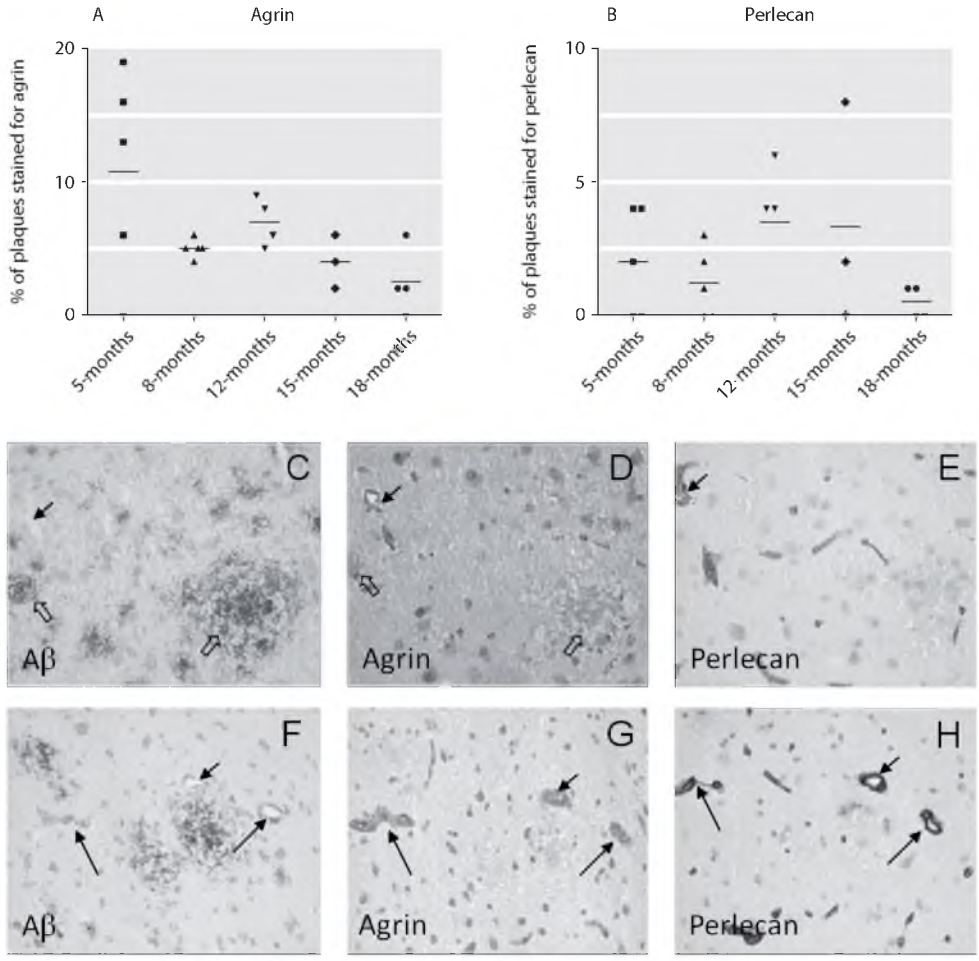

Figure 4: *Percentage of plaques positive for agrin (A) and perlecan (B). The number of agrin and perlecan positive plaques is very low (<10%). Immunohistochemical analysis of an 18-month-old mouse (C-E) demonstrated agrin-positive (open arrows in D) and perlecan-negative plaques (E). Aβ-positive vessels (long closed arrows; F) were positive for agrin (G) and perlecan (H). Normal vessels unaffected by Aβ deposition were also stained by antibodies against agrin and perlecan (short closed arrows in C-E). Magnification 200x.*

Discussion

Due to their close association with Aβ deposits in humans, HSPG are thought to play a crucial role in Aβ deposition. Using the APPswe/PS1dE9 mouse model for AD, we now establish that, although Aβ deposits do contain HSPG as detected by the HS GAG antibody JM403, deposition of HSPG in plaques is less abundant in this mouse model than in humans [254, 255]. In fact, co-deposition of the different HSPG subtypes (i.e. glypican-1, agrin and perlecan) with Aβ deposits was generally detected in less than 10% of the lesions. In contrast, agrin and glypican are present in virtually all cortical and hippocampal senile plaques of human AD patients [254, 263].

Deposition of Aβ in mouse models morphologically resembles deposition in humans, but there are also many differences [129]. Due to overexpression of human APP, its deposition in mice is a much faster process than the natural deposition observed in humans [197]. Mouse Aβ species often do not have the same posttranslational modifications as human Aβ [136] and compact deposits are less dense in mice. While human Aβ plaques can hardly be dissolved, mouse plaques are soluble in most detergent-containing buffers [129]. It was suggested that the increased solubility of mouse plaques compared to human plaques is due to the presence of glycoproteins in human, but not mouse, Aβ deposits [129]. Our data support this idea as we could not detect co-deposition of HSPG at the same level as observed in humans.

There is great variation between different mouse models in terms of AD pathology development. A previous study on HS co-deposition in sporadic AD patients and familiar PS1dE9 patients revealed that HS preferentially accumulated in Aβ40 deposits and were absent in most Aβ42 deposits [180]. Furthermore, in the Tg2576 model, that is known to accumulate substantially more Aβ40 than Aβ42 [122], more than 95% of Aβ deposits were positive for HS [180], although most HS-positive deposits contained both Aβ40 and Aβ42. One characteristic of the APPswe/PS1dE9 mouse model is that it demonstrates a shift in the Aβ40:Aβ42 ratio towards Aβ42 due to expression of the mutated PS1 gene [111]. Indeed, we found more abundant Aβ42 than Aβ40 staining in these mice. However, in contrast to the previous study on Tg2576 mice, in the APPswe/PS1dE9 model HS seem to preferentially, but not exclusively, accumulate in Aβ42-positive plaques. Further study, using more AD mouse models and AD patients, will perhaps elucidate if HS preferentially co-deposit with one particular Aβ species.

Previously, the membrane-bound HSPG glypican-1 and syndecan-3, but not agrin, perlecan or syndecans-1 and -2, were found co-deposited with Aβ in the Tg2576 mouse model [180], with these HSPG apparently expressed by astrocytes and microglia surrounding the Aβ deposits. Using the APPswe/PS1dE9 model, we could detect several HSPG subtypes, albeit in only a low percentage of Aβ plaques. Our glypican-1 antibody (M-95) also stained some astrocytes, suggesting that this cell type, along with other cells such as pericytes [244], may be responsible for expression of this HSPG.

As expected, in our APPswe/PS1dE9 mice we found an increase of Aβ plaque number with age. The decrease in plaque number at 18 months of age was unexpected but may be the result of inter-animal variation. The number of cerebral Aβ-positive vessels in our mouse model was low. Only at 18 months of age did we detect a reasonable number of CAA vessels. Previous immunohistochemical studies in this model [154] also showed late development (i.e. after 16 months) of vascular amyloidosis in this model, although others, using alternative techniques, demonstrated that APPswe/PS1dE9 mice could develop CAA as early as 6 months of age [82]. In any case, due to the low number

of CAA vessels, we could not reliably determine the co-deposition of the different HSPG species with vascular amyloidosis in the APPswe/PS1dE9 mouse model. Unlike glypican-1, agrin and perlecan were present in all cerebral blood vessels, a result that does reflect the human situation [255] and excludes the possibility that the antibodies used in this study did not detect murine HSPG.

In conclusion, we demonstrated minimal co-deposition of HSPG with Aβ in the APPswe/PS1dE9 mouse model for AD. This mouse model did develop progressive Aβ pathology but we did not detect a temporal relation between HSPG and Aβ deposition. Our data suggest that the molecular composition of Aβ deposits in a transgenic mouse model, with respect to the HSPG studied here, does not accurately replicate the composition of human cerebral Aβ deposits as commonly observed in AD brains. This may have important consequences for preclinical intervention studies aimed at removal of Aβ deposits from the brain, since the close interaction between HSPG and Aβ may be crucial for the success of such depletion strategies. The relative absence of HSPG in Aβ deposits in transgenic mouse models may therefore hinder the translation of intervention studies from mice to men. Future studies, using other models, may reveal whether our findings also apply to other transgenic mouse models of AD and to other Aβ-associated factors that are commonly found in human Aβ deposits.

Acknowledgments
This study was supported by a grant from the Internationale Stichting Alzheimer Onderzoek (ISAO, no. 07510), the Netherlands Organization for Scientific Research (NWO/ZonMW, Vidi program, no. 917.46.331) and the Hersenstichting Nederland (no. 14F06.18). We would like to thank Henk Arnts and his colleagues for their excellent care of the animals.

Chapter 5

Do amyloid β-associated factors co-deposit with Aβ in mouse models for Alzheimer's Disease

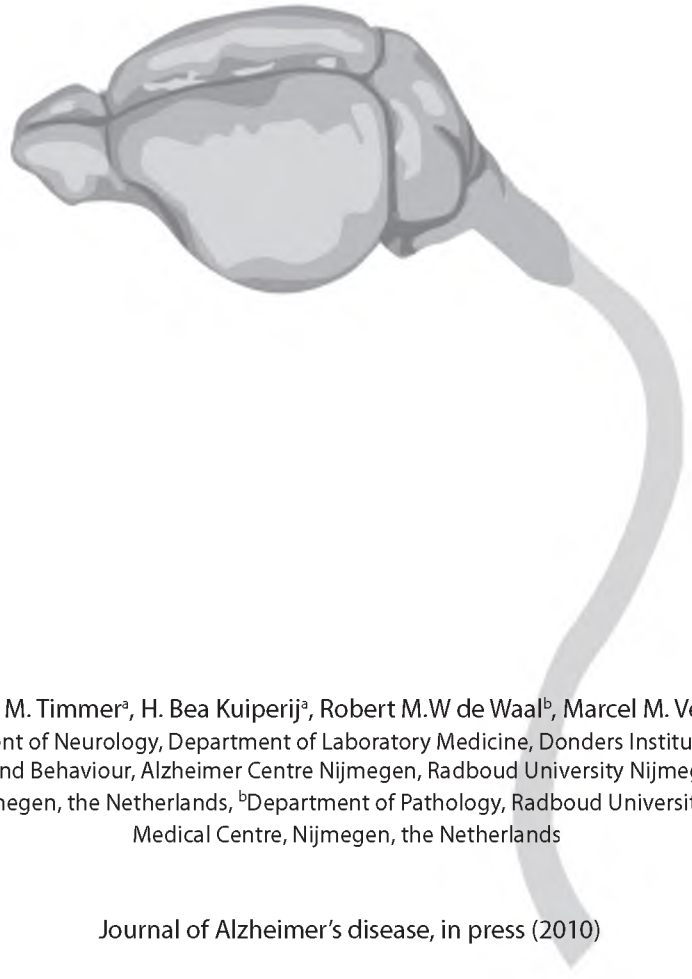

Nienke M. Timmer[a], H. Bea Kuiperij[a], Robert M.W de Waal[b], Marcel M. Verbeek[a]
[a]Department of Neurology, Department of Laboratory Medicine, Donders Institute for Brain, Cognition and Behaviour, Alzheimer Centre Nijmegen, Radboud University Nijmegen Medical Centre, Nijmegen, the Netherlands, [b]Department of Pathology, Radboud University Nijmegen Medical Centre, Nijmegen, the Netherlands

Journal of Alzheimer's disease, in press (2010)

Abstract

Senile plaques and cerebral amyloid angiopathy in Alzheimer's disease (AD) patients not only consist of the amyloid β protein (Aβ), but also contain many different Aβ-associated factors, such as heparan sulfate proteoglycans, apolipoproteins and complement factors. These factors may all influence Aβ deposition, aggregation and clearance and therefore seem important in the development of human Aβ deposits. To study AD pathology and test new therapeutic agents, many different mouse models have been created. By transgenic expression of the amyloid precursor protein, frequently in combination with other transgenes, these animals develop Aβ deposits that morphologically resemble their human counterparts. Whether this resemblance also applies to the presence of Aβ-associated factors is largely unclear. In this review, the co-deposition of factors known to associate with human Aβ deposits is summarized for several different AD mouse models.

Introduction

To investigate disease mechanisms and test new therapeutic agents, animal models are necessary tools. Even though the use of animals is ethically controversial, there are no other models available that are capable of reproducing the complex nature of human physiology. However, mimicking disease is not easy in animal models, since the biological pathways in animals are often not identical to those in humans. Therefore, most models are created as transgenics, expressing (mutated) human proteins implicated in human disease. But even in transgenic models, it remains difficult to accurately model symptoms and pathology of a human disease.

Alzheimer's disease (AD) is pathologically characterized by accumulation of the amyloid β (Aβ) protein in senile plaques (SP) and cerebral amyloid angiopathy (CAA) [85, 294] and by accumulation of hyperphosphorylated tau protein [12]. One of the earliest brain regions affected is the hippocampus, a brain region involved in memory formation. Indeed, memory impairment is one of the main symptoms of AD [24, 230]. The importance of Aβ in the pathogenesis of AD, has been emphasized by the discovery of multiple causative mutations in Aβ-related genes (amyloid precursor protein and presenilin genes) in familial AD [237].

Aβ is a cleavage product of the amyloid precursor protein (APP) and generally comprises either 40 (Aβ40) or 42 (Aβ42) amino acids. APP is a transmembrane protein that can be cleaved by several different secretases to release Aβ and a number of other cleavage products [45, 58, 288]. In the case of Aβ, APP is first cleaved by a γ-secretase [31] and then by a β- secretase [218, 260]. Many of the mutations in APP that cause the familial forms of AD are found close to these APP cleavage sites [237]. Aβ is normally cleared from the brain, but when this clearance process becomes impaired, for example due to aging, Aβ can start to oligomerize and eventually form fibrils. This fibrillization can then result in the formation of Aβ deposits throughout the brain. Besides mutations in APP, pathogenic mutations have also been found in presenilin-1 (PS1) and, to a lesser extent, presenilin-2 [29, 237]. Both these presenilins are part of the γ-secretase complex responsible for Aβ cleavage from APP [31, 289]. These mutations increase Aβ production, in particular of the more fibrillogenic Aβ42 variant [25].

In more than 99% of AD cases ageing is the most important risk factor to develop AD, whereas in less than 1% of cases the disease can be related to gene mutations. However, there are only a few animal species, including dogs and primates, that naturally develop AD-like pathology with advanced age [202]. To create models for AD with a faster development of Aβ pathology, transgenic (Tg) mouse models have been generated based on the introduction of human (mutated) APP, either alone or in combination with (mutated) presenilin genes [80]. Mice are usually the animals of choice for creating transgenics, since they are not only very susceptible to genetic manipulation, but are also relatively easy and cheap to maintain.

The first AD mouse model that was developed was the PDAPP model [79]. In this model, starting at an age of 6-9 months immunohistochemically detectable Aβ deposits developed, that become more dense upon ageing and finally morphologically resemble Aβ deposits found in humans. Furthermore, as seen in humans, the Aβ deposits in the PDAPP mice are surrounded by activated astrocytes and microglia and accompanied by a loss of synaptic density. PDAPP mice also develop cognitive deficits including memory impairment [68], further demonstrating their similarity to human AD patients.

Many more AD mouse models with Aβ pathology have been created since this

first model [80], all characterized by deposition of plaque-like Aβ, and most of them developing cognitive impairment [80]. Due to the different gene combinations and mutations used to create these mice, there are, however, many differences between models. For example, the age of pathology onset in AD models varies greatly. In some mice, such as the TgCRND8 model, deposition starts at an age of 3-6 months [42], while in others, such as the Tg2576 model, it starts at an age of 9-12 months [106]. In general, co-expression of PS1 lowers the age of onset [111], because APP in these mice is more readily cleaved by the γ-secretase [101]. Plaque morphology can also vary greatly between different models. For example, APP23 mice accumulate mostly compact deposits [232], while parenchymal Aβ deposits in TgSwDI mice are mostly diffuse [55]. Contrary to APP23 mice, that develop CAA next to parenchymal deposits [37], TgSwDI mice, but also for example APPDutch mice, accumulate Aβ mainly in the brain vasculature with limited parenchymal deposition [55, 96]. This characteristic makes these latter models suitable models for familial and sporadic cases of vascular amyloid pathology. APP and APP/PS1 models do not develop tau pathology, but tau transgenic mice have been developed [86, 151]. There is also a triple transgenic mouse model available, overexpressing tau, APP and PS1 [181].

Even though most AD mouse models demonstrate Aβ pathology that morphologically resembles human AD pathology, the Aβ deposited in mice is chemically different from human Aβ. In humans, Aβ species undergo posttranslational modifications, such as N-terminal degradation, cross-linking and isomerization. These modifications are either not found in AD mouse models or differ from the human situation [119, 136, 258]. Furthermore, Aβ deposits in mice are usually less compact than in humans, allowing mild extraction buffers to more easily extract Aβ from mouse brains relative to human brains. Finally, progressive AD pathology in humans is characterized by neurodegeneration, a characteristic that is rarely reproduced in AD mouse models [80]. Only the APP23 mouse model has been shown to have some neuronal loss in the CA1 region of the hippocampus [38].

In humans, Aβ deposits not only contain the Aβ protein, but immunohistochemical analyses also demonstrated many other proteins [1, 264, 281]. It is thought that because of their close association, these co-deposited molecules contribute to Aβ aggregation and deposition. Although this has not been proven for all co-depositing proteins, in vitro studies showed that heparan sulfate proteoglycans (HSPG), apolipoprotein E (apoE) and α1 chymotrypsin (α1-ACT), can indeed bind to Aβ, affect its aggregation, stabilize Aβ deposits and protect deposits against proteolytic degradation [156, 256, 286]. Because of their tight association with Aβ, these (glyco-) proteins may greatly influence the outcome of therapeutic intervention in humans, aimed at reducing Aβ aggregation and deposition. Since all new potential AD therapeutics are first tested in mouse models, it is important to know if these Aβ-associated factors are present in the various mouse models. In this review, we aim to examine the validity of AD mouse models with respect to the presence of the main Aβ co-depositing factors HSPG, apoE, complement factors, acute-phase proteins, ICAM-1, cystatin C and CLAC. An overview of the co-deposition of these factors in transgenic AD models is shown in Table 1 and discussed below.

Table 1: *Association of proteins that co-deposit with senile plaques in AD with Aβ deposits in different mouse models for AD.*

Co-depositing factor	AD mouse models						Reference
	Tg2576	PS/APP	APP23 [a]	TgSwDI [b]	APPswe/PS1dE9	APP-YAC	
Heparan sulfate proteoglycans			+				[26, 180, 242]
HS GAG	+				±		
Perlecan [c]	-				±		
Glypican-1	+				±		
Agrin	-						
Syndecans	±						
ApoE	+	+	+	+		+	[33, 134, 135,
ApoJ						+	206, 240, 258]
Complement							[76, 78, 162,
C1q	+	+	± / +	+			191, 206, 300]
C3	+		± / +	+			
C3d			± / +				
C4	+		-	+			
C4d			-				
C7			-				
C9			- / ±				
Acute phase proteins [d]							[132, 206]
Serum amyloid P			-				
α2-macroglobulin		+					
ICAM-1	+						[7]
Crystatin-c	+						[150]
CLAC		+ [e]					[133]

(- no co-deposition; ± weak co-deposition; + strong co-deposition)

[a] only compact Aβ deposits visible

[b] co-deposition with vascular Aβ

[c] expression in senile plaques in AD is controversial

[d] mice do not possess an α1-antichymotrypsin homologue [178]

[e] co-deposition with Aβ40- and Thioflavin S-negative plaques

Heparan sulfate proteoglycans (HSPG)

More than twenty years ago, close association of HSPG with Aβ deposits in humans, both parenchymal and vascular, was first described [220]. HSPG consist of a protein core with several highly sulfated glycosaminoglycan chains attached. These glycosaminoglycan chains consist of repeating disaccharide units. There are several different HSPG species, some membrane-associated (glypicans and syndecans) and some associated with the extracellular matrix (agrin, collagen XVIII and perlecan). HSPG are thought to be involved in numerous (developmental) processes, including neurogenesis, angiogenesis and blood brain barrier permeability [256]. Of the different HSPG species, agrin and glypican-1 are the only two HSPG found in association with all different types of Aβ deposits [52, 254, 255]. The association of perlecan with Aβ deposits is controversial, as one study described this HSPG to have the strongest association [220], whereas we have been unable to detect perlecan in CAA or SP [254, 255]. Overall though, HSPG are key components of human Aβ deposits. Indeed, in vitro analysis has demonstrated that HSPG can bind Aβ with high affinity, mainly through their glycosaminoglycan chains [219]. Through this binding, HSPG can enhance Aβ deposition [41, 52, 256], a process that seems to involve HSPG sulfate moieties [40].

There are only a few studies describing co-deposition of HSPG with Aβ deposits in mouse models. In a characterization study of APP23 mice, it is very briefly mentioned that HSPG co-localize with Aβ deposits [26]. A more elaborate study was done using 20-month-old Tg2576 mice [180]. It was demonstrated that antibodies against heparan sulfate stained more than 95% of the "doughnut"-shaped Aβ deposits visible in this model. Whereas in the APP23 mice no distinction was made between individual HSPG species, in the Tg2576 mice it was discovered that glypican-1 and syndecan-3, but not agrin, perlecan, syndecan-1 and -2, were found in the Aβ deposits. Therefore, in this mouse model the extensive co-deposition of HSPG seen in humans could only partly be reproduced. For example, agrin, a HSPG that is abundantly present in AD senile plaques, was absent from Aβ deposits in mice, demonstrating that the association of individual HSPG species with Aβ pathology may not always match the human situation.

We recently studied deposition of several HSPG species in the APPswe/PS1dE9 mouse model [242]. In this model, in general HSPG were associated with approximately 30% of Aβ deposits. Furthermore, co-localization of the different HSPG species (agrin, glypican-1 and perlecan) occurred in less than 10% of Aβ deposits for each of the species. Therefore, HSPG co-deposition was much less pronounced in this model than in the Tg2576 model or in humans. Due to a low number of detectable vascular deposits, co-deposition of HSPG with CAA vessels could not be determined in this model, nor was it investigated in the Tg2576 model.

Overall, the mouse models seem to differ from human AD pathology in either the type of HSPG species that co-deposit or the number of plaques in which HSPG co-deposition is observed. As previously hypothesized [129], it may be that the lack of glycoproteins, like HSPG, in Aβ deposits in mice is the reason that these deposits are generally less compact and more easily dissolved. It is important to note that HSPGs are an invariant component of all known human amyloidoses, both cerebral and in peripheral organs, pointing to a very important role in amyloidosis in general [225], a property that is apparently partly lacking in Tg mouse models for AD. As far as we know, co-deposition of HSPG has not been studied in mouse models for other types of amyloidosis.

Apoliprotein E

Apolipoprotein E (apoE) is the most prominant apolipoprotein in the central nervous system and mainly produced by astrocytes [27], although other cell types such as pericytes and smooth muscle cells also contribute to cerebral levels [30, 282]. ApoE binds to lipoproteins and mediates their interaction with lipoprotein receptors and endocytosis and in this manner regulates cholesterol homeostasis [185]. There are three isoforms of apoE (apoE2, 3 and 4), and the apoE4 isoform is a well-known risk factor for AD [231], whereas the apoE2 isoform seems to be protective for the development of AD. The exact role of apoE in AD, however, is still elusive [126]. In vitro studies have demonstrated a direct interaction between Aβ and apoE [231] and it is suggested that through this interaction apoE can influence Aβ aggregation and mediate Aβ clearance [126, 156, 286].

The fact that apoE can bind Aβ in vitro, suggests an interaction of these two proteins in vivo. Indeed, clear co-deposition of apoE with human Aβ deposits has been shown. ApoE immunoreactivity is observed in all senile plaques in AD brains, including in diffuse plaques and in the core of amyloid plaques [173, 174, 264, 287], although some authors described the co-deposition with diffuse deposits to be minor [213]. In these studies, apoE was also found in CAA vessels [264] and in dystrophic neurites surrounding plaques.

Co-deposition of apoE with Aβ deposits in mouse models has been well studied and in several models apoE was found co-localized with Aβ. Immunohistochemical analysis of deposits in Tg2576 [135, 240], APP23 [26, 206], PS/APP [33] and APP-YAC mice [134] revealed staining for apoE mostly in (Thioflavin-S positive) fibrillar deposits, with staining of some diffuse deposits. Furthermore, apoE colocalized with astrocyte markers [240], demonstrating that in mice, as in humans, astrocytes are likely responsible for apoE production. In the TgSwDI mouse model, that specifically deposits Aβ in the brain vasculature, apoE is found in close association with these vascular deposits [258]. All these findings in mice are therefore in concurrence with the apoE co-deposition found in humans.

Based on studies using brain material of Down-syndrome patients, it was suggested that apoE contributes to plaque maturation [144]. In these patients, Aβ42 was the first Aβ species to accumulate and apoE co-localization could be detected in these deposits before Aβ40 accumulates. In the Tg2576 model [240], Aβ42 also seems to be the initial Aβ species that deposits, with Aβ40 only visible in more mature deposits. Using the Tg2576 model, it was found that all Aβ deposits positive for apoE contained Aβ42, with only some containing Aβ40. Therefore, since apoE co-deposition in mice resembles that in humans, this suggests that apoE has a similar role in plaque maturation in mice as it has in humans. The function of apoE in Aβ deposition has also been investigated using apoE knockout mouse models. By crossing these knockout mice with AD mouse models [11, 103], it was discovered that apoE expression is key in developing Aβ deposition.

Recently, an increased risk for AD was linked to another apolipoprotein, apoJ [93, 142]. Indeed, this apolipoprotein, but also apoD, is known to co-deposit with Aβ [43, 174] and furthermore apoJ could decrease Aβ aggregation in vitro [161] and in vivo [64]. Co-deposition of apoD has not been studied in AD mouse models. In contrast, in the APP-YAC mouse model [134] co-deposition of apoJ with Aβ has been described. Therefore, in general, it appears that co-deposition of apolipoproteins with Aβ is well replicated in Tg mouse models for AD.

Complement factors

The complement system consists of a cascade of factors that can become activated as part of the innate immune response of the body. Although the liver is the main source of complement, brain glial cells can also produce complement factors [171]. The cascade is triggered when either factor C1q (classical pathway), C3 (alternative pathway) or lectins become activated. Ultimately, a membrane attack complex (MAC), consisting of factor C5b-9, is formed that lyses cells by forming a membrane pore. Besides foreign intruders, the Aβ protein is also known to trigger the complement system by binding to C1q or C3 [28, 115]. Indeed, in AD brain, expression of the complement system is upregulated [298] and recently a complement component receptor (CR1) was identified as a risk factor for AD [142]. Furthermore, several components of the complement system, including C1q, C3 and C5b-9, can be found clearly associated with Aβ deposits [73] and then mostly with fibrillar plaques [155]. Activation of the complement system in turn can stimulate Aβ aggregation [272]. Although the activated complement system can accelerate (Aβ-induced) neurodegeneration [212], there is also evidence that it can protect the brain from Aβ-induced damage [291].

Co-deposition of complement factors in mouse models has been well-studied. In two studies, C1q, C3 and C4 co-deposition in the Tg2576 model was investigated [78, 300]. Strong co-deposition of these three complement factors was found with (Thioflavin-S positive) Aβ deposits. C1q was also strongly expressed in Aβ deposits of PS/APP mice [162] and with the vascular deposits of TgSwDI mice [76]. In APP23 mice, not only was co-deposition of C1q studied, but also that of many more complement factors (C3, C3d, C4, C4d, C7, C9) [191, 206]. With the exception of C1q, C3 and C3d, co-deposition of these factors was weak, with co-deposition of complement factors further down in the cascade (C7, C9) being almost absent.

In summary, it appears that, unlike in human Aβ deposits, only the early components of the complement cascade (C1q, C3) can be detected in Aβ deposits of Tg mouse models. Although these early complement factors co-deposit with Aβ in mice, functionally they differ from their human equivalents. For example, it is known that mouse C1q does not bind human Aβ as efficiently as human C1q does [273] and that mouse C4 cannot activate C5 convertase [71]. Consequently, subsequent activation of the complement system in mice is also less efficient. Since complement can induce neurodegeneration [212], the less efficient activation of this system may explain the relatively low degree of neurodegeneration seen in mouse models [80]. Furthermore, the difference in complement co-deposition and activation between humans and mice may also provide some explanation for the different results that have been found in immunization studies in humans and mice aimed at finding new therapeutic agents [183, 203]. Despite the incomplete activation of the complement pathway in mice, it may still play a critical role in Aβ pathology in mouse models as was demonstrated by a reduction of inflammation and neurodegeneration in an AD mouse model crossed with complement knockout mice [78].

Acute-phase proteins

In AD brains, several acute-phase proteins co-deposit with Aβ, such as serum amyloid P (SAP), α2-macroglobulin (α2M) and α1-antichymotrypsin (α1-ACT) [2, 264]. Acute-phase proteins are proteins that become acutely upregulated in plasma in response to inflammation.

SAP is a glycoprotein that is closely associated with all Aβ deposits in humans [118, 264]. The proposed role for SAP in senile plaques is to protect Aβ fibrils from proteolysis [166]. Besides, SAP may activate the complement system by binding C1q [299]. Only two studies on SAP co-deposition in mouse models have been performed. In one AD mouse model (C57B6/SJL overexpressing APP), SAP did not co-localize with amyloid deposits [214, 215]. It was postulated that SAP, with a molecular weight of ~250 kDa, failed to readily pass the blood brain barrier (BBB). Only when SAP was administered intranasally to transgenic APP mice, could SAP be detected in association with Aβ deposits [215]. Since in humans, SAP can be detected in the AD brain and its production is exclusive to the liver, it was suggested that the integrity of the human BBB must be disturbed. In the APP23 model [206], SAP was also not detected in Aβ deposits, although staining in the periphery of deposits was visible. Therefore, functional disturbance of vessels of APP23 mice was apparently also not severe enough to allow BBB crossing of SAP into the brain [285]. The reduced transport of complement activator SAP into the brain may in turn contribute to the relative lack of complement activation in AD mouse models [206].

α2M, a protease inhibitor, co-localized with senile plaques in humans [252] and is thought to prevent accumulation of Aβ [107]. In a study aimed at investigating the role of α2M in AD, the co-localization of this protein in the PS/APP mouse model was characterized [132]. Starting from 3 months of age, these mice demonstrated Aβ deposition, with some deposits positive for α2M. The number of α2M -positive plaques then increased with age, with α2M mainly depositing in Thioflavin-S positive fibrillar senile plaques. This demonstrates that α2M co-deposition resembles the human situation.

Finally, the acute-phase protein α1-ACT is a serine protease inhibitor that co-deposits with human Aβ deposits [2]. Whereas some describe α1-ACT to enhance Aβ aggregation [75], others demonstrated an inhibition of fibril formation [156], possibly reflecting different effects of α1-ACT depending on the molar ratio between α1-ACT and Aβ [110]. However, as mice do not possess an α1-ACT homologue [178], co-deposition of this acute-phase protein in AD mouse models is not to be expected. Only by creating double transgenic mice for both human α1-ACT and APP, it was possible to study the in vivo role of α1-ACT on Aβ aggregation [178]. Thus, it was demonstrated that α1-ACT increased Aβ levels and plaque load in these mice.

Thus, co-deposition of acute-phase proteins has been studied in a few mouse models only and in these models co-deposition with Aβ was restricted to α2-macroglobulin.

ICAM-1, Cystatin C and CLAC

Besides the above mentioned factors, there are several more proteins that co-deposit with human Aβ, including intercellular adhesion molecule (ICAM)-1, the cysteine protease inhibitor cystatin C and collagenous Alzheimer amyloid plaque component (CLAC). ICAM-1 is closely associated with Aβ deposits in human AD brains, where it can be found in both classic and diffuse senile plaques in the cerebrum [267] and, specifically, in classic deposits in the cerebellum [266]. Similarly, co-deposition of ICAM-1 has been described in Tg2576 mice [7], although its expression is restricted to Thioflavin-S positive deposits.

Cystatin C has been found in both vascular and parenchymal Aβ deposits in AD [150]. On its own, cystatin C can form vascular amyloid deposits, as demonstrated in Icelandic patients suffering from hereditary cerebral hemorrhage with amyloidosis (HCHWA) [182]. Immunohistochemical analysis of 2-year old Tg2576 mice revealed that, similar to the human situation, cystatin C was detected in Aβ deposits of this model [150]. Other AD

mouse models have not yet been investigated for the expression of cystatin C, but the role of cystatin C in Aβ deposition has been studied by creating AD mouse models that overexpress human cystatin C. In these double transgenic mice, cystatin C reduced Aβ deposition [117, 170]. However, a reduction was also found when cystatin C was ablated [233].

By raising antibodies against extracted amyloid deposits, the co-deposition of CLAC with Aβ was discovered [95]. A subsequent in vitro study demonstrated that CLAC can bind Aβ, but only when Aβ is aggregated [95], making CLAC seemingly more selective in its binding than co-depositing proteins such as HSPG and apoE. In brain material of AD patients CLAC was found co-deposited with Aβ42-positive, but not with Aβ40- and Thioflavin S-positive plaques [133]. In the same study, a similar co-deposition of CLAC was found in PSAPP mice and it was suggested that CLAC co-deposited with Aβ in more AD mouse models (unpublished data).

Concluding remarks

Some proteins known to co-deposit with human Aβ also strongly associate with Aβ in mice, with apoE being the most prominent. However, there are also many factors that only partly co-deposit with Aβ in mice or that do not co-deposit at all, in contrast to the situation in AD brains (Table 1). For example, HSPG can be detected in Aβ deposits in mice, but their expression in Tg mouse brains is much more restricted than in humans. Since HSPG are known to stimulate Aβ aggregation and stabilize Aβ deposits, it seems likely that their limited association with Aβ deposits in mice is one of the reasons that these deposits are less compact and easier to dissolve than their human equivalents. Of the complement factors, only the early factors of the cascade co-deposit with Aβ in mice, resulting in a less efficient activation of the complement system and the lack of formation of the membrane attack complex. The absence of a robust complement activation, in turn, may explain the relative absence of neurodegeneration in mouse models for AD. In conclusion, although several transgenic mouse models are far from extensively studied for the association of Aβ-associated proteins with plaques, it appears that the composition of Aβ deposits in transgenic mice is markedly different from human Aβ deposits.

The less pronounced association of the above-mentioned factors may be a consequence of the rapid development of AD pathology in mouse models as compared to human AD patients. Indeed in transgenic mice individual plaques can form within weeks [295] or even within 24 hours [169], therefore, there is probably simply not enough time to allow co-deposition of these Aβ-associated proteins in the relatively constrained time period it takes for Aβ to accumulate in mice. The incomplete replication of the expression of Aβ-associated factors in mice and thus, the molecular composition of Aβ deposits in mice, may in turn imply that the results of Aβ-targeted therapeutics will likely be different in mice than in men. Indeed, there are many discrepancies in the outcomes of therapeutic interventions in mice and humans, with many human trials demonstrating side-effects not seen in mice [183]. Therefore, when using AD mouse models to study Aβ deposition or the effects of therapeutic agents on Aβ deposits, it is necessary to consider the differences in Aβ deposit composition between mice and humans when translating findings in mouse models to the human situation.

Acknowledgments
This work was supported by a grant from the Internationale Stichting Alzheimer Onderzoek (ISAO, no. 07510), the Netherlands Organization for Scientific Research (NWO/ZonMW, Vidi program, no. 917.46.331) and the Hersenstichting Nederland (no. 14F06.18).

Chapter 6

Enoxaparin treatment administered at both early and late stages of amyloid β deposition improves cognition of APPswe/PS1dE9 mice with differential effects on brain Aβ levels

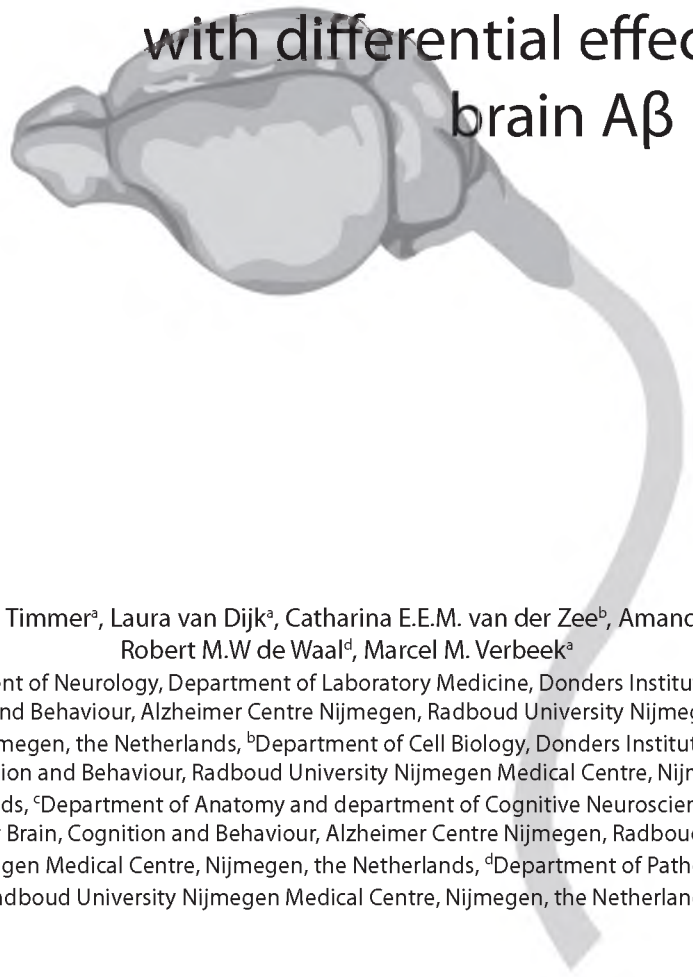

Nienke M. Timmer[a], Laura van Dijk[a], Catharina E.E.M. van der Zee[b], Amanda Kiliaan[c], Robert M.W de Waal[d], Marcel M. Verbeek[a]

[a]Department of Neurology, Department of Laboratory Medicine, Donders Institute for Brain, Cognition and Behaviour, Alzheimer Centre Nijmegen, Radboud University Nijmegen Medical Centre, Nijmegen, the Netherlands, [b]Department of Cell Biology, Donders Institute for Brain, Cognition and Behaviour, Radboud University Nijmegen Medical Centre, Nijmegen, the Netherlands, [c]Department of Anatomy and department of Cognitive Neurosciences, Donders Institute for Brain, Cognition and Behaviour, Alzheimer Centre Nijmegen, Radboud University Nijmegen Medical Centre, Nijmegen, the Netherlands, [d]Department of Pathology, Radboud University Nijmegen Medical Centre, Nijmegen, the Netherlands

Neurobiology of disease **40**(1), 340-347 (2010)

Abstract

Enoxaparin (Enox), a low molecular weight heparin, has been shown to lower brain amyloid β (Aβ) load in a mouse model for Alzheimer's disease. However, the effect of Enox on cognition was not studied. Therefore, we examined the effect of peripheral Enox treatment on cognition and brain Aβ levels in the APPswe/PS1dE9 mouse model by giving injections at an early (starting at 5 months of age) and late (starting at 10 and 12 months of age) stage of Aβ accumulation for three months. Although Enox had no effect on behaviour in the open field at any age, it improved spatial memory in the Morris water maze in 5-, 10- and 12-month-old mice. Furthermore, Enox treatment seemed to decrease guanidine HCl-extracted brain Aβ levels at 5 months of age, but significantly increased guanidine HCl-extracted Aβ42 and Aβ40 levels in both 10- and 12-month-old mice. In vitro, Enox increased aggregation of Aβ, even when Aβ was pre-aggregated.
In conclusion, Enox treatment, either at an early or a late stage of Aβ accumulation, could improve cognition in APPswe/PS1dE9 mice. However, since Enox treatment at an early stage of Aβ accumulation decreased guanidine HCl-extracted Aβ levels and Enox treatment at a late stage enhanced guanidine HCl-extracted Aβ levels, it seems that Enox influences Aβ deposition differently at different stages of Aβ pathology. In any case, our study suggests that enoxaparin treatment has potential as a therapeutic agent for Alzheimer's disease.

Introduction

Alzheimer's disease (AD) is characterized by atrophy of brain tissue caused by neuronal cell loss, particularly in regions involved in memory and learning [165]. Currently, only symptomatic treatment of AD is available and therefore, new therapeutic agents should be aimed at improving cognitive impairments by treating the underlying causes of the disease. One of the pathological hallmarks of AD is deposition of the amyloid β (Aβ) protein in the brain. Aβ is a 4kDa cleavage product of the amyloid precursor protein (APP) and Aβ aggregates, in particular soluble oligomeric aggregates, have been correlated to the extensive neuronal loss observed in AD patients [92, 128].

In the search for new therapeutic agents to prevent Aβ toxicity, compounds that inhibit the production of Aβ, reduce its aggregation or stimulate clearance of Aβ from the brain are being investigated. The success of the latter option has been demonstrated in several vaccination studies where induction of an immune response against Aβ resulted in cerebral Aβ clearance in mice [203] and in humans [177]. Moreover, a reduction was accompanied by improvement of cognition [100, 113]. However, due to serious side-effects (i.e. meningoencephalitis) preclinical trials had to be ended [183] and therefore immune therapy still requires further optimization.

Even though immune therapy is not yet suitable as a therapeutic intervention, it did provide some clues for a possible mechanism of Aβ clearance from the brain. Peripheral administration of Aβ antibodies (m266) led to a decrease in brain Aβ levels that was accompanied by an increase of plasma Aβ levels [61]. It was assumed that by binding to plasma Aβ, antibodies could trigger peripheral degradation of plasma Aβ, leading to a subsequent efflux of Aβ from the brain to reestablish the Aβ equilibrium between brain and plasma (i.e. peripheral sink hypothesis). Binding to plasma Aβ appears to be key, as other Aβ-binding substances, such as gelsolin and GM1, also triggered an efflux of Aβ from brain [163]. Proteins co-depositing with Aβ and with high binding affinity to Aβ are interesting candidates for (peripheral sink) clearance of Aβ.

Several proteins co-deposit with Aβ, such as small heat shock proteins [284] and heparan sulfate proteoglycans (HSPG) [254, 255]. HSPG are believed to play a key role in Aβ deposition by stimulating Aβ fibrillization and preventing Aβ proteolysis [256]. In an effort to inhibit amyloidosis, it was discovered that small sulfated molecules [127] and heparin, a highly sulfated HSPG analogue, could interfere with endogenous HSPG-induced fibrillization of Aβ. Even though heparin is a potential therapeutic agent, its use might lead to severe haemorrhages as it has anti-coagulant properties. Furthermore, because heparin is a mixture of polysaccharides with variable molecular weights ranging from 3,000 to 30,000 kDa, finding an effective therapeutic dose is difficult. In vivo experiments therefore have mostly used low molecular weight heparins, one of which is enoxaparin (Enox).

Enox is currently being used as anti-coagulant treatment in cardiovascular disease and does not lead to severe hemorrhages, proving that it can be tolerated by patients without serious side-effects. A first in vivo experiment, testing the effect of Enox on amyloidosis, was performed using a mouse model for inflammation-associated amyloid (AA) formation in the spleen [301] where Enox reduced AA amyloidosis. Next, in 2004, using the APP23 mouse model for Alzheimer's disease, animals were prophylactically treated with Enox [20] and it was found that Aβ levels had significantly lowered in Enox-treated mice compared to untreated mice. This lowering of Aβ levels was accompanied by a reduction in astrocyte activation, suggesting that Enox attenuated the proinflammatory

response of the brain. However, effects on cognition were not investigated in this mouse model and the exact mode of action of Enox remained unclear.
It was our aim to further investigate the effect of Enox, in both an early and late stage of the disease, on cognition and brain Aβ levels. To this end, we used the APPswe/PS1dE9 mouse model that develops Aβ plaque pathology as early as 4-6 months of age [82, 253] and which is accompanied by severe exploration deficits and cognition impairment [104, 139, 140].

Materials and Methods

APPswe/PS1dE9 (APP/PS1) mice

A colony of APPswe/PS1dE9 (APP/PS1) mice was established at the conventional department of the Central Animal Laboratory of the Radboud University Nijmegen Medical Centre, Nijmegen, The Netherlands, after obtaining the founder animals from Johns Hopkins University, Baltimore (MA), USA. In short, this model was created by co-injecting the two transgenes, with a prion protein promoter, in the pronucleus of single cell C57Bl/6 embryos [112].

Female APP/PS1 mice and non-transgenic (NT) C57Bl/6 littermates were group-housed in standard cages with nestlets and an igloo as cage enrichment. There was a 12 hour light-dark cycle (lights on at 7 am) with a constant temperature of 21±1°C, humidity control and background music during the light phase. Standard food pellets and acidified water (pH 2.5-3) were given ad libitum. This study was approved by the Animal Care Committee of the Radboud University Nijmegen Medical Centre (RU-DEC) and was performed according to the guidelines of the Dutch Council for Animal Care and the European Communities Council Directive of 24 November 1986 (86/609/EEC). Our study was also in concurrence with the European regulations on ethics and responsible conduct regarding scientific communication.

Treatment

Starting at either 5, 10 or 12 months of age, APP/PS1 mice received two (at 5 and 12 months) or three (at 10 months) intraperitoneal injections per week (0.1 ml per injection) of saline (PBS) (n=10, n=14 and n=9 respectively) or 2.5 mg/kg Enox (n=10, n=14 and n=8 respectively) (Sanofi-Aventis, Gouda, The Netherlands) for 12 consecutive weeks. Age-matched NT mice were handled, but not injected, when APP/PS1 mice received their injections (n=8, n=8 and n=6 respectively). Mice were regularly weighed during the injection period and did not show weight loss.

Behavioural analyses

During the injection period, behavioural analyses were performed. On a test day injections were given after the behavioural experiment was performed. Mice were excluded from the behavioural experiments if their vision appeared to be impaired (i.e. clouded eyes), as was the case in 1 mouse (PBS-injected) from the 5-month-old group, 2 mice (PBS-injected) from the 10-month-old group and 2 mice (PBS-injected) from the 12-month-old group.

Rotarod analysis

To test motor skills, mice were individually placed on a rotarod when the rod visibly started to rotate. The time mice spent on the rotarod while it accelerated to about 38 rpm was recorded, with a maximum of 300 seconds. Each mouse performed four trials with a 30 minute inter-trial rest period. Trial 1 was a pre-trial, trial 2 to 4 were averaged to determine the mean time (± standard error) spent on the rotarod.

Open Field

To analyze activity in a novel environment, open field behaviour was studied. The open field consisted of a 50 x 50 x 40 cm white Plexiglas box, placed below a video camera. Mice were placed in the centre of the box and were observed for 30 minutes each. They were

scored for time spent on different types of passive (sitting, grooming) and active (rearing, wall leaning, walking) behaviour, as previously defined [10].

Morris water maze

To test spatial memory, the Morris water maze was performed. A circular pool (diameter of 120 cm) was filled with water of 21-22 °C, until a platform placed in the north-east quadrant was 1 cm below the water surface. The water was made opaque with milk powder and spatial cues were placed around the pool (distance ~ 0.5m). Mice were placed in the pool at different starting positions during four trials per day. Each trial lasted two minutes or until the mouse reached the platform, after which the mice had to stay on the platform for 30 seconds before being removed from the pool. The time needed to find the platform (escape latency) was recorded for each trial. Each mouse performed four trials per day, with a 30-minute inter-trial rest period, for four days. Escape latencies of mice were averaged for each day. After 16 trials, a probe test was performed. In the probe test, the platform was removed and mice were allowed to swim for 2 minutes. DVD recordings of the probe trial were analysed using Ethovision® to score the number of crossings across the old platform location and the time they needed to first cross this location.

Reverse Morris water maze

Using the same pool and conditions as for the Morris water maze, mice again had to find a submerged platform in the reverse Morris water maze. This time the platform was moved to the south-west quadrant of the pool. The escape latency to find the new platform location was measured for two days (four trials/day) and followed by the probe test. Again, using DVD recordings of the probe trial, the same parameters as for the Morris water maze were analysed using Ethovision®.

Transcardial perfusion

After the behavioural tasks, mice were weighed and anesthetized with 2-4% isoflurane and transcardially perfused with sterile PBS (Roche, Mannheim, Germany) to remove blood from the tissues. After the perfusion, mice were decapitated and brains were collected. One hemisphere was snap-frozen in liquid nitrogen and stored at -80°C until further analysis.

Aβ extraction

A two-step extraction using carbonate buffer (soluble Aβ) and guanidine HCl (insoluble Aβ) was performed [55] on the frozen brain hemisphere. Prior to homogenization, the hemisphere was thawed on ice and the olfactory bulb and cerebellum were removed. Tissue was kept on ice until guanidine HCl was added. First, the hemisphere was weighed and homogenized in a tissue grinder with 10 µl/mg 1x carbonate buffer (0.1M carbonate, 50mM NaCl, 0.5% sodium azide, pH 11.5) containing protease inhibitors (Complete, Roche). To shear DNA, the carbonate extract was passed through a 21 gauge needle five times. The extract was then centrifuged for 20 min (4°C, 16,000 xg). The supernatant was collected and stored at -80°C (carbonate extract). The pellet was resuspended in 4 µl/mg of 5M guanidine HCl with protease inhibitors (Complete, Roche) and incubated for three hours on a rotamixer (room temperature). The extract was then centrifuged for 20 min (4°C, 16,000 xg) and the supernatant stored at -80°C (guanidine HCl extract).

ELISA of brain Aβ40 and Aβ42

The carbonate and guanidine HCl extracts of one brain hemisphere were analysed for human Aβ40 and Aβ42 levels by ELISA (Invitrogen, Paisley, UK) according to the manufacturers protocol. A protein assay (Pierce BCA, Thermo Fisher Scientific Inc, Rockford, IL, USA) was performed to determine total protein levels in the different extracts and Aβ levels were normalized to these total protein levels. In line with previous data [82], carbonate extracted (soluble) Aβ levels were much lower (>50 times) than guanidine HCl-extracted (insoluble) Aβ levels. Therefore, in the results we will only present guanidine HCl-extracted Aβ levels.

Thioflavin T analysis

For the Thioflavin-T assay, we used Aβ containing the Dutch mutation (Glu22-->Gln22) as found in HCHWA-D (DAβ1-40) as a model peptide, since this peptide has robust and reproducible aggregation and cytotoxic properties in vitro [54, 243]. DAβ1-40 (QCB; Hopkinton, Massachusetts, USA, 96% pure) was incubated up to 48 hours at 37°C (50 µM) with or without 250 µg/ml heparin (Sigma-Aldrich, St. Louis, MO, USA) or 250 µg/ml Enox in Tris/NaCl buffer (50 mM Tris, 150 mM NaCl, 0.01% sodium azide pH 7.4). In one sample, DAβ1-40 was incubated for 24 hours at 37°C (pre-aggregated DAβ1-40) before Enox was added for the remaining 24 hours. After various time intervals (1, 7, 24 and 48 hours), 20 µl samples were taken from the incubation mixture. These samples were added to 980 µl Thioflavin-T solution (50 mM glycine pH 9.2, 3 µM Thioflavin-T). Samples were excited at 450 nm (slit width 5 nm) and emission fluorescence was measured twice for each sample at 482 nm (slid width 10 nm). Mean emission fluorescence ± standard error was plotted as a function of time.

Statistical analysis

In general, groups were compared using independent unpaired T-tests. Time spent on active/passive behaviour in the open field and escape latencies in (reverse) Morris water maze were analyzed using a repeated measures analysis of variance (ANOVA). Learning curves of mice were also compared in this analysis. Results are presented as mean ± standard error. At each time point measured in the Thioflavin-T assay an unpaired two-sided t-test was performed to compare aggregation of DAβ1-40 with and without heparin or Enox. Statistical significance was reached at $p<0.05$, with $p<0.10$ considered a trend.

Results

Animals and body weight

During 12 weeks, three age groups of APP/PS1 mice received injections with either PBS or Enox. A non-transgenic (NT) group of C57Bl/6 mice served as a control. In both the 5- and 10-month-old group, one PBS-treated APP/PS1 mouse was lost during the injection period, but no Enox-treated APP/PS1 mice. In the 12-month-old group, one PBS-treated and two Enox-treated APP/PS1 mice were lost. No NT mice were lost during the injection period at any age. There were no significant body weight differences within injection groups over time or between injection groups at any point during the injection period (data not shown).

Two injections of Enox per week improved cognition and altered brain Aβ levels in 5- and 12-month-old APP/PS1 mice

We observed no differences in time spent on the rotarod between transgenic (PBS-treated) mice and NT mice or between injection groups at the ages tested (data not shown). The open field observations revealed that at 5 months of age, but not at 12 months of age, PBS-treated APP/PS1 mice tended to spend more time spent walking than NT mice and Enox-treated APP/PS1 mice (data not shown; $F(1,14) = 3.48$, $p=0.08$). There were no differences between NT, PBS-treated and Enox-treated mice in any of the other parameters (data not shown).

Spatial memory of mice was tested in the Morris water maze (Fig. 1). Over the four trial days, NT mice of the 5-month-old group showed a decrease in escape latency from 80 s to 40 s (Fig. 1A). The PBS-treated APP/PS1 mice had a significantly higher escape latency (Fig. 1A; $F(1,14) = 13.38$, $p=0.003$). Enox treatment seemed to lower escape latency of APP/PS1 mice compared to PBS treatment at day 3 and day 4 (Fig. 1A; $F(1,12) = 2.85$, $p=0.12$). The 12-month-old NT mice also showed a decrease in escape latency (from 100 s to 30 s) and PBS-treated APP/PS1 mice again had a significantly higher escape latency than NT mice (Fig. 1D; $F(1,9) = 19.24$, $p=0.002$). Enox-treated APP/PS1 mice had a significantly lower escape latency compared to PBS-treated APP/PS1 mice (Fig. 1D; $F(1,10) = 5.22$, $p=0.045$, day 2 until 4). Furthermore, PBS-treated APP/PS1 mice had a significantly less steeper slope of their learning curve than NT mice ($F(1,9) = 7.0$, $p=0.027$) and Enox-treated APP/PS1 mice ($F(1,10) = 5.63$, $p=0.04$) during the first three trial days (Fig. 1D).

In the probe test of the Morris water maze (Fig. 1 B, C, E and F), 5-month-old PBS-treated APP/PS1 mice had a seemingly lower number of platform crossings than age-matched NT mice (Fig. 1B; 2.0 ± 0.65 vs. 3.5 ± 1.25, $p=0.30$). In addition, PBS-treated animals needed near-significantly more time to cross the former platform location for the first time (Fig. 1C; 71.9 ± 18.0 sec vs. 31.0 ± 13.6 sec, $p=0.09$). Enox treatment of 5-month-old APP/PS1 mice seemed to increase the number of platform crossings (Fig. 1B; 4.2 ± 1.3, $p=0.14$) and significantly lowered the time needed to first cross the platform location (Fig. 1C; 21.7 ± 7.1 sec, $p=0.04$) compared to PBS-treated APP/PS1 mice. The 12-month-old PBS-treated APP/PS1 mice had a significantly lower number of platform crossings (Fig. 1E; 0.33 ± 0.21 vs. 3.80 ± 0.20, $p<0.0001$) and a significantly slower first crossing (Fig. 1F; 100.6 ± 14.7 sec vs. 17.8 ± 5.3 sec, $p=0.0009$) than NT mice. At this age, Enox treatment did not have an effect on the number of platform crossings (Fig. 1E) or on time-to-first-crossing (Fig. 1F) compared to PBS treatment.

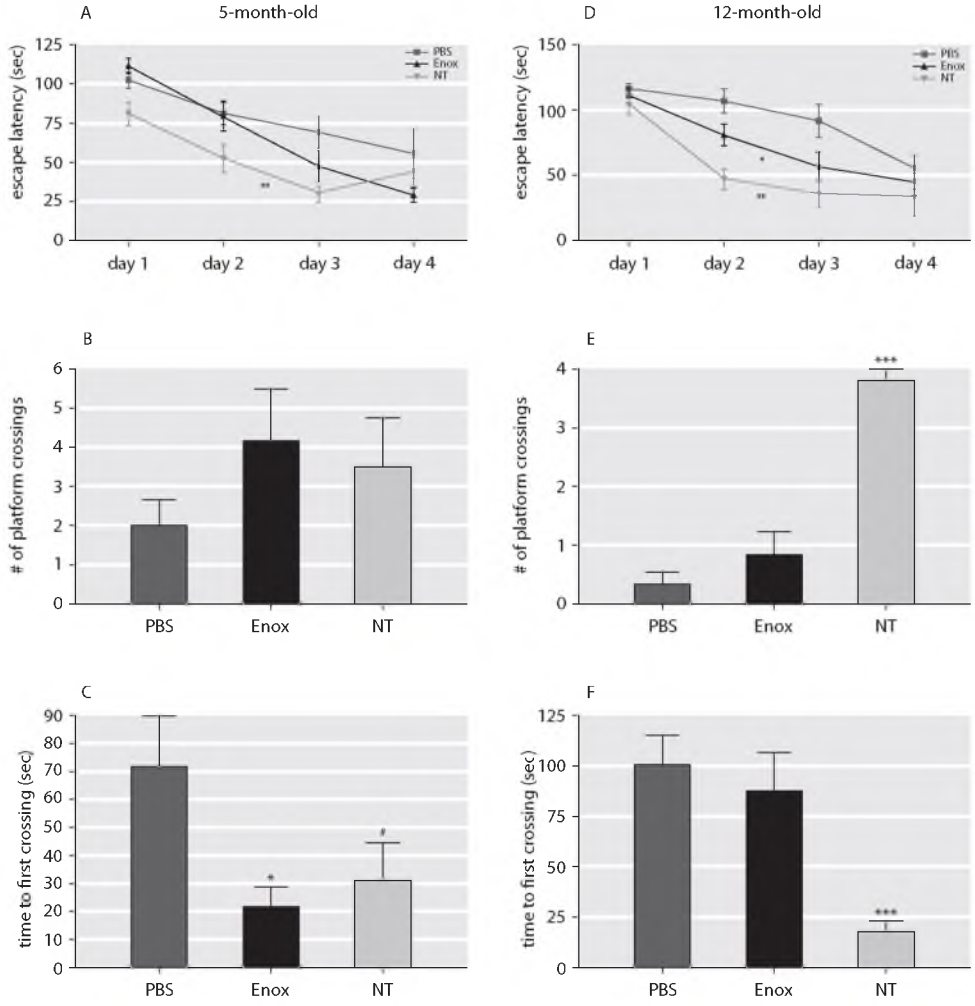

Figure 1: *Performance of 5- and 12-month-old APP/PS1 mice in the Morris water maze. In the acquisition trials, 5- (A) and 12-month-old (D) PBS-treated APPswe/PS1dE9 mice (n=8 and n= 6 respectively) had a significantly higher escape latency over four trial days than NT mice (n=8 and n=5 respectively). Enox treatment seemed to lower escape latency of 5-month-old APP/PS1 mice (n=6) and significantly lowered escape latency of 12-month-old APP/PS1 mice (n=6). In the probe trial of the Morris water maze (B, C, E and F), 5-month-old PBS-treated APPswe/PS1dE9 mice crossed the former platform location less often than NT mice (B) and 5-month-old PBS-treated APP/PS1 mice significantly less often than NT mice (E). At both ages, PBS-treated APP/PS1 mice needed (near-) significantly more time to first cross the old platform location (C and F respectively). Enox treatment increased the number of platform crossings (B) and significantly lowered the time needed to first cross the platform of 5-month-old PBS-treated APP/PS1 (C). In 12-month-old APP/PS1 mice, Enox treatment had no effect on the number of platform crossings (E) or the time to the first crossing (F).*
*# p<0.10, * p<0.05, ** p<0.01, *** p<0.001*

A reverse Morris water maze was performed for 2 days (four trials per day) to assess whether mice could unlearn irrelevant information and relearn a new platform location at the opposite end of the pool. In both the 5-month-old and 12-month-old group, the escape latency of NT mice, PBS-treated and Enox-treated APP/PS1 mice did not differ (data not shown). Similarly, the probe test of the reverse Morris water maze revealed for both 5- and 12-month-old animals no differences in the number of platform crossings between NT mice, PBS-treated APP/PS1 mice or Enox-treated APP/PS1 mice (data not shown). Both 5- and 12-month-old PBS-treated APP/PS1 mice seemed to need more time to first cross the platform compared to NT mice (data not shown; p=0.15 at both ages). The values of the Enox-treated groups were in between those of the other two groups (data not shown).

Aβ levels were determined in guanidine HCl extracts of one brain hemisphere (ng/mg total protein) (Fig. 2). Both brain Aβ40 and Aβ42 levels of 5- and 12-month-old NT mice were hardly detectable (<10 ng/mg). Enox treatment of 5- and 12-month-old APP/PS1 mice did not alter guanidine HCl-extracted brain Aβ42 level (Fig. 2C and D) compared to PBS-treated APP/PS1 mice. However, in 5-month-old Enox-treated APP/PS1 mice, the Aβ40 level was near-significantly lower compared to PBS-treated APP/PS1 mice (Fig. 2A: 0.76 ± 0.07 vs. 1.0 ± 0.10, p=0.07). Furthermore, Enox treatment significantly increased the Aβ40 level of 12-month-old APP/PS1 mice (Fig. 2B: 1.48 ± 0.06 vs. 1.0 ± 0.14, p=0.02).

Three injections of Enox per week improved cognition and altered brain Aβ levels of 10-month-old mice

Based on the above-described findings, we increased Enox treatment to three injections per week in APP/PS1 mice with an intermediary stage of disease (10-month-old). We observed no differences in time spent on the rotarod between NT mice, PBS-treated or Enox-treated APP/PS1 mice (data not shown). Furthermore, in the open field, PBS-treated APP/PS1 mice did not differ in activity from NT mice (data not shown) and Enox treatment did not alter the time spent any of the other parameters compared to PBS treatment (data not shown).

In the Morris water maze (Fig. 3), NT mice showed a decrease in escape latency from 110 s to 20 s over the four trial days (Fig. 3A). PBS-treated APP/PS1 mice had a significantly higher escape latency than NT mice ($F(1,16) = 16.76$, $p=0.001$). Furthermore, the slope of their learning curves was near-significantly less steep ($F(1,16) = 3.22$, $p=0.09$). Enox treatment seemed to slightly lower the escape latency on day 3 and 4 compared to PBS treatment, but this did not reach significance (Fig. 3A; $F(1,20) = 0.65$, $p=0.42$). Furthermore, the slope of the learning curve of Enox-treated APP/PS1 mice did not differ from PBS-treated APP/PS1 mice ($F(1,20) = 0.09$, $p=0.76$).

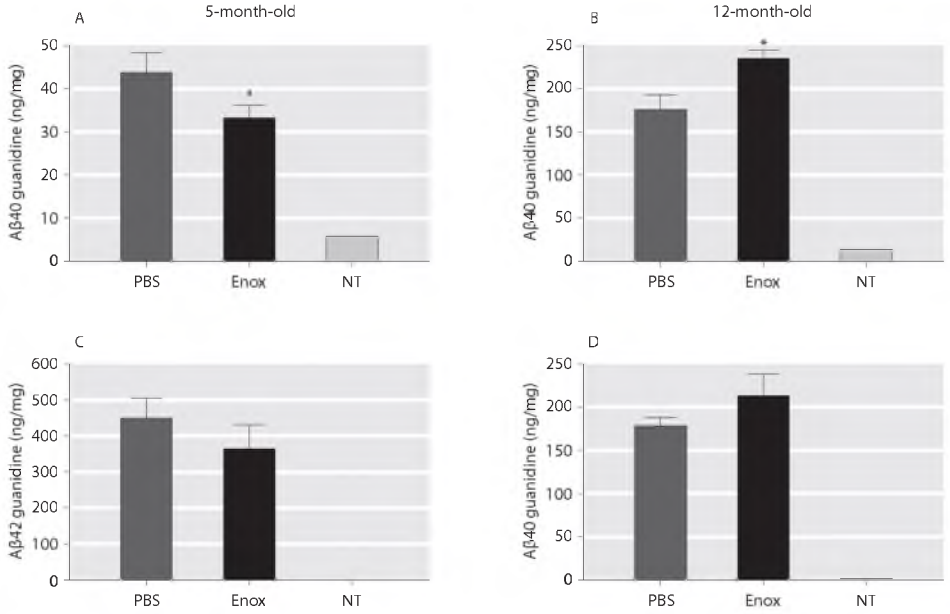

Figure 2: *Guanidine HCl-extracted brain Aβ40 levels (A and B) and Aβ42 levels (C and D) of 5- (A and C) and 12-month-old (B and D) APP/PS1 mice in ng/mg total protein. In 5-month-old APP/PS1 mice, Enox (n=10) had no effect on guanidine HCl-extracted Aβ42 levels (C) but near-significantly lowered guanidine HCl-extracted Aβ40 (A) levels compared to PBS (n=9). In 12-month-old APP/PS1 mice, Enox (n=6) treatment again did not alter guanidine HCl-extracted Aβ42 levels (D) of APP/PS1 mice but significantly increased guanidine HCl-extracted Aβ40 levels (F) compared to PBS (n=8). At both ages, Aβ levels of NT mice were hardly detectable. #p<0.10, * p<0.05*

In the probe test of the Morris water maze, PBS-treated APP/PS1 mice crossed the old platform location significantly less than NT mice (Fig. 3B: 2.1 ± 0.62 vs. 4.25 ± 0.53, p=0.02) and were significantly slower to first cross the platform (Fig. 3C: 52.4 ± 15.1 s vs. 15.3 ± 4.3 s, p=0.05). For the Enox-treated APP/PS1 mice, the number of platform crossings (Fig. 3B: 3.42 ± 0.70) was in between the values of the PBS and NT groups (p=0.18 compared to PBS treatment). The time to first crossing the platform by Enox-treated APP/PS1 mice was significantly reduced compared to PBS-treated APP/PS1 mice (Fig. 3C: 20.67 ± 4.87 s vs. 52.4 ± 15.1 s, p=0.04).

In the reverse Morris water maze, the escape latency of PBS-treated APP/PS1 mice did not differ from NT mice or Enox-treated APP/PS1 mice (data not shown). However, in the probe trial of the reverse Morris water maze (Fig. 4), PBS-treated APP/PS1 mice crossed the old platform location significantly (p=0.04) less than NT mice (Fig. 4A; 2.55 ± 0.64 vs. 4.63 ± 0.65, p=0.04) and they seemed to take more time to first cross the old platform location (Fig. 4B: 55.0 ± 14.5 sec vs. 26.1 ± 8.2 sec), although this was not significant (p=0.14). Enox treatment seemed to increase the number of platform crossings (Fig. 4A; 3.75 ± 0.73, p=0.23) and significantly lowered the time needed to first cross the platform location (Fig. 4B; 18.75 ± 3.71 s, p=0.02) compared to PBS treatment.

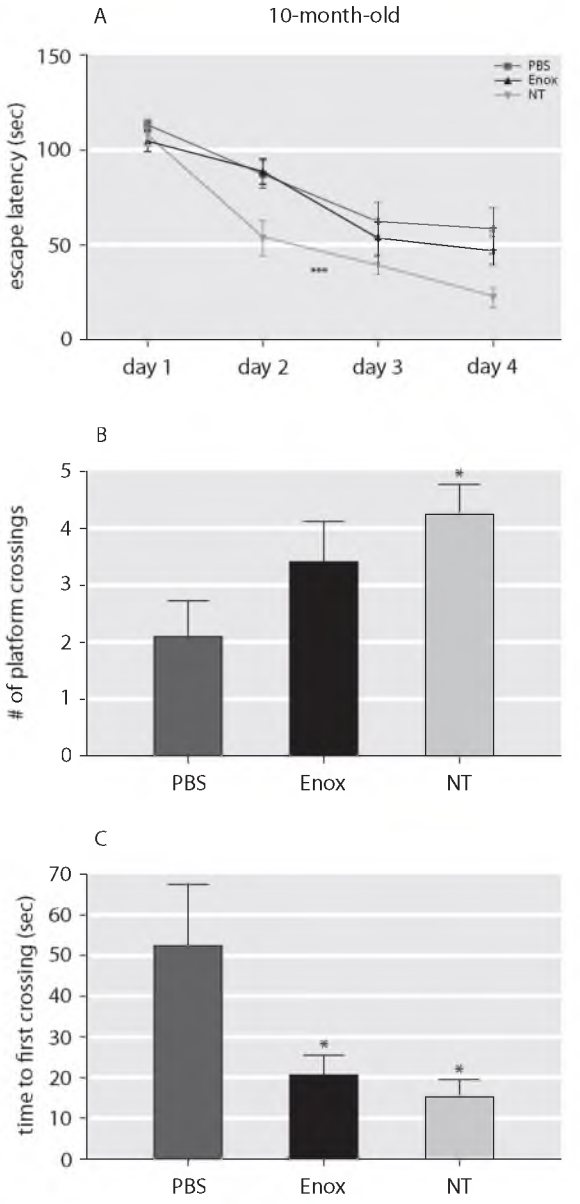

Figure 3: *Performance of 10-month-old APP/PS1 mice in the Morris water maze. In the acquisition trials, PBS-treated APP/PS1 mice (n=10) had a significantly higher escape latency over four trial days than NT mice (A). Treatment with Enox (n=12) had no effect on escape latency. In the probe trial of the Morris water maze (B and C), PBS-treated APP/PS1 mice crossed the former platform location significantly less often than NT mice (n=8) (B) and needed significantly more time to first cross this location (C). Enox treatment slightly increased the number of platform crossings and significantly lowered the time needed to first cross the platform. * $p<0.05$, *** $p<0.001$*

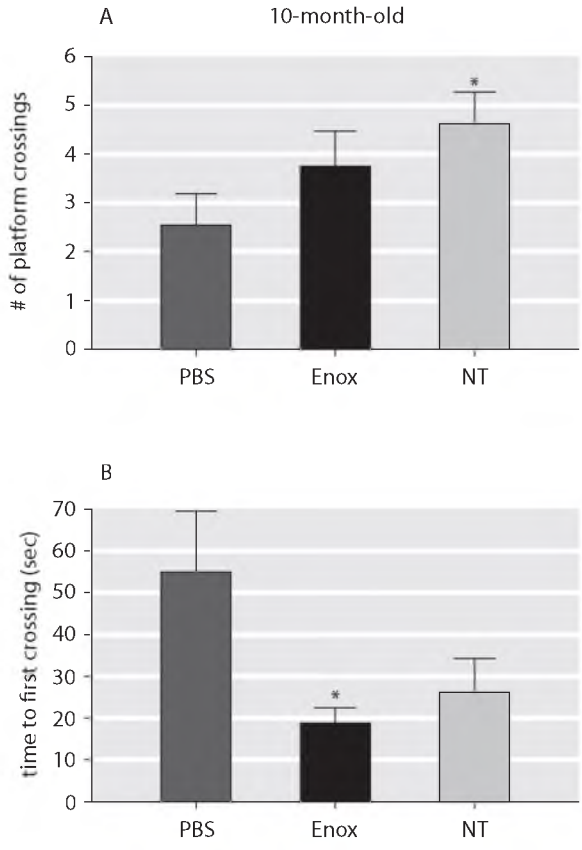

Figure 4: *Performance of 10-month-old APP/PS1 mice in the probe of the reverse Morris water maze. PBS-treated APP/PS1 mice (n=11) crossed the old platform location significantly less often than NT mice (n=8) (A) and seemed to need more time to first cross the location (B). Enox treatment (n=12) increased the number of platform crossings and significantly lowered the time needed to first cross the platform.* p<0.05*

In NT mice, guanidine HCl-extracted brain Aβ40 levels and Aβ42 levels were very low compared to PBS-treated APP/PS1 mice (Fig. 5). Enox treatment seemed to increase guanidine HCl-extracted Aβ40 levels compared to PBS-treated APP/PS1 mice (Fig. 5A: 1.44 ± 0.28 vs. 1.0 ± 0.13, p=0.16) and significantly increased guanidine HCl-extracted Aβ42 levels (Fig. 5B: 1.23 ± 0.07 vs. 1.0 ± 0.05, p=0.01).

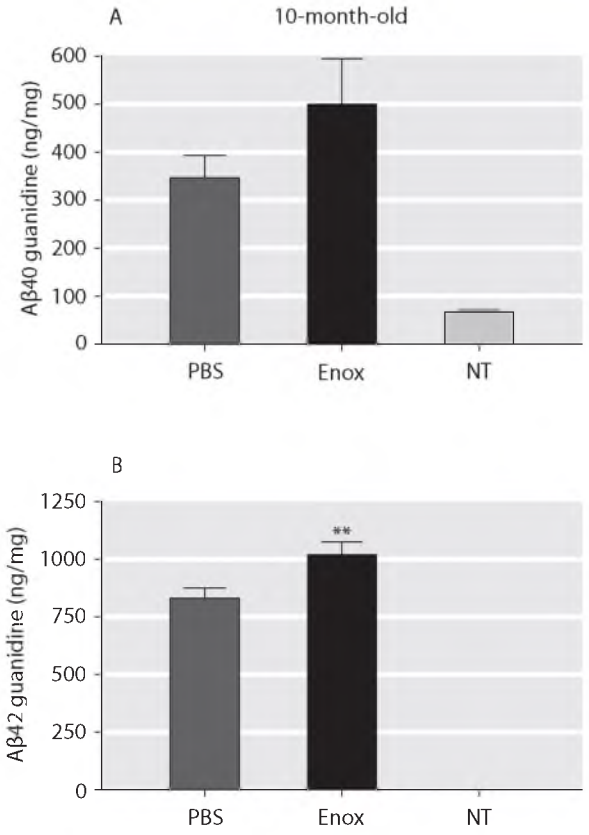

Figure 5: *Guanidine HCl-extracted brain Aβ40 (A) and Aβ42 (B) levels of 10-month-old APP/PS1 mice in ng/mg total protein. Enox (n= 14) seemed to increase guanidine HCl-extracted Aβ40 (A) and significantly increased guanidine HCl-extracted Aβ42 levels (B) compared to PBS (n=12). ** p=0.01*

Enox stimulates Aβ aggregation in vitro

To further investigate the effect of Enox on Aβ aggregation, we performed a Thioflavin T assay (Fig. 6). We used heparin as a positive control, since it is known that heparin stimulates Aβ aggregation [243]. Indeed, heparin significantly increased $DA\beta_{1\text{-}40}$ Thioflavin T fluorescence emission about two- to three-fold after 24 hours (p=0.02) and 48 hours (p=0.04) of incubation. Enox significantly increased $DA\beta_{1\text{-}40}$ fluorescence emission, and thus aggregation, three- to four-fold after 7 hours (p=0.02), 24 hours (p=0.01) and 48 hours of incubation (p=0.03). $DA\beta_{1\text{-}40}$ was also pre-aggregated from 0 to 24 hours, with Enox added from 24 to 48 hours. At 48 hours, Enox significantly enhanced aggregation of pre-aggregated $DA\beta_{1\text{-}40}$ compared to $DA\beta_{1\text{-}40}$ pre-aggregated for 24 hours or aggregated for 48 hours without Enox (p=0.05 and p=0.04 respectively).

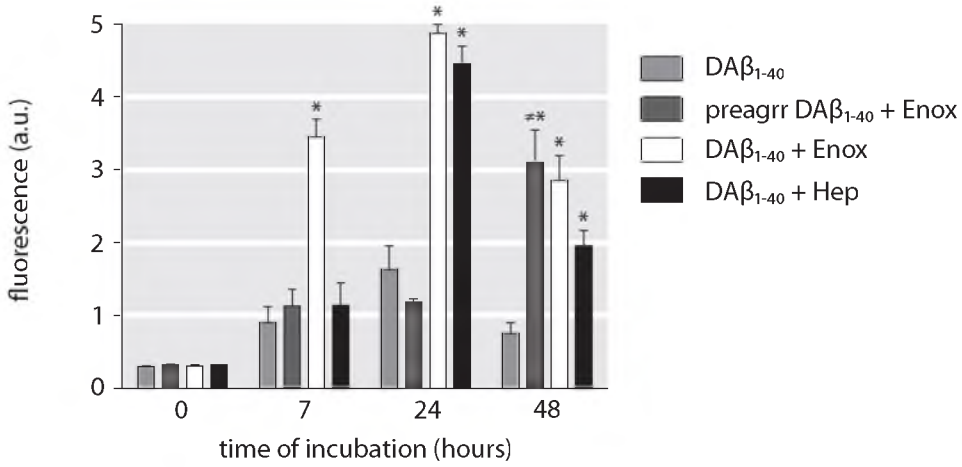

Figure 6: *Thioflavin-T analysis of DAβ$_{1-40}$ with heparin or Enox. DAβ$_{1-40}$ (black bars) was aggregated up to 48 hours (37°C) with either heparin (dark grey bars) or Enox (white bars). Heparin treatment significantly increased Thioflavin-T fluorescence at 24 and 48 hours of incubation. Enox significantly increased fluorescence at 7, 24 and 48 hours of incubation. When DAβ$_{1-40}$ was pre-aggregated for 24 hours (light grey bars), Enox also significantly increased fluorescence. * p<0.05 compared to DAβ$_{1-40}$; ǂ p<0.05 compared to pre-aggregated DAβ$_{1-40}$ (t=24 hours).*

Discussion

Previously it was demonstrated that enoxaparin, a low molecular weight heparin, was able to reduce brain Aβ levels in the APP23 mouse model for Alzheimer's disease [20]. In our study, using three different age groups of the APPswe/PS1dE9 mouse model, we demonstrated that enoxaparin treatment can improve cognition in both an early and late stage of Aβ pathology, but that 1) early treatment decreases (insoluble) brain Aβ levels, whereas 2) late treatment increases (insoluble) brain Aβ levels.

Since the APP23 model used in the previous study did not have significant cognitive impairment at the age tested (12 months old) [123], we chose the APPswe/PS1dE9 mouse model, a model with well-documented impairments in several behavioural tasks [104, 139, 140], to investigate the effect of enoxaparin on cognition. Indeed, we did find impaired spatial memory learning between non-transgenic mice and APPswe/PS1dE9 mice that were not due to impaired motor functions. In the open field, APPswe/PS1dE9 mice were hardly more active than non-transgenic mice, which was unexpected based on previous open field analyses of this model [104]. This finding is perhaps due to an age-related decrease in activity of C57Bl/6 NT mice [141]. Finally, Aβ levels of 5-month-old APPswe/PS1dE9 mice were generally lower than that of 10- and 12-month-old mice, which was as expected [82]. Strikingly, Aβ levels of our 12-month-old mice were generally lower than that of our 10-month-old mice, likely due to inter-assay differences.

In the different behavioural tests, the effects of Enox varied. For example, Enox treatment had no effect on open field activity of the APPswe/PS1dE9 mice tested in this study, neither when they received two injections per week nor when they received three injections per week. This may be the result of the absence of differences in activity levels between APPswe/PS1dE9 and NT mice or because the injection period or dose was insufficient to affect this type of behaviour. In the Morris water maze however, two injections of enoxaparin per week significantly improved spatial memory learning, as detected in the probe (5-month-old mice) and acquisition trial (12-month-old mice) of the Morris water maze. Following three injections per week, the 10-month-old group also demonstrated a significant improvement of cognition performance in the probe trials of both the Morris water maze and the reversal Morris water maze. It is known that mice can have great intertrial variation in performance in the Morris water maze [153] which might explain why in one age-group improved cognition is seen in the acquisition trials and in others in the probe trials. Overall, we conclude that Enox, when administered early or when given at a later stage of Aβ pathology, improves cognition in the APPswe/PS1dE9 mouse model.

We found that Enox seemed to decrease Aβ40 and Aβ42 levels in guanidine HCl extracts of 5-month-old APPswe/PS1dE9 mice. This result is similar to that previously found in APP23 mice treated early with Enox [20]. The effect of late administration of Enox has not yet been described, but we now observed that, unlike in the younger mice, Enox treatment enhanced guanidine HCl-extracted Aβ42 and Aβ40 levels of 12-month-old APP/PS1 mice compared to PBS treatment. A similar result was found when 10-month-old mice, that also have severe Aβ pathology, were injected with enoxaparin three times a week. Therefore, we conclude that Enox influences early Aβ pathology differently than late Aβ pathology.

It is unclear if Enox acts directly in the brain. Indeed, it has been shown that Enox may reduce the Aβ-induced activation of the complement and contact systems in blood [20]. To be able to act in the brain, Enox would have to cross the blood brain barrier (BBB), which appears to be unlikely considering its size (average 4500 dalton) and negative

charge. A similarly sized heparin-like macromolecule, pentosan polysulfate, was unable to cross an in vitro model of the BBB, whereas heparin derivatives of 3 kDa or smaller did cross [148]. It may be that, at least in the younger mice, Enox acted in the peripheral circulation as a peripheral sink agent, lowering brain Aβ levels by clearing Aβ from the blood. However, since in older APPswe/PS1dE9 mice guanidine HCl-extracted Aβ levels increased upon Enox treatment, an alternative mechanism may exist at a later stage of pathology.

It is known that transgenic models for AD can have a (age-dependent) disturbance of BBB integrity [246]. However, as far as we know, BBB integrity of the APPswe/PS1dE9 mouse model has not been investigated. Increased BBB permeability with age would allow easier passage of molecules like Enox across the BBB. As suggested by our in vitro aggregation assay, after entering the brain, Enox may stimulate Aβ aggregation, or enhance it when Aβ is already aggregated. In a previous study it was found that in vitro, Enox had no effect on aggregation of Aβ [20]. However, the time course for this study was only 30 minutes at room temperature, whereas we allowed Aβ to aggregate for a longer time and at physiological temperatures. Of course, the conditions of our in vitro aggregation assay may differ from in vivo conditions, since Aβ usually does not contain the Dutch mutation and the absolute concentrations and ratio of Aβ and Enox is likely different. Furthermore, in vivo other proteins may also influence the interaction between Aβ and Enox.

Since Aβ deposition is considered to be one of the major factors contributing to AD development [92, 165], most studies, aimed at finding new therapeutic agents, focus on improving cognition by decreasing Aβ levels. Indeed, many studies, including this study on early Enox treatment of APPswe/PS1dE9 mice, show that decreased Aβ levels are accompanied by improved cognition [167, 187]. However, our study now suggests that an improved cognition can also be accompanied by increased (guanidine HCl-extracted) brain Aβ levels at a later stage of disease development. It is assumed that low-n oligomeric species of Aβ (i.e. dimers and trimers) mediate neurotoxicity [269] and that these species are likely to be precursors of mature fibrils. Therefore, it may be that the increases in guanidine HCl-extracted Aβ levels we found in the older mice, reflect decreases in these more toxic species. It should be mentioned that we did not inject our NT mice with Enox and therefore it cannot be excluded that Enox improved cognition independent of its effects on Aβ levels.

In conclusion, our data confirm the previously demonstrated potency of enoxaparin as a therapeutic agent for Alzheimer's disease, although its exact effect on brain Aβ levels and exact mechanism of action remains unknown. A preclinical prophylactic study of enoxaparin has already been started [21], which should further elucidate the effects of enoxaparin in human AD patients.

Acknowledgments
This study was supported by a grant from the Internationale Stichting Alzheimer Onderzoek (ISAO, no. 07510), the Netherlands Organization for Scientific Research (NWO/ZonMW, Vidi program, no. 917.46.331) and the Hersenstichting Nederland (no. 14F06.18). We would like to thank Henk Arnts and his colleagues for their excellent care of the animals.

Chapter 7

The small heat shock protein αB crystallin slightly affects cerebral Aβ deposition, but not cognition mouse models for AD

Nienke M. Timmer[a], Laura van Dijk[a], Sharon Degener[a], Catharina E.E.M. van der Zee[b], Alexandra Versleijen[a], Wilbert Boelens[c], Amanda J. Kiliaan[d], William E. van Nostrand[e], H. Bea Kuiperij[a], Robert M.W de Waal[f], Marcel M. Verbeek[a]

[a]Department of Neurology, Department of Laboratory Medicine, Donders Institute for Brain, Cognition and Behaviour, Alzheimer Centre Nijmegen, Radboud University Nijmegen Medical Centre, Nijmegen, the Netherlands, [b]Department of Cell Biology, Donders Institute for Brain, Cognition and Behaviour, Radboud University Nijmegen Medical Centre, Nijmegen, the Netherlands, [c]Department of Biomolecular Medicine, Nijmegen Center for Molecular Life Sciences, Radboud University, Nijmegen, The Netherlands, [d]Department of Anatomy, Department of Cognitive Neuroscience, Donders Institute for Brain, Cognition and Behaviour, Alzheimer Centre Nijmegen, Radboud University Nijmegen Medical Centre, Nijmegen, the Netherlands, [e]Neurosurgery and Medicine, Stony Brook University, Stony Brook, New York, USA, [f]Department of Pathology, Radboud University Nijmegen Medical Centre, Nijmegen, the Netherlands

Abstract

Amyloid β (Aβ) accumulation in Alzheimer's disease (AD) is aggravated by disturbed cerebral clearance. Currently, there is no curative treatment for AD. According to the peripheral sink hypothesis, peripheral administration of Aβ-binding agents may reduce blood Aβ levels and drain Aβ from the brain across the blood-brain barrier. One small heat shock protein, αB-crystallin, binds Aβ with high affinity. Therefore, we tested if αB-crystallin can act as a peripheral sink agent. We injected APPswe/PS1dE9 and TgSwDI mice with αB-crystallin for three months and investigated the effect on behaviour and brain Aβ levels. In APPswe/PS1dE9 mice, αB-crystallin had no effect on activity or cognition and slightly increased Aβ40 levels. In TgSwDI mice, αB-crystallin normalized activity (i.e. walking and sitting) to levels of controls and decreased brain Aβ42 levels, without affecting cognition. Overall, we conclude that there is currently no evidence that αB-crystallin could serve as an effective therapeutic agent for AD.

Introduction

Alzheimer's disease (AD) is pathologically characterized by accumulation of amyloid β (Aβ) protein in the brain. Aβ is a 4kDa cleavage product of the amyloid precursor protein (APP) that is normally removed from the brain by degradation or clearance [149]. There are two peptidases involved in extracellular Aβ degradation, insulin degrading enzyme (IDE) [188] and neprilysin (NEP) [109]. There is also evidence for phagocytosis of Aβ by microglia and subsequent intracellular degradation [16, 203]. Furthermore, Aβ can be transported across the blood brain barrier by, for instance, LDL-receptor-related protein 1 (LRP-1) [216]. With age, Aβ removal from the brain becomes less efficient [149], Aβ levels in brain rise and Aβ starts to deposit, forming (senile) plaques in the parenchyma and accumulations in the vascular walls. However, not the fibrillar deposits but soluble, oligomeric Aβ species have been correlated to the extensive neuronal loss observed in AD patients [92, 128]. Currently there is no cure for AD, only symptomatic treatment can be administered.

There is much interest in compounds that enhance removal of Aβ from the brain. One extensively studied therapeutic approach is immune therapy that relies on the induction of an immune response against Aβ to reduce brain Aβ levels. Ideally, these reduced Aβ levels should be accompanied by improvements in cognitive behaviour. Vaccination studies of mice [203] and humans [177] have indeed demonstrated a reduction in brain Aβ levels as a result of cerebral Aβ clearance, accompanied by improved cognition [100, 113]. However, a follow-up study investigating long term effects of immunization did not demonstrate any effect on cognition, even though mean brain Aβ levels were lower than unimmunized controls [102]. Furthermore, due to serious side-effects (i.e. meningoencephalitis) preclinical trials had to be ended [183]. Therefore, immune therapy still requires further optimization before being applicable as a therapeutic intervention.

Even though immunization is not yet suitable for therapeutic intervention, it did provide some clues to a possible mechanism of Aβ clearance from the brain. Peripheral administration of Aβ antibodies (m266) led to a decrease in brain Aβ levels that was accompanied by an increase in plasma Aβ levels [61]. It was assumed that by binding to plasma Aβ, antibodies could trigger peripheral degradation, leading to a subsequent efflux of Aβ from the brain to reestablish the Aβ equilibrium between brain and plasma (i.e. peripheral sink hypothesis). Binding to plasma Aβ appears to be key as other Aβ-binding substances, such as gelsolin and GM1, also trigger an efflux of Aβ from the brain [163]. Proteins co-depositing with Aβ are likely to have high binding affinity to Aβ and are less likely to generate the side-effects seen with antibody treatment, making these proteins interesting candidates for (peripheral sink) clearance of Aβ.

Previously, we examined the interaction of small heat shock proteins (sHsp) with Aβ. Small Hsp are chaperone proteins involved in proper folding of proteins [32]. In total, ten human sHsp have been described [121], all possessing an α-crystallin domain. Since misfolding of Aβ is the main reason for its accumulation, it would be expected that sHsp are associated with Aβ in the brain. Indeed, several members of the sHsp family can be detected in Aβ deposits. Hsp20, Hsp27, HspB2/B3 and HspB8 can be found co-localized with senile plaques, with HspB2/B3 also co-localized with cerebral amyloid angiopathy (CAA) [284]. The only sHsp that is not co-localized with Aβ deposits in vivo is αB-crystallin. However, in vitro αB-crystallin demonstrated the strongest association with Aβ [279]. This sHsp strongly inhibited Aβ-induced cellular toxicity, suppressed β-sheet conformation of aggregating Aβ and had the strongest binding affinity to Aβ of all sHsp tested.

Since αB-crystallin can strongly bind Aβ in vitro, we aimed to investigate if αB-

crystallin can reduce brain Aβ levels and act as a peripheral sink agent in vivo. To this end, we used two different mouse models for AD. The APPswe/PS1dE9 mouse model develops Aβ plaque pathology as early as 4-6 months of age and has severely impaired cognition [82, 253]. The TgSwDI model accumulates Aβ mainly in the vasculature, starting at an age of about 3 months [55]. This specific vascular accumulation of Aβ is due to a reduced affinity of LRP-1 to Aβ with Dutch and Iowa mutations [56], preventing this latter model to sustain a peripheral sink mechanism [259].

Materials and Methods

APPswe/PS1dE9 and TgSwDI mice

A colony of APPswe/PS1dE9 (APP/PS1) mice was established at the conventional department of the Central Animal Laboratory of the Radboud University Nijmegen Medical Centre, Nijmegen, The Netherlands, after obtaining founder animals from Johns Hopkins University, Baltimore (MA), USA. In short, this model was created by co-injection of two transgenes for APP with the swedish mutation and PS1 with a deletion in exon 9, under control of a prion protein promoter, in the pronucleus of single cell C57Bl/6 embryos [112]. An additional colony of transgenic mice expressing human APP with the Swedish, Dutch and Iowa mutations (TgSwDI), under control of the Thy-1 promoter, was also established at the Central Animal Laboratory of the Radboud University Nijmegen Medical Centre. Founder animals of this transgenic line were obtained from Stony Brook University, Stony Brook (NY), USA [55].

Female APP/PS1 mice, TgSwDI mice and non-transgenic (WT) C57Bl/6 control mice were group-housed in standard cages with nestlets and an igloo as cage enrichment. There was a 12 hour light-dark cycle (lights on at 7 am), with a constant temperature of 21±1°C, humidity control and background music during the light phase. Standard food pellets and acidified water (pH 2.5-3) were given ad libitum. This study was approved by the Animal Care Committee of the Radboud University Nijmegen Medical Centre (RU-DEC) and was performed according to the guidelines of the Dutch Council for Animal Care and the European Communities Council Directive of 24 November 1986 (86/609/EEC). Our study was also in concurrence with the European regulations on ethics and responsible conduct regarding scientific communication.

Recombinant mouse αB-crystallin production

To minimize the induction of an immune response, mouse αB-crystallin was used. Mouse αB-crystallin was either purified by column chromatography or by affinity chromatography using a histidine tag, generating mouse-αB-crystallin and mouse αB-crystallin-His respectively. For αB-crystallin without His-tag, the coding region was cloned into a pET16b vector. Subsequently, mouse αB-crystallin was expressed in Rosetta DE3 plysS competent cells (Invitrogen, Paisley, UK). A culture inoculated from a single colony was incubated for 3 hours at 37 °C. Production of mouse αB-crystallin was induced by addition of isopropyl-thio-β-D-galactopyranoside (IPTG) at a final concentration of 0.37 mM. Cells were harvested in TEG (25 mM Tris pH 8.0, 2 mM EDTA, 50 mM glucose) with protease inhibitors (Complete mini EDTA-free, Roche, Mannheim, Germany) and lysed by sonication. Purification of mouse αB-crystallin was performed using a DEAE-Sepharose Fast Flow column (Pharmacia, Freiburg, Germany) and a linear NaCl gradient from 0 up to 1M in TNE buffer (25 mM Tris pH 8.0, 1M NaCl, 2mM EDTA). For further purification a Source 15 Q column (Amersham, Uppsala, Sweden) was used, again with a linear NaCl gradient in TNE buffer (0-1 M, pH 8.5). Finally, the buffer was exchanged to phosphate buffered saline (PBS) using iCon concentrator spin columns (9 kDa cut-off, Thermo Fisher Scientific, San Jose, CA, USA).

For the production of mouse αB-crystallin-His, the pET46EK vector was used to introduce a N-terminal His-tag sequence, was used. Again, mouse αB-crystallin was expressed in Bl21(DE3) plysS competent cells and production was induced by addition of 0.375 mM IPTG. Cells were lysed by sonication in native lysis buffer (NLB) (50 mM NaH-2PO4, 300 mM NaCl, pH 8.0) supplemented with EDTA-free protease inhibitors (Complete,

Roche). For purification of the protein, Ni-NTA agarose beads (Qiagen, Hilden, Germany) were used. Mouse αB-crystallin-His was allowed to bind to the agarose beads for 1 hour (4°C), after which beads were brought into a polypropylene column (Qiagen) and washed and eluted with NLB supplemented with increasing amounts of imidazole (Sigma-Aldrich, St. Louis, MO, USA). Eluted fractions were collected and analyzed using 12% SDS-page gels, to determine which fraction contained the purified protein. An iCON concentrator spin column was used to concentrate mouse αB-crystallin-His and to exchange the buffer to PBS. For both mouse αB-crystallin and mouse αB-crystallin-His, a BCA protein assay (Pierce BCA, Thermo Fisher Scientific Inc, Rockford, IL, USA) was performed to determine protein concentration. Purity of both mouse αB-crystallin and mouse αB-crystallin-His was >95%.

Treatment

Starting at an age of 12 months, APP/PS1 mice received two intraperitoneal injections per week (0.1 ml per injection) of PBS (n=9) or 750 µg/kg mouse αB-crystallin in PBS (n=12) for 12 consecutive weeks. Age-matched WT mice (n=6) were handled similarly, but not injected, when the transgenic mice received their injections. Similarly, 9-month-old TgSwDI mice received three intraperitoneal injections per week of PBS (n=12) or 750 µg/kg mouse αB-crystallin-His (n=11). Again, age-matched WT mice (n=12) were handled when the transgenic mice received their injections. Mice were regularly weighed during the injection period.

Behavioural analyses

After 5 weeks of injections, behavioural analysis was started. Injections continued during the behavioural testing, but on a test day injections were given after the behavioural experiment was performed. Mice were excluded from the behavioural experiments if they were blind (i.e. cloudy eyes) and therefore we excluded 2 animals (one in the PBS-group and one in the αB-crystallin-group) from the TgSwDI group. Because of the low number of surviving animals in the αB-crystallin-treated group of APP/PS1 mice, in this group we did not exclude data of mice that were blind in one eye (n=2). These blind mice performed similarly to non-blind αB-crystallin-treated mice in the behavioural analyses.

Rotarod analysis

To test motor skills, mice were individually placed on a rotarod, after the rod had started to visibly rotate. The time mice spent on the rotarod while it accelerated to about 38 rpm was recorded, with a maximum of 300 seconds. Each mouse performed four trials with a 30 minute inter-trial rest period. Trial 1 was a pre-trial, trial 2 to 4 were averaged to determine the mean time (± standard error) spent on the rotarod.

Open Field

To analyze exploration and activity in a novel environment, open field behaviour was studied. The open field consisted of a 50 x 50 x 40 cm white Plexiglas box, placed below a video camera. Mice were placed in the centre of the box and were observed for 30 minutes each. They were scored for time spent on different types of passive (sitting, grooming) and active (rearing, wall leaning, walking) behaviours, as previously defined [10].

Morris water maze

To test spatial memory, the Morris water maze was performed. A circular pool (diameter of 120 cm) was filled with water of 21-22 °C, until a platform placed in the north-east quadrant was 1 cm below the water surface. The water was made opaque with milk powder and spatial cues were placed around the pool (distance ~ 0.5m). Mice were placed in the pool at different starting positions during four trials per day. Each trial lasted two minutes or until the mouse reached the platform, after which the mouse had to stay on the platform for 30 seconds before being removed from the pool. The time needed to find the platform (escape latency) was recorded for each trial. Each mouse performed four trials per day, with a 30-minute inter-trial rest period, for four days. Escape latencies of mice were averaged for each day. After 16 trials, a probe test was performed. In the probe test, the platform was removed and mice were allowed to swim for 2 minutes. DVD recordings of the probe trial were analysed using Ethovision®, to score the number of crossings across the old platform location and the time they needed to first cross this location.

Reverse Morris water maze

Using the same pool and conditions as for the Morris water maze, mice again had to find a submerged platform in the reverse Morris water maze. This time the platform was moved to the south-west quadrant of the pool. After two days (four trials/day), mice had to perform the probe test. Again, using DVD recordings of the probe trial, the same parameters as for the Morris water maze were analysed using Ethovision®.

Transcardial perfusion

After the behavioural tasks, mice were weighed, anesthetized with 2-4% isoflurane and transcardially perfused with sterile PBS (Roche, Mannheim, Germany). After the perfusion, mice were decapitated and brains were collected. One hemisphere was snap-frozen in liquid nitrogen and stored at -80°C until further analysis.

Aβ extraction

A two-step extraction using carbonate buffer (soluble Aβ) and guanidine-HCl (insoluble Aβ) was performed on a frozen brain hemisphere. Prior to homogenization, the hemisphere was thawed on ice and the olfactory bulb and cerebellum were removed. Tissue was kept on ice extraction until guanidine-HCl was added. First, the hemisphere was weighed and homogenized in a tissue grinder with 10 µl/mg 1x carbonate buffer (0.1M carbonate, 50mM NaCl, 0.5% sodium azide, pH 11.5) containing protease inhibitors (Complete, Roche). To shear DNA, the carbonate extract was passed five times through a 21 gauge needle. The extract was then centrifuged for 20 min (4°C, 16.000 rcf). The supernatant was collected and stored at -80°C (carbonate extract). The pellet was resuspended in 4 µl/mg of 5M guanidine-HCl with protease inhibitors (Complete, Roche) and incubated for three hours on a rotamixer (room temperature). The extract was then centrifuged for 20 min (4°C, 16.000 rcf) and the supernatant was stored at -80°C (guanidine-HCl extract).

ELISA of brain Aβ40 and Aβ42

The carbonate and guanidine-HCl extracts of one brain hemisphere were analysed for human Aβ40 and Aβ42 levels by ELISA (Invitrogen, Paisley, UK). The ELISAs were performed according to the manufacturer's protocol. In short, extracts were diluted with diluent buffer provided in the kit. Dilutions varied per model, and were therefore optimized for both

models. To dilute the standards, 1x carbonate buffer or 5 M guanidine-HCl was added to the diluent buffer to create the same dilution and conditions as used for the samples. After incubating the extracts for 3 hours with detection antibody on a shaker (room temperature), plates were incubated for 30 minutes with anti-rabbit IgG-HRP diluted in HRP-diluent. Finally, stabilized chromogen (tetramethylbenzidine) was added to the wells and incubated for 30 minutes in the dark (room temperature), after which the reaction was stopped with stop solution from the kit. The O.D. was measured at 450 nm. Using the standard curve, the concentration of each mouse extract (in duplicate) could be determined (in pg/ml) and averaged for each treatment group. A protein assay (Pierce BCA, Thermo Fisher Scientific Inc, Rockford, IL, USA) was performed to determine total protein levels in the different extracts. Aβ levels were normalized to this protein level (ng/mg). In line with previous data [82], carbonate-extracted (soluble) Aβ levels were much lower (>100 times) in both transgenic models than guanidine HCl-extracted (insoluble) Aβ levels. Therefore, in the results we only present guanidine HCl-extracted Aβ levels.

Statistical analysis

Injection groups were compared using independent unpaired T-tests. Time spent on active/passive behaviour in the open field and escape latencies in (reverse) Morris water maze were analyzed using a repeated measures analysis of variance (ANOVA). Learning curves of mice were also compared in this analysis. Results are presented as mean ± standard error. Statistical significance was set at $p<0.05$, with $p<0.10$ considered a trend.

Results

Animals and body weight

During 12 weeks, 12-month old APP/PS1 and 9-month-old TgSwDI mice received injections with either PBS or αB-crystallin at an age when Aβ deposition in these models was prominent (12 and 9 months of age respectively). Wildtype (WT) C57Bl/6 mice served as controls. There were no significant body weight differences in WT or PBS- or αB-crystallin-treated transgenic groups at any point during the injection period (data not shown). During the experiment with the APP/PS1 mice, 1 PBS-treated and 8 αB-crystallin-treated mice were lost (resp. n=8 and n=4 left). For the TgSwDI mice, 6 PBS-treated and 2 αB-crystallin-treated mice were lost (resp. n=6 and n=9 left). No WT mice were lost during the injection period of the APP/PS1 or TgSwDI mice.

αB-crystallin does not affect activity or cognition but increases brain Aβ40 levels in 12-month-old APP/PS1 mice

The rotarod test was performed to test motor function of the mice. We observed no significant differences in time spent on the rotarod between transgenic (PBS- or αB-crystallin treated) mice and WT mice (data not shown). The open field observations revealed that WT mice and APP/PS1 mice that were treated with PBS or αB-crystallin for 3 months did not differ in the time spent on walking, sitting rearing, wall leaning or grooming (data not shown).

Spatial memory of mice was tested in the Morris water maze (Fig. 1). Over the four trial days, WT mice showed a decrease in escape latency from 100 s to 30 s, with PBS-treated APP/PS1 mice having a significantly higher escape latency than WT mice (Fig. 1A; $F(1,9) = 19.24$, $p=0.002$). On average, treatment with αB-crystallin had no effect on escape latency compared to PBS treatment (Fig. 2A). Furthermore, PBS-treated APP/PS1 mice had a significantly less steep slope of their learning curve than WT mice ($F(1,9) = 7.0$, $p=0.027$) and a near-significantly less steep slope than αB-crystallin-treated APP/PS1 mice ($F(1,7) = 5.36$, $p=0.054$) during the first three trial days (Fig. 1A) .

In the probe test of the Morris water maze, PBS-treated APP/PS1 mice had a significantly lower number of platform crossings (Fig. 1B; 0.33 ± 0.21 vs. 3.80 ± 0.20, $p<0.0001$) and a significantly slower first crossing (Fig. 1C; 100.6 ± 14.7 sec vs. 17.8 ± 5.3 sec, $p=0.0009$) than WT mice. Treatment with αB-crystallin non-significantly ($p=0.21$) increased the number of platform crossings (Fig. 1B: 1.0 ± 0.56 vs. 0.33 ± 0.21) and non-significantly ($p=0.26$) decreased the time-to-first-crossing compared to PBS treatment (Fig. 1C: 66.0 ± 28.1 sec. vs. 100.6 ± 14.7 sec.).

A reverse Morris water maze was performed for 2 days (four trials per day) to assess whether mice could unlearn irrelevant information and relearn a new platform location at the opposite side of the pool. In the acquisition trials of the reverse Morris water maze, the escape latency was not significantly different between the three treatments groups (data not shown). In the probe test of the reverse Morris water maze, the number of platform crossing was similar for WT mice, PBS-treated APP/PS1 mice or αB-crystallin-treated APP/PS1 mice (data not shown). PBS-treated APP/PS1 mice did seem to need more time to first cross the platform compared to WT mice, but these differences were not significant due to large variation in values ($p=0.15$). The αB-crystallin-treated group crossed the platform location a similar number of times as the PBS-treated group (data not shown) and needed a similar amount of time to first cross the platform location (data not shown).

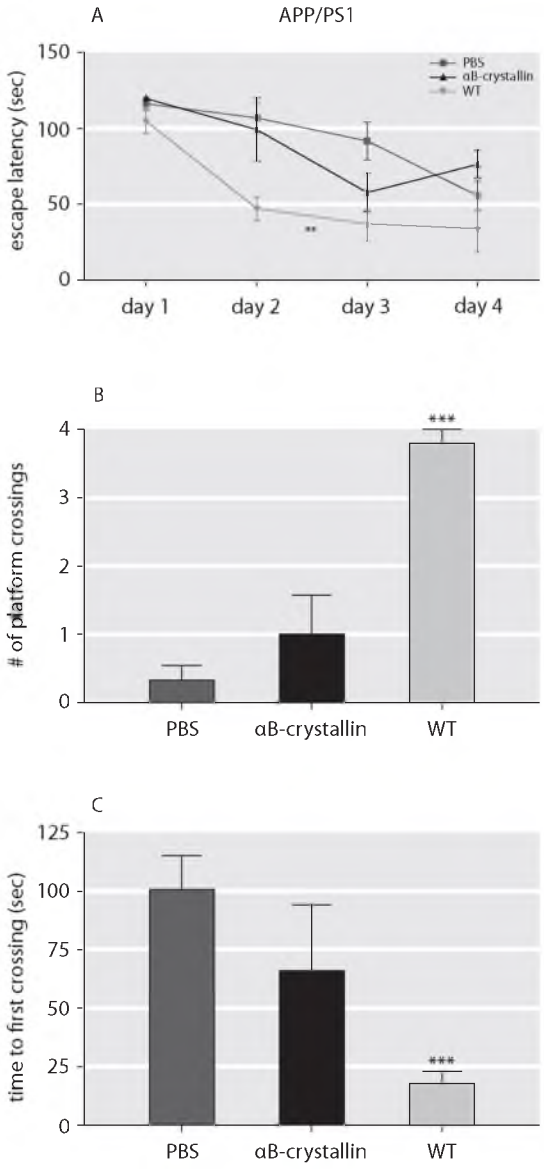

Figure 1: *Performance of APPswe/PS1dE9 mice in the Morris water maze. In the acquisition trials (A), PBS-treated mice (n=6) had a significantly higher escape latency over four trial days than WT mice (n=5). Treatment with αB-crystallin (n=3) had no effect on escape latency. In the probe trial of the Morris water maze, PBS-treated APPswe/PS1dE9 mice crossed the former platform location significantly less often than WT mice (B) and needed significantly more time to first cross the old platform location (C). Treatment with αB-crystallin had no effect on the number of platform crossings (B) or the time to the first crossing (C).*
*** p<0.01, *** p<0.001*

Aβ levels were determined in guanidine HCl extracts of one brain hemisphere (ng/mg total protein) (Fig. 2). Brain Aβ40 and Aβ42 levels of age-matched WT mice were hardly detectable (13.6 and 1.6 ng/mg respectively). Treatment with αB-crystallin did not alter the Aβ42 (Fig. 2B) level in APP/PS1 mice compared to PBS treatment, but it near-significantly increased Aβ40 (Fig. 2A: 434.1 ± 96.4 ng/mg vs. 266.6 ± 34.5 ng/mg, p=0.06).

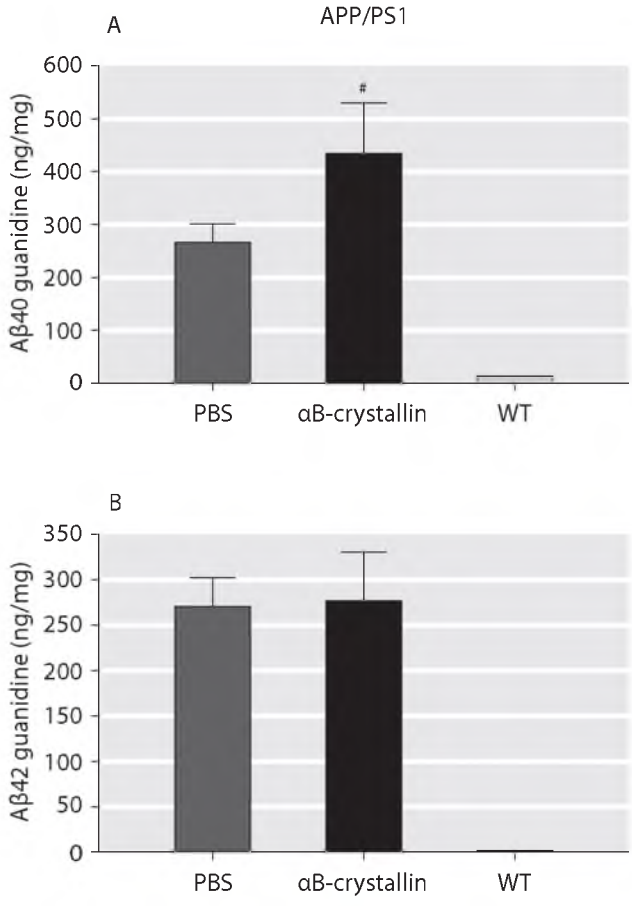

Figure 2: *Guanidine HCl-extracted brain Aβ levels (ng/mg total protein) of APPswe/PS1dE9 mice. Treatment with αB-crystallin (n=4) did not alter Aβ42 levels compared to PBS treatment (n=8) (B), but near-significantly increased Aβ40 levels (A). #p<0.10*

αB-crystallin affects activity, but not cognition, and lowers brain Aβ42 levels of TgSwDI mice. When we used TgSwDI mice, we observed no differences in time spent on the rotarod between WT mice, PBS-treated or αB-crystallin-treated mice (data not shown). In the open field, PBS-treated TgSwDI mice were generally more active than WT mice, with significantly more time spent on walking (Fig.3A: $F(1,15) = 4.99$, $p=0.04$) and wall leaning (Fig. 3C; $F(1,15)=5.92$, $p=0.03$) and significantly less time sitting (Fig. 3B: $F(1,15) =11.34$, $p=0.004$). There was no difference between these two groups in time spent on grooming (Fig.

3D). Treatment with αB-crystallin non-significantly increased the time spent on walking (Fig. 3A: F(1,11) = 1.08, p=0.32) and decreased the time spent on sitting (Fig. 3B F(1,11) =2.11, p=0.17) compared to PBS treatment, although these effects were not significant. The time spent on wall leaning was significantly lowered with αB-crystallin treatment (Fig. 3C: F(1,11) =8.26, p=0.02) and the time spent on grooming was significantly increased compared to PBS treatment (Fig. 3D: F(1,11) = 8.93, p=0.01).

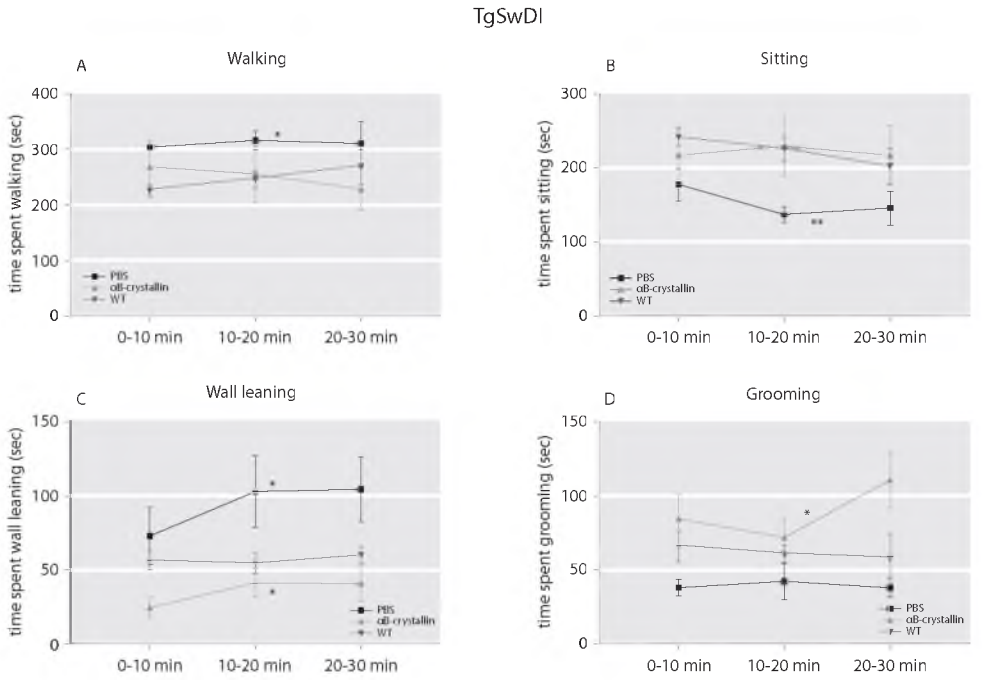

Figure 3: *The time TgSwDI and WT mice spent on the open field parameters walking (A), sitting (B), wall leaning (C) and grooming (D) was recorded for 30 minutes and depicted in 3 periods of 10 minutes. PBS-treated TgSwDI mice (n=5) spent significantly more time on walking (A) and wall leaning (C) and significantly less time on sitting (B) than WT mice (n=12). Treatment with αB-crystallin (n=8) significantly reduced the time spent on wall leaning (C) and significantly increased the time spent on grooming (D) compared to PBS treatment. * p<0.05, ** p<0.01*

In the Morris water maze, WT mice showed a decrease in escape latency (Fig. 4), from 120 s to 70 s over the four trial days. PBS-treated TgSwDI mice had a significantly lower escape latency than WT mice (Fig. 4A: F(1,15) = 8.44, p=0.01), although the slope of their learning curve was not different (F(1,15) = 2.76, p=0.12). Overall, treatment with αB-crystallin had no effect on escape latency compared to PBS treatment or compared to WT mice (Fig. 4A). Only on the fourth trial day, the escape latency of αB-crystallin-treated TgSwDI mice was significantly lower than PBS-treated TgSwDI mice (18.6 ± 7.5 s vs. 71.75 ± 12.9 s, p=0.01). Furthermore, the slope of the learning curve of αB-crystallin-treated TgSwDI mice was significantly less steep than that of PBS-treated TgSwDI mice (Fig. 4A:

F(1,11) = 20.53, p=0.01). In the probe test of the Morris water maze, PBS-treated TgSwDI mice had a non-significantly higher number of platform crossings than WT mice (Fig. 4B: 2.2 ± 0.73 vs. 1.1 ± 0.33, p=0.13). The number of platform crossings of the αB-crystallin-treated TgSwDI mice were in between those of the other two groups (Fig. 4B). The time PBS-treated and αB-crystallin-treated TgSwDI mice needed to first cross the platform was not significantly different to the time WT mice needed (Fig.4C).

In the reverse Morris water maze, the escape latency of PBS-treated TgSwDI mice in the acquisition trials did not differ from WT mice or αB-crystallin-treated TgSwDI mice (data not shown). Furthermore, in the probe trial of the reverse Morris water maze, there were no significant differences between the treatment groups on the number of platform crossings and the time needed to first cross the old platform location (data not shown).

Finally, compared to PBS treatment, treatment with αB-crystallin non-significantly (p=0.32) increased guanidine HCl-extracted Aβ40 levels compared to PBS-treated TgSwDI mice (Fig. 5A: 122.0 ± 19.8 ng/mg vs. 96.6 ± 4.2 ng/mg). Furthermore, αB-crystallin treatment significantly decreased Aβ42 levels (Fig. 5B: 3.67 ± 0.60 vs. 2.43 ± 0.25, p=0.05). Guanidine HCl-extracted Aβ levels of WT mice were too low to be detected.

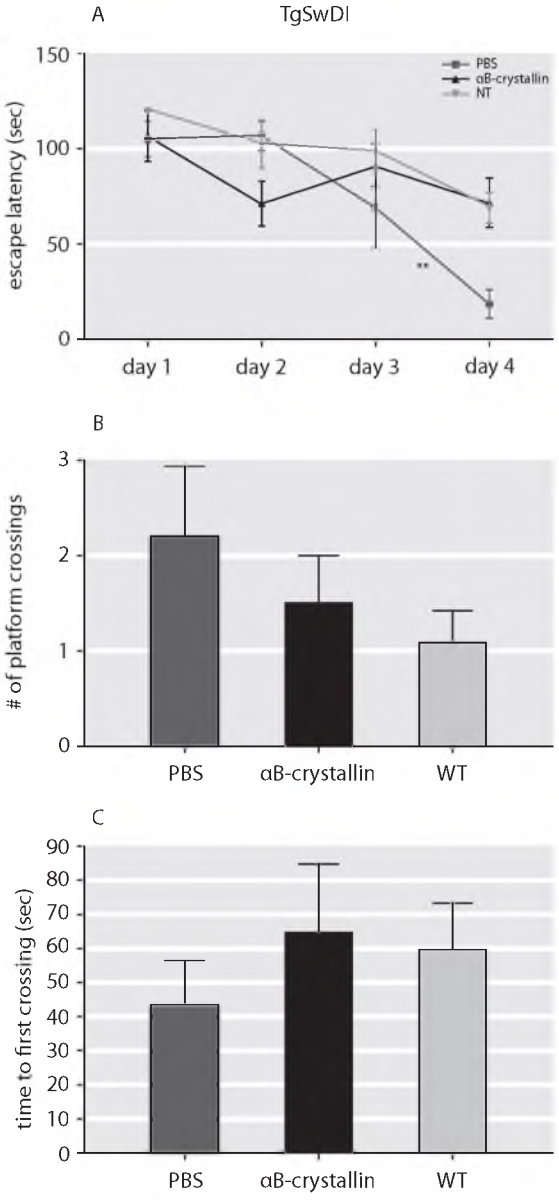

Figure 4: *Performance of TgSwDI mice in the Morris water maze. In the acquisition trials (A), PBS-treated mice (n=5) had a significantly lower escape latency over four trial days than WT mice (n=12). Treatment with αB-crystallin (n=8) had no effect on escape latency. In the probe trial of the Morris water maze, PBS-treated TgSwDI mice non-significantly crossed the former platform location more often than WT mice (B) but needed a similar amount of time to first cross the old platform location (C). Treatment with αB-crystallin had no effect on the number of platform crossings (B) or the time to the first crossing (C). ** p<0.01*

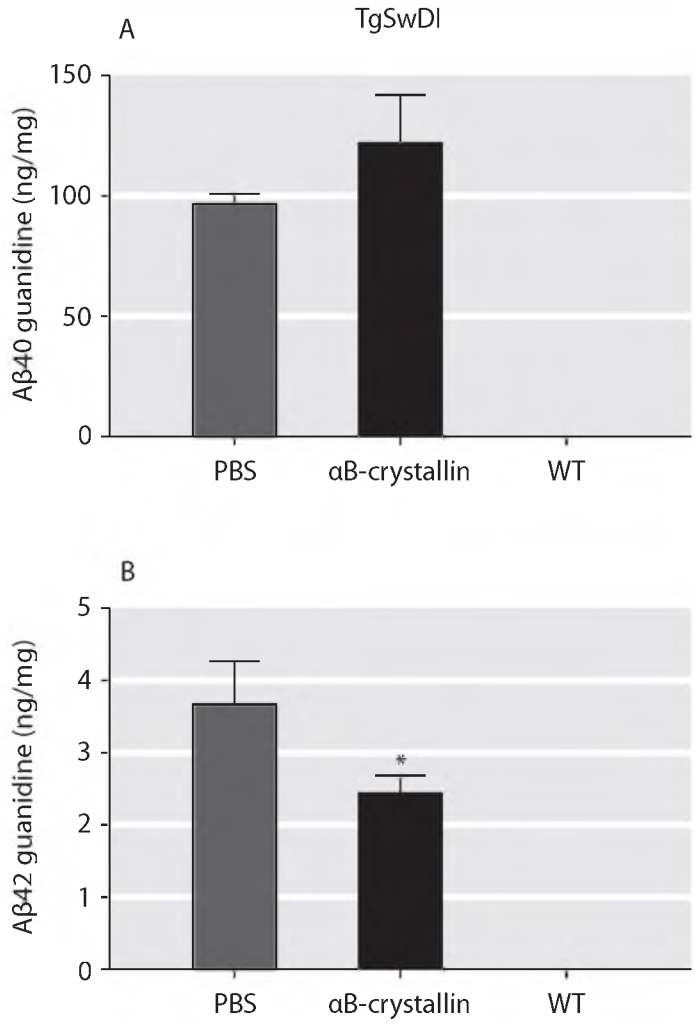

Figure 5: *Guanidine HCl-extracted brain Aβ levels of TgSwDI mice (ng/mg total protein). Treatment with αB-crystallin (n=6) slightly increased Aβ40 levels (A) compared to PBS-treated mice (n=9), whereas it significantly decreased Aβ42 levels (B). *p<0.05*

Discussion

Previously, we demonstrated that αB-crystallin can bind Aβ and influence its aggregation [279], making this small heat shock protein a candidate agent for therapeutic intervention in Alzheimer's disease. In the present study, using the APPswe/PS1dE9 and TgSwDI mouse model for AD, we demonstrated that αB-crystallin 1) had no effect on cognition in both models, 2) had some effect on activity levels in the TgSwDI model, 2) slightly increased guanidine HCl-extracted brain Aβ40 levels in the APP/PS1 model and 3) lowered guanidine HCl-extracted brain Aβ42 levels in the TgSwDI model.

Both the APPswe/PS1dE9 and the TgSwDI mouse model have previously demonstrated well-documented impairments in several behavioural tasks [104, 139, 140, 292]. We also found impaired spatial memory learning in our APPswe/PS1dE9 mice, but not in our TgSwDI mice. In the Morris water maze, APPswe/PS1dE9 mice needed significantly more time finding a hidden platform than WT mice, while TgSwDI mice performed similar to WT mice or even better. This latter result appears to be caused by the relatively weak performance of the WT mice in this behavioural test, although it is also important to mention that 67% of our PBS-treated TgSwDI mice were lost during the injection period. The loss was likely not due to the PBS, as the same PBS solution was used to dilute the αB-crystallin and only 18% of the αB-crystallin-treated TgSwDI mice were lost. However, in this experiment the TgSwDI mice proved to be very sensitive to the combined stress of injections and behavioural testing, resulting in the death of many mice. It may be that αB-crystallin somehow lowered the stress response of these mice, thereby protecting them from stress-related death. In any case, because of this loss, the lack of a difference between TgSwDI and WT mice may also reflect a selection bias. As APPswe/PS1dE9 and TgSwDI mice performed equally well on the rotarod as their non-transgenic controls, any differences we found between non-transgenic mice and transgenic mice were not due to impaired motor functions.

In the open field, it was the APPswe/PS1dE9 model that hardly differed from non-transgenic controls, while the TgSwDI mice were (significantly) more active than WT mice. Both these results were unexpected. In a previous open field analysis of the APPswe/PS1dE9 model, these mice were more active than non-transgenic controls [104]. And, previously, TgSwDI were similarly active to non-transgenic controls in an open field analysis, although the open field test was performed slightly different [292]. Again, it may be the increased sensitivity to stress that causes our TgSwDI mice to in this case be more active compared to wildtype controls. Finally, as expected from a previous characterization of the TgSwDI model [55], we found that Aβ40 levels of this model were considerably higher than Aβ42 levels. The APPswe/PS1dE9 model is known to have a higher amount of insoluble Aβ42 compared to Aβ40 [82], but in our hands Aβ40 and Aβ42 levels in 12-month-old APPswe/PS1dE9 mice were comparable. This latter discrepancy is perhaps due to the different extraction methods used in our study compared to the previous study.

In both mouse models, αB-crystallin had some effect on brain Aβ levels; it near-significantly increased guanidine HCl-extracted Aβ40 levels in APPswe/PS1dE9 mice and significantly lowered guanidine HCl-extracted Aβ42 levels in TgSwDI mice. The fact that αB-crystallin could influence brain Aβ levels in our TgSwDI mice, advocates against this sHsp acting as a peripheral sink agent, as it is known that TgSwDI mice cannot sustain a peripheral sink mechanism [259]. Therefore, our results suggest that αB-crystallin acted directly in the brain, although based on mere size, BBB crossing of this sHsp seems unlikely. Differential effects of αB-crystallin on brain Aβ species may be due to the addition

of a His-tag to the αB-crystallin injected in the TgSwDI mice or perhaps due to the larger number of injections received by the TgSwDI mice. Previously, it was demonstrated that addition of a His-tag to HSC70 altered the molecular state of this Hsp, because the His-tag stabilized the dimeric form of HSC70 [6]. However, we have previously found that this His-tagged sHsp had similar effects on protein aggregation and cellular toxicity as their untagged versions (unpublished data). It may be that differences in Aβ accumulation of the two models used, provide an explanation to the differential result of αB-crystallin, as they have different types of Aβ deposits and opposite Aβ40:Aβ42 ratios [55, 82].

Considering the Aβ40:Aβ42 ratios, it is striking that αB-crystallin affects concentrations of the Aβ species that is less abundant in both models, i.e. Aβ40 in APPswe/PS-1dE9 mice and Aβ42 in TgSwDI mice. This result raises the question if αB-crystallin-induced changes in brain Aβ levels are sufficient to affect cognitive function. Indeed, in our hands αB-crystallin injection hardly had an effect on cognition in any of the performed behavioural tests; only in the TgSwDI mice, αB-crystallin restored parameters of the open field to WT levels. However, as with the comparison between the transgenic and non-transgenic mice, when interpreting the results of the αB-crystallin treatment, the substantial loss of mice in the αB-crystallin-treated APPswe/PS1dE9 mice and the PBS-treated TgSwDI mice should be taken into consideration. Again, this may have lead to selection biases and thereby influenced the interpretation of our experiments. Furthermore, since we did not include a control group injected with either a nonsense protein or a sHsp that did not interact with Aβ in vitro (e.g. Hsp27) [19], we cannot conclude that the observed effects on Aβ levels are only the result of injection with the high affinity sHsp αB-crystallin. Finally, it should be mentioned that in this study only mice with severe Aβ pathology were examined. It may be that administration of αB-crystallin at an earlier age, when more soluble Aβ is present, can reveal stronger effects of αB-crystallin on cognition and brain Aβ load and perhaps even demonstrate a peripheral sink action of αB-crystallin.

In conclusion, we have no indication that peripheral administration of αB-crystallin is a suitable treatment option for AD (mouse models), nor did our experiments reveal that αB-crystallin can act as a peripheral sink for Aβ. Further investigation, using more mice at different stages of Aβ pathology, may provide more conclusive evidence on a therapeutic action of αB-crystallin. Furthermore, (small) Hsp may also act as therapeutic agents in other ways than examined in our study. For example, it is known that Hsp not only bind the Aβ protein, but are also highly immunogenic [304]. When Hsp form a complex with Aβ they may enhance the immune response against Aβ, thereby enhancing Aβ clearance. Indeed, immunization with an Aβ/Hsp70 complex induced a markedly higher immune response in APPswe mice than immunization with Aβ alone, although in this case the increased immune response was accompanied by an increase in brain Aβ levels [130]. Another approach to using Hsp as therapeutic agents is by pharmacologically inducing their expression in the brain. For example, induction of Hsp70 by the plant-derived compound celastrol has neuroprotective effects in animal models for neurodegenerative diseases such as Parkinson's disease [48] and amyotrophic lateral sclerosis [125]. It is suggested that a similar effect may occur in AD [3, 5]. As far as we know, the pharmacological induction of Hsp has not yet been tested in AD models. Therefore, even though administration of Hsp such as αB-crystallin may not be effective, Hsp do have many characteristics making them interesting therapeutic targets and should therefore be further explored in the search for new therapeutic agents.

Acknowledgments
This study was supported by a grant from the Internationale Stichting Alzheimer Onderzoek (ISAO, no. 07510), the Netherlands Organization for Scientific Research (NWO/ZonMW, Vidi program, no. 917.46.331) and the Hersenstichting Nederland (no. 14F06.18). We would like to thank Henk Arnts, Karin de Haas-Cremers and their colleagues for the excellent care of the animals.

Chapter 8
Summary and discussion

Summary

Heparan sulfate proteoglycans and Aβ

In humans suffering from Alzheimer's disease (AD), heparan sulfate proteoglycans (HSPG) are found in close association with amyloid β (Aβ) pathology [254, 255]. The extracellular matrix HSPG agrin and the cell surface HSPG glypican-1 seem to have a particularly strong association, as these are the only two HSPG that can be found in all the different types of AD lesions, i.e. parenchymal plaques and cerebral amyloid angiopathy (CAA). In vitro studies have demonstrated that HSPG affect Aβ deposition at many levels, from regulating Aβ cleavage [17, 204] to triggering Aβ aggregation and maintaining Aβ deposits [41, 52, 87]. Vice versa, Aβ can protect HSPG from proteolysis [13]. As it was known that Aβ can induce the expression of a number of genes [195], we wanted to investigate if Aβ could also influence production of HSPG such as agrin and glypican-1, as an explanation for the accumulation of HSPG species with Aβ deposits. As we describe in **Chapter 2**, we found that Aβ increased protein and mRNA production of the HSPG agrin and glypican-1 by human brain pericytes (HBP), suggesting a local production of HSPG by cerebrovascular cells in CAA. Furthermore, both HSPG accumulated at the cell surface of cerebrovascular cells, apparently retained there by the Aβ fibrils attached to the cell membranes, which provides a plausible molecular basis of co-deposition of HSPG, and perhaps also of other co-depositing proteins (**Chapter 5**), with Aβ.

After the initial production of core proteins, proteoglycan glycosaminoglycan (GAG) chains are stepwise attached to the protein core. Furthermore, the chains are enzymatically modified until they ultimately consist of both highly sulfated and relatively unmodified regions [22, 91, 256]. We have found evidence that Aβ is involved in at least one of these modifications, as Aβ can induce an increased sulfate incorporation into GAG chains (**Chapter 2**). These sulfate moieties in turn are essential in mediating the stimulatory effect of HSPG on Aβ aggregation [40]. Indeed, in **Chapter 3**, we demonstrate that removal of O- and particularly N-sulfates from heparin, a HSPG analogue, could eliminate induction of Aβ aggregation by heparin. Furthermore, whereas fully sulfated heparin inhibited Aβ-induced cellular toxicity, this effect was lost when heparin was (partially) desulfated. By immunohistochemistry we then determined that GAG chains near CAA vessels are differentially sulfated (**Chapter 3**), again suggesting that variation in sulfation patterns is relevant.

HSPG are part of a family of proteoglycans, including chondroitin sulfate, dermatan sulfate and keratan sulfate [256], each characterized by the presence of different GAG chains with differing numbers of sulfate moieties. Although less abundant than HSPG, these different proteoglycans can be detected near Aβ deposits as well [65, 221, 223], suggesting they may also influence Aβ aggregation, perhaps dependent on their level of sulfation. When comparing the effects of different GAGs on Aβ aggregation (**Chapter 3**) it seemed in general that highly sulfated GAGs (i.e. heparin and dextran sulfate, a GAG-related macromolecule) increased Aβ aggregation most effectively. Furthermore, both heparin and heparan sulfate protected against Aβ-induced toxicity of cerebrovascular cells, while the less sulfated chondroitin sulfate had no effect.

Aβ-associated proteins in AD mouse models

In order to investigate pathology development and test new therapeutic agents, many transgenic mouse models for AD have been created by inserting human AD-related genes (i.e. amyloid precursor protein and presenilin) carrying one or more familial mutations

into the mouse genome. For the experiments described in **Chapters 4, 6** and **7**, we used the APPswe/PS1dE9 mouse model. In this model, expression of human amyloid precursor protein (APP) with the Swedish mutation and presenilin-1 (PS1) with a deletion in exon 9, leads to Aβ deposition starting from 4-6 months of age [82, 253]. Furthermore, this Aβ deposition is accompanied by severely impaired cognition [139, 140]. In **Chapter 7** we also describe experiments performed using the TgSwDI mouse model, a model that mainly accumulates vascular Aβ deposits from about 3 months of age [55] and that also demonstrates robust cognitive impairment [292].

It is known that there are marked differences between human and mouse Aβ deposits with regards to Aβ modifications and compaction [119, 136, 258]. As HSPG are such an intrinsic part of Aβ deposits in AD patients [254, 255, 257] and as they are clearly involved in Aβ deposition in vitro (**Chapters 2** and **3**), we wanted to investigate if Aβ deposits in a transgenic AD mouse model demonstrate a similar relation between Aβ and HSPG. In **Chapter 4**, we describe that, unlike in humans, the co-deposition of HS GAG chains and the HSPG species perlecan, glypican-1 and agrin with Aβ deposits in APPswe/PS1dE9 mice was limited. Only about 30% of Aβ deposits was positive for heparan sulfate (HS) GAG chains and less than 10% of deposits was positive for any of the different HSPG species. Furthermore, we could not find a temporal relation between the (limited) deposition of HSPG and the robust Aβ deposition.

Besides HSPG, a whole number of other proteins, including apoliporotein E (apoE) [173], complement factors [73] and acute-phase proteins [264] are also found in or near Aβ deposits. We therefore reviewed the literature on co-deposition of Aβ-associated factors in different mouse models for AD (**Chapter 5**). We determined that only apoE co-deposition was robustly modeled in many AD mouse models, while the other factors (i.e. HSPG, complement, acute phase proteins, ICAM-1, Cystatin C and CLAC) only partly co-deposited or were not found co-localized with Aβ at all. Therefore, it appears that the composition of Aβ deposits in transgenic mice is very different from that of Aβ deposits in humans, perhaps explaining why therapeutic agents proven to modulate brain Aβ levels in mouse models often do not have a similar effect in patients. It should be mentioned that for many factors, the number of studies was limited to only one or two mouse models. As these factors appear crucial in human Aβ deposition, we suggested that co-deposition of these factors should be studied in more mouse models.

New therapeutic agents

Until now, there are few options to treat AD. There are only a handful of approved agents and these merely treat the symptoms of the disease [175], but not the underlying pathology. There are, however, many new therapeutic approaches under development. Many of these approaches target the Aβ protein, as this protein appears to be a key player in AD pathology.

One new approach receiving much attention has been immune therapy, aimed at triggering an immune response against Aβ. However, clinical trials revealed that immune therapy is not suitable for treatment yet, as it was accompanied by serious negative side-effects [183]. As HSPG demonstrate such a clear affinity for Aβ, a characteristic they share with many potential therapeutic agents including immune therapy, we wanted to investigate if HSPG could be used as therapeutic agents (**Chapter 6**). To this end, we used the low molecular weight heparin enoxaparin, that was previously shown to reduce brain Aβ levels in the APP23 mouse model [20]. Furthermore, we previously demonstra-

ted that several small heat shock proteins (sHsp) have affinity for Aβ [279], many of which can be found co-deposited with Aβ deposits [280, 284]. Of all sHsp, αB-crystallin had the strongest binding affinity with Aβ and through this binding could reduce Aβ aggregation and Aβ-induced toxicity [279]. In **Chapter 7**, we investigated the potential of the small heat shock protein αB-crystallin to act as a therapeutic agent. Both enoxaparin and αB-crystallin were administered peripherally and we hypothesized that they may act as so-called peripheral sink agents, as both are considered too large (~4500 kDa and 22 kDa respectively) to cross the blood brain barrier (BBB). The peripheral sink hypothesis (Fig. 1) states that peripherally administered agents that bind Aβ with high affinity can lower the plasma Aβ pool when binding Aβ in the peripheral circulation, as complexes of Aβ and the peripheral sink agent become targeted for peripheral degradation. This then triggers an efflux of Aβ from the brain to the blood in order to restore the equilibrium that is known to exist between brain and blood Aβ pools [61].

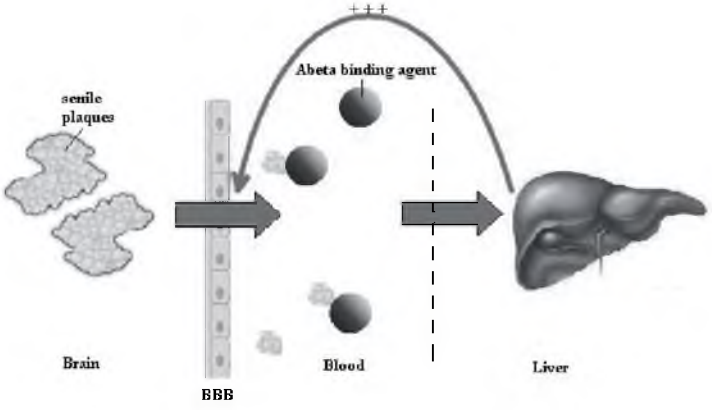

Figure 1: *The peripheral sink hypothesis. Peripherally administered Aβ-binding agents bind Aβ with high affinity in the plasma. These complexes, in turn, become targeted for degradation in organs such as the liver. This peripheral degradation depletes the plasma pool of Aβ, triggering an efflux of Aβ from the brain to the blood.*

Using APPswe/PS1dE9 mice, we found that both enoxaparin (**Chapter 6**) and αB-crystallin (**Chapter 7**) altered brain Aβ levels, although only enoxaparin could significantly improve cognition, as measured in the Morris water maze. At an early stage of Aβ deposition in APPswe/PS1dE9 mice (5 months of age), enoxaparin lowered guanidine-HCl extracted Aβ40, which confirmed the results of the previous prophylactic enoxaparin treatment of APP23 mice [20]. However, we found an opposite effect on Aβ levels in APPswe/PS1dE9 mice with intermediate to severe Aβ pathology (10 and 12 months old respectively). At these stages, enoxaparin increased guanidine HCl-extractable Aβ40 and Aβ42 levels. Although αB-crystallin could not improve cognition of APPswe/PS1dE9 mice, it did normalize activity levels of these mice as measured in the open field. Furthermore, αB-crystallin slightly increased guanidine HCl-extractable Aβ40 levels (**Chapter 7**). Overall, we conclude that enoxaparin, but not αB-crystallin, may be a potential therapeutic agent.

The results of our experiments in APPswe/PS1dE9 mice did not provide us with clear evidence on a peripheral sink action of either protein. We also treated TgSwDI mice

with αB-crystallin (**Chapter 7**). As Aβ clearance from the brain by transport across the BBB is minimal in these mice [55], it is a suitable model to at least exclude a peripheral sink action. In these mice, αB-crystallin had no effect on cognition or activity parameters, again demonstrating its unsuitability as a therapeutic agent. However, guanidine HCl-extracted Aβ42 levels were reduced, suggesting that αB-crystallin possibly affects brain Aβ levels independent of a peripheral sink function.

In summary, the main conclusions of our in vitro and in vivo experiments are that:

1. Aβ can induce protein and mRNA expression of HSPG agrin and glypican-1
2. The molecular basis for HSPG co-deposition with Aβ may be the retention of HSPG, such as agrin and glypican-1, by Aβ fibrils e.g. on the cell surface.
3. Sulfate moieties of HSPG (i.e. heparin) modulate the influence of HSPG on Aβ aggregation and their inhibitory effect on Aβ-induced toxicity of cerebrovascular cells.
4. In the APPswe/PS1dE9 model, a robust Aβ deposition with age (starting at 5 months of age) is accompanied by limited co-deposition of HSPG species (<30%).
5. In general, AD mouse models do not seem to co-deposit Aβ-associated factors to the same extent as humans, limiting the translation of results of therapies aimed at Aβ removal obtained in mouse models to the human situation.
6. αB-crystallin is not a suitable therapeutic agent, as it has no effect on cognition and only slightly influences brain Aβ levels in APPswe/PS1dE9 and TgSwDI mice.
7. Enoxaparin may be a new therapeutic agent, improving cognitive impairment and altering brain Aβ levels.

Discussion

Aβ-induced expression of co-depositing proteins

Previously it has been described that Aβ is capable of inducing gene expression of a number of proteins [195]. Although there is no evidence that these proteins are involved in Aβ aggregation, some of them could be detected in (vascular) Aβ deposits. We have now demonstrated that Aβ can also induce protein expression of the co-depositing heparan sulfate proteoglycans (HSPG) agrin and glypican-1 in cerebrovascular cells (**Chapter 2**). It would be interesting to investigate if Aβ can also induce other co-depositing proteins, such as apoE and acute phase proteins.

As Aβ can stimulate the expression of HSPG, it seems puzzling that co-deposition of HSPG in the APPswe/PS1dE9 mouse model was low (**Chapter 4**). It may simply be that in mouse cells, HSPG are not as easily induced as in human cells. However, it should be mentioned that the low detection of HSPG does not necessarily reflect low HSPG production. Indeed, the APPswe/PS1dE9 model highly expresses Aβ [112] and therefore enough Aβ should be present to stimulate production of HSPG. It may be that due to the rapid deposition of Aβ in mouse models [169, 295], HSPG are not able to co-deposit with Aβ. Furthermore, HSPG may be more readily degraded in the brains of these mice. To determine if Aβ can actually trigger the production of HSPG in APPswe/PS1dE9 mice, gene expression and mRNA production of HSPG should be analyzed in brain tissue of transgenic mice and wildtype controls. Analysis of expression and activity of HSPG-degrading heparinases within mouse brains may reveal if HSPG are more easily degraded in the brains of our model compared to the brains of AD patients.

Finally, our in vitro analysis demonstrated that Aβ fibrils can act as a HSPG reservoir (**Chapter 2**). As the APPswe/PS1dE9 model has a robust deposition of Aβ (**Chapter 4**), it should be able to trap HSPG during deposition. Perhaps the chemical differences between Aβ expressed in humans and several mouse models [119, 136, 258] or the above-mentioned rapid deposition of Aβ in mouse models compared to humans [169, 295], can explain the fact that Aβ hardly traps HSPG in APPswe/PS1dE9 mice. Furthermore, these explanations can perhaps also be extended to the co-deposition of other proteins, as our review summarizes that, in general, co-deposition of these proteins is different in transgenic mice compared to AD patients (**Chapter 5**).

Aβ-induced modifications of GAG chains

Aβ not only induces protein expression of agrin and glypican-1, it also triggers sulfate incorporation into GAG chains (**Chapter 2**). It was already described that the sulfate moieties of HSPG are necessary mediators of the HSPG-induced aggregation of Aβ [40], a role that we have now further established for HSPG-induced aggregation of vascular Aβ (**Chapter 3**). However, it remains to be investigated if Aβ indeed triggers sulfate incorporation of HS GAG chains, since sulfate could also have been incorporated into proteoglycans less involved in Aβ deposition, such as chondroitin sulfate. There are enzymes that specifically degrade these other proteoglycans (i.e. chondroitinases), allowing for a more targeted study of HS GAG chain modulation by Aβ.

The formation of HS GAG chains is a multi-step process, involving several different enzymatic modifications [256]. Even sulfation is not a one-step modification, as it involves sulfation of N- and (subsequently) O-glycans. Indeed, N- and O-sulfates each appear to have specific roles, as they do not have the same capability to induce Aβ aggregation (**Chapter 3**). It may therefore be interesting to investigate if Aβ can modulate any of

these or other steps, e.g. affect enzyme levels involved in sulfation.

Risks of, and possible alternatives to, enoxaparin and αB-crystallin as therapeutic agents
Of the two potential therapeutic agents we tested, only enoxaparin appeared to be a potential therapeutic agent, as it not only altered brain Aβ levels but improved cognition in several groups of APPswe/PS1dE9 mice (**Chapter 6**), although αB-crystallin also affected brain Aβ levels (**Chapter 7**). However, αB-crystallin did not improve the symptoms of AD (e.g. cognitive impairment) and therefore it did not seem useful to further investigate peripheral αB-crystallin administration for future therapeutic use in AD patients. An alternative strategy would be to administer αB-crystallin into the ventricles of the brain, assuming αB-crystallin can diffuse to areas rich in Aβ deposits. However, when manipulating brain protein levels of αB-crystallin it should be realized that αB-crystallin as a chaperone protein likely also affects proteins other than Aβ. This may therefore prove more detrimental rather than any positive effects of intracerebroventricular administration of αB-crystallin on Aβ deposition.

In our experiments, we could not detect any adverse effect of peripherally administrated enoxaparin or αB-crystallin. If anything, αB-crystallin appeared to protect mice from (stress-induced) death during the experiments (**Chapter 7**). Enoxaparin is a known anti-coagulant and may therefore trigger (micro)hemorrhaging. However, we have no evidence of hemorrhaging in our enoxaparin-treated APPswe/PS1dE9 mice. Furthermore, to anticipate to any future side-effects of enoxaparin treatment in humans, we used an enoxaparin dose that has been demonstrated to be tolerated by humans. The use of even smaller enoxaparin-related agents, such as Neuroparin, may reduce the risk of hemorrhaging even further. Neuroparin has already been proven to act as a neuroprotective agent [198] and is able to cross the BBB [157], although as far as we know, it has not been administered to transgenic Aβ-depositing mice yet.

Finally, it remains to be established if enoxaparin has the same positive effects in AD patients. As we have described, there are marked differences between Aβ deposits in transgenic mice and humans (**Chapter 4** and **5**). Mouse Aβ deposits are known to be more easily dissolved in mild extraction buffers, perhaps explained by a relative lack of HSPG co-deposition AD mouse models (**Chapter 4**), and this characteristic may make them more easily manipulated by exogenously administered proteins than human Aβ deposits.

Peripheral sink or an alternative mechanism of action
Both enoxaparin and αB-crystallin influenced brain Aβ levels of APP/PS1dE9 mice (**Chapter 6** and **7**), but the question remains how these proteins mediated this effect. Based on size, binding affinity and the chosen route of administration (i.e. intraperitoneally), we assumed that enoxaparin and αB-crystallin should be able to act as peripheral sink agents. However, the results presented in this thesis gave us little evidence to conclude that enoxaparin and αB-crystallin indeed acted as peripheral sink agents. Generally, peripheral sink agents increase plasma Aβ levels [61, 146] and lower brain Aβ levels without entering the brain [163]. Therefore, to further investigate a potential peripheral sink action of enoxaparin or αB-crystallin, plasma Aβ levels should be determined and/or mouse brains should be investigated for the presence of these agents. It should be noted that plasma Aβ levels are not always altered when known peripheral sink agents are administrated [163, 184], perhaps because effects on plasma Aβ levels are transient, with a new equilibrium quickly establishing. Furthermore, it should be taken into consideration

that antibodies that recognize peripherally administered proteins, will likely also detect endogenous proteins. To distinguish peripherally administered proteins from endogenous proteins and easily track distribution of an agent within the body, labeled versions of enoxaparin or αB-crystallin may be administered to mice. For example, 125I-labeled heparins are available, suggesting a similar labeling should be possible for enoxaparin. Of course, the size of the label should be carefully chosen, as it should not hamper the potential entry of enoxaparin or αB-crystallin into the brain.

For enoxaparin, several other mechanisms of action could be considered. For example, enoxaparin may have protected the brain by its ability to reduce Aβ-induced complement activation and thus detrimental brain inflammation [20]. In the present study we did not investigate complement activation, but this could be considered for future experiments, keeping in mind that not all components of the complement system behave as they do in humans (**Chapter 5**). Furthermore, as an anti-coagulant, enoxaparin may have acted on Aβ and mouse cognition by altering perfusion of the brain. It would therefore be interesting to investigate cerebral blood flow and cerebral blood volume in transgenic, but also wildtype, mice treated with enoxaparin.

In conclusion, we describe in this thesis that HSPG have an important role in Aβ pathology. Not only are several HSPG upregulated by Aβ, HSPG also influence Aβ aggregation and Aβ-induced cellular toxicity, with an important function for their sulfate moieties. Although an AD mouse model may not fully replicate the repertoire of Aβ-associated proteins, we demonstrated that HSPG analogues (i.e. enoxaparin) may be useful as potential therapeutic agents. The co-deposition of sHsp in AD mouse models remains to be investigated, but in any case, the use of αB-crystallin as a peripherally administered therapeutic agent was unsuccessful.

Nederlandse Samenvatting

De ziekte van Alzheimer en het amyloid β eiwit

De ziekte van Alzheimer is een ouderdomsgerelateerde aandoening die in Nederland 130.000 patiënten kent en wordt gekenmerkt door symptomen als geheugenverlies, apathie en depressie. Er wordt geschat dat met de vergrijzing het aantal patiënten de komende jaren zal groeien naar zeker 300.000, waarbij er in 2050 wereldwijd zelfs 100 miljoen Alzheimer patiënten zullen zijn. Een juiste diagnose en effectieve behandeling zijn daarom zeer belangrijk. Echter, het stellen van met name een vroegtijdige diagnose is tot op heden niet mogelijk. Bovendien zijn er momenteel slechts vijf goedgekeurde medicijnen. De meeste van deze medicijnen zijn gericht zijn op het verhinderen van de afbraak van de neurotransmitter acetylcholine. Alzheimer patiënten hebben namelijk minder acetylcholine, omdat als gevolg van de ziekte met name de cholinerge neuronen, die normaliter de neurotransmitter acetylcholine afgeven, worden aangetast. Met deze medicijnen worden echter alleen de symptomen van de ziekte behandeld en niet de oorzaken van de ziekte. Daarom blijft het van groot belang meer inzicht te krijgen in de pathologie van de ziekte van Alzheimer en gaat de zoektocht naar nieuwe medicijnen nog altijd voort.

Kenmerkend voor de hersenen van Alzheimer patiënten zijn ophopingen van het eiwit amyloid bèta (Aβ). Deze ophopingen bevinden zich niet alleen tussen zenuwcellen (neuronen), als zogenaamde seniele plaques (SP), maar zitten ook rondom bloedvaten als zogenaamd cerebraal amyloid angiopathie (CAA). Bij Alzheimer patiënten gaat er door ouderdom iets mis met het opruimen van het Aβ eiwit. Normaliter wordt Aβ namelijk opgeruimd na productie, enerzijds door enzymen in de hersenen, anderzijds door transport van Aβ uit de hersenen naar de bloedsomloop. Wanneer deze processen verstoord zijn, kan het Aβ eiwit samenklonteren (aggregeren) en ophopen in de hersenen. Hierbij aggregeren afzonderlijke (monomere) Aβ eiwitten samen tot zogenaamde oligomeren bestaande uit 2 tot 20 monomere Aβ eiwitten. Vervolgens ontstaan protofibrillen en fibrillen, steeds langere ketens van Aβ eiwitten. Uiteindelijk kunnen deze fibrillen plaques en CAA vormen. Aggregatie van Aβ kan ook het gevolg zijn van genetische mutaties in bijvoorbeeld het amyloid precursor eiwit (APP), maar dit verklaard slechts een klein percentage patiënten (<1%).

Heparan sulfaat proteoglycanen

Eerdere studies hebben aangetoond dat in plaques en CAA ook andere eiwitten ophopen, waaronder heparan sulfaat proteoglycanen (HSPG). Proteoglycanen bestaan uit een eiwit met daaraan lange gesulfateerde suikergroepen. Naast HSPG zijn er ook chondroitine sulfaat, keratan sulfaat en dermatan sulfaat proteoglycanen. De vier verschillende proteoglycanen onderscheiden zich in de opbouw van hun suikerketen; elke proteoglycaan bevat een unieke (herhalende) disaccharide unit. Er zijn ook nog eens verschillende HSPG, elk met een ander eiwit. Drie van deze HSPG zijn geassocieerd met de extracellulaire matrix tussen cellen (perlecan, agrine en collageen VXIII) en twee HSPG bevinden zich op het celoppervlak (glypican en syndecan).

Omdat al deze HSPG, en dan met name agrine en glypican-1, samen worden gevonden met Aβ, wordt aangenomen dat ze een interactie aangaan met het laatstgenoemde eiwit en een rol spelen bij de aggregatie van Aβ. Om te bepalen of het omgekeerde ook het geval is, namelijk dat Aβ ook invloed heeft op het ophopen van HSPG in onder meer CAA, hebben wij in **hoofdstuk 2** gekeken of Aβ de productie en de cellulaire locatie van agrine en glypican-1 kan beïnvloeden. Hierbij is gebruik gemaakt van pericyten, cellen die zich rondom bloedvaten bevinden en daarom een mogelijke bron van HSPG kun-

nen zijn in CAA. Het bleek dat Aβ de eiwit en mRNA expressie van agrine en glypican-1 kon verhogen en dat de geproduceerde HSPG geassocieerd waren met Aβ fibrillen op het celoppervlak van de pericyten. Bovendien werden onder invloed van Aβ meer sulfaatgroepen ingebouwd in de suikerketens van proteoglycanen, wat suggereert dat ook de opbouw van de suikerketens van HSPG door Aβ kan worden beïnvloed. Dit laatste is een interessante bevinding aangezien eerder is aangetoond dat de sulfaatgroepen van belang zijn bij de invloed die HSPG hebben op de ophoping van Aβ. Dit blijkt ook uit de experimenten beschreven in **hoofdstuk 3**, waarbij (deels) desulfateren van HSPG de stimulerende werking van HSPG op Aβ aggregatie en de bescherming van HSPG tegen Aβ-geïnduceerde cellulaire toxiciteit kon wegnemen.

In **hoofdstuk 3** is bovendien onderzocht in welke mate andere proteoglycanen, zoals chondroitine sulfaat, Aβ aggregatie beïnvloeden. Hierbij bleek nogmaals dat de sulfaatgroepen een bepalende rol spelen in het stimuleren van Aβ aggregatie, aangezien de sterker gesulfateerde proteoglycanen aggregatie sterker bevorderden dan minder gesulfateerde proteoglycanen. Tenslotte is gevonden dat in CAA, HSPG terug te vinden waren met verschillende patronen van sulfatering, wat wederom aangeeft dat de sulfaatgroepen een belangrijke component zijn van HSPG als het gaat om Aβ aggregatie.

Muismodellen en amyloid β-geassocieerde eiwitten

Om meer te weten te komen over de ziekte van Alzheimer en nieuwe therapieën te testen, wordt veel gebruik gemaakt van muismodellen. Het is namelijk mogelijk om ook in de hersenen van muizen het Aβ eiwit te laten aggregeren. Hiervoor moet dan wel een menselijk gen voor APP, met één of meerdere van de in mensen beschreven mutaties, aan het genoom van de muis worden toegevoegd. Als gevolg van de Aβ aggregaten in hun hersenen, verslechterd bij veel van deze muismodellen het geheugen van de muizen, wat zich uit in een verstoord leergedrag.

Omdat bij de mens HSPG zo'n belangrijk onderdeel zijn van Aβ aggregaten, wilden wij onderzoeken of een soortgelijke relatie tussen HSPG en Aβ bestaat in een muismodel (**hoofdstuk 4**). Als model hebben wij gekozen voor APPswe/PS1dE9 muizen. Deze muizen brengen APP tot expressie met daarin de zogenaamde Zweedse mutatie (Swe). Deze mutatie zorgt ervoor dat Aβ makkelijker uit het gemuteerde APP wordt geknipt dan wanneer de mutatie afwezig zou zijn. Bovendien wordt ook humaan preseniline-1 (PS1) tot expressie gebracht in deze muis, met een deletie in exon 9 (dE9). Dit eiwit is onderdeel van één van de secretases die Aβ uit APP knipt. Gecombineerd zorgen deze genen ervoor dat Aβ al vanaf een leeftijd van 4-6 maanden oud gaat aggregeren in de hersenen van deze muizen.

In **hoofdstuk 4** beschrijven we dat, in tegenstelling tot bij de mens de Aβ depositities in APPswe/PS1dE9 muizen slechts beperkt geassocieerd zijn met HSPG. Bij nadere bestudering van de literatuur (**hoofdstuk 5**) bleek dat ook veel andere eiwitten die in de mens samen met Aβ terug te vinden zijn, zoals complement factoren en acute fase eiwitten, in verschillende muismodellen in mindere mate of zelfs helemaal niet terug te vinden zijn. Deze resultaten geven duidelijk aan dat de samenstelling van Aβ aggregaten in muismodellen zeer kan verschillen van menselijke Aβ aggregaten. Aangezien de samenstelling van een Aβ aggregaat mede bepaald hoe makkelijk het aggregaat te verwijderen is, verklaart dit verschil tussen muis en mens mogelijk waarom een behandeling in mensen soms andere resultaten geeft dan dezelfde behandeling in een muismodel.

HSPG en het kleine heat shock eiwit αB-crystalline als medicatie voor de ziekte van Alzheimer

Omdat HSPG een belangrijke rol spelen bij Aβ aggregatie, is er in **hoofdstuk 6** onderzocht of HSPG ook als medicijn kunnen dienen. Hierbij is voor de behandeling gekozen om gebruik te maken van enoxaparine, een heparine met een laag moleculair gewicht. Heparines op hun beurt zijn sterk gesulfateerde varianten van HSPG. Enoxaparine wordt al gebruikt bij de behandeling van hart- en vaatziekten en het is aangetoond dat het in een muismodel voor de ziekte van Alzheimer (APP23 muis), bij behandeling op jonge leeftijd, het Aβ gehalte in de hersenen kon verlagen. Om het effect van enoxaparine op Aβ verder te onderzoeken en bovendien het effect op het leergedrag van muizen te bestuderen, hebben wij APPswe/PS1dE9 muizen van verschillende leeftijden 3 maanden lang behandeld met enoxaparine (**hoofdstuk 6**).

Wij vonden dat bij APPswe/PS1dE9 muizen, waarbij de behandeling met enoxaparine vroeg in het aggregatie proces (leeftijd van 5 maanden oud) startte, de hoeveelheid Aβ40 in de hersenen daalde, zoals ook al werd waargenomen in APP23 muizen. Echter, in een intermediair (10 maanden oud) en laat (12 maanden oud) stadium van aggregatie verhoogde enoxaparine juist de hoeveelheid (geaggregeerd) Aβ in de hersenen. Dit laatste resultaat komt overeen met onze bevinding dat enoxaparine, wanneer het in direct contact komt met Aβ, de aggregatie van Aβ bevordert (**hoofdstuk 6**). Er wordt echter aangenomen dat enoxaparine niet rechtstreeks in de hersenen zijn werking heeft; de barrière die bestaat tussen bloed en hersenen belemmert namelijk de doorgang van veel grote moleculen. Wellicht is de bloed-hersen barrière in de oudere muizen beschadigd, wat het voor enoxaparine mogelijk maakt om de hersenen in te komen en aggregatie van Aβ te bevorderen.

In de jongere muizen heeft enoxaparine mogelijk gewerkt als een zogenaamde perifere sink. Een molecuul dat als perifere sink werkt, kan het Aβ gehalte in de hersenen namelijk doen dalen door te binden aan Aβ dat circuleert in de bloedsomloop (perifere circulatie). Aβ dat in het bloed gebonden is aan een ander molecuul kan makkelijker worden herkend voor afbraak in perifere organen zoals de lever of de nieren. Deze afbraak verstoort vervolgens het evenwicht dat bestaat tussen het Aβ gehalte in de hersenen en het bloed. Om dit evenwicht te herstellen zal Aβ vanuit de hersenen het Aβ gehalte in het bloed weer aanvullen met als gevolg dat het Aβ gehalte van het brein lager wordt. Om meer informatie te krijgen over de werking van enoxaparine, zou dus ook het Aβ gehalte in het bloed gemeten moeten worden. Het labelen van enoxaparine zou bovendien mogelijk kunnen uitwijzen of enoxaparine de bloed-hersen barrière passeert. Onafhankelijk van het precieze mechanisme waarmee enoxaparine het Aβ gehalte in de hersenen beïnvloedt, is het opvallend dat enoxaparine-geïnduceerde veranderingen van Aβ gepaard gingen met een verbetering van het leergedrag van de muizen. Dit duidt erop dat enoxaparine potentie heeft als medicijn voor de ziekte van Alzheimer.

Uit eerdere studies is gebleken dat niet alleen HSPG, maar ook kleine heat shock eiwitten ophopen met het Aβ eiwit. Heat shock eiwitten zijn stresseiwitten die betrokken zijn bij de juiste vouwing van eiwitten en het is dan ook niet verwonderlijk dat ze een interactie aangaan met Aβ. Het is gebleken dat met name het kleine heat shock eiwit αB-crystalline een sterke binding heeft met Aβ, wat kan betekenen dat het mogelijk als perifere sink kan dienen. In **hoofdstuk 7** is daarom, op een vergelijkbare manier als in hoofdstuk 6 voor enoxaparine, onderzocht of αB-crystalline de hoeveelheid Aβ in de hersenen van APPswe/PS1dE9 muizen kan beïnvloeden en het leergedrag van de muizen kan

verbeteren. Hierbij is ook een ander muismodel behandeld met αB-crystalline, het TgSwDI model. In dit model, dat APP tot expressie brengt met de Zweedse (Sw), Nederlandse (D; Dutch) en Iowa (I) mutatie, aggregeert Aβ voornamelijk in de bloedvaten. Het bleek dat αB-crystalline een kleine verhoging gaf van Aβ in de hersenen van APPswe/PS1dE9 muizen en een verlaging in de TgSwDI muizen. Het is bekend dat TgSwDI muizen geen transport van Aβ over de bloed-hersen barrière toelaten. Dit laatste resultaat duidt erop dat αB-crystalline mogelijk niet als perifere sink heeft gewerkt. Het αB-crystalline zelf is echter ook te groot voor transport over deze barrière; kortom het exacte werkingsmechanisme is ook hier nog onduidelijk. Echter, aangezien αB-crystalline geen verbetering gaf van het leergedrag van de APPswe/PS1dE9 of de TgSwDI muizen, lijkt het erop dat dit klein heat shock eiwit, in tegenstelling tot enoxaparine, geen potentie heeft als medicijn tegen de ziekte van Alzheimer.

Conclusie

In dit proefschrift wordt de rol van HSPG bij Aβ aggregatie beschreven. Het is gebleken dat Aβ de expressie van enkele van deze HSPG reguleert. HSPG beïnvloeden op hun beurt weer de aggregatie van Aβ en de Aβ-geïnduceerde cellulaire toxiciteit, waarbij de sulfaatgroepen van groot belang blijken. En hoewel er in dit proefschrift wordt beschreven dat een muismodel voor de ziekte van Alzheimer geen compleet model is als het gaat om de co-depositie van factoren zoals HSPG, is er met behulp van het APPswe/PS1dE9 model wel aangetoond dat een analoog van HSPG, enoxaparine, potentie heeft om als medicijn te dienen in de behandeling voor de ziekte van Alzheimer. Perifeer toedienen van een klein heat shock eiwit zoals αB crystalline daarentegen heeft nauwelijks effect op Aβ depositie en cognitie.

References

[1] Abraham CR, Potter H (1989) The protease inhibitor, alpha 1-antichymotrypsin, is a component of the brain amyloid deposits in normal aging and Alzheimer's disease. *Ann Med* **21**, 77-81.

[2] Abraham CR, Selkoe DJ, Potter H (1988) Immunochemical identification of the serine protease inhibitor alpha 1-antichymotrypsin in the brain amyloid deposits of Alzheimer's disease. *Cell* **52**, 487-501.

[3] Adachi H, Katsuno M, Waza M, Minamiyama M, Tanaka F, Sobue G (2009) Heat shock proteins in neurodegenerative diseases: pathogenic roles and therapeutic implications. *Int J Hyperthermia* **25**, 647-654.

[4] Akiyama H, Barger S, Barnum S, Bradt B, Bauer J, Cole GM, Cooper NR, Eikelenboom P, Emmerling M, Fiebich BL, Finch CE, Frautschy S, Griffin WS, Hampel H, Hull M, Landreth G, Lue L, Mrak R, Mackenzie IR, McGeer PL, O'Banion MK, Pachter J, Pasinetti G, Plata-Salaman C, Rogers J, Rydel R, Shen Y, Streit W, Strohmeyer R, Tooyoma I, Van Muiswinkel FL, Veerhuis R, Walker D, Webster S, Wegrzyniak B, Wenk G, Wyss-Coray T (2000) Inflammation and Alzheimer's disease. *Neurobiol Aging* **21**, 383-421.

[5] Allison AC, Cacabelos R, Lombardi VR, Alvarez XA, Vigo C (2001) Celastrol, a potent antioxidant and anti-inflammatory drug, as a possible treatment for Alzheimer's disease. *Prog Neuropsychopharmacol Biol Psychiatry* **25**, 1341-1357.

[6] Amor-Mahjoub M, Suppini JP, Gomez-Vrielyunck N, Ladjimi M (2006) The effect of the hexahistidine-tag in the oligomerization of HSC70 constructs. *J Chromatogr B Analyt Technol Biomed Life Sci* **844**, 328-334.

[7] Apelt J, Lessig J, Schliebs R (2002) Beta-amyloid-associated expression of intercellular adhesion molecule-1 in brain cortical tissue of transgenic Tg2576 mice. *Neurosci Lett* **329**, 111-115.

[8] Asai M, Hattori C, Szabo B, Sasagawa N, Maruyama K, Tanuma S, Ishiura S (2003) Putative function of ADAM9, ADAM10, and ADAM17 as APP alpha-secretase. *Biochem Biophys Res Commun* **301**, 231-235.

[9] Bacskai BJ, Kajdasz ST, McLellan ME, Games D, Seubert P, Schenk D, Hyman BT (2002) Non-Fc-mediated mechanisms are involved in clearance of amyloid-beta in vivo by immunotherapy. *J Neurosci* **22**, 7873-7878.

[10] Balemans MC, Huibers MM, Eikelenboom NW, Kuipers AJ, van Summeren RC, Pijpers MM, Tachibana M, Shinkai Y, van Bokhoven H, Van der Zee CE (2009) Reduced exploration, increased anxiety, and altered social behavior: Autistic-like features of euchromatin histone methyltransferase 1 heterozygous knockout mice. *Behav Brain Res.*

[11] Bales KR, Verina T, Cummins DJ, Du Y, Dodel RC, Saura J, Fishman CE, DeLong CA, Piccardo P, Petegnief V, Ghetti B, Paul SM (1999) Apolipoprotein E is essential for amyloid deposition in the APP(V717F) transgenic mouse model of Alzheimer's disease. *Proc Natl Acad Sci U S A* **96**, 15233-15238.

[12] Ballatore C, Lee VM, Trojanowski JQ (2007) Tau-mediated neurodegeneration in Alzheimer's disease and related disorders. *Nat Rev Neurosci* **8**, 663-672.

[13] Bame KJ, Danda J, Hassall A, Tumova S (1997) Abeta(1-40) prevents heparanase-catalyzed degradation of heparan sulfate glycosaminoglycans and proteoglycans in vitro. A role for heparan sulfate proteoglycan turnover in Alzheimer's disease. *J Biol Chem* **272**, 17005-17011.

[14] Barber AJ, Lieth E (1997) Agrin accumulates in the brain microvascular basal lamina during development of the blood-brain barrier. *Dev Dyn* **208**, 62-74.

[15] Bard F, Barbour R, Cannon C, Carretto R, Fox M, Games D, Guido T, Hoenow K, Hu K, Johnson-Wood K, Khan K, Kholodenko D, Lee C, Lee M, Motter R, Nguyen M, Reed A, Schenk D, Tang P, Vasquez N, Seubert P, Yednock T (2003) Epitope and isotype specificities of antibodies to beta -amyloid peptide for protection against Alzheimer's disease-like neuropathology. *Proc Natl Acad Sci U S A* **100**, 2023-2028.

[16] Bard F, Cannon C, Barbour R, Burke RL, Games D, Grajeda H, Guido T, Hu K, Huang J, Johnson-Wood K, Khan K, Kholodenko D, Lee M, Lieberburg I, Motter R, Nguyen M, Soriano F, Vasquez N, Weiss K, Welch B, Seubert P, Schenk D, Yednock T (2000) Peripherally administered antibodies against amyloid beta-peptide enter the central nervous system and reduce pathology in a mouse model of Alzheimer disease. *Nat Med* **6**, 916-919.

[17] Beckman M, Holsinger RM, Small DH (2006) Heparin activates beta-secretase (BACE1) of Alzheimer's disease and increases autocatalysis of the enzyme. *Biochemistry* **45**, 6703-6714.

[18] Behl C, Davis JB, Lesley R, Schubert D (1994) Hydrogen peroxide mediates amyloid beta protein toxicity. *Cell* **77**, 817-827.

[19] Bentahir M, Nyabi O, Verhamme J, Tolia A, Horre K, Wiltfang J, Esselmann H, De Strooper B (2006) Presenilin clinical mutations can affect gamma-secretase activity by different mechanisms. *J Neurochem* **96**, 732-742.

[20] Bergamaschini L, Rossi E, Storini C, Pizzimenti S, Distaso M, Perego C, De Luigi A, Vergani C, De Simoni MG (2004) Peripheral treatment with enoxaparin, a low molecular weight heparin, reduces plaques and beta-amyloid accumulation in a mouse model of Alzheimer's disease. *J Neurosci* **24**, 4181-4186.

[21] Bergamaschini L, Rossi E, Vergani C, De Simoni MG (2009) Alzheimer's disease: another target for heparin therapy. *ScientificWorldJournal* **9**, 891-908.

[22] Bernfield M, Gotte M, Park PW, Reizes O, Fitzgerald ML, Lincecum J, Zako M (1999) Functions of cell surface heparan sulfate proteoglycans. Annu Rev *Biochem* **68**, 729-777.

[23] Bharadwaj PR, Dubey AK, Masters CL, Martins RN, Macreadie IG (2009) Abeta aggregation and possible implications in Alzheimer's disease pathogenesis. J *Cell Mol Med* **13**, 412-421.

[24] Blennow K, de Leon MJ, Zetterberg H (2006) Alzheimer's disease. *Lancet* **368**, 387-403.

[25] Borchelt DR, Thinakaran G, Eckman CB, Lee MK, Davenport F, Ratovitsky T, Prada CM, Kim G, Seekins S, Yager D, Slunt HH, Wang R, Seeger M, Levey AI, Gandy SE, Copeland NG, Jenkins NA, Price DL, Younkin SG, Sisodia SS (1996) Familial Alzheimer's disease-linked presenilin 1 variants elevate Abeta1-42/1-40 ratio in vitro and in vivo. *Neuron* **17**, 1005-1013.

[26] Bornemann KD, Staufenbiel M (2000) Transgenic mouse models of Alzheimer's disease. *Ann N Y Acad Sci* **908**, 260-266.

[27] Boyles JK, Pitas RE, Wilson E, Mahley RW, Taylor JM (1985) Apolipoprotein E associated with astrocytic glia of the central nervous system and with nonmyelinating glia of the peripheral nervous system. *J Clin Invest* **76**, 1501-1513.

[28] Bradt BM, Kolb WP, Cooper NR (1998) Complement-dependent proinflammatory properties of the Alzheimer's disease beta-peptide. *J Exp Med* **188**, 431-438.

[29] Brouwers N, Sleegers K, Van Broeckhoven C (2008) Molecular genetics of Alzheimer's disease: an update. *Ann Med* **40**, 562-583.

[30] Bruinsma IB, Wilhelmus MM, Kox M, Veerhuis R, de Waal RM, Verbeek MM (2009) Apolipoprotein E protects cultured pericytes and astrocytes from D-Abeta(1-40)-mediated cell death. *Brain Res.*

[31] Brunkan AL, Goate AM (2005) Presenilin function and gamma-secretase activity. *J Neurochem* **93**, 769-792.

[32] Buchner J (1996) Supervising the fold: functional principles of molecular chaperones. *FASEB J* **10**, 10-19.

[33] Burns MP, Noble WJ, Olm V, Gaynor K, Casey E, LaFrancois J, Wang L, Duff K (2003) Co-localization of cholesterol, apolipoprotein E and fibrillar Abeta in amyloid plaques. *Brain Res Mol Brain Res* **110**, 119-125.

[34] Buttini M, Masliah E, Barbour R, Grajeda H, Motter R, Johnson-Wood K, Khan K, Seubert P, Freedman S, Schenk D, Games D (2005) Beta-amyloid immunotherapy prevents synaptic degeneration in a mouse model of Alzheimer's disease. *J Neurosci* **25**, 9096-9101.

[35] Buxbaum JD, Christensen JL, Ruefli AA, Greengard P, Loring JF (1993) Expression of APP in brains of transgenic mice containing the entire human APP gene. *Biochem Biophys Res Commun* **197**, 639-645.

[36] Caccamo A, Oddo S, Sugarman MC, Akbari Y, LaFerla FM (2005) Age- and region-dependent alterations in Abeta-degrading enzymes: implications for Abeta-induced disorders. *Neurobiol Aging* **26**, 645-654.

[37] Calhoun ME, Burgermeister P, Phinney AL, Stalder M, Tolnay M, Wiederhold KH, Abramowski D, Sturchler-Pierrat C, Sommer B, Staufenbiel M, Jucker M (1999) Neuronal overexpression of mutant amyloid precursor protein results in prominent deposition of cerebrovascular amyloid. *Proc Natl Acad Sci U S A* **96**, 14088-14093.

[38] Calhoun ME, Wiederhold KH, Abramowski D, Phinney AL, Probst A, Sturchler-Pierrat C, Staufenbiel M, Sommer B, Jucker M (1998) Neuron loss in APP transgenic mice. *Nature* **395**, 755-756.

[39] Castillo GM, Cummings JA, Yang W, Judge ME, Sheardown MJ, Rimvall K, Hansen JB, Snow AD (1998) Sulfate content and specific glycosaminoglycan backbone of perlecan are critical for perlecan's enhancement of islet amyloid polypeptide (amylin) fibril formation. *Diabetes* **47**, 612-620.

[40] Castillo GM, Lukito W, Wight TN, Snow AD (1999) The sulfate moieties of glycosaminoglycans are critical for the enhancement of beta-amyloid protein fibril formation. *J Neurochem* **72**, 1681-1687.

[41] Castillo GM, Ngo C, Cummings J, Wight TN, Snow AD (1997) Perlecan binds to the beta-amyloid proteins (A beta) of Alzheimer's disease, accelerates A beta fibril formation, and maintains A beta fibril stability. *J Neurochem* **69**, 2452-2465.

[42] Chishti MA, Yang DS, Janus C, Phinney AL, Horne P, Pearson J, Strome R, Zuker N, Loukides J, French J, Turner S, Lozza G, Grilli M, Kunicki S, Morissette C, Paquette J, Gervais F, Bergeron C, Fraser PE, Carlson GA, George-Hyslop PS, Westaway D (2001) Early-onset amyloid deposition and cognitive deficits in transgenic mice expressing a double mutant form of amyloid precursor protein 695. *J Biol Chem* **276**, 21562-21570.

[43] Choi-Miura NH, Ihara Y, Fukuchi K, Takeda M, Nakano Y, Tobe T, Tomita M (1992) SP-40,40 is a constituent of Alzheimer's amyloid. *Acta Neuropathol* **83**, 260-264.

[44] Chow VW, Mattson MP, Wong PC, Gleichmann M (2010) An overview of APP processing enzymes and products. *Neuromolecular Med* **12**, 1-12.

[45] Citron M (2000) Identifying proteases that cleave APP. *Ann N Y Acad Sci* **920**, 192-196.

[46] Citron M (2004) Strategies for disease modification in Alzheimer's disease. *Nat Rev Neurosci* **5**, 677-685.

[47] Clark CM, Davatzikos C, Borthakur A, Newberg A, Leight S, Lee VM, Trojanowski JQ (2008) Biomarkers for early detection of Alzheimer pathology. *Neurosignals* **16**, 11-18.

[48] Cleren C, Calingasan NY, Chen J, Beal MF (2005) Celastrol protects against MPTP- and 3-nitropropionic acid-induced neurotoxicity. *J Neurochem* **94**, 995-1004.

[49] Codita A, Winblad B, Mohammed AH (2006) Of mice and men: more neurobiology in dementia. *Curr Opin Psychiatry* **19**, 555-563.

[50] Corder EH, Saunders AM, Risch NJ, Strittmatter WJ, Schmechel DE, Gaskell PC, Jr., Rimmler JB, Locke PA, Conneally PM, Schmader KE, . (1994) Protective effect of apolipoprotein E type 2 allele for late onset Alzheimer disease. *Nat Genet* **7**, 180-184.

[51] Corder EH, Saunders AM, Strittmatter WJ, Schmechel DE, Gaskell PC, Small GW, Roses AD, Haines JL, Pericak-Vance MA (1993) Gene dose of apolipoprotein E type 4 allele and the risk of Alzheimer's disease in late onset families. *Science* **261**, 921-923.

[52] Cotman SL, Halfter W, Cole GJ (2000) Agrin binds to beta-amyloid (Abeta), accelerates abeta fibril formation, and is localized to Abeta deposits in Alzheimer's disease brain. *Mol Cell Neurosci* **15**, 183-198.

[53] Das P, Howard V, Loosbrock N, Dickson D, Murphy MP, Golde TE (2003) Amyloid-beta immunization effectively reduces amyloid deposition in FcRgamma-/- knock-out mice. *J Neurosci* **23**, 8532-8538.

[54] Davis J, Van Nostrand WE (1996) Enhanced pathologic properties of Dutch-type mutant amyloid beta-protein. *Proc Natl Acad Sci U S A* **93**, 2996-3000.

[55] Davis J, Xu F, Deane R, Romanov G, Previti ML, Zeigler K, Zlokovic BV, Van Nostrand WE (2004) Early-onset and robust cerebral microvascular accumulation of amyloid beta-protein in transgenic mice expressing low levels of a vasculotropic Dutch/Iowa mutant form of amyloid beta-protein precursor. *J Biol Chem* **279**, 20296-20306.

[56] Davis J, Xu F, Miao J, Previti ML, Romanov G, Ziegler K, Van Nostrand WE (2006) Deficient cerebral clearance of vasculotropic mutant Dutch/Iowa Double Ass in human AssPP transgenic mice. *Neurobiol Aging* **27**, 946-954.

[57] De Boeck H, Lories V, David G, Cassiman JJ, Van den Berghe H (1987) Identification of a 64 kDa heparan sulphate proteoglycan core protein from human lung fibroblast plasma membranes with a monoclonal antibody. *Biochem J* **247**, 765-771.

[58] De Strooper B., Vassar R, Golde T (2010) The secretases: enzymes with therapeutic potential in Alzheimer disease. *Nat Rev Neurol* **6**, 99-107.

[59] Deane R, Du YS, Submamaryan RK, LaRue B, Jovanovic S, Hogg E, Welch D, Manness L, Lin C, Yu J, Zhu H, Ghiso J, Frangione B, Stern A, Schmidt AM, Armstrong DL, Arnold B, Liliensiek B, Nawroth P, Hofman F, Kindy M, Stern D, Zlokovic B (2003) RAGE mediates amyloid-beta peptide transport across the blood-brain barrier and accumulation in brain. *Nat Med* **9**, 907-913.

[60] Deane R, Wu Z, Sagare A, Davis J, Du YS, Hamm K, Xu F, Parisi M, LaRue B, Hu HW, Spijkers P, Guo H, Song X, Lenting PJ, Van Nostrand WE, Zlokovic BV (2004) LRP/amyloid beta-peptide interaction mediates differential brain efflux of Abeta isoforms. *Neuron* **43**, 333-344.

[61] DeMattos RB, Bales KR, Cummins DJ, Dodart JC, Paul SM, Holtzman DM (2001) Peripheral anti-A beta antibody alters CNS and plasma A beta clearance and decreases brain A beta burden in a mouse model of Alzheimer's disease. *Proc Natl Acad Sci U S A* **98**, 8850-8855.

[62] DeMattos RB, Bales KR, Cummins DJ, Paul SM, Holtzman DM (2002) Brain to plasma amyloid-beta efflux: a measure of brain amyloid burden in a mouse model of Alzheimer's disease. *Science* **295**, 2264-2267.

[63] DeMattos RB, Bales KR, Parsadanian M, O'Dell MA, Foss EM, Paul SM, Holtzman DM (2002) Plaque-associated disruption of CSF and plasma amyloid-beta (Abeta) equilibrium in a mouse model of Alzheimer's disease. *J Neurochem* **81**, 229-236.

[64] DeMattos RB, O'Dell MA, Parsadanian M, Taylor JW, Harmony JA, Bales KR, Paul SM, Aronow BJ, Holtzman DM (2002) Clusterin promotes amyloid plaque formation and is critical for neuritic toxicity in a mouse model of Alzheimer's disease. *Proc Natl Acad Sci U S A* **99**, 10843-10848.

[65] DeWitt DA, Silver J, Canning DR, Perry G (1993) Chondroitin sulfate proteoglycans are associated with the lesions of Alzheimer's disease. *Exp Neurol* **121**, 149-152.

[66] Dodart JC, Bales KR, Gannon KS, Greene SJ, DeMattos RB, Mathis C, DeLong CA, Wu S, Wu X, Holtzman DM, Paul SM (2002) Immunization reverses memory deficits without reducing brain Abeta burden in Alzheimer's disease model. *Nat Neurosci* **5**, 452-457.

[67] Dodart JC, Mathis C, Bales KR, Paul SM (2002) Does my mouse have Alzheimer's disease? *Genes Brain Behav* **1**, 142-155.

[68] Dodart JC, Meziane H, Mathis C, Bales KR, Paul SM, Ungerer A (1999) Behavioral disturbances in transgenic mice overexpressing the V717F beta-amyloid precursor protein. *Behav Neurosci* **113**, 982-990.

[69] Donahue JE, Berzin TM, Rafii MS, Glass DJ, Yancopoulos GD, Fallon JR, Stopa EG (1999) Agrin in Alzheimer's disease: altered solubility and abnormal distribution within microvasculature and brain parenchyma. *Proc Natl Acad Sci U S A* **96**, 6468-6472.

[70] Dumont M, Wille E, Calingasan NY, Tampellini D, Williams C, Gouras GK, Liby K, Sporn M, Nathan C, Flint BM, Lin MT (2009) Triterpenoid CDDO-methylamide improves memory and decreases amyloid plaques in a transgenic mouse model of Alzheimer's disease. *J Neurochem* **109**, 502-512.

[71] Ebanks RO, Isenman DE (1996) Mouse complement component C4 is devoid of classical pathway C5 convertase subunit activity. *Mol Immunol* **33**, 297-309.

[72] Eikelenboom P, Hack CE, Kamphorst W, Rozemuller JM (1992) Distribution pattern and functional state of complement proteins and alpha 1-antichymotrypsin in cerebral beta/A4 deposits in Alzheimer's disease. *Res Immunol* **143**, 617-620.

[73] Eikelenboom P, Stam FC (1982) Immunoglobulins and complement factors in senile plaques. An immunoperoxidase study. *Acta Neuropathol (Berl)* **57**, 239-242.

[74] Elder GA, Gama Sosa MA, De Gasperi R (2010) Transgenic Mouse Models of Alzheimer's Disease. *Mt Sinai J Med* **77**, 69-81.

[75] Eriksson S, Janciauskiene S, Lannfelt L (1995) Alpha 1-antichymotrypsin regulates Alzheimer beta-amyloid peptide fibril formation. *Proc Natl Acad Sci U S A* **92**, 2313-2317.

[76] Fan R, DeFilippis K, Van Nostrand WE (2007) Induction of complement proteins in a mouse model for cerebral microvascular A beta deposition. *J Neuroinflammation* **4**, 22.

[77] Fenili D, Brown M, Rappaport R, McLaurin J (2007) Properties of scyllo-inositol as a therapeutic treatment of AD-like pathology. J Mol Med 85, 603-611.

[78] Fonseca MI, Zhou J, Botto M, Tenner AJ (2004) Absence of C1q leads to less neuropathology in transgenic mouse models of Alzheimer's disease. *J Neurosci* **24**, 6457-6465.

[79] Games D, Adams D, Alessandrini R, Barbour R, Berthelette P, Blackwell C, Carr T, Clemens J, Donaldson T, Gillespie F (1995) Alzheimer-type neuropathology in transgenic mice overexpressing V717F beta-amyloid precursor protein. *Nature* **373**, 523-527.

[80] Games D, Buttini M, Kobayashi D, Schenk D, Seubert P (2006) Mice as models: transgenic approaches and Alzheimer's disease. *J Alzheimers Dis* **9**, 133-149.

[81] Gandy S (2005) The role of cerebral amyloid beta accumulation in common forms of Alzheimer disease. *J Clin Invest* **115**, 1121-1129.

[82] Garcia-Alloza M, Robbins EM, Zhang-Nunes SX, Purcell SM, Betensky RA, Raju S, Prada C, Greenberg SM, Bacskai BJ, Frosch MP (2006) Characterization of amyloid deposition in the APPswe/PS1dE9 mouse model of Alzheimer disease. *Neurobiol Dis.*

[83] Gelinas DS, DaSilva K, Fenili D, St George-Hyslop P, McLaurin J (2004) Immunotherapy for Alzheimer's disease. *Proc Natl Acad Sci U S A* **101 Suppl 2**, 14657-14662.

[84] Ghosh AK, Kumaragurubaran N, Hong L, Kulkarni S, Xu X, Miller HB, Reddy DS, Weerasena V, Turner R, Chang W, Koelsch G, Tang J (2008) Potent memapsin 2 (beta-secretase) inhibitors: design, synthesis, protein-ligand X-ray structure, and in vivo evaluation. *Bioorg Med Chem Lett* **18**, 1031-1036.

[85] Glenner GG, Wong CW (1984) Alzheimer's disease: initial report of the purification and characterization of a novel cerebrovascular amyloid protein. *Biochem Biophys Res Commun* **120**, 885-890.

[86] Gotz J, Chen F, Barmettler R, Nitsch RM (2001) Tau filament formation in transgenic mice expressing P301L tau. *J Biol Chem* **276**, 529-534.

[87] Gupta-Bansal R, Frederickson RC, Brunden KR (1995) Proteoglycan-mediated inhibition of A beta proteolysis. A potential cause of senile plaque accumulation. *J Biol Chem* **270**, 18666-18671.

[88] Halfter W, Dong S, Schurer B, Cole GJ (1998) Collagen XVIII is a basement membrane heparan sulfate proteoglycan. *J Biol Chem* **273**, 25404-25412.

[89] Handler M, Yurchenco PD, Iozzo RV (1997) Developmental expression of perlecan during murine embryogenesis. *Dev Dyn* **210**, 130-145.

[90] Hansen RA, Gartlehner G, Webb AP, Morgan LC, Moore CG, Jonas DE (2008) Efficacy and safety of donepezil, galantamine, and rivastigmine for the treatment of Alzheimer's disease: a systematic review and meta-analysis. *Clin Interv Aging* **3**, 211-225.

[91] Hardingham TE, Fosang AJ (1992) Proteoglycans: many forms and many functions. *FASEB J* **6**, 861-870.

[92] Hardy J, Selkoe DJ (2002) The amyloid hypothesis of Alzheimer's disease: progress and problems on the road to therapeutics. *Science* **297**, 353-356.

[93] Harold D, Abraham R, Hollingworth P, Sims R, Gerrish A, Hamshere ML, Pahwa JS, Moskvina V, Dowzell K, Williams A, Jones N, Thomas C, Stretton A, Morgan AR, Lovestone S, Powell J, Proitsi P, Lupton MK, Brayne C, Rubinsztein DC, Gill M, Lawlor B, Lynch A, Morgan K, Brown KS, Passmore PA, Craig D, McGuinness B, Todd S, Holmes C, Mann D, Smith AD, Love S, Kehoe PG, Hardy J, Mead S, Fox N, Rossor M, Collinge J, Maier W, Jessen F, Schurmann B, van den Bussche H, Heuser I, Kornhuber J, Wiltfang J, Dichgans M, Frolich L, Hampel H, Hull M, Rujescu D, Goate AM, Kauwe JS, Cruchaga C, Nowotny P, Morris JC, Mayo K, Sleegers K, Bettens K, Engelborghs S, De Deyn PP, Van Broeckhoven C, Livingston G, Bass NJ, Gurling H, McQuillin A, Gwilliam R, Deloukas P, Al-Chalabi A, Shaw CE, Tsolaki M, Singleton AB, Guerreiro R, Muhleisen TW, Nothen MM, Moebus S, Jockel KH, Klopp N, Wichmann HE, Carrasquillo MM, Pankratz VS, Younkin SG, Holmans PA, O'Donovan M, Owen MJ, Williams J (2009) Genome-wide association study identifies variants at CLU and PICALM associated with Alzheimer's disease. *Nat Genet* **41**, 1088-1093.

[94] Hasegawa M, Crowther RA, Jakes R, Goedert M (1997) Alzheimer-like changes in microtubule-associated protein Tau induced by sulfated glycosaminoglycans. Inhibition of microtubule binding, stimulation of phosphorylation, and filament assembly depend on the degree of sulfation. *J Biol Chem* **272**, 33118-33124.

[95] Hashimoto T, Wakabayashi T, Watanabe A, Kowa H, Hosoda R, Nakamura A, Kanazawa I, Arai T, Takio K, Mann DM, Iwatsubo T (2002) CLAC: a novel Alzheimer amyloid plaque component derived from a transmembrane precursor, CLAC-P/collagen type XXV. *EMBO J* **21**, 1524-1534.

[96] Herzig MC, Winkler DT, Burgermeister P, Pfeifer M, Kohler E, Schmidt SD, Danner S, Abramowski D, Sturchler-Pierrat C, Burki K, van Duinen SG, Maat-Schieman ML, Staufenbiel M, Mathews PM, Jucker M (2004) Abeta is targeted to the vasculature in a mouse model of hereditary cerebral hemorrhage with amyloidosis. *Nat Neurosci* **7**, 954-960.

[97] Hickman-Davis JM, Davis IC (2006) Transgenic mice. *Paediatr Respir Rev* **7**, 49-53.

[98] Higgins LS, Catalano R, Quon D, Cordell B (1993) Transgenic mice expressing human beta-APP751, but not mice expressing beta-APP695, display early Alzheimer's disease-like histopathology. *Ann N Y Acad Sci* **695**, 224-227.

[99] Hock C, Konietzko U, Papassotiropoulos A, Wollmer A, Streffer J, von Rotz RC, Davey G, Moritz E, Nitsch RM (2002) Generation of antibodies specific for beta-amyloid by vaccination of patients with Alzheimer disease. *Nat Med* **8**, 1270-1275.

[100] Hock C, Konietzko U, Streffer JR, Tracy J, Signorell A, Muller-Tillmanns B, Lemke U, Henke K, Moritz E, Garcia E, Wollmer MA, Umbricht D, de Quervain DJ, Hofmann M, Maddalena A, Papassotiropoulos A, Nitsch RM (2003) Antibodies against beta-amyloid slow cognitive decline in Alzheimer's disease. *Neuron* **38**, 547-554.

[101] Holcomb L, Gordon MN, McGowan E, Yu X, Benkovic S, Jantzen P, Wright K, Saad I, Mueller R, Morgan D, Sanders S, Zehr C, O'Campo K, Hardy J, Prada CM, Eckman C, Younkin S, Hsiao K, Duff K (1998) Accelerated Alzheimer-type phenotype in transgenic mice carrying both mutant amyloid precursor protein and presenilin 1 transgenes. *Nat Med* **4**, 97-100.

[102] Holmes C, Boche D, Wilkinson D, Yadegarfar G, Hopkins V, Bayer A, Jones RW, Bullock R, Love S, Neal JW, Zotova E, Nicoll JA (2008) Long-term effects of Abeta42 immunisation in Alzheimer's disease: follow-up of a randomised, placebo-controlled phase I trial. *Lancet* **372**, 216-223.

[103] Holtzman DM, Fagan AM, Mackey B, Tenkova T, Sartorius L, Paul SM, Bales K, Ashe KH, Irizarry MC, Hyman BT (2000) Apolipoprotein E facilitates neuritic and cerebrovascular plaque formation in an Alzheimer's disease model. *Ann Neurol* **47**, 739-747.

[104] Hooijmans CR, Van der Zee CE, Dederen PJ, Brouwer KM, Reijmer YD, van Groen T, Broersen LM, Lutjohann D, Heerschap A, Kiliaan AJ (2009) DHA and cholesterol containing diets influence Alzheimer-like pathology, cognition and cerebral vasculature in APPswe/PS1dE9 mice. *Neurobiol Dis* **33**, 482-498.

[105] Horwitz J (1992) Alpha-crystallin can function as a molecular chaperone. *Proc Natl Acad Sci U S A* **89**, 10449-10453.

[106] Hsiao K, Chapman P, Nilsen S, Eckman C, Harigaya Y, Younkin S, Yang F, Cole G (1996) Correlative memory deficits, Abeta elevation, and amyloid plaques in transgenic mice. *Science* **274**, 99-102.

[107] Hughes SR, Khorkova O, Goyal S, Knaeblein J, Heroux J, Riedel NG, Sahasrabudhe S (1998) Alpha2-macroglobulin associates with beta-amyloid peptide and prevents fibril formation. *Proc Natl Acad Sci U S A* **95**, 3275-3280.

[108] Iozzo RV (1998) Matrix proteoglycans: from molecular design to cellular function. *Annu Rev Biochem* **67**, 609-652.

[109] Iwata N, Tsubuki S, Takaki Y, Watanabe K, Sekiguchi M, Hosoki E, Kawashima-Morishima M, Lee HJ, Hama E, Sekine-Aizawa Y, Saido TC (2000) Identification of the major Abeta1-42-degrading catabolic pathway in brain parenchyma: suppression leads to biochemical and pathological deposition. *Nat Med* **6**, 143-150.

[110] Janciauskiene S, Rubin H, Lukacs CM, Wright HT (1998) Alzheimer's peptide Abeta1-42 binds to two beta-sheets of alpha1-antichymotrypsin and transforms it from inhibitor to substrate. *J Biol Chem* **273**, 28360-28364.

[111] Jankowsky JL, Fadale DJ, Anderson J, Xu GM, Gonzales V, Jenkins NA, Copeland NG, Lee MK, Younkin LH, Wagner SL, Younkin SG, Borchelt DR (2004) Mutant presenilins specifically elevate the levels of the 42 residue beta-amyloid peptide in vivo: evidence for augmentation of a 42-specific gamma secretase. *Hum Mol Genet* **13**, 159-170.

[112] Jankowsky JL, Slunt HH, Ratovitski T, Jenkins NA, Copeland NG, Borchelt DR (2001) Co-expression of multiple transgenes in mouse CNS: a comparison of strategies. *Biomol Eng* **17**, 157-165.

[113] Janus C, Pearson J, McLaurin J, Mathews PM, Jiang Y, Schmidt SD, Chishti MA, Horne P, Heslin D, French J, Mount HT, Nixon RA, Mercken M, Bergeron C, Fraser PE, St George-Hyslop P, Westaway D (2000) A beta peptide immunization reduces behavioural impairment and plaques in a model of Alzheimer's disease. *Nature* **408**, 979-982.

[114] Jarrett JT, Berger EP, Lansbury PT, Jr. (1993) The carboxy terminus of the beta amyloid protein is critical for the seeding of amyloid formation: implications for the pathogenesis of Alzheimer's disease. *Biochemistry* **32**, 4693-4697.

[115] Jiang H, Burdick D, Glabe CG, Cotman CW, Tenner AJ (1994) beta-Amyloid activates complement by binding to a specific region of the collagen-like domain of the C1q A chain. *J Immunol* **152**, 5050-5059.

[116] Jung SS, Zhang W, Van Nostrand WE (2003) Pathogenic A beta induces the expression and activation of matrix metalloproteinase-2 in human cerebrovascular smooth muscle cells. *J Neurochem* **85**, 1208-1215.

[117] Kaeser SA, Herzig MC, Coomaraswamy J, Kilger E, Selenica ML, Winkler DT, Staufenbiel M, Levy E, Grubb A, Jucker M (2007) Cystatin C modulates cerebral beta-amyloidosis. *Nat Genet* **39**, 1437-1439.

[118] Kalaria RN, Grahovac I (1990) Serum amyloid P immunoreactivity in hippocampal tangles, plaques and vessels: implications for leakage across the blood-brain barrier in Alzheimer's disease. *Brain Res* **516**, 349-353.

[119] Kalback W, Watson MD, Kokjohn TA, Kuo YM, Weiss N, Luehrs DC, Lopez J, Brune D, Sisodia SS, Staufenbiel M, Emmerling M, Roher AE (2002) APP transgenic mice Tg2576 accumulate Abeta peptides that are distinct from the chemically modified and insoluble peptides deposited in Alzheimer's disease senile plaques. *Biochemistry* **41**, 922-928.

[120] Kanemitsu H, Tomiyama T, Mori H (2003) Human neprilysin is capable of degrading amyloid beta peptide not only in the monomeric form but also the pathological oligomeric form. *Neurosci Lett* **350**, 113-116.

[121] Kappe G, Franck E, Verschuure P, Boelens WC, Leunissen JA, de Jong WW (2003) The human genome encodes 10 alpha-crystallin-related small heat shock proteins: HspB1-10. *Cell Stress Chaperones* **8**, 53-61.

[122] Kawarabayashi T, Younkin LH, Saido TC, Shoji M, Ashe KH, Younkin SG (2001) Age-dependent changes in brain, CSF, and plasma amyloid (beta) protein in the Tg2576 transgenic mouse model of Alzheimer's disease. *J Neurosci* **21**, 372-381.

[123] Kelly PH, Bondolfi L, Hunziker D, Schlecht HP, Carver K, Maguire E, Abramowski D, Wiederhold KH, Sturchler-Pierrat C, Jucker M, Bergmann R, Staufenbiel M, Sommer B (2003) Progressive age-related impairment of cognitive behavior in APP23 transgenic mice. *Neurobiol Aging* **24**, 365-378.

[124] Kheterpal I, Williams A, Murphy C, Bledsoe B, Wetzel R (2001) Structural features of the Abeta amyloid fibril elucidated by limited proteolysis. *Biochemistry* **40**, 11757-11767.

[125] Kiaei M, Kipiani K, Petri S, Chen J, Calingasan NY, Beal MF (2005) Celastrol blocks neuronal cell death and extends life in transgenic mouse model of amyotrophic lateral sclerosis. *Neurodegener Dis* **2**, 246-254.

[126] Kim J, Basak JM, Holtzman DM (2009) The role of apolipoprotein E in Alzheimer's disease. *Neuron* **63**, 287-303.

[127] Kisilevsky R, Lemieux LJ, Fraser PE, Kong X, Hultin PG, Szarek WA (1995) Arresting amyloidosis in vivo using small-molecule anionic sulphonates or sulphates: implications for Alzheimer's disease. *Nat Med* **1**, 143-148.

[128] Klein WL, Krafft GA, Finch CE (2001) Targeting small Abeta oligomers: the solution to an Alzheimer's disease conundrum? *Trends Neurosci* **24**, 219-224.

[129] Kokjohn TA, Roher AE (2009) Amyloid precursor protein transgenic mouse models and Alzheimer's disease: understanding the paradigms, limitations, and contributions. *Alzheimers Dement* **5**, 340-347.

[130] Koller MF, Mohajeri MH, Huber M, Wollmer MA, Roth Z'graggen BV, Sandmeier E, Moritz E, Tracy J, Nitsch RM, Christen P (2004) Active immunization of mice with an Abeta-Hsp70 vaccine. *Neurodegener Dis* **1**, 20-28.

[131] Kolm V, Sauer U, Olgemooller B, Schleicher ED (1996) High glucose-induced TGF-beta 1 regulates mesangial production of heparan sulfate proteoglycan. *Am J Physiol* **270**, F812-F821.

[132] Kondo T, Tooyama I (2003) Deposition of Alpha2-Macroglobulin in Fibrillar Type of Senile Plaques in the Brain of PS/APP-Transgenic Mice. *Acta Histochemica et Cytochemica* **36**, 215-220.

[133] Kowa H, Sakakura T, Matsuura Y, Wakabayashi T, Mann DM, Duff K, Tsuji S, Hashimoto T, Iwatsubo T (2004) Mostly separate distributions of CLAC- versus Ab40- or Thioflavin S-reactivities in senile plaques reveal two distinct subpopulations of b-amyloid deposits. *Am J Pathol* **165**, 273-281.

[134] Kulnane LS, Lamb BT (2001) Neuropathological characterization of mutant amyloid precursor protein yeast artificial chromosome transgenic mice. *Neurobiol Dis* **8**, 982-992.

[135] Kuo YM, Crawford F, Mullan M, Kokjohn TA, Emmerling MR, Weller RO, Roher AE (2000) Elevated A beta and apolipoprotein E in A betaPP transgenic mice and its relationship to amyloid accumulation in Alzheimer's disease. *Mol Med* **6**, 430-439.

[136] Kuo YM, Kokjohn TA, Beach TG, Sue LI, Brune D, Lopez JC, Kalback WM, Abramowski D, Sturchler-Pierrat C, Staufenbiel M, Roher AE (2001) Comparative analysis of amyloid-beta chemical structure and amyloid plaque morphology of transgenic mouse and Alzheimer's disease brains. *J Biol Chem* **276**, 12991-12998.

[137] Kurup S, Wijnhoven TJ, Jenniskens GJ, Kimata K, Habuchi H, Li JP, Lindahl U, van Kuppevelt TH, Spillmann D (2007) Characterization of anti-heparan sulfate phage display antibodies AO4B08 and HS4E4. *J Biol Chem* **282**, 21032-21042.

[138] LaFerla FM, Green KN, Oddo S (2007) Intracellular amyloid-beta in Alzheimer's disease. *Nat Rev Neurosci* **8**, 499-509.

[139] Lalonde R, Kim HD, Fukuchi K (2004) Exploratory activity, anxiety, and motor coordination in bigenic APPswe + PS1/DeltaE9 mice. *Neurosci Lett* **369**, 156-161.

[140] Lalonde R, Kim HD, Maxwell JA, Fukuchi K (2005) Exploratory activity and spatial learning in 12-month-old APP(695)SWE/co+PS1/DeltaE9 mice with amyloid plaques. *Neurosci Lett* **390**, 87-92.

[141] Lalonde R, Strazielle C (2009) Exploratory activity and motor coordination in old versus middle-aged C57BL/6J mice. *Arch Gerontol Geriatr* **49**, 39-42.

[142] Lambert JC, Heath S, Even G, Campion D, Sleegers K, Hiltunen M, Combarros O, Zelenika D, Bullido MJ, Tavernier B, Letenneur L, Bettens K, Berr C, Pasquier F, Fievet N, Barberger-Gateau P, Engelborghs S, De Deyn P, Mateo I, Franck A, Helisalmi S, Porcellini E, Hanon O, de Pancorbo MM, Lendon C, Dufouil C, Jaillard C, Leveillard T, Alvarez V, Bosco P, Mancuso M, Panza F, Nacmias B, Bossu P, Piccardi P, Annoni G, Seripa D, Galimberti D, Hannequin D, Licastro F, Soininen H, Ritchie K, Blanche H, Dartigues JF, Tzourio C, Gut I, Van Broeckhoven C, Alperovitch A, Lathrop M, Amouyel P (2009) Genome-wide association study identifies variants at CLU and CR1 associated with Alzheimer's disease. *Nat Genet* **41**, 1094-1099.

[143] Lanz TA, Hosley JD, Adams WJ, Merchant KM (2004) Studies of Abeta pharmacodynamics in the brain, cerebrospinal fluid, and plasma in young (plaque-free) Tg2576 mice using the gamma-secretase inhibitor N2-[(2S)-2-(3,5-difluorophenyl)-2-hydroxyethanoyl]-N1-[(7S)-5-methyl-6-oxo -6,7-dihydro-5H-dibenzo[b,d]azepin-7-yl]-L-alaninamide (LY-411575). *J Pharmacol Exp Ther* **309**, 49-55.

[144] Lemere CA, Blusztajn JK, Yamaguchi H, Wisniewski T, Saido TC, Selkoe DJ (1996) Sequence of deposition of heterogeneous amyloid beta-peptides and APO E in Down syndrome: implications for initial events in amyloid plaque formation. *Neurobiol Dis* **3**, 16-32.

[145] Lemere CA, Maron R, Spooner ET, Grenfell TJ, Mori C, Desai R, Hancock WW, Weiner HL, Selkoe DJ (2000) Nasal A beta treatment induces anti-A beta antibody production and decreases cerebral amyloid burden in PD-APP mice. *Ann N Y Acad Sci* **920**, 328-331.

[146] Lemere CA, Spooner ET, LaFrancois J, Malester B, Mori C, Leverone JF, Matsuoka Y, Taylor JW, DeMattos RB, Holtzman DM, Clements JD, Selkoe DJ, Duff KE (2003) Evidence for peripheral clearance of cerebral Abeta protein following chronic, active Abeta immunization in PSAPP mice. *Neurobiol Dis* **14**, 10-18.

[147] Leveugle B, Ding W, Durkin JT, Mistretta S, Eisle J, Matic M, Siman R, Greenberg BD, Fillit HM (1997) Heparin promotes beta-secretase cleavage of the Alzheimer's amyloid precursor protein. *Neurochem Int* **30**, 543-548.

[148] Leveugle B, Ding W, Laurence F, Dehouck MP, Scanameo A, Cecchelli R, Fillit H (1998) Heparin oligosaccharides that pass the blood-brain barrier inhibit beta-amyloid precursor protein secretion and heparin binding to beta-amyloid peptide. *J Neurochem* **70**, 736-744.

[149] LeVine H, III (2004) The Amyloid Hypothesis and the clearance and degradation of Alzheimer's beta-peptide. *J Alzheimers Dis* **6**, 303-314.

[150] Levy E, Sastre M, Kumar A, Gallo G, Piccardo P, Ghetti B, Tagliavini F (2001) Codeposition of cystatin C with amyloid-beta protein in the brain of Alzheimer disease patients. *J Neuropathol Exp Neurol* **60**, 94-104.

[151] Lewis J, McGowan E, Rockwood J, Melrose H, Nacharaju P, Van SM, Gwinn-Hardy K, Paul MM, Baker M, Yu X, Duff K, Hardy J, Corral A, Lin WL, Yen SH, Dickson DW, Davies P, Hutton M (2000) Neurofibrillary tangles, amyotrophy and progressive motor disturbance in mice expressing mutant (P301L) tau protein. *Nat Genet* **25**, 402-405.

[152] Lindahl B, Eriksson L, Lindahl U (1995) Structure of heparan sulphate from human brain, with special regard to Alzheimer's disease. *Biochem J* **306 (Pt 1)**, 177-184.

[153] Lipp HP, Wolfer DP (1998) Genetically modified mice and cognition. Curr Opin *Neurobiol* **8**, 272-280.

[154] Liu L, Herukka SK, Minkeviciene R, van Groen T, Tanila H (2004) Longitudinal observation on CSF Abeta42 levels in young to middle-aged amyloid precursor protein/presenilin-1 doubly transgenic mice. *Neurobiol Dis* **17**, 516-523.

[155] Loeffler DA (2004) Using animal models to determine the significance of complement activation in Alzheimer's disease. *J Neuroinflammation* **1**, 18.

[156] Ma J, Yee A, Brewer HB, Jr., Das S, Potter H (1994) Amyloid-associated proteins alpha 1-antichymotrypsin and apolipoprotein E promote assembly of Alzheimer beta-protein into filaments. *Nature* **372**, 92-94.

[157] Ma Q, Dudas B, Hejna M, Cornelli U, Lee JM, Lorens S, Mervis R, Hanin I, Fareed J (2002) The blood-brain barrier accessibility of a heparin-derived oligosaccharides C3. *Thromb Res* **105**, 447-453.

[158] Maier M, Seabrook TJ, Lazo ND, Jiang L, Das P, Janus C, Lemere CA (2006) Short amyloid-beta (Abeta) immunogens reduce cerebral Abeta load and learning deficits in an Alzheimer's disease mouse model in the absence of an Abeta-specific cellular immune response. *J Neurosci* **26**, 4717-4728.

[159] Mandelkow EM, Mandelkow E (1998) Tau in Alzheimer's disease. *Trends Cell Biol* **8**, 425-427.

[160] Masliah E, Hansen L, Adame A, Crews L, Bard F, Lee C, Seubert P, Games D, Kirby L, Schenk D (2005) Abeta vaccination effects on plaque pathology in the absence of encephalitis in Alzheimer disease. *Neurology* **64**, 129-131.

[161] Matsubara E, Soto C, Governale S, Frangione B, Ghiso J (1996) Apolipoprotein J and Alzheimer's amyloid beta solubility. *Biochem J* **316** (Pt 2), 671-679.

[162] Matsuoka Y, Picciano M, Malester B, LaFrancois J, Zehr C, Daeschner JM, Olschowka JA, Fonseca MI, O'Banion MK, Tenner AJ, Lemere CA, Duff K (2001) Inflammatory responses to amyloidosis in a transgenic mouse model of Alzheimer's disease. *Am J Pathol* **158**, 1345-1354.

[163] Matsuoka Y, Saito M, LaFrancois J, Saito M, Gaynor K, Olm V, Wang L, Casey E, Lu Y, Shiratori C, Lemere C, Duff K (2003) Novel therapeutic approach for the treatment of Alzheimer's disease by peripheral administration of agents with an affinity to beta-amyloid. *J Neurosci* **23**, 29-33.

[164] Matsuoka Y, Shao L, Debnath M, LaFrancois J, Becker A, Gray A, Aisen P, Mathis C, Klunk W, Duff K (2005) An Abeta sequestration approach using non-antibody Abeta binding agents. *Curr Alzheimer Res* **2**, 265-268.

[165] Mattson MP (2004) Pathways towards and away from Alzheimer's disease. *Nature* **430**, 631-639.

[166] McGeer EG, Yasojima K, Schwab C, McGeer PL (2001) The pentraxins: possible role in Alzheimer's disease and other innate inflammatory diseases. *Neurobiol Aging* **22**, 843-848.

[167] McLaurin J, Kierstead ME, Brown ME, Hawkes CA, Lambermon MH, Phinney AL, Darabie AA, Cousins JE, French JE, Lan MF, Chen F, Wong SS, Mount HT, Fraser PE, Westaway D, St George-Hyslop P (2006) Cyclohexanehexol inhibitors of Abeta aggregation prevent and reverse Alzheimer phenotype in a mouse model. *Nat Med* **12**, 801-808.

[168] McLean CA, Cherny RA, Fraser FW, Fuller SJ, Smith MJ, Beyreuther K, Bush AI, Masters CL (1999) Soluble pool of Abeta amyloid as a determinant of severity of neurodegeneration in Alzheimer's disease. *Ann Neurol* **46**, 860-866.

[169] Meyer-Luehmann M, Spires-Jones TL, Prada C, Garcia-Alloza M, de Calignon A, Rozkalne A, Koenigsknecht-Talboo J, Holtzman DM, Bacskai BJ, Hyman BT (2008) Rapid appearance and local toxicity of amyloid-beta plaques in a mouse model of Alzheimer's disease. *Nature* **451**, 720-724.

[170] Mi W, Pawlik M, Sastre M, Jung SS, Radvinsky DS, Klein AM, Sommer J, Schmidt SD, Nixon RA, Mathews PM, Levy E (2007) Cystatin C inhibits amyloid-beta deposition in Alzheimer's disease mouse models. *Nat Genet* **39**, 1440-1442.

[171] Morgan BP, Gasque P (1996) Expression of complement in the brain: role in health and disease. *Immunol Today* **17**, 461-466.

[172] Morgan D, Diamond DM, Gottschall PE, Ugen KE, Dickey C, Hardy J, Duff K, Jantzen P, DiCarlo G, Wilcock D, Connor K, Hatcher J, Hope C, Gordon M, Arendash GW (2000) A beta peptide vaccination prevents memory loss in an animal model of Alzheimer's disease. *Nature* **408**, 982-985.

[173] Namba Y, Tomonaga M, Kawasaki H, Otomo E, Ikeda K (1991) Apolipoprotein E immunoreactivity in cerebral amyloid deposits and neurofibrillary tangles in Alzheimer's disease and kuru plaque amyloid in Creutzfeldt-Jakob disease. *Brain Res* **541**, 163-166.

[174] Navarro A, Del VE, Astudillo A, Gonzalez del RC, Tolivia J (2003) Immunohistochemical study of distribution of apolipoproteins E and D in human cerebral beta amyloid deposits. *Exp Neurol* **184**, 697-704.

[175] Neugroschl J, Sano M (2010) Current treatment and recent clinical research in Alzheimer's disease. *Mt Sinai J Med* **77**, 3-16.

[176] Nicoll JA, Burnett C, Love S, Graham DI, Dewar D, Ironside JW, Stewart J, Vinters HV (1997) High frequency of apolipoprotein E epsilon 2 allele in hemorrhage due to cerebral amyloid angiopathy. *Ann Neurol* **41**, 716-721.

[177] Nicoll JA, Wilkinson D, Holmes C, Steart P, Markham H, Weller RO (2003) Neuropathology of human Alzheimer disease after immunization with amyloid-beta peptide: a case report. *Nat Med* **9**, 448-452.

[178] Nilsson LN, Bales KR, DiCarlo G, Gordon MN, Morgan D, Paul SM, Potter H (2001) Alpha-1-antichymotrypsin promotes beta-sheet amyloid plaque deposition in a transgenic mouse model of Alzheimer's disease. *J Neurosci* **21**, 1444-1451.

[179] Nunan J, Small DH (2000) Regulation of APP cleavage by alpha-, beta- and gamma-secretases. *FEBS Lett* **483**, 6-10.

[180] O'Callaghan P, Sandwall E, Li JP, Yu H, Ravid R, Guan ZZ, van Kuppevelt TH, Nilsson LN, Ingelsson M, Hyman BT, Kalimo H, Lindahl U, Lannfelt L, Zhang X (2008) Heparan sulfate accumulation with Abeta deposits in Alzheimer's disease and Tg2576 mice is contributed by glial cells. *Brain Pathol* **18**, 548-561.

[181] Oddo S, Caccamo A, Shepherd JD, Murphy MP, Golde TE, Kayed R, Metherate R, Mattson MP, Akbari Y, LaFerla FM (2003) Triple-transgenic model of Alzheimer's disease with plaques and tangles: intracellular Abeta and synaptic dysfunction. *Neuron* **39**, 409-421.

[182] Olafsson I, Thorsteinsson L, Jensson O (1996) The molecular pathology of hereditary cystatin C amyloid angiopathy causing brain hemorrhage. *Brain Pathol* **6**, 121-126.

[183] Orgogozo JM, Gilman S, Dartigues JF, Laurent B, Puel M, Kirby LC, Jouanny P, Dubois B, Eisner L, Flitman S, Michel BF, Boada M, Frank A, Hock C (2003) Subacute meningoencephalitis in a subset of patients with AD after Abeta42 immunization. *Neurology* **61**, 46-54.

[184] Park JH, Widi GA, Gimbel DA, Harel NY, Lee DH, Strittmatter SM (2006) Subcutaneous Nogo receptor removes brain amyloid-beta and improves spatial memory in Alzheimer's transgenic mice. *J Neurosci* **26**, 13279-13286.

[185] Pitas RE, Boyles JK, Lee SH, Hui D, Weisgraber KH (1987) Lipoproteins and their receptors in the central nervous system. Characterization of the lipoproteins in cerebrospinal fluid and identification of apolipoprotein B,E(LDL) receptors in the brain. *J Biol Chem* **262**, 14352-14360.

[186] Priller C, Bauer T, Mitteregger G, Krebs B, Kretzschmar HA, Herms J (2006) Synapse formation and function is modulated by the amyloid precursor protein. *J Neurosci* **26**, 7212-7221.

[187] Puzzo D, Staniszewski A, Deng SX, Privitera L, Leznik E, Liu S, Zhang H, Feng Y, Palmeri A, Landry DW, Arancio O (2009) Phosphodiesterase 5 inhibition improves synaptic function, memory, and amyloid-beta load in an Alzheimer's disease mouse model. *J Neurosci* **29**, 8075-8086.

[188] Qiu WQ, Walsh DM, Ye Z, Vekrellis K, Zhang J, Podlisny MB, Rosner MR, Safavi A, Hersh LB, Selkoe DJ (1998) Insulin-degrading enzyme regulates extracellular levels of amyloid beta-protein by degradation. *J Biol Chem* **273**, 32730-32738.

[189] Rabenstein DL (2002) Heparin and heparan sulfate: structure and function. *Nat Prod Rep* **19**, 312-331.

[190] Rapraeger A (1989) Transforming growth factor (type beta) promotes the addition of chondroitin sulfate chains to the cell surface proteoglycan (syndecan) of mouse mammary epithelia. *J Cell Biol* **109**, 2509-2518.

[191] Reichwald J, Danner S, Wiederhold KH, Staufenbiel M (2009) Expression of complement system components during aging and amyloid deposition in APP transgenic mice. *J Neuroinflammation* **6**, 35.

[192] Reisberg B, Doody R, Stoffler A, Schmitt F, Ferris S, Mobius HJ (2003) Memantine in moderate-to-severe Alzheimer's disease. *N Engl J Med* **348**, 1333-1341.

[193] Rensink AA, de Waal RM, Kremer B, Verbeek MM (2003) Pathogenesis of cerebral amyloid angiopathy. *Brain Res Brain Res Rev* **43**, 207-223.

[194] Rensink AA, Otte-Holler I, de Boer R, Bosch RR, ten Donkelaar HJ, de Waal RM, Verbeek MM, Kremer B (2004) Insulin inhibits amyloid beta-induced cell death in cultured human brain pericytes. *Neurobiol Aging* **25**, 93-103.

[195] Rensink AA, Otte-Holler I, ten Donkelaar HJ, de Waal RM, Kremer B, Verbeek MM (2004) Differential gene expression in human brain pericytes induced by amyloid-beta protein. *Neuropathol Appl Neurobiol* **30**, 279-291.

[196] Rensink AA, Verbeek MM, Otte-Holler I, ten Donkelaar HT, de Waal RM, Kremer B (2002) Inhibition of amyloid-beta-induced cell death in human brain pericytes in vitro. *Brain Res* **952**, 111-121.

[197] Roher AE, Kokjohn TA (2002) Of mice and men: The relevance of transgenic mice Abeta immunizations to Alzheimer's disease. *J Alzheimers Dis* **4**, 431-434.

[198] Rose M, Dudas B, Cornelli U, Hanin I (2004) Glycosaminoglycan C3 protects against AF64A-induced cholinotoxicity in a dose-dependent and time-dependent manner. *Brain Res* **1015**, 96-102.

[199] Ruegg MA (1996) Agrin, laminin beta 2 (s-laminin) and ARIA: their role in neuromuscular development. *Curr Opin Neurobiol* **6**, 97-103.

[200] Sagare A, Deane R, Bell RD, Johnson B, Hamm K, Pendu R, Marky A, Lenting PJ, Wu Z, Zarcone T, Goate A, Mayo K, Perlmutter D, Coma M, Zhong Z, Zlokovic BV (2007) Clearance of amyloid-beta by circulating lipoprotein receptors. *Nat Med* **13**, 1029-1031.

[201] Salmivirta M, Lidholt K, Lindahl U (1996) Heparan sulfate: a piece of information. *FASEB J* **10**, 1270-1279.

[202] Sarasa M, Pesini P (2009) Natural non-trasgenic animal models for research in Alzheimer's disease. *Curr Alzheimer Res* **6**, 171-178.

[203] Schenk D, Barbour R, Dunn W, Gordon G, Grajeda H, Guido T, Hu K, Huang J, Johnson-Wood K, Khan K, Kholodenko D, Lee M, Liao Z, Lieberburg I, Motter R, Mutter L, Soriano F, Shopp G, Vasquez N, Vandevert C, Walker S, Wogulis M, Yednock T, Games D, Seubert P (1999) Immunization with amyloid-beta attenuates Alzheimer-disease-like pathology in the PDAPP mouse. *Nature* **400**, 173-177.

[204] Scholefield Z, Yates EA, Wayne G, Amour A, McDowell W, Turnbull JE (2003) Heparan sulfate regulates amyloid precursor protein processing by BACE1, the Alzheimer's beta-secretase. *J Cell Biol* **163**, 97-107.

[205] Schubert W, Prior R, Weidemann A, Dircksen H, Multhaup G, Masters CL, Beyreuther K (1991) Localization of Alzheimer beta A4 amyloid precursor protein at central and peripheral synaptic sites. *Brain Res* **563**, 184-194.

[206] Schwab C, Hosokawa M, McGeer PL (2004) Transgenic mice overexpressing amyloid beta protein are an incomplete model of Alzheimer disease. *Exp Neurol* 188, 52-64.

[207] Schwab C, McGeer PL (2008) Inflammatory aspects of Alzheimer disease and other neurodegenerative disorders. *J Alzheimers Dis* **13**, 359-369.

[208] Selkoe DJ (1998) The cell biology of beta-amyloid precursor protein and presenilin in Alzheimer's disease. *Trends Cell Biol* **8**, 447-453.

[209] Selkoe DJ (2001) Alzheimer's disease: genes, proteins, and therapy. *Physiol Rev* **81**, 741-766.

[210] Selkoe DJ (2001) Clearing the brain's amyloid cobwebs. *Neuron* **32**, 177-180.

[211] Selkoe DJ (2004) Alzheimer disease: mechanistic understanding predicts novel therapies. *Ann Intern Med* **140**, 627-638.

[212] Shen Y, Halperin JA, Lee CM (1995) Complement-mediated neurotoxicity is regulated by homologous restriction. *Brain Res* **671**, 282-292.

[213] Sheng JG, Mrak RE, Griffin WS (1996) Apolipoprotein E distribution among different plaque types in Alzheimer's disease: implications for its role in plaque progression. *Neuropathol Appl Neurobiol* **22**, 334-341.

[214] Shi J, Perry G, Aliev G, Smith MA, Ashe KH, Friedland RP (1999) Serum amyloid P is not present in amyloid beta deposits of a transgenic animal model. *Neuroreport* **10**, 3229-3232.

[215] Shi J, Perry G, Berridge MS, Aliev G, Siedlak SL, Smith MA, LaManna JC, Friedland RP (2002) Labeling of cerebral amyloid beta deposits in vivo using intranasal basic fibroblast growth factor and serum amyloid P component in mice. *J Nucl Med* **43**, 1044-1051.

[216] Shibata M, Yamada S, Kumar SR, Calero M, Bading J, Frangione B, Holtzman DM, Miller CA, Strickland DK, Ghiso J, Zlokovic BV (2000) Clearance of Alzheimer's amyloid-ss(1-40) peptide from brain by LDL receptor-related protein-1 at the blood-brain barrier. *J Clin Invest* **106**, 1489-1499.

[217] Siemers ER, Quinn JF, Kaye J, Farlow MR, Porsteinsson A, Tariot P, Zoulnouni P, Galvin JE, Holtzman DM, Knopman DS, Satterwhite J, Gonzales C, Dean RA, May PC (2006) Effects of a gamma-secretase inhibitor in a randomized study of patients with Alzheimer disease. *Neurology* **66**, 602-604.

[218] Sinha S, Anderson JP, Barbour R, Basi GS, Caccavello R, Davis D, Doan M, Dovey HF, Frigon N, Hong J, Jacobson-Croak K, Jewett N, Keim P, Knops J, Lieberburg I, Power M, Tan H, Tatsuno G, Tung J, Schenk D, Seubert P, Suomensaari SM, Wang S, Walker D, Zhao J, McConlogue L, John V (1999) Purification and cloning of amyloid precursor protein beta-secretase from human brain. *Nature* **402**, 537-540.

[219] Snow AD, Kinsella MG, Parks E, Sekiguchi RT, Miller JD, Kimata K, Wight TN (1995) Differential binding of vascular cell-derived proteoglycans (perlecan, biglycan, decorin, and versican) to the beta-amyloid protein of Alzheimer's disease. *Arch Biochem Biophys* **320**, 84-95.

[220] Snow AD, Mar H, Nochlin D, Kimata K, Kato M, Suzuki S, Hassell J, Wight TN (1988) The presence of heparan sulfate proteoglycans in the neuritic plaques and congophilic angiopathy in Alzheimer's disease. *Am J Pathol* **133**, 456-463.

[221] Snow AD, Mar H, Nochlin D, Kresse H, Wight TN (1992) Peripheral distribution of dermatan sulfate proteoglycans (decorin) in amyloid-containing plaques and their presence in neurofibrillary tangles of Alzheimer's disease. *J Histochem Cytochem* **40**, 105-113.

[222] Snow AD, Mar H, Nochlin D, Sekiguchi RT, Kimata K, Koike Y, Wight TN (1990) Early accumulation of heparan sulfate in neurons and in the beta-amyloid protein-containing lesions of Alzheimer's disease and Down's syndrome. *Am J Pathol* **137**, 1253-1270.

[223] Snow AD, Nochlin D, Sekiguichi R, Carlson SS (1996) Identification in immunolocalization of a new class of proteoglycan (keratan sulfate) to the neuritic plaques of Alzheimer's disease. *Exp Neurol* **138**, 305-317.

[224] Snow AD, Sekiguchi R, Nochlin D, Fraser P, Kimata K, Mizutani A, Arai M, Schreier WA, Morgan DG (1994) An important role of heparan sulfate proteoglycan (Perlecan) in a model system for the deposition and persistence of fibrillar A beta-amyloid in rat brain. *Neuron* **12**, 219-234.

[225] Snow AD, Wight TN (1989) Proteoglycans in the pathogenesis of Alzheimer's disease and other amyloidoses. *Neurobiol Aging* **10**, 481-497.

[226] Snow AD, Willmer J, Kisilevsky R (1987) Sulfated glycosaminoglycans: a common constituent of all amyloids? *Lab Invest* **56**, 120-123.

[227] Solomon B (2008) Immunological approaches for amyloid-beta clearance toward treatment for Alzheimer's disease. *Rejuvenation Res* **11**, 349-357.

[228] Solomon B, Koppel R, Frankel D, Hanan-Aharon E (1997) Disaggregation of Alzheimer beta-amyloid by site-directed mAb. *Proc Natl Acad Sci U S A* **94**, 4109-4112.

[229] Solomon B, Koppel R, Hanan E, Katzav T (1996) Monoclonal antibodies inhibit in vitro fibrillar aggregation of the Alzheimer beta-amyloid peptide. *Proc Natl Acad Sci U S A* **93**, 452-455.

[230] Sperling RA, Dickerson BC, Pihlajamaki M, Vannini P, LaViolette PS, Vitolo OV, Hedden T, Becker JA, Rentz DM, Selkoe DJ, Johnson KA (2010) Functional alterations in memory networks in early Alzheimer's disease. *Neuromolecular Med* **12**, 27-43.

[231] Strittmatter WJ, Saunders AM, Schmechel D, Pericak-Vance M, Enghild J, Salvesen GS, Roses AD (1993) Apolipoprotein E: high-avidity binding to beta-amyloid and increased frequency of type 4 allele in late-onset familial Alzheimer disease. *Proc Natl Acad Sci U S A* **90**, 1977-1981.

[232] Sturchler-Pierrat C, Abramowski D, Duke M, Wiederhold KH, Mistl C, Rothacher S, Ledermann B, Burki K, Frey P, Paganetti PA, Waridel C, Calhoun ME, Jucker M, Probst A, Staufenbiel M, Sommer B (1997) Two amyloid precursor protein transgenic mouse models with Alzheimer disease-like pathology. *Proc Natl Acad Sci U S A* **94**, 13287-13292.

[233] Sun B, Zhou Y, Halabisky B, Lo I, Cho SH, Mueller-Steiner S, Devidze N, Wang X, Grubb A, Gan L (2008) Cystatin C-cathepsin B axis regulates amyloid beta levels and associated neuronal deficits in an animal model of Alzheimer's disease. *Neuron* **60**, 247-257.

[234] Takasugi N, Tomita T, Hayashi I, Tsuruoka M, Niimura M, Takahashi Y, Thinakaran G, Iwatsubo T (2003) The role of presenilin cofactors in the gamma-secretase complex. *Nature* **422**, 438-441.

[235] Takata K, Hirata-Fukae C, Becker AG, Chishiro S, Gray AJ, Nishitomi K, Franz AH, Sakaguchi G, Kato A, Mattson MP, LaFerla FM, Aisen PS, Kitamura Y, Matsuoka Y (2007) Deglycosylated anti-amyloid beta antibodies reduce microglial phagocytosis and cytokine production while retaining the capacity to induce amyloid beta sequestration. *Eur J Neurosci* **26**, 2458-2468.

[236] Tanabe C, Hotoda N, Sasagawa N, Sehara-Fujisawa A, Maruyama K, Ishiura S (2007) ADAM19 is tightly associated with constitutive Alzheimer's disease APP alpha-secretase in A172 cells. *Biochem Biophys Res Commun* **352**, 111-117.

[237] Tandon A, Rogaeva E, Mullan M, St George-Hyslop PH (2000) Molecular genetics of Alzheimer's disease: the role of beta-amyloid and the presenilins. *Curr Opin Neurol* **13**, 377-384.

[238] Tanzi RE (2005) The synaptic Abeta hypothesis of Alzheimer disease. *Nat Neurosci* **8**, 977-979.

[239] Ten Dam GB, Kurup S, van de Westerlo EM, Versteeg EM, Lindahl U, Spillmann D, van Kuppevelt TH (2006) 3-O-sulfated oligosaccharide structures are recognized by anti-heparan sulfate antibody HS4C3. *J Biol Chem* **281**, 4654-4662.

[240] Terai K, Iwai A, Kawabata S, Sasamata M, Miyata K, Yamaguchi T (2001) Apolipoprotein E deposition and astrogliosis are associated with maturation of beta-amyloid plaques in betaAPPswe transgenic mouse: Implications for the pathogenesis of Alzheimer's disease. *Brain Res* **900**, 48-56.

[241] Thal DR, Griffin WS, de Vos RA, Ghebremedhin E (2008) Cerebral amyloid angiopathy and its relationship to Alzheimer's disease. *Acta Neuropathol* **115**, 599-609.

[242] Timmer NM, Herbert MK, Kleinovink JW, Kiliaan AJ, de Waal RM, Verbeek MM (2010) Limited expression of heparan sulfate proteoglycans associated with Abeta deposits in the APPswe/PS1dE9 mouse model for Alzheimer's disease. *Neuropathol Appl Neurobiol.* **36**, 478-486

[243] Timmer NM, Schirris TJ, Bruinsma IB, Otte-Holler I, van Kuppevelt TH, de Waal RM, Verbeek MM (2010) Aggregation and cytotoxic properties towards cultured cerebrovascular cells of Dutch-mutated Abeta40 (DAbeta(1-40)) are modulated by sulfate moieties of heparin. *Neurosci Res.* **66**, 380-389

[244] Timmer NM, van Horssen J, Otte-Holler I, Wilhelmus MM, David G, van Beers J, de Waal RM, Verbeek MM (2009) Amyloid beta induces cellular relocalization and production of agrin and glypican-1. *Brain Res* **1260**, 38-46.

[245] Tokuda T, Calero M, Matsubara E, Vidal R, Kumar A, Permanne B, Zlokovic B, Smith JD, Ladu MJ, Rostagno A, Frangione B, Ghiso J (2000) Lipidation of apolipoprotein E influences its isoform-specific interaction with Alzheimer's amyloid beta peptides. *Biochem J* **348 Pt 2**, 359-365.

[246] Ujiie M, Dickstein DL, Carlow DA, Jefferies WA (2003) Blood-brain barrier permeability precedes senile plaque formation in an Alzheimer disease model. *Microcirculation* **10**, 463-470.

[247] Van Dam D, De Deyn PP (2006) Drug discovery in dementia: the role of rodent models. *Nat Rev Drug Discov* **5**, 956-970.

[248] Van den Born J, van den Heuvel LP, Bakker MA, Veerkamp JH, Assmann KJ, Berden JH (1992) A monoclonal antibody against GBM heparan sulfate induces an acute selective proteinuria in rats. *Kidney Int* **41**, 115-123.

[249] Van den Born J, van den Heuvel LP, Bakker MA, Veerkamp JH, Assmann KJ, Berden JH (1994) Monoclonal antibodies against the protein core and glycosaminoglycan side chain of glomerular basement membrane heparan sulfate proteoglycan: characterization and immunohistological application in human tissues. *J Histochem Cytochem* **42**, 89-102.

[250] Van den Heuvel LP, van den Born J, van de Velden TJ, Veerkamp JH, Monnens LA, Schroder CH, Berden JH (1989) Isolation and partial characterization of heparan sulphate proteoglycan from the human glomerular basement membrane. *Biochem J* **264**, 457-465.

[251] Van Duinen SG, Castano EM, Prelli F, Bots GT, Luyendijk W, Frangione B (1987) Hereditary cerebral hemorrhage with amyloidosis in patients of Dutch origin is related to Alzheimer disease. *Proc Natl Acad Sci U S A* **84**, 5991-5994.

[252] Van Gool D, De Strooper B, Van Leuven F, Triau E, Dom R (1993) alpha 2-Macroglobulin expression in neuritic-type plaques in patients with Alzheimer's disease. *Neurobiol Aging* **14**, 233-237.

[253] Van Groen T, Kiliaan AJ, Kadish I (2006) Deposition of mouse amyloid beta in human APP/PS1 double and single AD model transgenic mice. *Neurobiol Dis* **23**, 653-662.

[254] Van Horssen J, Kleinnijenhuis J, Maass CN, Rensink AA, Otte-Holler I, David G, van den Heuvel LP, Wesseling P, de Waal RM, Verbeek MM (2002) Accumulation of heparan sulfate proteoglycans in cerebellar senile plaques. *Neurobiol Aging* **23**, 537-545.

[255] Van Horssen J, Otte-Holler I, David G, Maat-Schieman ML, van den Heuvel LP, Wesseling P, de Waal RM, Verbeek MM (2001) Heparan sulfate proteoglycan expression in cerebrovascular amyloid beta deposits in Alzheimer's disease and hereditary cerebral hemorrhage with amyloidosis (Dutch) brains. *Acta Neuropathol (Berl)* **102**, 604-614.

[256] Van Horssen J, Wesseling P, van den Heuvel LP, de Waal RM, Verbeek MM (2003) Heparan sulphate proteoglycans in Alzheimer's disease and amyloid-related disorders. *Lancet Neurol* **2**, 482-492.

[257] Van Horssen J, Wilhelmus MM, Heljasvaara R, Pihlajaniemi T, Wesseling P, de Waal RM, Verbeek MM (2002) Collagen XVIII: a novel heparan sulfate proteoglycan associated with vascular amyloid depositions and senile plaques in Alzheimer's disease brains. *Brain Pathol* **12**, 456-462.

[258] Van Vickle GD, Esh CL, Daugs ID, Kokjohn TA, Kalback WM, Patton RL, Luehrs DC, Walker DG, Lue LF, Beach TG, Davis J, Van Nostrand WE, Castano EM, Roher AE (2008) Tg-SwDI transgenic mice exhibit novel alterations in AbetaPP processing, Abeta degradation, and resilient amyloid angiopathy. *Am J Pathol* **173**, 483-493.

[259] Vasilevko V, Xu F, Previti ML, Van Nostrand WE, Cribbs DH (2007) Experimental investigation of antibody-mediated clearance mechanisms of amyloid-beta in CNS of Tg-SwDI transgenic mice. *J Neurosci* **27**, 13376-13383.

[260] Vassar R, Bennett BD, Babu-Khan S, Kahn S, Mendiaz EA, Denis P, Teplow DB, Ross S, Amarante P, Loeloff R, Luo Y, Fisher S, Fuller J, Edenson S, Lile J, Jarosinski MA, Biere AL, Curran E, Burgess T, Louis JC, Collins F, Treanor J, Rogers G, Citron M (1999) Beta-secretase cleavage of Alzheimer's amyloid precursor protein by the transmembrane aspartic protease BACE. *Science* **286**, 735-741.

[261] Vekrellis K, Ye Z, Qiu WQ, Walsh D, Hartley D, Chesneau V, Rosner MR, Selkoe DJ (2000) Neurons regulate extracellular levels of amyloid beta-protein via proteolysis by insulin-degrading enzyme. *J Neurosci* **20**, 1657-1665.

[262] Verbeek MM, de Waal RM, Schipper JJ, Van Nostrand WE (1997) Rapid degeneration of cultured human brain pericytes by amyloid beta protein. *J Neurochem* **68**, 1135-1141.

[263] Verbeek MM, Otte-Holler I, van den BJ, van den Heuvel LP, David G, Wesseling P, de Waal RM (1999) Agrin is a major heparan sulfate proteoglycan accumulating in Alzheimer's disease brain. *Am J Pathol* **155**, 2115-2125.

[264] Verbeek MM, Otte-Holler I, Veerhuis R, Ruiter DJ, de Waal RM (1998) Distribution of A beta-associated proteins in cerebrovascular amyloid of Alzheimer's disease. *Acta Neuropathol (Berl)* **96**, 628-636.

[265] Verbeek MM, Otte-Holler I, Wesseling P, Ruiter DJ, de Waal RM (1994) Induction of alpha-smooth muscle actin expression in cultured human brain pericytes by transforming growth factor-beta 1. *Am J Pathol* **144**, 372-382.

[266] Verbeek MM, Otte-Holler I, Wesseling P, Ruiter DJ, de Waal RM (1996) Differential expression of intercellular adhesion molecule-1 (ICAM-1) in the A beta-containing lesions in brains of patients with dementia of the Alzheimer type. *Acta Neuropathol* **91**, 608-615.

[267] Verbeek MM, Otte-Holler I, Westphal JR, Wesseling P, Ruiter DJ, de Waal RM (1994) Accumulation of intercellular adhesion molecule-1 in senile plaques in brain tissue of patients with Alzheimer's disease. *Am J Pathol* **144**, 104-116.

[268] Von Bernhardi R (2010) Immunotherapy in Alzheimer's disease: where do we stand? Where should we go? *J Alzheimers Dis* **19**, 405-421.

[269] Walsh DM, Klyubin I, Fadeeva JV, Rowan MJ, Selkoe DJ (2002) Amyloid-beta oligomers: their production, toxicity and therapeutic inhibition. *Biochem Soc Trans* **30**, 552-557.

[270] Wang YJ, Zhou HD, Zhou XF (2006) Clearance of amyloid-beta in Alzheimer's disease: progress, problems and perspectives. *Drug Discov Today* **11**, 931-938.

[271] Watanabe N, Araki W, Chui DH, Makifuchi T, Ihara Y, Tabira T (2004) Glypican-1 as an Abeta binding HSPG in the human brain: its localization in DIG domains and possible roles in the pathogenesis of Alzheimer's disease. *FASEB J* **18**, 1013-1015.

[272] Webster S, O'Barr S, Rogers J (1994) Enhanced aggregation and beta structure of amyloid beta peptide after coincubation with C1q. *J Neurosci Res* **39**, 448-456.

[273] Webster SD, Tenner AJ, Poulos TL, Cribbs DH (1999) The mouse C1q A-chain sequence alters beta-amyloid-induced complement activation. *Neurobiol Aging* **20**, 297-304.

[274] Weldon DT, Rogers SD, Ghilardi JR, Finke MP, Cleary JP, O'Hare E, Esler WP, Maggio JE, Mantyh PW (1998) Fibrillar beta-amyloid induces microglial phagocytosis, expression of inducible nitric oxide synthase, and loss of a select population of neurons in the rat CNS in vivo. *J Neurosci* **18**, 2161-2173.

[275] Weller RO, Massey A, Newman TA, Hutchings M, Kuo YM, Roher AE (1998) Cerebral amyloid angiopathy: amyloid beta accumulates in putative interstitial fluid drainage pathways in Alzheimer's disease. *Am J Pathol* **153**, 725-733.

[276] Whitehouse PJ, Price DL, Struble RG, Clark AW, Coyle JT, Delon MR (1982) Alzheimer's disease and senile dementia: loss of neurons in the basal forebrain. *Science* **215**, 1237-1239.

[277] Wijnhoven TJ, van de Westerlo EM, Smits NC, Lensen JF, Rops AL, van der Vlag J, Berden JH, van den Heuvel LP, van Kuppevelt TH (2008) Characterization of anticoagulant heparinoids by immunoprofiling. *Glycoconj J* **25**, 177-185.

[278] Wilcock DM, Alamed J, Gottschall PE, Grimm J, Rosenthal A, Pons J, Ronan V, Symmonds K, Gordon MN, Morgan D (2006) Deglycosylated anti-amyloid-beta antibodies eliminate cognitive deficits and reduce parenchymal amyloid with minimal vascular consequences in aged amyloid precursor protein transgenic mice. *J Neurosci* **26**, 5340-5346.

[279] Wilhelmus MM, Boelens WC, Otte-Holler I, Kamps B, de Waal RM, Verbeek MM (2006) Small heat shock proteins inhibit amyloid-beta protein aggregation and cerebrovascular amyloid-beta protein toxicity. *Brain Res* **1089**, 67-78.

[280] Wilhelmus MM, Boelens WC, Otte-Holler I, Kamps B, Kusters B, Maat-Schieman ML, de Waal RM, Verbeek MM (2006) Small heat shock protein HspB8: its distribution in Alzheimer's disease brains and its inhibition of amyloid-beta protein aggregation and cerebrovascular amyloid-beta toxicity. *Acta Neuropathol (Berl)* **111**, 139-149.

[281] Wilhelmus MM, de Waal RM, Verbeek MM (2007) Heat shock proteins and amateur chaperones in amyloid-Beta accumulation and clearance in Alzheimer's disease. *Mol Neurobiol* **35**, 203-216.

[282] Wilhelmus MM, Otte-Holler I, Davis J, Van Nostrand WE, de Waal RM, Verbeek MM (2005) Apolipoprotein E genotype regulates amyloid-beta cytotoxicity. *J Neurosci* **25**, 3621-3627.

[283] Wilhelmus MM, Otte-Holler I, van Triel JJ, Veerhuis R, Maat-Schieman ML, Bu G, de Waal RM, Verbeek MM (2007) Lipoprotein receptor-related protein-1 mediates amyloid-beta-mediated cell death of cerebrovascular cells. *Am J Pathol* **171**, 1989-1999.

[284] Wilhelmus MM, Otte-Holler I, Wesseling P, de Waal RM, Boelens WC, Verbeek MM (2006) Specific association of small heat shock proteins with the pathological hallmarks of Alzheimer's disease brains. *Neuropathol Appl Neurobiol* **32**, 119-130.

[285] Winkler DT, Bondolfi L, Herzig MC, Jann L, Calhoun ME, Wiederhold KH, Tolnay M, Staufenbiel M, Jucker M (2001) Spontaneous hemorrhagic stroke in a mouse model of cerebral amyloid angiopathy. *J Neurosci* **21**, 1619-1627.

[286] Wisniewski T, Castano EM, Golabek A, Vogel T, Frangione B (1994) Acceleration of Alzheimer's fibril formation by apolipoprotein E in vitro. *Am J Pathol* **145**, 1030-1035.

[287] Wisniewski T, Frangione B (1992) Apolipoprotein E: a pathological chaperone protein in patients with cerebral and systemic amyloid. *Neurosci Lett* **135**, 235-238.

[288] Wolfe MS (2001) Secretase targets for Alzheimer's disease: identification and therapeutic potential. *J Med Chem* **44**, 2039-2060.

[289] Wolfe MS, Haass C (2001) The Role of presenilins in gamma-secretase activity. *J Biol Chem* **276**, 5413-5416.

[290] Woods AG, Cribbs DH, Whittemore ER, Cotman CW (1995) Heparan sulfate and chondroitin sulfate glycosaminoglycan attenuate beta-amyloid(25-35) induced neurodegeneration in cultured hippocampal neurons. *Brain Res* **697**, 53-62.

[291] Wyss-Coray T, Yan F, Lin AH, Lambris JD, Alexander JJ, Quigg RJ, Masliah E (2002) Prominent neurodegeneration and increased plaque formation in complement-inhibited Alzheimer's mice. *Proc Natl Acad Sci U S A* **99**, 10837-10842.

[292] Xu F, Grande AM, Robinson JK, Previti ML, Vasek M, Davis J, Van Nostrand WE (2007) Early-onset subicular microvascular amyloid and neuroinflammation cor relate with behavioral deficits in vasculotropic mutant amyloid beta-protein precursor transgenic mice. *Neuroscience* **146**, 98-107.

[293] Yamaguchi F, Richards SJ, Beyreuther K, Salbaum M, Carlson GA, Dunnett SB (1991) Transgenic mice for the amyloid precursor protein 695 isoform have impaired spatial memory. *Neuroreport* **2**, 781-784.

[294] Yamaguchi H, Hirai S, Morimatsu M, Shoji M, Harigaya Y (1988) Diffuse type of senile plaques in the brains of Alzheimer-type dementia. *Acta Neuropathol* **77**, 113-119.

[295] Yan P, Bero AW, Cirrito JR, Xiao Q, Hu X, Wang Y, Gonzales E, Holtzman DM, Lee JM (2009) Characterizing the appearance and growth of amyloid plaques in APP/PS1 mice. *J Neurosci* **29**, 10706-10714.

[296] Yan SD, Chen X, Fu J, Chen M, Zhu H, Roher A, Slattery T, Zhao L, Nagashima M, Morser J, Migheli A, Nawroth P, Stern D, Schmidt AM (1996) RAGE and amyloid-beta peptide neurotoxicity in Alzheimer's disease. *Nature* **382**, 685-691.

[297] Yasojima K, Akiyama H, McGeer EG, McGeer PL (2001) Reduced neprilysin in high plaque areas of Alzheimer brain: a possible relationship to deficient degradation of beta-amyloid peptide. *Neurosci Lett* **297**, 97-100.

[298] Yasojima K, Schwab C, McGeer EG, McGeer PL (1999) Up-regulated production and activation of the complement system in Alzheimer's disease brain. *Am J Pathol* **154**, 927-936.

[299] Ying SC, Gewurz AT, Jiang H, Gewurz H (1993) Human serum amyloid P component oligomers bind and activate the classical complement pathway via residues 14-26 and 76-92 of the A chain collagen-like region of C1q. *J Immunol* **150**, 169-176.

[300] Zhou J, Fonseca MI, Pisalyaput K, Tenner AJ (2008) Complement C3 and C4 expression in C1q sufficient and deficient mouse models of Alzheimer's disease. *J Neurochem* **106**, 2080-2092.

[301] Zhu H, Yu J, Kindy MS (2001) Inhibition of amyloidosis using low-molecular-weight heparins. *Mol Med* **7**, 517-522.

[302] Zilka N, Novak M (2006) The tangled story of Alois Alzheimer. *Bratisl Lek Listy* **107**, 343-345.

[303] Zlokovic BV (2004) Clearing amyloid through the blood-brain barrier. *J Neurochem* **89**, 807-811.

[304] Zugel U, Kaufmann SH (1999) Role of heat shock proteins in protection from and pathogenesis of infectious diseases. *Clin Microbiol Rev* **12**, 19-39.

Curriculum Vitae

Nienke Timmer werd op 30 oktober 1979 geboren in Groningen, waar zij in 1998 haar VWO diploma behaalde aan het Willem Lodewijk Gymnasium. In 1999, na een jaar verschillende (administratieve) baantjes gehad te hebben, begon zij met de opleiding Biologie aan de Rijksuniversiteit Groningen. Vanwege haar interesse in anatomie en pathologie, koos zij na het eerste jaar met algemene biologievakken voor de richting Medische Biologie. Haar drie onderzoeksstages lagen vervolgens allen binnen de neurobiologie. Zo onderzocht zij tijdens haar eerste stage bij de afdeling Medische Fysiologie te Groningen, de mogelijkheid om neuronale stamcellen *in vitro* tot oligodendrocyten te differentiëren voor de behandeling van multiple sclerose (begeleider: Dr. J.C.V.M. Copray en Prof. Dr. H.W.G.M Boddeke). Tijdens haar tweede stage in Groningen bij de afdeling Moleculaire Neurobiologie (begeleider: Dr. K. van der Borght en Prof. Dr. P.G.M. Luiten) onderzocht zij of neuronale stamcellen getransplanteerd konden worden in de hersenen van muizen. Tenslotte vertrok zij voor een derde stage naar de universiteit van Szeged in Hongarije waar zij op de afdelingen Anatomie en Fysiologie onderzoek deed naar het effect van diazoxide op ischemie bij ratten met een operatief opgelegde chronische cerebrale hypoperfusie (begeleider: Dr. E. Farkas en prof. dr. F. Bari). Tijdens haar opleiding heeft Nienke bovendien meerdere student-assistentschappen gedaan, waaronder de begeleiding van practica anatomie en histologie voor eerste- en tweedejaars biologie studenten.

In april 2005 studeerde Nienke af in de richting Medische Biologie, waarna zij in september 2005 begon aan haar promotie op de afdeling Neurologie van het Universitair Medisch Centrum St. Radboud te Nijmegen onder supervisie van promotor Prof. Dr. H.P.H. Kremer (afd. Neurologie, Groningen) en copromotoren Dr. Ir. M.M Verbeek (afd. Neurologie, Nijmegen) en Dr. R.M.W. de Waal (afd. Pathologie, Nijmegen). Tijdens haar promotie, beschreven in dit proefschrift, begeleidde zij meerdere studenten tijdens hun stage. Daarnaast presenteerde zij haar onderzoeksresultaten op verschillende (internationale) bijeenkomsten, in de vorm van posters en mondelinge presentaties.
Vanaf december 2009 is zij werkzaam als postdoc op het LeARN project (CTMM) onder begeleiding van Dr. Ir. M.M. Verbeek. Binnen dit project doet zij onderzoek naar glutamaatgerelateerde metabolieten als potentiële biomarkers voor de ziekte van Alzheimer.

Full papers

Timmer NM, Kuiperij HB, de Waal RM, Verbeek MM (2010) Do amyloid β-associated factors co-deposit with Aβ in mouse models for Alzheimer's disease? *J Alzheimers Dis*

Timmer NM, van Dijk L, van der Zee CE, Kiliaan A, de Waal RM, Verbeek MM (2010) Enoxaparin treatment administered at both early and late stages of amyloid beta deposition improves cognition of APPswe/PS1dE9 mice with differential effects on brain A beta levels. *Neurobiol Dis.* **40**(1), 340-347

Timmer NM, Herbert MK, Kleinovink JW, Kiliaan AJ, de Waal RM, Verbeek MM (2010) Limited expression of heparan sulfate proteoglycans associated with Abeta deposits in the APPswe/PS1dE9 mouse model for Alzheimer's disease. *Neuropathol Appl Neurobiol.* **36**, 478-486

Timmer NM, Schirris TJ, Bruinsma IB, Otte-Holler I, van Kuppevelt TH, de Waal RM, Verbeek MM (2010) Aggregation and cytotoxic properties towards cultured cerebrovascular cells of Dutch-mutated Abeta40 (DAbeta(1-40)) are modulated by sulfate moieties of heparin. *Neurosci Res.* **66(4)**, 380-389

Timmer NM, van Horssen J, Otte-Holler I, Wilhelmus MM, David G, van Beers J, de Waal RM, Verbeek MM (2009) Amyloid beta induces cellular relocalization and production of agrin and glypican-1. *Brain Res* **1260**, 38-46

Farkas E, **Timmer NM**, Domoki F, Mihály A, Luiten PG, Bari F. (2005) Post-ischemic administration of diazoxide attenuates long-term microglial activation in the rat brain after permanent carotid artery occlusion. Neurosci Lett. 387(3), 168-172

Balasubramaniyan V, **Timmer N**, Kust B, Boddeke E, Copray S (2004) Transient expression of Olig1 initiates the differentiation of neural stem cells into oligodendrocyte progenitor cells. *Stem cells* **22(6)**, 878-882

Abstracts

Timmer NM, Degener S, Bergervoet N, Kiliaan AJ, van der Zee I, de Waal RMW, Verbeek MM (2009) Enoxaparin improves cognition of APPswe/PS1dE9 and TgSwDI mice with minor effect on amyloid β levels, *Alzheimers Dement* **5**(4) supplement (International Conference on Alzheimer's Disease), P416-417

Timmer N, de Waal R, Verbeek M (2008) Glycosaminoglycan sulfate moieties and chain length important for heparan sulfate proteoglycan interactions with amyloid-beta, *Alzheimers Dement* **4**(4) supplement (International Conference on Alzheimer's Disease), T350

Timmer NM, van Dijk L, Bergervoet N, Kiliaan A, van der Zee CEEM, de Waal RMW, Verbeek MM (2008) Treatment of APPswe/PS1dE9 mice with Enoxaparin improves cognitive impairment, *Alzheimers Dement* **4**(4) supplement (International Conference on Alzheimer's Disease), T763

Timmer NM, van Dijk L, Bergervoet N, Kiliaan A, van der Zee CEEM, de Waal RMW, Verbeek MM (2008) A peripheral sink for amyloid beta protein clearance, *7th Dutch Endo Neuro Psycho meeting*

Timmer N, van Beers J, de Waal R, Verbeek M (2006) Heparan sulphate proteoglycans may affect the biological activity of Aβ, *5th Dutch Endo Neuro Psycho meeting*

Timmer NM, Copray JCVM, Küst B, Balasubramaniyan V, Baron W, Wiersema A, De Haan G, Boddeke HWGM (2003) Induction of Oligodendrocyte differentiation in bone marrow derived neural stem cells, *2th Dutch Endo Neuro Psycho meeting*

Dankwoord

Dankwoord

Nu de wetenschappelijke inhoud van dit boekje afgerond (en gelezen?) is, is het tijd voor het dankwoord. Ik hoop natuurlijk dat ik niemand ben vergeten, zo ja, dan zal ik overwegen een beetje van mijn eigen medicijn te gebruiken…

Ik wil dit dankwoord beginnen met Marcel en Rob, mijn beide co-promotoren. Beiden waren aanwezig bij mijn allereerste stappen in het promotieonderzoek, oftewel de sollicitatie, en nu ook bij de uiteindelijke promotie.
Marcel, jij was de co-promotor die voor de dagelijkse begeleiding zorgde. Ik heb je leren kennen als een gedreven persoon die het serieuze werk van onderzoeker combineert met een flinke dosis humor en sarcasme. Met name de vrijheid die je mij tijdens het werk gaf, en nog steeds geeft, heb ik altijd als zeer fijn ervaren. Bovendien ben je, ondanks je drukke schema, altijd makkelijk benaderbaar. Bedankt voor de goede samenwerking de afgelopen jaren, wat mij betreft gaan we nog even op dezelfde voet door.
Rob, waarschijnlijk met name door de wat grotere fysieke afstand van onze werkplekken, hebben wij de afgelopen jaren eigenlijk met name contact gehad tijdens de wekelijkse werkbesprekingen. Bij deze besprekingen blijkt telkens weer je grote interesse in een breed scala aan onderwerpen, zowel binnen als buiten de wetenschap, wat de werkbesprekingen altijd weer net iets interessanter maakt. Ook wil ik je bedanken voor je nauwkeurige nakijkwerk van mijn artikelen. Jij bent altijd degene die tekstueel letterlijk de 'puntjes op de i' zet.

Beste Berry, als promotor bent u pas laat bij mijn promotie betrokken geraakt. Ik waardeer het dan ook zeer dat u, zelfs nu u in Groningen werkt, nog bereid was om mij tijdens de laatste loodjes van mijn promotie te begeleiden. Daarvoor dan ook mijn dank.

Ilona, al een half jaartje nadat ik was begonnen, kwam jij bij ons in de groep en sindsdien hebben wij eigenlijk al onze promotiebeslommeringen gedeeld. Bij jou vond ik een klankbord voor de experimenten die ik wilde uitvoeren en het is fijn om te weten dat ik altijd bij je kan komen emmeren over van alles en nog wat (en vice versa!). Laten we ook buiten het werk om veel contact houden, onze etentjes en tripjes, naar steden als Den Bosch en Groningen, zijn namelijk altijd zeer gezellig! Ik vond het niet meer dan logisch om jou bij mijn promotiedag te betrekken als paranimf en ben blij dat jij deze taak wilt vervullen. Kun je alvast een klein beetje oefenen voor je eigen promotie…

Toen ik bij Marcel op het toenmalige lab Kindergeneeskunde en Neurologie begon te werken, was ik naast Micha de enige promovendus binnen de "Alzheimer groep". Inmiddels is onze groep flink uitgebreid en dit is de sfeer op ons lab, wat mij betreft, zeer ten goede gekomen. Bea, van jouw kennis op onderzoeksgebied kan ik nog veel opsteken en ik hoop dat we nog vaak ook buiten het werk om samen gaan eten en kletsen. Ik meen dat we nog steeds een keertje sushi gaan maken, kan niet wachten!
Inge, Kim, Megan en Mareike, als "nieuwe" aio's binnen onze groep wil ik jullie bedanken voor de gezelligheid op het lab én in de kantoortuin en jullie heel veel succes wensen met jullie eigen promoties. Alexandra, bedankt voor je hulp met het zuiveren van αB-crystalline. Helaas is ons artikel (nog) niet gepubliceerd, maar je staat als co-auteur in ieder geval wel in dit boekje.

Voor mijn onderzoek heb ik veel samengewerkt met andere onderzoekers. Amanda en Ineke, zonder jullie input zouden veel van mijn muizen studies niet zijn uitgevoerd. Kortom, bedankt voor jullie muizen(kennis) en bijdrages aan dit proefschrift.
Bill, I want to thank you and your colleagues for providing us with the TgSwDI mouse model and the occasional protocol and suggestion. In the end, we hardly used the TgSwDI mice for the publications in this thesis, but we will continue to work with this model and hopefully produce some interesting articles in the near future.
Ook al mijn andere co-auteurs wil ik hier natuurlijk bedanken. Micha, bedankt dat je me op weg hebt geholpen als aio en ik hoop dat we (wetenschappelijk) contact blijven houden. Aan jouw werk wordt in ieder geval nog steeds gerefereerd en dan niet alleen op wetenschappelijk gebied; gevleugelde uitspraken als "dat is flut" en "lekker bezig" komen nog steeds wel eens langs.
Jack en Irene, ik wil jullie beiden bedanken voor de samenwerking. Jack, veel van jouw werk was de basis voor dit proefschrift en Irene, van jouw expertise op het gebied van amyloid β en electronen microscopie heb ik veel profijt gehad. Tenslotte wil ik ook Joyce van Beers, Wilbert Boelens, Guido David en Toin van Kuppevelt nog bedanken voor hun bijdrage aan mijn onderzoek en de tijd die ze hebben gestoken in mijn artikelen.

Hoewel ik hoofdzakelijk werkzaam was bij de afdeling Kindergeneeskunde en Neurologie, heb ik ook andere afdelingen bezocht tijdens mijn promotie. Ik wil hierbij vooral de afdeling pathologie, en dan met name Ine, Kiek, Cathy en Riki, bedanken voor de gastvrijheid de afgelopen jaren. Niet alleen heb ik veel celkweek en immunohistochemie bij jullie kunnen uitvoeren, ook veel van mijn studenten hebben hun werk bij pathologie kunnen uitvoeren.
Hierbij kom ik automatisch op de volgende groep die ik wil bedanken, namelijk de studenten die ik heb mogen begeleiden. In chronologische volgorde waren dit: Jelle, Wan Ying, Samantha, Laura, Niek, Tom, Sharon, Jan-Willem en Mieke. Slechts een aantal van jullie staat als co-auteur op mijn artikelen vermeld, maar jullie hebben allemaal een belangrijke bijdrage geleverd aan mijn onderzoek. Speciale dank ook aan de studenten die zich dagen achter elkaar hebben opgesloten in de "gedragskamer" om voor mij de muizen te testen.
Mijn muizenwerk is vrijwel allemaal uitgevoerd op het CDL en hier werken dan ook veel mensen die hebben bijgedragen aan mijn onderzoek. Zo hebben de dierverzorgers van de afdeling VGD mijn muizen de afgelopen jaren goed verzorgt. Hierbij wil ik met name Henk noemen, mijn contactpersoon binnen het CDL. Henk, bedankt voor je hulp bij vrijwel alle praktische, en vaak ook administratieve, aspecten van het muizenwerk. Ik hoop dat onze samenwerking ook de komende tijd op dezelfde gezellige en efficiënte manier kan worden voortgezet.

Van al mijn collega's heb ik buiten het werk om nog het meest contact met Herman. Herman, ik wil je dan ook bedanken voor je "opvang" hier in Nijmegen, samen met jou heb ik deze, voor mij eerst vreemde, stad goed leren kennen. Onze etentjes, concert- en filmbezoeken zijn altijd gezellig en wat mij betreft blijven we deze uitstapjes gewoon doen. En natuurlijk moeten we ook blijven borrelen in "stamkroeg" de Mug, al dan niet samen met collega's waaronder Inge K., Francien en Marijke. Ook alle overige (oud-) collega's van Q en P hebben natuurlijk bijgedragen aan de goede sfeer die ik heb ervaren tijdens het werk, de koffiepauzes en de vele uitjes, daarvoor mijn dank! Hierbij wil ik ook

nog een tweetal oud-collega's bij naam noemen; Mieke en Suus, ik hoop dat we contact kunnen blijven houden!
Carlijn, jou wil ik, als oud-collega binnen het Alzheimer veld, bedanken voor je gezelligheid en kordaatheid tijdens het genotyperen van de muizen en tijdens onze congresavonturen! Inmiddels werk je al weer even op het CDL, waar ik je helaas veel te weinig tegenkom. Hopelijk kunnen we af een toe nog een lunch inplannen.

Naast alle collega's wil ik graag ook een heel aantal mensen bedanken die misschien niet direct naast mij aan de labtafel werken, maar wel veel ontspanning brengen na het werk. Marleen, onze vakanties (en reizen!) door heel Europa en inmiddels ook Amerika, zijn altijd supergezellig. Dit is eigenlijk al zo vanaf de eerste nacht dat we een tent deelden, toen we elkaar nog maar nauwelijks kenden. Jij hebt inmiddels, als vaste reisgenoot en goede vriendin, veel van mijn werkperikelen meegekregen en ik ben dan ook heel blij dat je bij mijn promotie aanwezig bent.
Al in mijn eerste week van de opleiding Biologie in Groningen, kreeg ik contact met de "biologievrienden" (en inmiddels ook de aanhang) die ik nu nog steeds met wisselende regelmatigheid zie. Ciska, Eva, Willemien en Sonja, samen met Marleen hebben we al menig gezellig weekendje gehad en ik hoop dat we dit de komende jaren kunnen voortzetten. Nu Willemien in New York zit, wordt het tijd ons "Landal" gebied uit te breiden. En Cis en Son, bij deze wil ik jullie alvast heel veel succes wensen met jullie promoties!
Ook Peter, Melian, Douwe Jaap, Carmen, Arjen, Marloes, Janneke en Sander wil ik bedanken voor de gezellige etentjes/logeerfeestjes/filmpjes de afgelopen jaren. Ons contact is misschien niet meer zo regelmatig, maar ik hoop dat jullie bij mijn promotie kunnen zijn. Marte en Hiltje, ik hoop ook dat wij de komende jaren ons contact kunnen blijven onderhouden.

En dan wil ik natuurlijk ook mijn familie bedanken. We zijn maar met een klein clubje, maar wat mij betreft daarom juist best hecht. Met alle onderwijzers, bèta's en zelfs een analiste in de familie, kon het haast niet missen dat ik ben gaan promoveren in de neurobiologie. Helaas kan niet iedereen van de familie mijn promotie meemaken. Met name Gerda zou ik graag nog bedanken voor de interesse die ze altijd toonde voor mijn werk en de adviezen die ze mij tijdens mijn promotietijd heeft gegeven. Ik ben in ieder geval trots mijn promotiedag met (een deel) van mijn familie te mogen delen, waaronder Joke, Marja, Minke, Johan, Tanja, Egbert en Rienk.

Tenslotte mijn lieve ouders, "broertje" en schoonzus. Jan-Rienk, we zien elkaar helaas niet zo veel meer nu we niet meer samen in één huis wonen, maar ik vind het erg leuk dat jij mijn paranimf wilt zijn en dat jij je bovendien ook op mijn lay-out wilde storten. Samen met Henk (bedankt Henk!) hebben we er een mooi boekje van gemaakt. Overigens zou je zelf ook makkelijk kunnen promoveren, het discussiëren en kritisch denken gaat jou veel makkelijker af dan mij! Je wordt zelfs al een beetje een filosoof, maar kijk uit, om met Theo Maassen te spreken, filosofen zijn mensen die de hele dag nadenken over de zin van het leven. Ik weet niet wat de zin van het leven is, maar volgens mij in ieder geval niet om daar de hele dag over na te lopen denken.

Chantal, als wij aan de lijn hangen of als ik op bezoek kom, is het altijd gezellig. Ook onze bezoekjes aan "Jim" musicals zijn inmiddels een traditie geworden die ik er graag in wil houden. Bij ons in de familie sta je bekend om je brede en goede kledingsmaak en ik heb hier al veel van mogen profiteren. Ik denk dus dat ik je bij voorbaat alvast mag bedanken voor de hulp bij het uitzoeken van mijn promotie garderobe.

Pap en mam, last but definitely not least, het klinkt waarschijnlijk cliché, maar ik had volgens mij geen betere ouders kunnen hebben. Pap, het is altijd weer leuk om met jou op pad te gaan in de weekenden en ik wil je bedanken voor alle klusjes die je altijd (ongevraagd) voor mij uitvoert. Mam, jij zag al een onderzoeker in mij toen ik dat nog helemaal niet zag. Ik hoop dat jij de komende jaren veel rust en plezier vindt in je eigen werkzaamheden. In ieder geval is het fijn om te weten dat ik altijd bij jullie terecht kan voor een babbeltje, advies, gezelligheid en een dosis noordelijke nuchterheid. Bedankt dat jullie mij door dik en dun steunen, dit boekje is dan ook voor jullie!

Nienke

Series Donders Institute for Brain, Cognition and Behaviour

1. van Aalderen-Smeets, S.I. (2007). *Neural dynamics of visual selection.* Maastricht University, Maastricht, The Netherlands.
2. Schoffelen, J.M. (2007). *Neuronal communication through coherence in the human motor system.* Radboud University Nijmegen, Nijmegen, The Netherlands.
3. de Lange, F.P. (2008). *Neural mechanisms of motor imagery.* Radboud University Nijmegen, Nijmegen, The Netherlands.
4. Grol, M.J. (2008). *Parieto-frontal circuitry in visuomotor control.* University Utrecht, Utrecht, The Netherlands.
5. Bauer, M. (2008). *Functional roles of rhythmic neuronal activity in the human visual and somatosensory system.* Radboud University Nijmegen, Nijmegen, The Netherlands.
6. Mazaheri, A. (2008). *The Influence of Ongoing Oscillatory Brain Activity on Evoked Responses and Behaviour.* Radboud University Nijmegen, Nijmegen, The Netherlands.
7. Hooijmans, C.R. (2008). *Impact of nutritional lipids and vascular factors in Alzheimer's Disease.* Radboud University Nijmegen, Nijmegen, The Netherlands.
8. Gaszner, B. (2008). *Plastic responses to stress by the rodent urocortinergic Edinger-Westphal nucleus.* Radboud University Nijmegen, Nijmegen, The Netherlands.
9. Willems, R.M. (2009). *Neural reflections of meaning in gesture, language and action.* Radboud University Nijmegen, Nijmegen, The Netherlands.
10. Van Pelt, S. (2009). *Dynamic neural representations of human visuomotor space.* Radboud University Nijmegen, Nijmegen, The Netherlands.
11. Lommertzen, J. (2009). *Visuomotor coupling at different levels of complexity.* Radboud University Nijmegen, Nijmegen, The Netherlands.
12. Poljac, E. (2009). *Dynamics of cognitive control in task switching: Looking beyond the switch cost.* Radboud University Nijmegen, Nijmegen, The Netherlands.
13. Poser, B.A. (2009) *Techniques for BOLD and blood volume weighted fMRI.* Radboud University Nijmegen, Nijmegen, The Netherlands.
14. Baggio, G. (2009). *Semantics and the electrophysiology of meaning. Tense, aspect, event structure.* Radboud University Nijmegen, Nijmegen, The Netherlands.
15. van Wingen, G.A. (2009). *Biological determinants of amygdala functioning.* Radboud University Nijmegen Medical Centre, Nijmegen, The Netherlands.
16. Bakker, M. (2009). *Supraspinal control of walking: lessons from motor imagery.* Radboud University Nijmegen Medical Centre, Nijmegen, The Netherlands.
17. Aarts, E. (2009). *Resisting temptation: the role of the anterior cingulate cortex in adjusting cognitive control.* Radboud University Nijmegen, Nijmegen, The Netherlands.
18. Prinz, S. (2009). *Waterbath stunning of chickens – Effects of electrical parameters on the electroencephalogram and physical reflexes of broilers.* Radboud University Nijmegen, Nijmegen, The Netherlands.
19. Knippenberg, J.M.J. (2009). *The N150 of the Auditory Evoked Potential from the rat amygdala: In search for its functional significance.* Radboud University Nijmegen, Nijmegen, The Netherlands.

20. Dumont, G.J.H. (2009). *Cognitive and physiological effects of 3,4-methylenedioxy methamphetamine (MDMA or 'ecstasy') in combination with alcohol or cannabis in humans*. Radboud University Nijmegen, Nijmegen, The Netherlands.
21. Pijnacker, J. (2010). *Defeasible inference in autism: a behavioral and electrophysiogical approach*. Radboud Universiteit Nijmegen, The Netherlands.
22. de Vrijer, M. (2010). *Multisensory integration in spatial orientation*. Radboud University Nijmegen, Nijmegen, The Netherlands.
23. Vergeer, M. (2010). *Perceptual visibility and appearance: Effects of color and form*. Radboud University Nijmegen, Nijmegen, The Netherlands.
24. Levy, J. (2010). *In Cerebro Unveiling Unconscious Mechanisms during Reading*. Radboud University Nijmegen, Nijmegen, The Netherlands.
25. Treder, M. S. (2010). *Symmetry in (inter)action*. Radboud University Nijmegen, Nijmegen, The Netherlands.
26. Horlings C.G.C. (2010). *A Weak balance; balance and falls in patients with neuromuscular disorders*. Radboud University Nijmegen, Nijmegen, The Netherlands
27. Snaphaan, L.J.A.E. (2010). *Epidemiology of post-stroke behavioural consequences*. Radboud University Nijmegen Medical Centre, Nijmegen, The Netherlands.
28. Dado – Van Beek, H.E.A. (2010). *The regulation of cerebral perfusion in patients with Alzheimer's disease*. Radboud University Nijmegen Medical Centre, Nijmegen, The Netherlands.
29. Derks, N.M. (2010). *The role of the non-preganglionic Edinger-Westphal nucleus in sex-dependent stress adaptation in rodents*. Radboud University Nijmegen, Nijmegen, The Netherlands.
30. Wyczesany, M. (2010). *Covariation of mood and brain activity. Integration of subjective self-report data with quantitative EEG measures*. Radboud University Nijmegen, Nijmegen, The Netherlands.
31. Beurze S.M. (2010). *Cortical mechanisms for reach planning*. Radboud University Nijmegen, Nijmegen, The Netherlands.
32. van Dijk, J.P. (2010). *On the Number of Motor Units*. Radboud University Nijmegen, The Netherlands .
33. Lapatki, B.G. (2010). *The Facial Musculature – Characterization at a Motor Unit Level*. Radboud University Nijmegen, Nijmegen, The Netherlands.
34. Kok, P. (2010). *Word Order and Verb Inflection in Agrammatic Sentence Production*. Radboud University Nijmegen, Nijmegen, The Netherlands.
35. van Elk, M. (2010). *Action semantics: Functional and neural dynamics*. Radboud University Nijmegen, Nijmegen, The Netherlands.
36. Majdandzic, J. (2010). *Cerebral mechanisms of processing action goals in self and others*. Radboud University Nijmegen, Nijmegen, The Netherlands.
37. Snijders, T.M. (2010). *More than words – neural and genetic dynamics of syntactic unification*. Radboud University Nijmegen, Nijmegen, The Netherlands.
38. Grootens, K.P. (2010). *Cognitive dysfunction and effects of antipsychotics in schizophrenia and borderline personality disorder*. Radboud University Nijmegen Medical Centre, Nijmegen, The Netherlands.
39. Nieuwenhuis, I.L.C. (2010). *Memory consolidation: A process of integration – Converging evidence from MEG, fMRI and behavior*. Radboud University Nijmegen Medical Centre, Nijmegen, The Netherlands.

40. Menenti, L.M.E. (2010). *The right language: differential hemispheric contributions to language production and comprehension in context*. Radboud University Nijmegen, Nijmegen, The Netherlands.
41. van Dijk, H.P. (2010). *The state of the brain, how alpha oscillations shape behaviour and event related responses*. Radboud University Nijmegen, Nijmegen, The Netherlands.
42. Meulenbroek, O.V. (2010). *Neural correlates of episodic memory in healthy aging and Alzheimer's disease*. Radboud University Nijmegen, Nijmegen, The Netherlands.
43. Oude Nijhuis, L.B. (2010). *Modulation of human balance reactions*. Radboud University Nijmegen, Nijmegen, The Netherlands.
44. Qin, S. (2010). *Adaptive memory: imaging medial temporal and prefrontal memory systems*. Radboud University Nijmegen, The Netherlands.
45. Timmer, N.M. (2011). *The interaction of heparan sulfate proteoglycans with the amyloid β protein*. Radboud University Nijmegen, Nijmegen, The Netherlands.

Figures in full colour

Figures in full colour

***Chapter 1**: Figure 1*

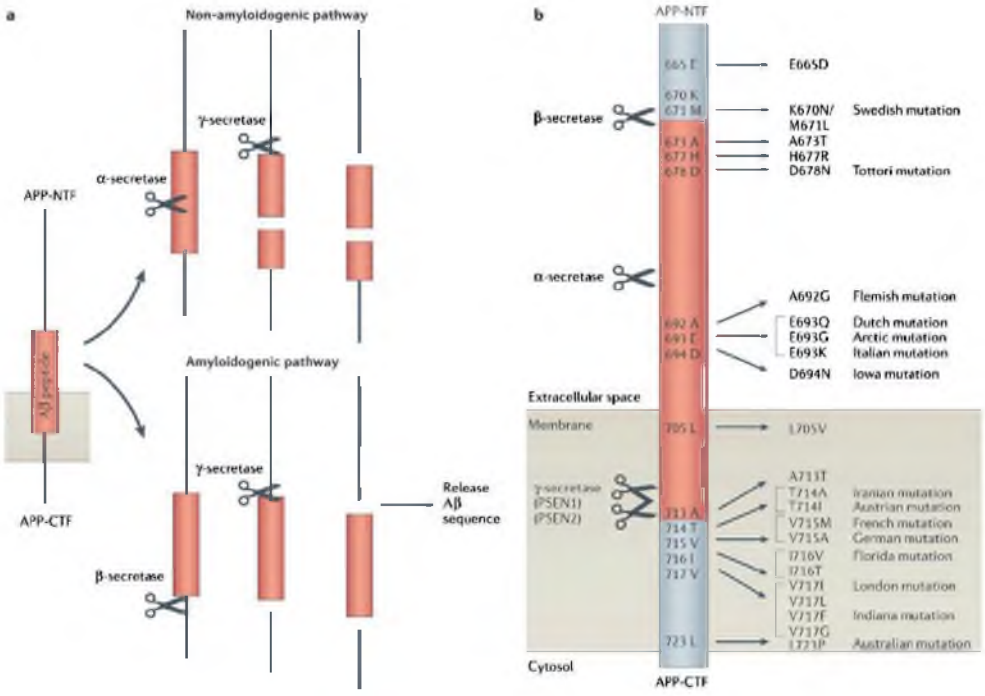

Figure 1: *Amyloid precursor protein (APP) processing involves proteolytic cleavage by several secretases (A). The non-amyloidogenic pathway is initiated by α-secretase cleavage, which occurs in the middle of the amyloid β (Aβ) sequence (red), and results in the release of several soluble APP fragments. The amyloidogenic pathway releases Aβ peptides through cleavage by α- and β-secretases. (B) Part of the APP amino-acid sequence; mutations associated with early-onset Alzheimer's disease have been highlighted. Most mutations are clustered in the close vicinity of secretase-cleavage sites, thereby influencing APP processing, and are named after the nationality or location of the first family in which that specific mutation was demonstrated. The Aβ sequence is indicated in red. Reprinted with permission from Macmillan Publishers Ltd: [Nature Reviews Drug Discovery] [247], copyright (2006)*

***Chapter 1**: Figure 2*

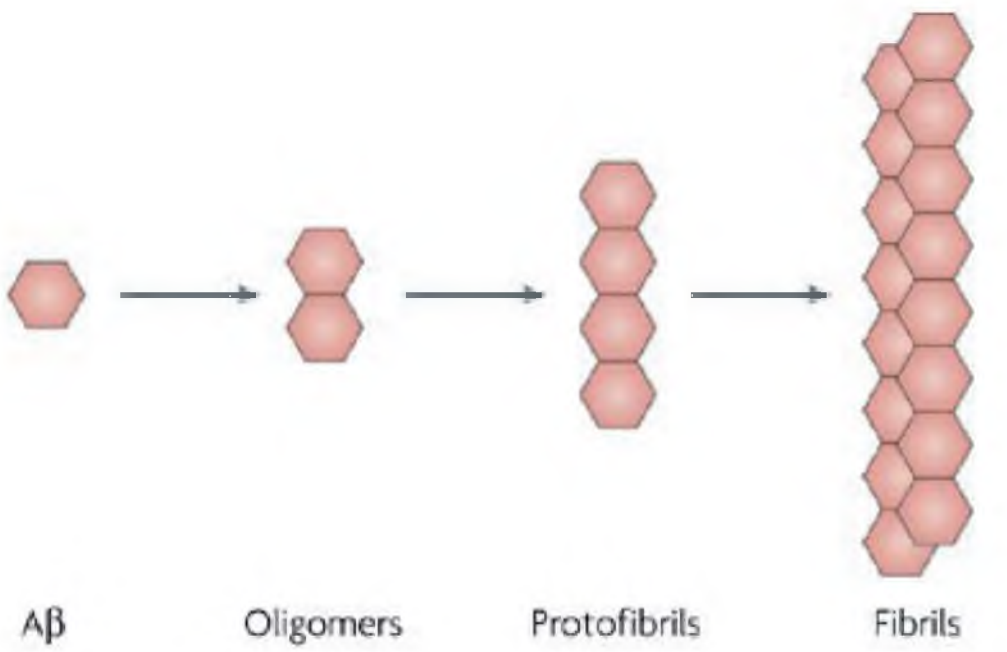

Figure 2: *Amyloid β (Aβ) can exist in multiple assembly states — monomers, oligomers, protofibrils and fibrils. In its monomeric state, Aβ does not appear to be neurotoxic. By contrast, oligomeric and protofibrillar species are considered potent blockers of long-term potentiation, a form of synaptic plasticity. Reprinted with permission from Macmillan Publishers Ltd: [Nature Reviews Neuroscience] [138], copyright (2007).*

***Chapter 1**: Figure 3*

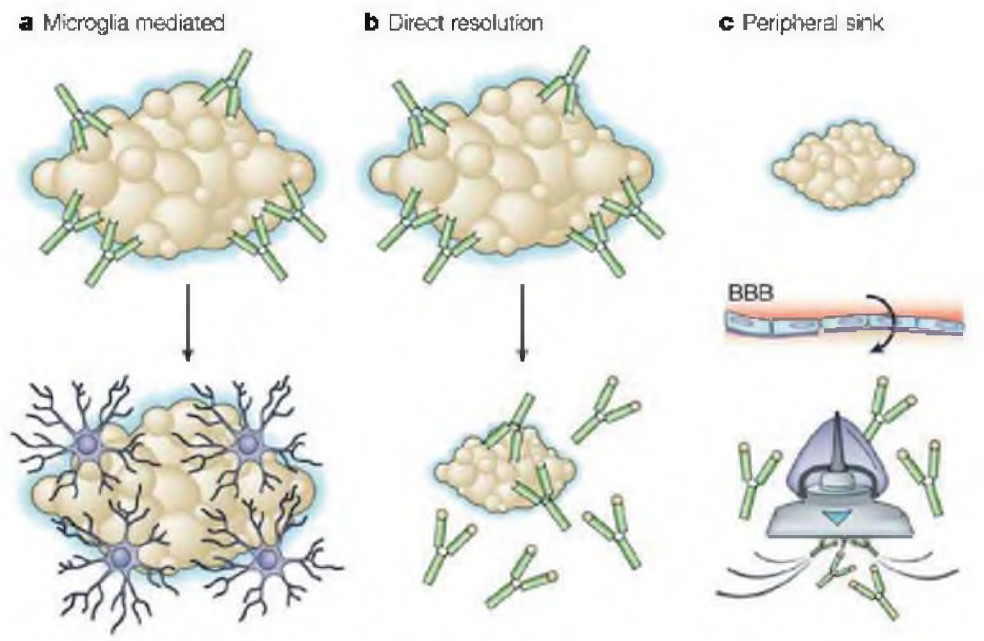

Figure 3: *Three biological mechanisms that are not mutually exclusive have been proposed. Small amounts of anti-amyloid antibodies reach amyloid deposits in the brain and trigger a phagocytic response by microglia (A). Anti-amyloid antibodies reach amyloid deposits in the brain and resolve them directly through interaction of the antibody with the amyloid deposit (B). Anti-amyloid antibodies act as a peripheral sink for soluble amyloid β species, leading ultimately to the resolution of brain deposits by mass action (B). BBB, blood–brain barrier. Reprinted with permission from Macmillan Publishers Ltd: [Nature Reviews Neuroscience] [46], copyright (2004).*

***Chapter 2**: Figure 1*

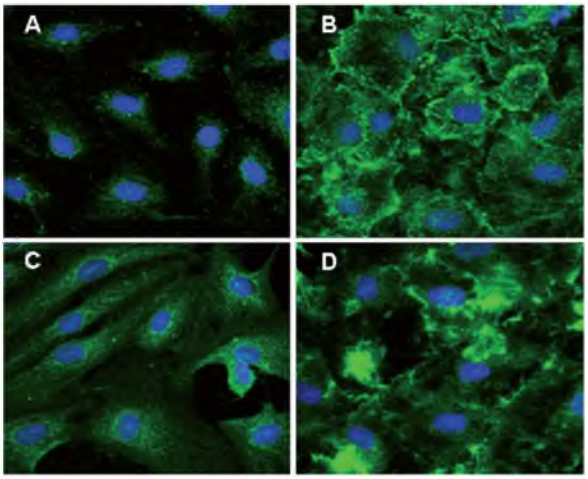

Figure 1: *Immunofluorescence staining of untreated (A, C) and DAβ$_{1-40}$–treated (B, D) HBP for agrin (A, B) and glypican-1 (C, D). Protein expression of both agrin and glypican-1 was increased after treatment. Original magnification 630x.*

***Chapter 3**: Figure 5*

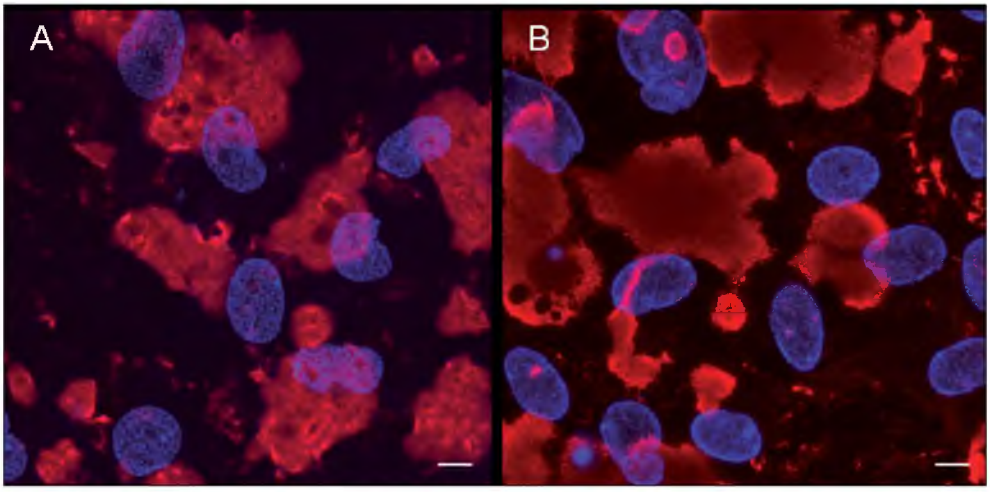

Figure 5: *Immunofluorescent staining of confluent cultures of HBP incubated with DAβ$_{1-40}$ alone (A) or in combination with heparin (B). No obvious change in the association of Aβ (40-4; red) with the cultured cells (Topro-3; blue nuclei) was visible when DAβ$_{1-40}$ was incubated with heparin. Magnification 630x. Scale bar: 1 mm*

***Chapter 3**: Figure 10*

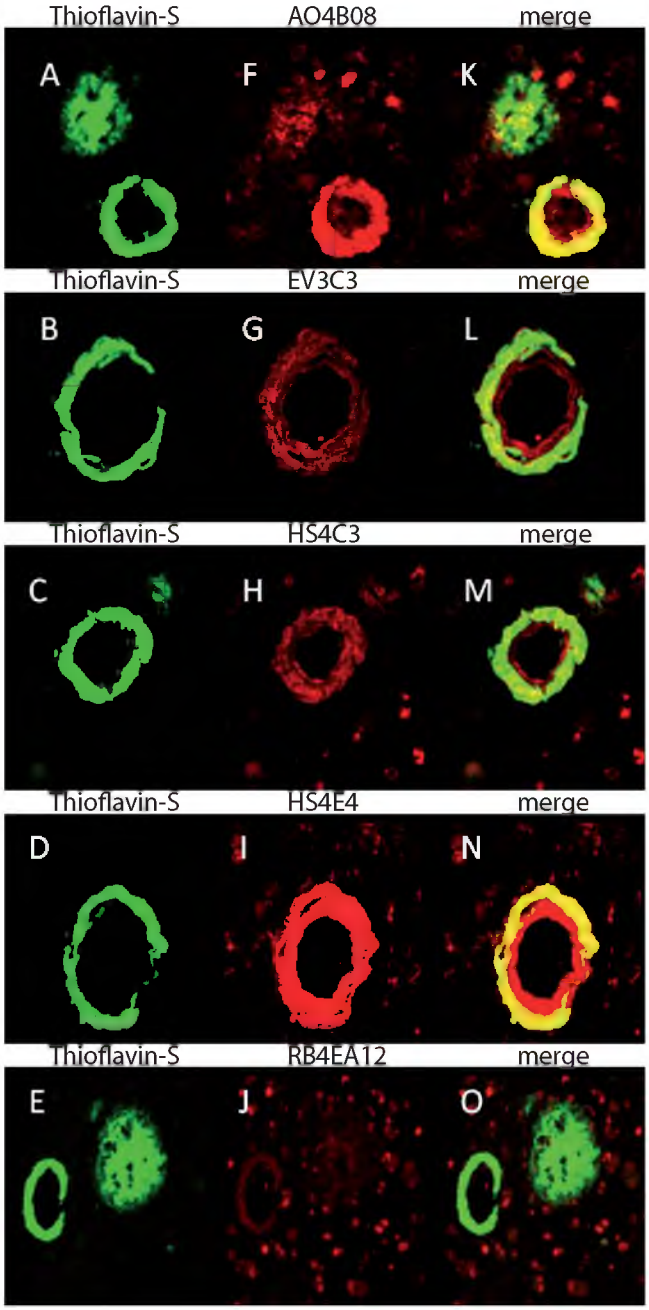

Figure 10: *Immunofluorescent staining of Thioflavin-S positive cortical vessels of an AD patient (A-E) with different phage display antibodies that recognize different HS sulfate motives (F-J). In K-O, Thioflavin-S and HS staining is merged. Vessels with fibrillar Aβ deposits were positive for most antibodies (K-N), but negative for RB4EA12 (O). Original magnification 630x.*

***Chapter 4**: Figures 1C and 1D*

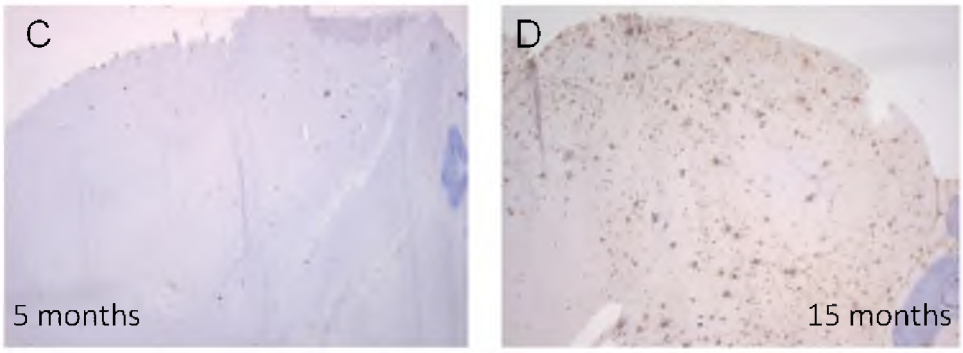

Figure 1: *The average Aβ plaque number (±S.E.M.) increased with age in the APPswe/PS1dE9 mouse model (A), whereas the average number of Aβ-positive blood vessels (±S.E.M.) was low (B), except in the 18-month-old mice. Sagittal sections (5 µm) of mice aged 5 months (C) or 15 months (D) were stained for Aβ using the 6C6 antibody and plaques and Aβ-positive vessels were counted in 8 sections per mouse. (A) * p<0.05 compared to 5 months old. ^ p<0.05 compared to 8 months old. (B) * p<0.05 compared to all other groups. Magnification 200x.*

***Chapter 4**: Figures 2C, 2D and 2E*

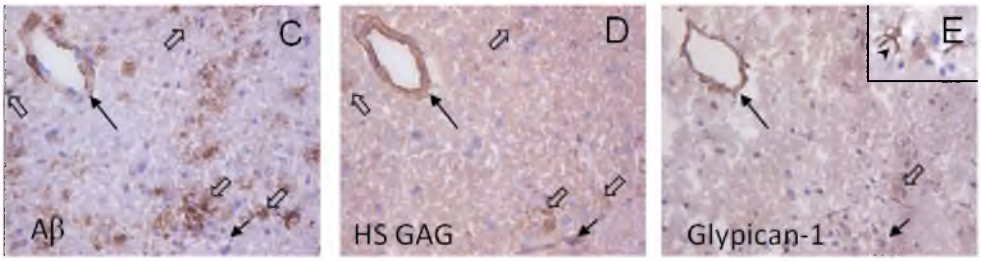

Figure 2: *Percentage of plaques positive for HS GAG (A) and glypican-1 (B). At and above the age of 8 months, the number of HS GAG-positive plaques increased with age (A). However, in 5-month-old mice there was more HS GAG (29%) co-deposition with Aβ than in 8-month-old mice (18%) but this was not significant (p>0.05). The number of glypican-1 positive plaques was low and remained constant with increasing age (B). Immunohistochemical analysis (C-E) of a 15-month-old mouse demonstrated HS GAG and glypican-1 positive plaques (open arrows). An Aβ-negative vessel was positive for HS-GAG (short closed arrow; D) and an Aβ-positive vessel (long closed arrow) was positive for both HS GAG (D) and glypican-1 (E). The inset (E) shows a glial cell positive for glypican-1 (arrowhead). Magnification 200x; magnification inset 400x.*

F

***Chapter 4**: Figures 3A, 3B and 3C*

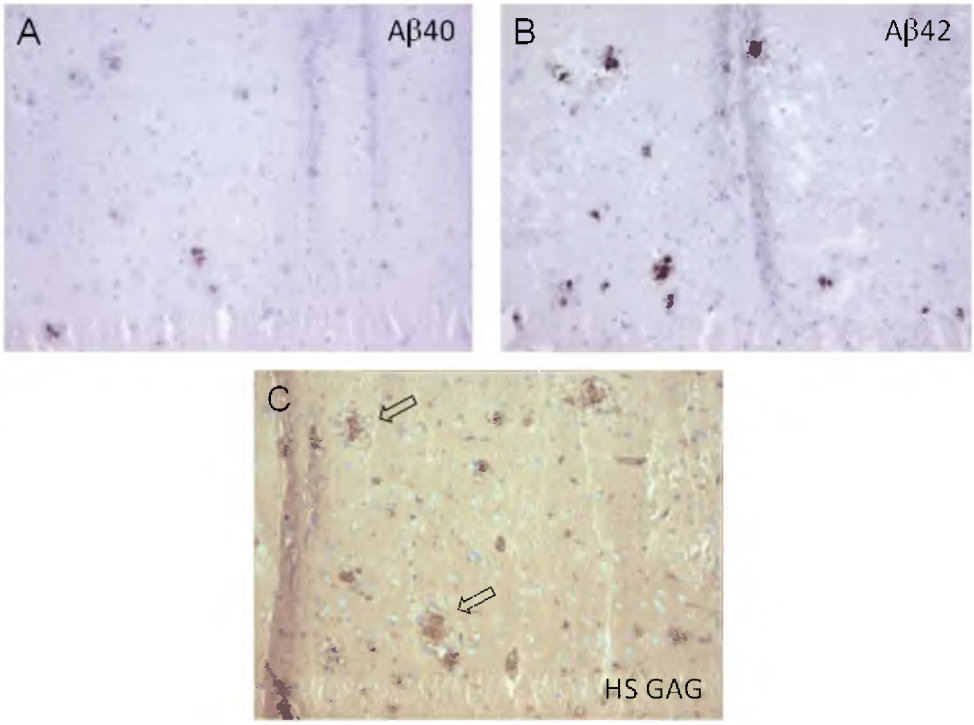

Figure 3: *Aβ40- (A) and Aβ42-positive (B) plaques and co-deposition with HS GAG (C) in a 15-month-old APPswe/PS1dE9 mouse. Aβ42-positive plaques were more numerous than Aβ40-positive plaques. All Aβ40-positive plaques were positive for Aβ42. HS GAG staining could be observed in both Aβ42- and Aβ40-containing plaques (open arrows).*

***Chapter 4**: Figures 4C, 4D, 4E, 4F, 4G and 4H*

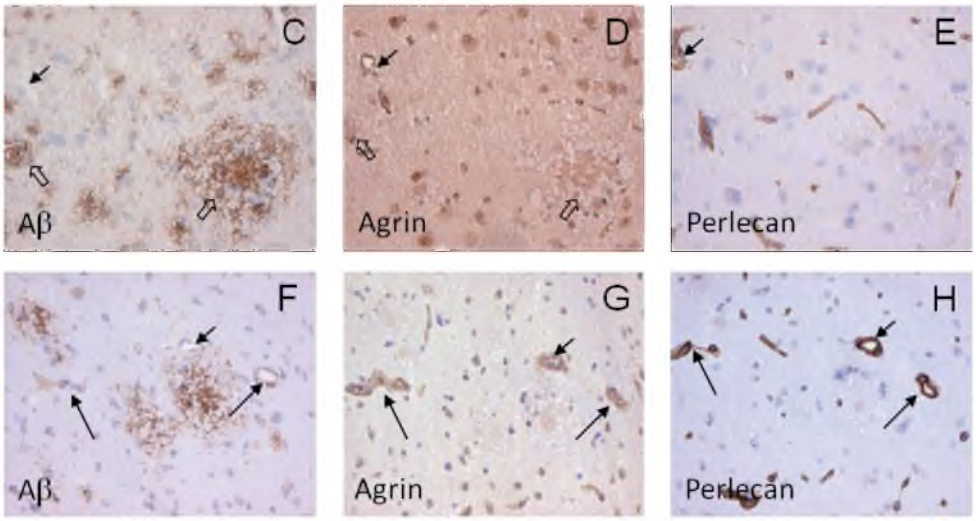

Figure 4: *Percentage of plaques positive for agrin (A) and perlecan (B). The number of agrin and perlecan positive plaques is very low (<10%). Immunohistochemical analysis of an 18-month-old mouse (C-E) demonstrated agrin-positive (open arrows in D) and perlecan-negative plaques (E). Aβ-positive vessels (long closed arrows; F) were positive for agrin (G) and perlecan (H). Normal vessels unaffected by Aβ deposition were also stained by antibodies against agrin and perlecan (short closed arrows in C-E). Magnification 200x.*

***Chapter 8**: Figure 1*

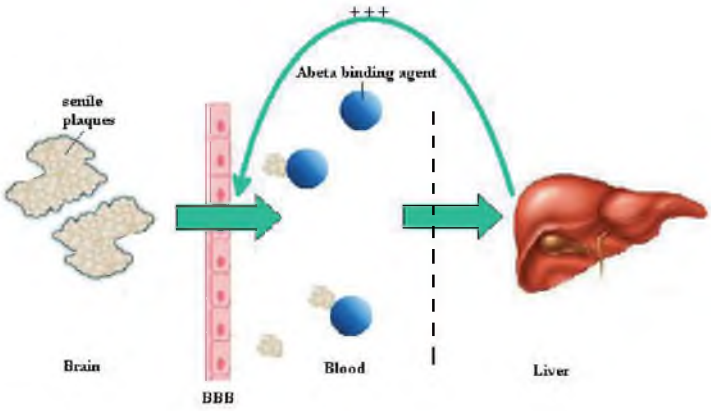

Figure 1: *The peripheral sink hypothesis. Peripherally administered Aβ-binding agents bind Aβ with high affinity in the plasma. These complexes, in turn, become targeted for degradation in organs such as the liver. This peripheral degradation depletes the plasma pool of Aβ, triggering an efflux of Aβ from the brain to the blood.*